UNIVERSITÀ DEGLI STUDI DI TRIESTE

XXXII CICLO DEL DOTTORATO DI RICERCA IN AMBIENTE E VITA

Geochemical characterization and redox properties of humic substances in lagoon environments

Settore scientifico-disciplinare: AGR/13

DOTTORANDO
CARLO BRAVO

COORDINATORE
PROF. GIORGIO ALBERTI

SUPERVISORE DI TESI
PROF. MARIA DE NOBILI

ANNO ACCADEMICO 2018/2019

UNIVERSITÀ DEGLI STUDI DI TRIESTE

XXXII CICLO DEL DOTTORATO DI RICERCA IN AMBIENTE E VITA

Geochemical characterization and redox properties of humic substances in lagoon environments

Settore scientifico-disciplinare: AGR/13

DOTTORANDO
CARLO BRAVO

COORDINATORE
PROF. GIORGIO ALBERTI

SUPERVISORE DI TESI
PROF. MARIA DE NOBILI

ANNO ACCADEMICO 2018/2019

« Προσπάθησε σε αυτά τα πράγματα,
εξάσκησε τα, χρειάζεται να τα αγαπάς: αυτά
θα σε φέρουν στα ίχνη της Θείας αρετής »

STATEMENT OF ORIGINAL CONTRIBUTION

The research presented in this thesis is an original contribution in the field of soil chemistry, focusing on humic substances in lagoon environments. Due to the multidisciplinary nature of the research project, the accomplished results had been possible thanks to fruitful collaborations with national and international research groups, in particular: the group of Electrochemistry of the University of Udine, with prof. Rosanna Toniolo as referee; the group of Marine Geochemistry of the Oceanographic Institute of the University of São Paolo (BR), with prof. Christian Millo as referee; the group of Research and Development of the Embrapa Instrumentation Center (São Carlos – BR), with Dr. Ladislau Martin-Neto as referee.

The manuscripts included in this thesis are organized in six chapters:

Chapter 1. De Nobili M., Bravo C., Chen Y. The spontaneous secondary synthesis of soil organic matter components: A critical examination of the Soil Continuous Model theory. *Submitted to Applied Soil Ecology*.

Chapter 2. Bravo C., Khakbaz A., Contin M., Goi D., De Nobili M. Is alkalinity of extractants responsible of artefacts formation during humic substances extraction? *Forthcoming submission*.

Chapter 3. Bravo C., Toniolo R., Contin M., De Nobili M. Redox behavior of humic acids after aerobic and anaerobic peat incubations. *Submitted to Biogeochemistry*.

Chapter 4. Bravo C., Toniolo R., Contin M., Martin-Neto L., Nascimento O.R., De Nobili M. Electron donating capacity of humic substances in relation to fast electron shuttling mechanisms at environmentally meaningful pH. *Forthcoming submission.*

Chapter 5. Bravo C., Millo C., Covelli S., Contin M., De Nobili M. Terrestrial-marine continuum of sedimentary organic matter in a mid-latitude estuarine system. *Journal of Soils and Sediments, 20(2), 1074-1086.* https://doi.org/10.1007/s11368-019-02457-6.

Chapter 6. Bravo C., Millo C., Toniolo R., Contin M., Martin-Neto L., De Nobili M. Electron donating properties of humic acids in saltmarsh soils. *Forthcoming submission*.

ABSTRACT

The humification model and, consequently, the existence of humic substances (HS), were recently harshly questioned in favor of a new vision of soil organic matter, the Soil Continuum Model, proposed by Lehmann and Kleber. For this reason, the first part of this thesis examines the integrity of the alkaline extraction of HS, both by a review of the related scientific literature and by performing suitable experiments. The aim of the review was to put to scrutiny the criticism regarding the so called 'humic substances paradigm', and to discuss and examine the argumentations of the Soil Continuum Model theory in the light of recent existing literature. A vast volume of interdisciplinary scientific evidences supports the formation of relevant non-pre-existing complex molecules exhibiting various types of structures. These molecules form during degradation and decay of biological cell components, a process in which pedofauna has a chemically active role.

Because of the lack of a systematic and straightforward investigation of the problem in the literature, a series of experiments was carried out to verify the possible formation of artefacts during alkaline extraction of HS. Sphagnum moss and peats at different stages of decomposition were extracted by both alkaline (sodium hydroxide and sodium pyrophosphate) and neutral (neutral sodium pyrophosphate and water) solutions and extracts were fractionated according to the classic solubility scheme. Results show that extraction yields vary with the extractant pH: alkaline extractants extract more organic matter from the different substrates. Spectroscopic properties are conserved when different extractants are used. Moreover, substances extracted from sphagnum differ both in their solubility properties and in their spectroscopic characteristics from HS extracted from peat. This allowed to observe structural differences among HS extracted from substrates at different stages of humification.

After having ascertained the reliability of the humic substances approach, the thesis examines the capability of HS to undergo redox reactions mediated by microorganisms. Therefore, electrochemical and structural changes which peat humic acids (HA) undergo when exposed to either

aerobic or anaerobic incubation are investigated. Under anaerobic conditions, HA may act as terminal electron acceptors, allowing facultative anaerobic bacteria to obtain energy from anaerobic respiration. In peatlands, extended drought periods induced by climate change could alter redox properties of HA and affect ratios of greenhouse gases emissions. Cyclic voltammetry experiments showed that microbial reduction increases the number of electrons that can be directly transferred from HA and that a wide potential distribution of redox-active moieties is present in HA molecules. Pseudo-first order kinetic constants indicate that, after reduction, HA can act as faster electron shuttles.

The kinetics of the oxidation of HS were then investigated using the redox mediator ABTS. The co-existence of fast and slow reaction steps was highlighted using electron paramagnetic resonance (EPR) spectroscopy. This allowed to set up a method to define the electron donating capacity (EDC) of HS.

The last part of the thesis examines the terrestrial and marine contributions to HS in sediments and saltmarsh soils along a river-lagoon transect (Marano and Grado Lagoon, Northern Adriatic Sea, Italy). The investigation of HS in sediments highlighted the existence of a complex but continuous pattern of terrestrial and marine contributions to C sequestration and humification, even in transitional environments where allochthonous humic C inputs are restricted due to insolubilization of humic substances by Ca^{2+}.

Geochemical characteristics of humic acids extracted from sediments were then compared to those extracted from saltmarshes of the same lagoon, and finally correlated with the electron donating capacity. The results obtained confirm the importance of contributions of aromatic structures of terrestrial origin for the EDC capacity of HA in transitional environments. The geochemical characteristics of soil organic matter and HS strongly affect the electron donating capacity of HS and should be taken into account when studying redox processes in transitional environments.

RIASSUNTO

Il modello di umificazione e di conseguenza l'esistenza delle sostanze umiche (HS) sono stati recentemente messi duramente in discussione a favore di una nuova visione della sostanza organica del suolo, il Soil Continuum Model, proposto da Lehmann e Kleber. Per questa ragione, la prima parte di questa tesi esamina l'integrità dell'estrazione alcalina delle sostanze umiche, sia con una revisione della relativa letteratura scientifica che svolgendo idonei esperimenti. Lo scopo della revisione è di esaminare attentamente le critiche relative al cosiddetto "paradigma delle sostanze umiche" e, alla luce della recente letteratura, di discutere le argomentazioni proposte dal Soil Continuum Model.

Un vasto volume di evidenze scientifiche interdisciplinari supporta la formazione di rilevanti molecole complesse non-preesistenti che esibiscono diversi tipi di strutture. Queste molecole si formano durante la degradazione e decomposizione di componenti cellulari biologiche, un processo in cui la pedofauna svolge un ruolo chimicamente attivo.

A supporto di questa analisi della letteratura, un'investigazione sperimentale è stata condotta per verificare la possibile formazione di artefatti durante l'estrazione alcalina di HS. Sfagno e torbe a differenti fasi di decomposizione sono stati estratti con soluzioni alcaline (idrossido di sodio e sodio pirofosfato) e neutre (sodio pirofosfato neutro e acqua) e gli estratti sono stati frazionati secondo lo schema di solubilità classico. I risultati hanno mostrato che le rese di estrazione variano con il pH degli estraenti: estraenti alcalini estraggono più materia organica dai diversi substrati. Le proprietà spettroscopiche sono conservate quando diversi estraenti sono utilizzati. Inoltre, le sostanze estratte dallo sfagno differiscono dagli HS estratti dalla torba sia per le proprietà di solubilità che per le caratteristiche spettroscopiche. Questo ha permesso di osservare differenze strutturali tra HS estratti dai substrati in diverse fasi di umificazione.

Dopo aver accertato l'affidabilità dell'approccio delle sostanze umiche, la tesi esamina la capacità delle HS di essere sottoposte a reazioni redox mediate dai microorganismi. Pertanto, i

cambiamenti elettrochimici e strutturali che subiscono gli acidi umici (HA) di torba quando sono esposti a incubazione aerobica o anaerobica sono stati esaminati. In condizioni anaerobiche, gli HA fungono da accettori terminali di elettroni, permettendo a batteri anaerobici facoltativi di ottenere energia dalla respirazione anaerobica. Esperimenti di voltammetria ciclica hanno mostrato che la riduzione microbica aumenta il numero di elettroni che possono essere direttamente trasferiti dagli HA e che un vasto intervallo di gruppi funzionali, con un vasto intervallo di potenziali redox, sono presenti in molecole di HA. Le costanti cinetiche di pseudo primo ordine indicano che, dopo la riduzione, gli HA possono donare elettroni più velocemente.

La cinetica dell'ossidazione delle sostanze umiche è ampiamente analizzata usando il mediatore redox ABTS. La coesistenza di fasi di reazioni veloci e lente è evidenziata usando la spettroscopia di risonanza elettronica paramagnetica (EPR).

L'ultima parte della tesi esamina il contributo terrestre e marino delle HS nei sedimenti e suoli di barena lungo un transetto fiume-laguna (Laguna di Marano e Grado, Mare Adriatico Settentrionale, Italia). I risultati evidenziano l'esistenza di un pattern complesso ma continuo di contributi terrestri e marini al sequestro di C e all'umificazione, anche in un ambiente di transizione dove input di C umico alloctono sono ristretti a causa dell'insolubilità di sostanze umiche da Ca^{2+}.

Le caratteristiche geochimiche degli HA estratti dai sedimenti sono stati poi confrontati con quelli estratti da barene della stessa laguna e alla fine correlate con la capacità di donare elettroni (EDC). I risultati ottenuti in questo lavoro confermano l'importanza dei contributi di strutture aromatiche di origine terrestre per la capacità di EDC degli HA in ambienti di transizione. Inoltre, le caratteristiche geochimiche dei suoli e degli acidi umici sono fortemente legate alla capacità di donare elettroni degli HA, e devono essere presi in considerazione quando processi di ossidoriduzione sono studiati in ambienti di transizione.

TABLE OF CONTENTS

STATEMENT OF ORIGINAL CONTRIBUTION i

ABSTRACT iii

RIASSUNTO v

THESIS' AIM AND STRUCTURE 1

CHAPTER 1 3

CHAPTER 2 49

CHAPTER 3 67

CHAPTER 4 89

CHAPTER 5 109

CHAPTER 6 125

FUTURE RESEARCH PERSPECTIVES 145

APPENDIX ix

ACKNOWLEDGMENTS xliii

THESIS' AIM AND STRUCTURE

The aim of this PhD thesis was to investigate the environmental role of humic substances in redox processes in recurrently flooded soils, such as those that are everyday subject to tidal fluctuations. Existing literature, in fact, suggests that humic substances play a key role when anoxic conditions occur in submerged soils, being involved as electron shuttles between microorganisms and metals and acting as terminal electron acceptors for the anaerobic respiration.

Different multidisciplinary approaches were adopted in order to give new insights on i) the capacity of humic acids to act as terminal electron acceptors, ii) the possible mechanisms of redox reactions involving humic substances, iii) the electron donating capacity of humic substances in a lagoon environment in relation to their geochemical characteristics.

The humification model, and consequently the existence of humic substances, was recently harshly questioned in favour of a new vision of soil organic matter (the Soil Continuum Model, proposed by Lehmann and Kleber). For this reason, Chapter 1 of this thesis examines the integrity of the alkaline extraction of humic substances. The aim is to put to scrutiny the criticism regarding the so called 'humic substances paradigm', discussing and examining the argumentations of the Soil Continuum Model theory in the light of recent existing literature. To support such literature analysis, an experimental investigation was carried out to verify the possible formation of artefacts during alkaline extraction of HS and results are reported in Chapter 2.

After having ascertained the reliability of the humic substances approach, the thesis proceeds with Chapter 3, where electrochemical and structural changes which peat humic acids undergo when exposed to either aerobic or anaerobic incubation are examined. In Chapter 4, the kinetics of the oxidation of humic substances are investigated throughout using the redox mediator ABTS, and the co-existence of fast and slow reaction steps is highlighted.

Once the interaction between humic substances and ABTS has been deeply investigated, in Chapter 5 it is presented the terrestrial and marine contribution of humic acids in sediments along a river-lagoon transect (Marano and Grado Lagoon, Northern Adriatic Sea, Italy). In Chapter 6, geochemical characteristics of humic acids extracted from sediments were then compared to those extracted from saltmarshes of the same lagoon, and finally correlated with the electron donating capacity.

In the end, the project "Stable isotope characterization of humic acids and retention capacity for Pb and other metals in the Cananéia-Iguape coastal system (Sao Paulo – Brazil)" is presented as future research perspectives and some preliminary results are provided.

All chapters have been written in the form of individual papers and are introduced by a short preface. Chapter 5 has already been published in the Journal of Soils and Sediments; all the other chapters only need to be properly finalized according to the chosen journal specific requirements before submission.

All the Supporting Information of the individual chapters are reported in the Appendix, which is structured according to the chapters' order.

CHAPTER 1

This work was carried out with the aim to critically examine the Soil Continuum Model proposed by Lehmann and Kleber. It is presented as a review of the vast volume of interdisciplinary scientific evidences related to the formation of relevant non-pre-existing complex molecules (humic substances) in soils and sediments, exhibiting various types of structures. The active role of pedofauna in the humification process was also considered. Two sections were dedicated to the color and molecular weights of humic substances.

The Spontaneous Secondary Synthesis of Soil Organic Matter Components: A Critical Examination of the Soil Continuous Model Theory

Maria De Nobili, Carlo Bravo* and Yona Chen

M. De Nobili and C. Bravo, Department of Agro-environmental, Food and Animal Sciences, University of Udine, via delle Scienze 208, 33100 Udine, Italy;

C. Bravo, Department of Life Sciences, University of Trieste, Via Licio Giorgieri 5, 34128, Trieste, Italy;

Y. Chen, Department of Soil and Water Sciences, The Robert H. Smith Faculty of Agriculture, Food and Environment, The Hebrew University of Jerusalem, POB 12, Rehovot, 7610010, Israel.

*Corresponding author: carlo.bravo@uniud.it

Keywords: humic substances; secondary synthesis; polyphenol-oxidases; pedofauna

Abbreviations list

SCM soil continuous model

SOM soil organic matter

HS humic substances

HA humic acids

FA fulvic acids

ESI FT-ICR MS electrospray ionization Fourier transform ion cyclotron resonance mass spectrometry

NMR nuclear magnetic resonance

OM organic matter

DOM dissolved organic matter

DOC dissolved organic carbon

HiDOC hydrophilic dissolved organic carbon

HoA hydrophobic acids

HoN hydrophobic neutral fraction

HoB hydrophobic bases fraction

HiN Hydrophilic neutrals fraction

PO polyphenoloxidases

POD peroxidases

SEC size exclusion chromatography

ESI electro spray ionization

M_n number average molecular weight

M_w weight average molecular weight

MW molecular weight

Core ideas

i) Secondary synthesis of humic substances does not require energy investments.

ii) Non pre-existing complex molecules are produced by phenoloxidases and peroxidase.

iii) Strongly alkaline conditions are present in the mid-gut of pedofauna.

iv) Large molecular weight HS are theoretically possible.

v) All current, different but complementary, approaches need to be maintained.

Abstract

The “Soil Continuous Model” questions the occurrence of any independent natural process of secondary synthesis that generates compounds structurally distinct from plant or microbial metabolites. This review shows that a vast volume of interdisciplinary scientific evidences supports the formation of relevant non-pre-existing complex molecules exhibiting various types of structures. These molecules form during degradation and decay of biological cell components. The spontaneous abiotic and enzymatically catalyzed reactions of components of organic residues and of their oxidative decomposition products suggested by state-of-the-art studies are indeed those proposed by the most classic humification theory. The chemically active role of pedofauna is also highlighted, explaining why the apparently harsh conditions of alkaline extraction of HS cannot be considered un-natural. Many insects and larvae feeding on foliage of plants with a high content of tannins have a midgut pH above 9. Albeit reducing conditions are often maintained to avoid oxidation, peroxidases are active in the intestinal tract and pass on to faeces. Polyphenols are then immediately enzymatically oxidized to their reactive quinone form, once faeces are excreted and exposed to oxygen. Implications of our current knowledge on the reactivity of plant components in soil is discussed in relation with present state of the art research on humic substances. Contrary to claims by the “Soil Continuous Model” theory, all current, different but complementary, approaches need to be maintained to understand the extremely complex nature of soil organic matter.

1. Introduction

Recently a novel model theory, the "Soil Continuous Model" (SCM), has been put forward challenging the most widely accepted current views on soil organic matter (SOM) transformations (Lehmann and Kleber, 2015). The authors claim the SCM model to be able to overcome all current contradictions and uncertainties in SOM research by viewing it as a continuum spanning from intact plant material to highly oxidized carbon. They argue that "the available evidence does not support the formation of large-molecular-size and persistent 'humic substances' (HS) in soils" and that "the evidence available to date does not support the assumption that processes of secondary synthesis create quantitatively significant proportions of "chemically reactive, yet recalcitrant" materials in natural environments" (Kleber and Lehmann, 2019). Their criticism of the empirical approach by which HS are extracted from soil with alkaline extractants, has been extensively questioned by Olk et al. (2019a, 2019b), who provided justifications for the extraction procedure and reviewed related literature, demonstrating that HS can be successfully used as a proxy of SOM in the investigation of many important agronomic and environmental issues. Contrary to what Lehmann and Kleber (2015) reiteratively stressed in their criticism of the "classic humification theory", early research on HS was never limited to a single extraction method. During the second half of the last century, several scientists had independently and repeatedly put under scrutiny, the extraction procedure, employing different extractants (Choudhri and Stevenson, 1957; Hayes et al., 1975) spanning from neutral salts (Bremner, 1949; Okuda and Ori, 1956), to diluted acids (Yuant, 1964), organic solvents (Piccolo, 1988) and chelating substances (Martin and Reeve, 1957; Evans, 1959).

Different extractants extract HS from soil with different yields, ash content and slightly different composition, which is - not surprising at all, this being the expected trend for many classes of ionisable organic compounds, whose solubility strongly depends on the pH and polarity of the extractant (Hayes and Clapp, 2001). None of the scientists that carried out extractions with neutral extractants ever concluded that the brown substances solubilized from soil under mild, un-altering conditions, were of a different nature compared to those extracted under harsh alkaline conditions.

Indeed, scrutiny of the isolates from alkaline and neutral extraction and different solvents allowed researchers to conclude that structural differences among humic acids (HA) extracted from different soils are indeed more pronounced than differences observed in isolates obtained from the same soil by different extraction procedures (Dick and Burba, 1999; Hayes and Clapp, 2001).

Extraction by sodium hydroxide solutions was never the only option, but it prevailed with time, being substantiated by a vast and varied amount of acquired experimental knowledge, that demonstrated that 0.5 M NaOH: a) extracted HS of very close chemical characteristics; and b) it allowed in most cases larger extraction yields.

The assertion "HS have not been observed by modern analytical techniques" (Lehmann and Kleber, 2015) is not actually true. The most advanced techniques are currently bringing evidence in favour of the most classical views on structure and origin of HS. Tandem mass spectrometry, based on infrared multiphoton dissociation, identified labile fragments of fulvic acid (FA) molecules, whose chemical formulas could be linked to plausible structures consistent with degraded lignin fragments (Di Donato et al., 2016). Not only conclusions drawn from earlier investigations carried out by ^{1}H and ^{13}C nuclear magnetic resonance (NMR) (Kelleher and Simpson, 2006) have been critically examined (Albers et al., 2008; Bell et al., 2014; Knicker et al., 2016), but at present, the most advanced instrumental techniques suggest that HS differ from a simple mixture of plant or microbial metabolites and belong to classes of recognizable organic compounds with a known defined structure (Bell et al., 2015; Cao and Schmitt-Rohr, 2018). Electrospray ionization Fourier transform ion cyclotron resonance mass spectrometry (ESI FT-ICR MS) has given new insight into the distinctive molecular characteristics of HA which provides a basis to the hypothesis that suggests a possible pathway to their formation (Ikeia et al., 2015). Furthermore, dipolar dephasing ^{13}C NMR and graphical-statistical analysis of pyrolysis compounds (Almendros et al., 2018) allowed to highlight the origin of unsaturated HA structures and differentiated from pyrogenic aromatic structures.

Lehmann and Kleber (2015) further criticize what they call the "classic humification" approach denying that HS can be considered as a proxy for SOM. Indeed, HS may very well be just

a sizeable fraction (up to 60-75%) of SOM, yet they are responsible for most of the beneficial roles fulfilled by SOM. Ample justification, for this, is provided by the huge number of studies, recently reviewed by Olk et al. (2019a, 2019b), who demonstrated the practicability of the approach in agriculture, pedology and environmental sciences. Existing occasional disagreements among scientists are another argument used to foster the rejection of the HS concept, as terms such as humification, humus and HS are indeed used with sometimes widely different connotations prevailing in different disciplines. However, we argue that contradictions followed by synthesis, are an integral part of the evolution of science. Examples of this kind can be found in any discipline and were almost in all instances a tool leading to the advancement of science. The essential conditions to such achievements are common sense, respect to other opinions, honesty and humbleness that have to accompany any criticism.

In this review, starting from an examination of the affirmations which make up the base of the criticism to the complex and still not unified concept of HS, we will demonstrate, through a novel independent type of approach, that the existing apparent contradictions do not undermine the correctness of currently accepted views of SOM.

A large part of this review will focus on the huge recent scientific evidence available from disciplines other than SOM research, such as Food Science, Botany and Entomology, that indeed supports the most classic humification theory. This review examines current knowledge of the chemical reactivity of plant components exposing the predictable spontaneous formation of non-pre-existing chemical structures, when or even before residues enter the soil. In particular, it highlights the chemically active role of pedofauna, explaining why the apparently harsh conditions of alkaline extraction of HS cannot be actually considered un-natural.

In the last part of the review we discuss implications of our current knowledge on the reactivity of plant components inputs to soil in relation with present state of the art research on HS and the need to maintain all current different yet complementary approaches to understand the extremely complex nature of SOM.

2. Decomposition of organic matter and selective preservation by sorption

According to the SCM model, "organic matter exists as a continuum of organic fragments that are continuously processed by the decomposer community towards smaller molecular size. The breakdown of large molecules leads to a decrease in the size of the main components of primary plant material with concurrent increases in polar and ionizable groups, and thus to increased solubility in water." Increased polarity is expected to favour sorption onto soil mineral surfaces and inclusion into soil aggregates: the whole process is supposed to foster protection against further decomposition, only by regulating substrates availability in the water phase. These assumptions, unfortunately, are neither supported by experimental evidence, nor by theory. In fact, the anticipated increases in polar and ionizable groups of the small molecules produced by hydrolysis reactions may indeed be assumed to increase solubility and therefore dissolved organic matter (DOC), but not sorption, which is well known to be preferentially driven by the larger entropy changes associated to hydrophobic interactions (Jardine et al., 1989; Kaiser and Zech, 1997).

In the absence of mineral surfaces, such as during composting, decomposition of organic matter (OM) is accompanied by a considerable steady decline in dissolved organic matter (DOM or DOC) (Zmora-Nahum et al., 2005). A larger proportion of soluble highly polar hydrophilic DOC (HiDOC) is found in composts before stabilization: its production during OM decomposition represents therefore only a transient stage and not a final attainment. Concurrently with the fact that hydrolysis reactions rates are generally much slower than bio-oxidation rates (D'Imporzano and Adani, 2007), an overall decrease of HiDOC is indeed observed with composting time (Said-Pullicino and Gigliotti, 2007). Conversely, studies on the composition of DOM during composting, agree with the above statement by showing that hydrophobic acids (HoA), the dominant components of the hydrophobic fraction, exhibit a moderate increase with time (Chefetz et al., 1998a; 1998b; Straathof and Comans, 2015). At the same time, the hydrophobic neutral (HoN) fraction of DOM also increases sharply, while the hydrophobic bases (HoB) fraction decreases. Hydrophilic neutrals (HiN) represent the major fraction of the dissolved hydrophiles until 120 days of composting and decrease thereafter

by 38% (Chefetz et al., 1998b). The ^{13}C-NMR spectra of the unfractionated DOM revealed an increasing level of aromatic structures in the residual DOM with composting time. Concomitantly, ^{13}C-NMR spectra of the HoA fraction basically implied a polyphenol-humic structure, whereas the HoN spectra exhibited strong aliphatic features. This information strongly suggests co-existence of complex mechanisms with a preferential turnover of hydrophilic fractions during decomposition of organic substrates, while hydrophobics remain relatively conserved (Chefetz et al., 1998a; 1998b; Straathof and Comans, 2015). The progressive increase in solubility of SOM during decomposition, which should be expected on the basis of the SCM model and which, in the absence of sorption on mineral surfaces, would be directly reflected in an increase of DOM, does not therefore occur and is, at best, only a transient phenomenon often observed during the first part of the thermophilic stage. It could be argued that the observed decrease in DOM could be brought about by increased mineralization, triggered by availability of water-soluble substrates. However, this is not the case, because, the decrease in DOM is actually accompanied by a concomitant decrease in microbial respiration (Said-Pullicino and Gigliotti, 2007) and a consistent increase of the HS concentration of the compost.

In composts, the OM fraction largely exceeds that of the mineral components, whereas in soils the mineral fraction is the dominant one. Therefore, in composts, sorption does not contribute to mask DOM trends. In soils, however, all DOM components enter the sorption/de-sorption equilibria with the surfaces of soil minerals (Avneri-Katz et al., 2017). However, sorption of highly soluble polysaccharide-derived DOM on mineral surfaces is weaker, whereas the hydrophobic acid (HoA) fraction undergoes preferential adsorption (up to 70% of total adsorbed C) by soil mineral surfaces (Kaiser and Guggenberger, 2000). Adsorptive and desorptive processes strongly favour the accumulation of the more recalcitrant lignin-derived DOM (Leinemann et al., 2018). Highly oxidized polyphenols are preferentially retained via ligand-exchange, preserved and eventually partially de-sorbed and maintain, in the soil solution, a total concentration ranging from 6–15 to a few hundred mg phenol-C kg^{-1} depending on soil mineralogy, pH and prevailing cations (Curtin et al., 2016).

3. Molecular reactivity

The SCM model "excludes any secondary synthesis of 'humic substances'". Yet, sorbed polyphenols, such as catechin, have been shown to undergo spontaneous, non-catalyzed, abiotic polymerization (Pal et al., 1994; Chen et al., 2010) and Mn-, Fe- and Al-oxides were extensively shown to be able to catalyze formation of humic like substances in vitro (Huang and Hardie, 2009; Fukuchi et al., 2010).

Many, among the simple molecules present in plant residues, released by roots (Cesco et al., 2012) or produced during degradation of plant tissues, are far from being non-reactive and - undergo spontaneous abiotic oxidation and polymerization (Dec et al., 2003). Being at the base of many browning reactions in food, which are of great concern to the food processing industry (Friedman, 1996), polyphenols are probably the most studied. Browning reactions occur very rapidly in damaged plant tissues (Martinez and Whitaker, 1995; Tomas-Barberan et al., 1997; García et al., 2017), whenever the strict compartmentalization that prevents these substances from reacting with other cell metabolites is mechanically destroyed by industrial processing or insect chewing. Enzymes able to catalyse the oxidation and polymerization of polyphenols are contemporarily released by these actions (Lagrimi, 1991). They are thus free to act on their designed and non-designed substrates in a disordered and uncontrolled way so that the end result is the formation of brown-coloured adducts (Robards et al., 1999; Lattanzio, 2003).

Phenoloxidases (PO), which catalyse the addition of an oxygen in a position *ortho*- to an existing hydroxyl group in an aromatic ring (Martinez and Whitaker, 1995), are for instance responsible of the fast browning of lacerated or crumpled leaves, when exposed to oxygen (Tomas-Barberan et al., 1997). The spontaneous browning of damaged tissues is chemically initiated by the enzymatic oxidation of di-phenols to quinones, which subsequently may polymerize in the presence of oxygen or eventually suffer attack by nucleophilic compounds such as amino sugars and amino acids (Friedman, 1996; Mishra and Gautam, 2016).

It is well-known that browning of fresh cut fruits and vegetables is accelerated, in cut or damaged leaves, by spontaneous induction of enzymes (Tomas-Barberan et al., 1997; García et al., 2017), such as phenylalanine ammonia lyase, which catalyses the synthesis of phenylpropanoid moieties. It is also equally well known, that the formed phenolic moieties (Robards et al., 1999; Lattanzio, 2003) are enzymatically oxidized by PO resulting in the secondary synthesis of brown adducts, and that this class of enzymes is common in soils (Sinsabaugh, 2010; Zavarzina et al., 2018).

Notwithstanding existing overlaps, PO are often classified according to substrate specificity and mechanism of action into three main classes: laccases (EC 1.10.3.2), catechol oxidases (EC 1.10.3.1) and tyrosinases (EC 1.14.18.1).

Laccases (Chaurasia et al., 2013) are a widespread class of multi-copper containing enzymes, also active in soil (Eichlerová et al., 2012), which perform both anabolic and catabolic functions, presiding, among other things, over both the radical polymerization of lignin and its decomposition. They represent the dominant type of ligninolytic fungal and bacterial oxidative exo-enzymes which display p-diphenol oxidase activity (Baldrian, 2006; Witayakran and Ragauskas, 2009; Liers et al., 2011). Notwithstanding their well-defined metabolic roles, laccases are not substrate specific, but catalyze the coupling of most hydroxylated aromatic substrates with other types of molecules to produce heteromolecular hybrids (Fig. 1). Laccases are not only highly stable in solution (Riva, 2006; Witayakran and Ragauskas, 2009), but they do maintain their activity even when grafted to organic or inorganic solid surfaces (Zdarta et al., 2018). Their reactions may occur at room temperature, mild pH, and in the presence of oxygen (Rodríguez Couto and Toca Herrera, 2006; Ortner et al., 2015). This high stability and efficiency in catalysing the polymeryzation of new materials (Ba and Kumar, 2017) and decontamination of wastewaters from phenols, amines and other types of pollutants (Riva, 2006) has made them highly promising in a wide range of potential industrial applications (Mikolasch and Schauer, 2009; Witayakran and Ragauskas, 2009; Ba and Kumar, 2017).

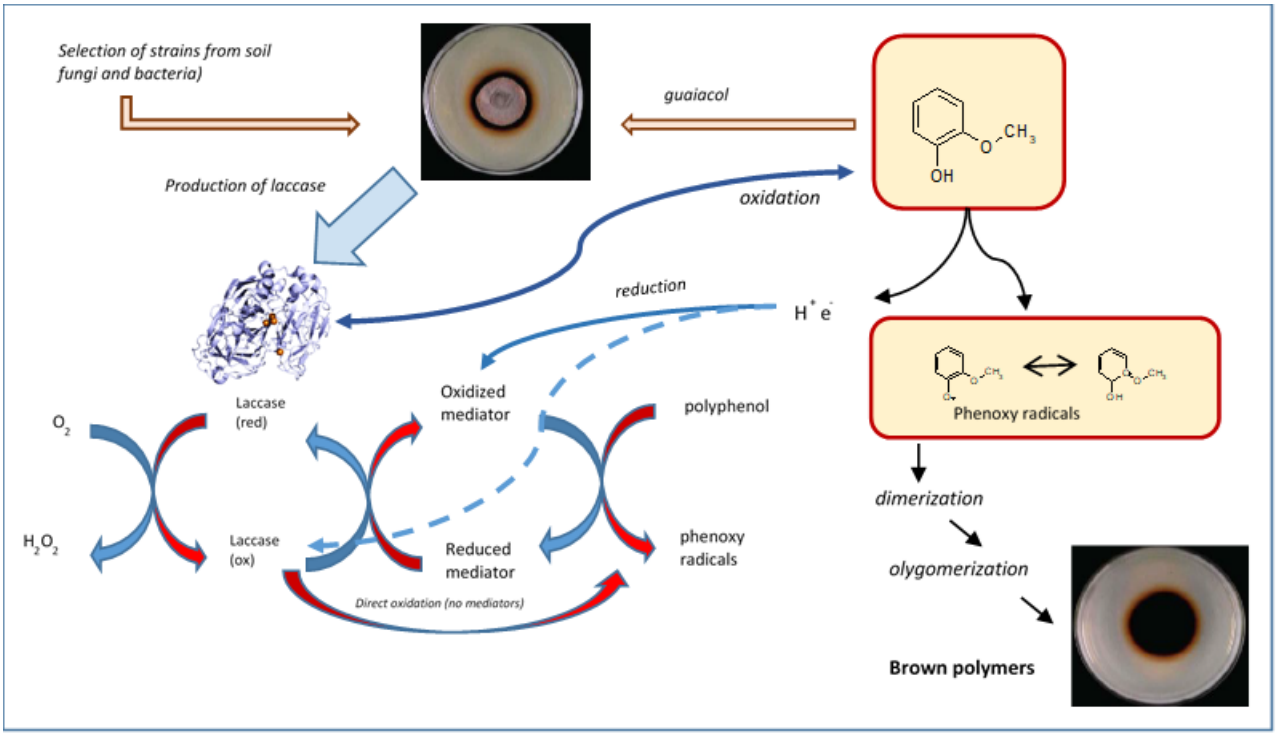

Fig. 1. Oxidation of guaiacol and production of brown polymers by laccases from fungi and bacteria strains selected from soil (petri dish images from Devasia et al., 2016).

Coupling reactions catalyzed by laccases are hypothesized to proceed by formation of a radical cation which then deprotonates to give a radical (Fig. 1). The radical afterwards produces a quinonoid derivative or undergoes nucleophilic attack by a similar radical producing dimer, oligomers and eventually even larger molecules (Wong, 2009; Ćirić-Marjanović et al., 2017). Until recently, laccases were thought to have only a limited role in the degradation of lignin, because of their low redox potential. This limits the types of phenolic structures which could be theoretically oxidized, and which are actually oxidized in the absence of mediators (Cañas and Camarero, 2010). Free radicals of fungal metabolites or lignin degradation products may, on the contrary, play as redox mediators (Morozova et al., 2007; Lundell et al., 2010) and have access to potential reaction sites within the complex three-dimensional structural network of lignin. Similarly, phenoxyl radical fragments generated by the same enzyme or by other PO, can oxidize nonphenolic residues within the lignin polymer backbone causing its decomposition. Organic and organo-mineral horizons of both broadleaved and coniferous forest soils display high laccase activity (Criquet et al., 1999; Luis et al., 2004). This enzyme, which plays a fundamental role in the transformation of SOM (Baldrian and

262 Šnajdr, 2011; Zavarzina et al., 2018), is also active in agricultural or meadow soils (Eichlerová et al.,
263 2012).

264 A very large number of examples of well documented and thoroughly studied enzymatically
265 catalyzed reactions that lead to structural transformations of polyphenols, which strongly resemble
266 those hypothesized for the formation of HS, can be found in food science and green chemistry studies
267 (Richard-Forget and Gauillard, 1997; Lundell et al., 2010). Besides laccases, also peroxidases (POD)
268 (Hofrichter, 2002) show high reactivity for generating free radicals from phenols, but POD are unable
269 to control the coupling selectivity and therefore are more likely to produce highly disordered adducts,
270 rather than polymers. The activity of POD (Kellner et al., 2014) is limited by the availability of
271 hydrogen peroxide, but in the presence of PO, these enzymes enhance together the oxidation of
272 phenols and cause the progressive browning of fruit juices (Richard-Forget and Gauillard, 1997). In
273 fact, it was shown that during phenol oxidation, PO generate variable amounts of hydrogen peroxide
274 and moreover, that POD can eventually use quinones as proxy for the peroxide substrate.

275 Under natural soil conditions, reactions such as those reported in Fig. 2, are probably unlikely
276 to lead to a massive formation of high molecular weight molecules, because of progressive
277 consumption of reagents and enzyme inactivation. However, the process is likely to initiate and to
278 result in the formation of an array of mixed oligomeric compounds which were not originally present
279 in living cells and do not correspond to any known plant metabolite and which in turn can further
280 react with other intermediate products of decomposition.

281 These compounds, indeed, possess all the chemical characteristics described by the classic
282 views of HS (Stevenson, 1994).

283 The variety of new molecules that can be potentially synthesized within dead cells through
284 these uncontrolled and disordered, but well recognized reaction mechanisms, is huge. Even larger is
285 the number of compounds that can eventually originate from them in soil, where plant metabolites
286 may diffuse from damaged tissues and react with bacterial or fungal metabolites. Since their substrate
287 is a large insoluble biopolymer, most fungal laccases and peroxidases are in fact exocellular enzymes,

and are continuosly released in soil by fungi in order to free N containing compounds and carbohydrates from wooden residues.

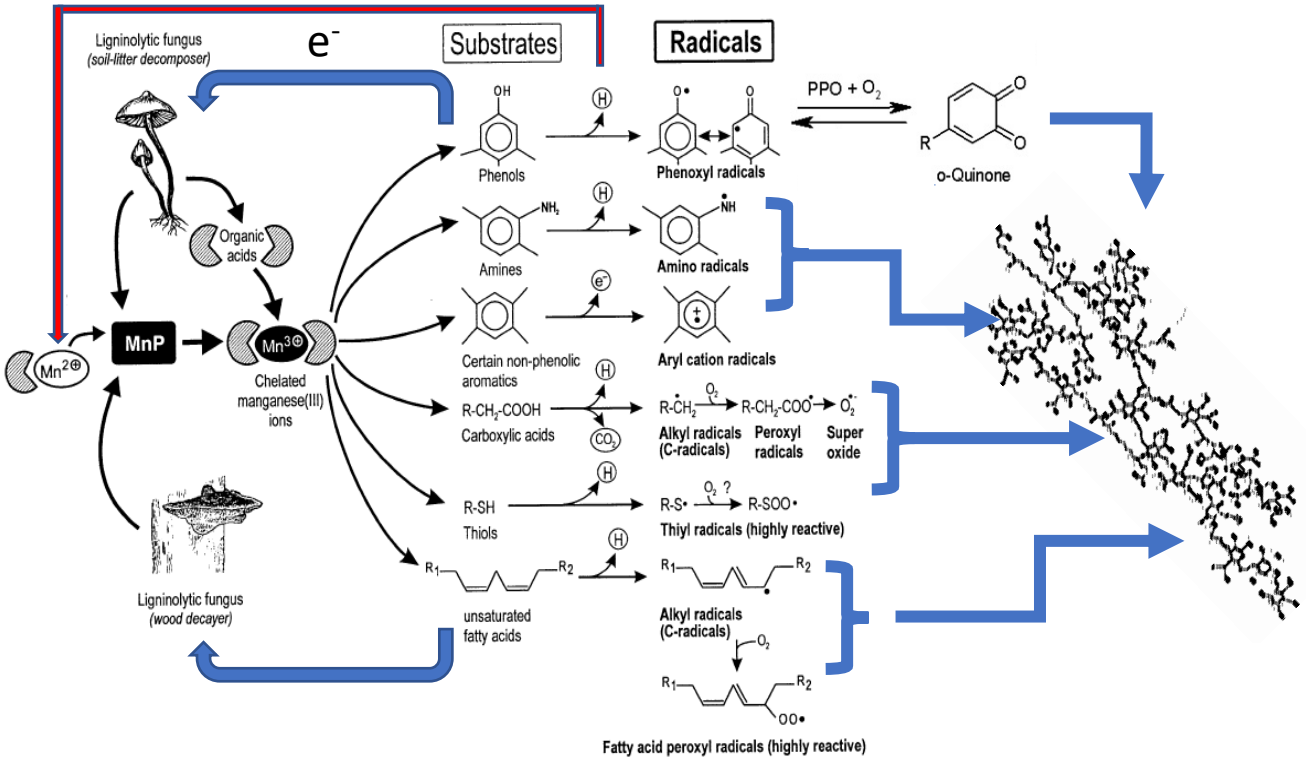

Fig. 2. Example of the action of fungal Mn peroxidases (MnP) coupled to that of phenoloxidase (PO) to produce HS. From Hoftrichter (2002), modified.

Phenols also react spontaneously with proteins (Hagerman, 2012): the phenomenon of astringency, that occurs in the mouth every time we taste unripe persimmon fruits or other tannin rich food, testifies how readily polyphenols may precipitate proline rich proteins (Ozdal et al., 2013).

Among these, those with an alkaline isoelectric point, are more effective in binding polyphenols than those with acidic ones, particularly in binding tannins (Kroll and Rawel, 2001; Ozdal et al., 2013). In most fruit juices, the presence of tannins with a high degree of polymerization also intensifies the development of turbidity and increases formation of adducts and precipitates. Complex tannins can bind to several exposed reactive sites on a protein's surface or even to several proteins or protein units at the same time. These enzymatically driven reactions are also accompanied by visible browning (Nicolas et al. 1994; Robards et al., 1999).

Formation of adducts may occur through hydrogen bonds and hydrophobic interactions, but covalent bonds may also be established (Kroll and Rawel, 2001). Here we will focus on the formation of covalent adducts as this represents a permanent, non-reversible mechanism for the modification of the known chemical structure of a defined organic compound into what could become a precursor for a non-biologically directed synthesis of phenol – protein adducts and finally of humic molecules.

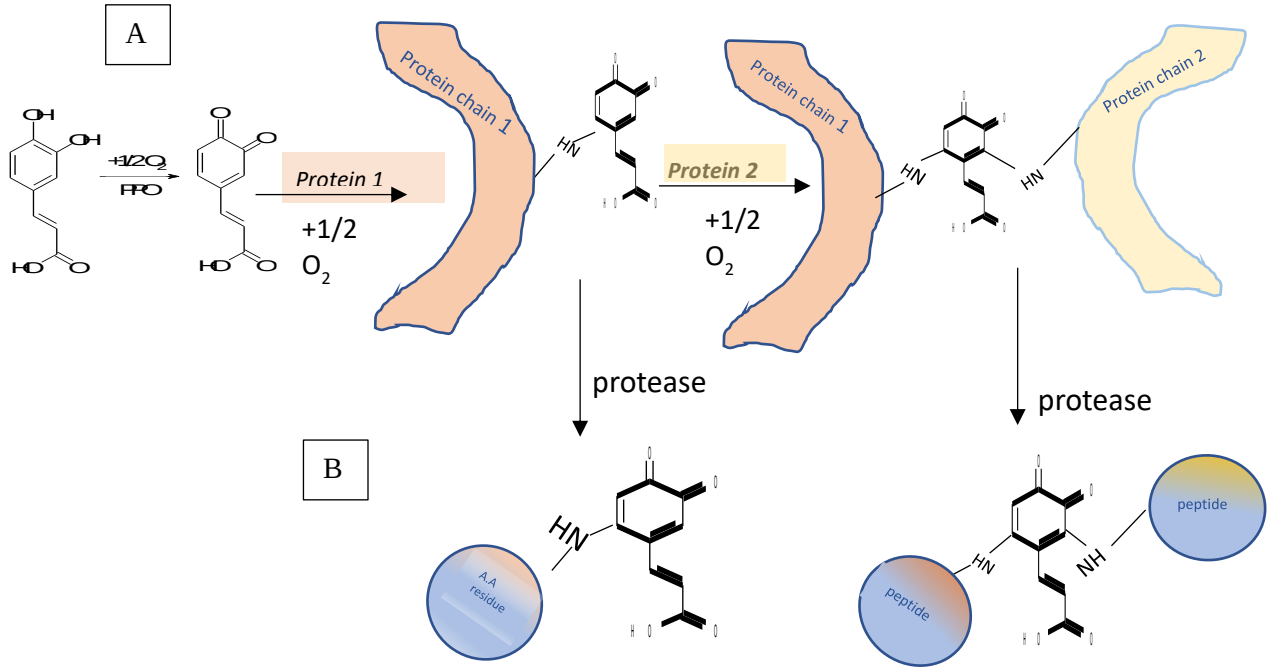

Fig. 3. Oxidation of a polyphenol by PPO and its crosslinking reaction with two protein molecules (A). Subsequent attack by proteases results in the release of amino acid or peptide adducts with reacted polyphenols (B).

The primary products of the enzymatic oxidation of o-diphenols, besides reacting with other quinones to produce brown polymers, can themselves readily undergo attack by nucleophilic residues located in proteins. This results in the formation of covalent bonds with the protein backbone and in concomitant changes in its physicochemical, structural and biological properties (Fig. 3). Further oxidation of the addition product may lead to a second addition, which may be accompanied by formation of cross-linked protein adducts (Zhang et al., 2010).

For instance, mushroom tyrosinase (EC 1.14.18.1) induces the formation of cross-linkages in α-lactalbumin and β-lactoglobulin through the formation of covalent bonds with caffeic acid or other low molecular weight polyphenols (Thalmann and Lötzbeyer, 2002). The optimum pH for this

321 reaction is between 4 and 5, but in the case of lysozyme, which has a higher isoelectric point, the
322 optimum is at pH 7.

323 These reactions involve common phenolic compounds such as ferulic-, caffeic-, chlorogenic-
324 and gallic acid as well as *m*-, *o*-, *p*-dihydroxyphenols (Rawel et al., 2000; Kroll and Rawel, 2001) and
325 occur spontaneously (Hurrel and Finot, 1985) even in the absence of enzymatic catalysis and at room
326 temperature, under pH conditions commonly found in soils (5–9). For flavonoids, the occurrence of
327 two adjacent (ortho) aromatic hydroxyl groups such as in kaempferol, quercetin and myricetin is a
328 necessary structural feature for auto-oxidation and therefore for reactivity (Zhang et al., 2010).

329 The main reactive groups involved in the formation of covalent bonds with proteins are
330 situated in exposed free amino groups (e.g. lysine side chains) (Baxter et al., 1997). Also the
331 heterocyclic N in tryptophan is highly reactive, as testified by the decrease in fluorescence intensity
332 which follows the formation of the adducts (Ozdal et al., 2013). Tyrosine residues are also involved,
333 as laccase has been shown to catalyze the polymerization and cross-linking of tyrosine containing
334 peptides (Mattinen et al., 2005).

335 Formation of adducts with phenols impairs the hydrolytic activity of proteases and availability
336 of aminoacids (Hurrel and Finot, 1985; Rawel et al., 2000). Obviously, hydrolysis is not hampered
337 far from reaction sites and most of the protein chains will still undergo decomposition. Yet amino
338 acid residue and small peptides, located near the non peptidic bonds, will resist the action of proteases.
339 These reactions provide a rationale for the presence of peptide N in HS detected by ^{1}H and ^{13}C NMR
340 and for the relative recalcitrance of this N to further decomposition (Fig. 3).

341

342 **4. The color of humic substances**

According to Lehmann and Kleber (2015), the dark colour of HS is "generated in laboratory experiments". This is definitely not true: not only because organic layers in soil and even mineral soils are indeed naturally brown (Allison, 2006), but also decaying organic matter spontaneously becomes brown with time (Sugahara et al., 1979; Khan et al., 2009). SOM extracts obtained with neutral buffers and sometimes even water extracts of soils, or leachates of composts and peat) as well as many natural freshwater bodies are innately brown or very dark brown (Fig. 4).

Fig. 4. Humic substances dissolve in rainwater draining from organic matter rich soils and colour this forest brook in Karelia.

As repeatedly mentioned before, browning reactions occur spontaneously and rapidly in processed food and beverages and involve many common mechanisms besides the well-known Maillard reaction responsible for non-enzymatic browning. The Maillard reaction, however, although having been suggested as a possible mechanism of formation of HS (Stevenson, 1994), is probably not likely to occur extensively in soil, being driven by extreme pH or high temperatures.

Although non-enzymatic oxidation of phenols caused by alkaline treatments does results in browning, the same darkening effect ensues by even more rapid enzymatic mechanisms even under very mild conditions (Li et al. 2008). The pH optimum for fungal laccases is, in fact, acidic and mostly within a pH range between 3.5–6 (Baldrian, 2006).

Intracellular laccases are responsible for the formation of melanins (Nagai et al., 2003). These polymers are synthesized by fungi to protect themselves from environmental stresses, but, following cell death, the uncontrolled action of intracellular laccases which can act on a relatively wide range of possible substrates, can result in post-harvest browning of mushrooms (Martinez and Whitaker, 1995; Lin and Su, 2019).

Non-enzymatic browning may also be initiated by the formation of a complex between polyphenols and metals (Cheng and Crisosto, 1997). Polyvalent cations such as Fe^{3+} and Cu^{2+} easily form complexes with phenolic compounds (Slabbert, 1992), catalyzing their oxidation. In fact, they enhance formation of hazes in fruit juice, which is caused by insoluble adducts produced by reaction with carbohydrates and proteins (Beveridge and Wrolstad, 1997). Tannins with a high degree of polymerization also increase the extent of haze formation as they can bind to several sites cross-linking amino-acid chains or even different proteins. The ensuing precipitates are coloured and become brown with time.

Brown coloured products (Fig. 5) are also produced within a few minutes during lignin oxidation by laccase in the presence of oxygen (Ortner et al., 2015).

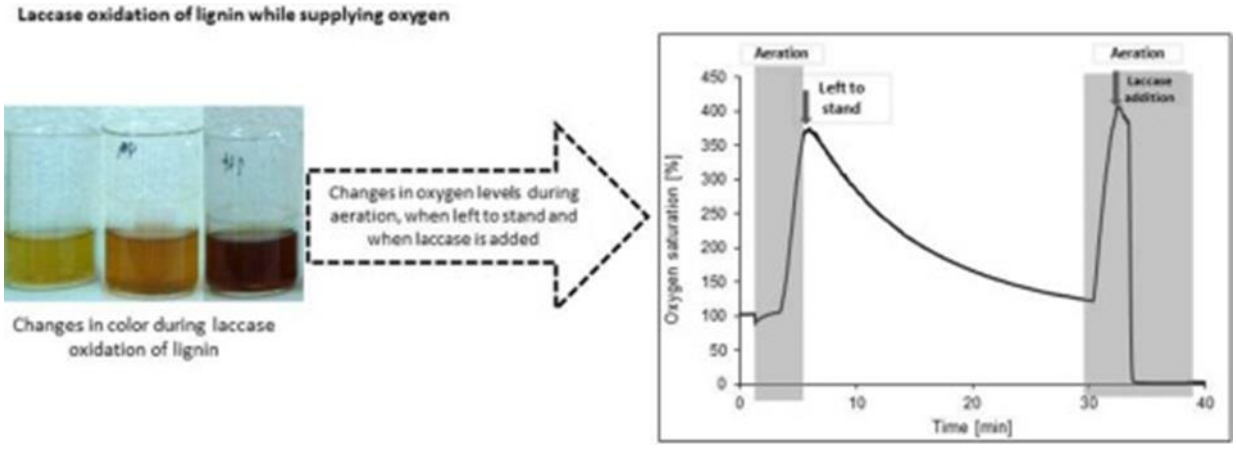

Fig. 5. Changes in colour during laccase oxidation of lignin. Colour development occurs within a few minutes from the start of the aeration (from Ortner et al. 2015).

Coloured soluble and insoluble high molecular weight reaction products are even formed from the coupling of amino acids with lipid oxidation products (Hidalgo and Zamora, 2000). The role of

lipids in these reactions is similar to that of carbohydrates in the Maillard reaction or of phenols in the enzymatic browning. Polyunsaturated fatty acids are enzymatically oxidized either by lipoxygenases or cyclooxygenases to hydro or endoperoxides, which, in turn, produce carbonyl compounds, that react readily with amino groups to form both small and large coloured substances (Adams et al., 2009).

The potential industrial applications of laccase catalyzed homo- and hetero-coupling have been exhaustively investigated. An example is the production of polymers with antioxidant properties, not only through grafting of low-molecular weight molecules onto lignocellulose materials, but also through cross-linking and oligomerisation of peptides with polyphenols, (Mikolasch and Schauer, 2009).

5. The SCM model does not consider the action of pedofauna

Soils are complex ecosystems that harbour highly biodiverse and abundant communities of permanent or temporary edaphic invertebrate populations, which process a large fraction of incoming organic materials and directly or indirectly affect SOM turnover (Wolters, 2000; Zanella et al., 2018).

The humic horizon of moder and amphimull humus forms (Zanella et al., 2018a), which in many forest soils can be several centimeters thick, is actually - made up from 70 to 100% in volume, roots excluded, of zoogenically transformed materials consisting in droppings of epigeic earthworms, of macro and microarthropods, of insect larvae and enchytraeids (Zanella et al., 2018b).

The OM of these droppings derives from chewed and digested litter residues that passed through the gut of pedofauna (Dillon and Dillon, 2004), which is often characterized by strongly alkaline conditions. Lepidoptera and Diptera feeding on foliage of plants with a high content of tannins and on Solanaceae often have a midgut pH above 9 (Clark, 1999). A decreased, but still alkaline midgut pH (near 8), displayed by some lepidopteran species may be an adaptive response that overrides selection of the normally high pH for insects feeding on foliage of plants containing

terpenes, glucosinolates, and pyrrolizidine alkaloids (Shao et al., 2012; Chou et al.; 2018). In general, Lepidopterans and sawflies possess strongly alkaline gut conditions from pH 8 to 10 (Appel, 1994). The highest pH values, among soil dwelling beetle larvae, are found among the Scarabaeidae: larvae of the African scarab *Pachnoda ephippiata*, for instance, have an alkaline midgut pH above 10 (Lemke et al., 2003), but also some species of higher termites possess a mid-gut pH above 10 (Bignell and Eggleton, 1995). Many arthropods have intestinal tracts characterized by strongly reducing redox conditions (Johnson and Barbehenn, 2000): this is a likely a defence strategy meant to protect these animals against the high content of phenols in their diet (Shao et al., 2012). Reducing conditions impede oxidation of phenols, but peroxidases are active in the intestinal tract and are passed on to feces. Polyphenols become immediately enzymatically oxidized to their quinone form once the alkaline feces are excreted and, therefore, exposed to oxygen. In silkworms, for instance, the blackening of the insect feces, which are green inside the gut (Fig. 6), is due to an activated form of PO, which serves to regulate the number of bacteria in the hindgut (Shao et al., 2012).

Due to all the above, the assumption made by Lehmann and Kleber (2015), namely, that strongly alkaline conditions are extraneous to soil is therefore unrealistic. Even in acid soils, leaves, stems and roots, either eaten living or dead, are incorporated into non particulate SOM, after transiting through the alkaline feeding tract of insects and larvae. They have, therefore, already experienced pH values that are not very much higher than those of an alkaline extractant.

Even in acid soils, HS are liable to have been naturally exposed to alkaline pH conditions and most likely right at the time of the initial stages of their formation.

Many of the reactions that were described in the previous paragraphs are indeed particularly favored by passage through the feeding apparatus and strongly alkaline digestive tract of insects.

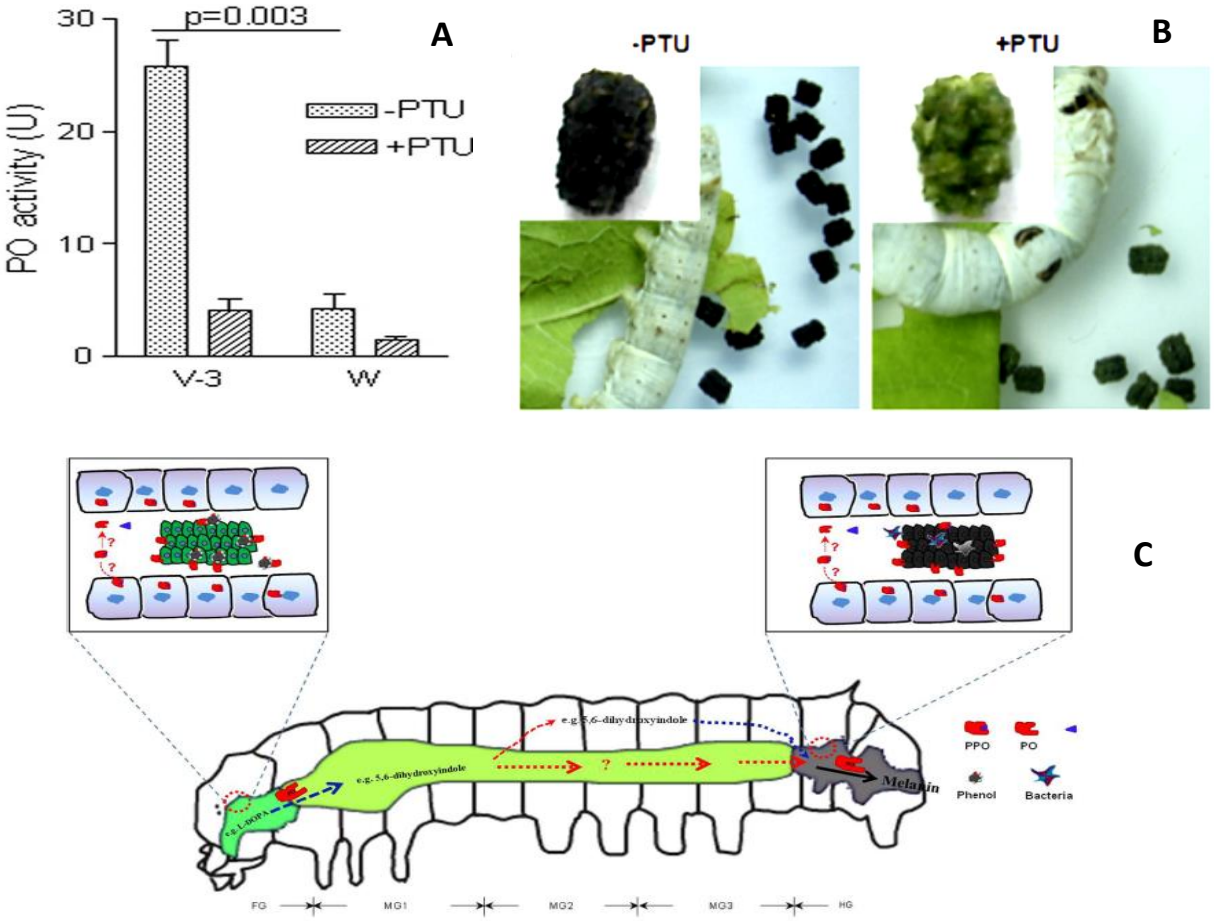

Fig. 6. Melanization of silkworm feces is inhibited by the PO inhibitor PTU. A) PO activity during the feeding stage (V-3) and wandering stage of silkworm larvae is inhibited by a PPO inhibitor (PTU). C) melanisation occurs in the last part of the intestinal tract were pro-phenoloxidases (PPO) secreted in the foregut are activated to PO: feces excreted by PTU-fed silkworm larvae were green. From Shao et al. (2012) and Wu et al. (2015).

The quantity and variety of reactive molecules is also concomitantly enhanced, increasing the number of possible reaction products. Gut microflora may contribute to enrich feces with fungal and bacterial metabolites. Locust fecal pellets for instance contain guaiacol produced from decarboxylation of vanillic acid carried out by gut saprophytes. But insects themselves may contribute: among the pheromones of locusts are phenolic compounds released from their feces (Obeng-Ofori et al., 1994).

6. The problem of molecular weights

The extremely diverse polydisperse mixture of randomly generated molecules, spanning from simple intramolecularly bonded products of the spontaneous oxidation of polyphenols to partly

443 hydrolysed condensation reactions products of adducts between proteins and tannins must, by force,
444 be characterized by a relatively wide range of possible molecular weights. Unfortunately, in many
445 official definitions HS are still described as “large molecules”, and this poorly accurate affirmation
446 has become one of the recurrent arguments put forward against the “classic humification model”. A
447 quick review of the current literature, however, highlights the tendency of most scientists to be,
448 conversely, in favour of the exclusive presence in HS of small molecules, eventually forming
449 supramolecular associations (Sutton and Sposito, 2005; Šmejkalová and Piccolo, 2008). Olk et al.
450 (2019b) concluded that the molecular size of HS is generally much less than thought by Stevenson
451 (1994) and others of his era.

452 FA and aquatic HS, for instance, have low molecular weights (number average molecular
453 weights between 545 and 1630 Da) and do not comprise large molecules (Chin et al., 1994). The
454 positive-ion ESI FTICR broadband mass spectrum of FA from the Suwannee River yielded molecular
455 ions in the range between 316 and 1098 Da (Stenson et al., 2003); However, one should bear in mind
456 the limitation of the procedure, especially the fact that less than 5–10% of the sample pass the
457 chromatography column and reach the spectrometry analysis (see discussion below).

458 Overestimation and underestimation of molecular sizes of HS has occurred in the past because
459 of improper use of size exclusion chromatography and/or misunderstanding of the implications
460 involved in the application of separation techniques to polydisperse mixtures (De Nobili and Chen,
461 1999). The determination of molecular weights on a mixture with a large number of components,
462 generates either number average (M_n) or weight average (M_w) molecular weights. Using techniques
463 that give Mn average molecular weights, such as those based on colligative properties or
464 concentration mediated measurements, the response is biased towards low molecular weights
465 (Perminova et al., 2003). For instance, average M_n of peat and soil HA measured by size exclusion
466 chromatography (SEC), range respectively from 6.4 to 7 kDa but, average Mw range between 18 and
467 19.2 kDa. The outcome is mediated by the type of detector used: a UV-vis detector, whose response
468 is number of molecules dependent, will produce a different MW than a DOC detector, whose response

469 is based on the total number of dissolved carbon atoms, irrespectively from whether they are
470 contained in a single molecule or in several smaller ones. Another frequently overlooked problem is
471 the fact that SEC columns need to be calibrated in order to provide meaningful indications on the
472 absolute molecular size of molecules. A proper set of standards of the same kind of molecules should
473 be employed to this purpose because shape, charge density and hydration, contribute to the exclusion
474 effect that is at the base of the separation. This is not possible for HS and therefore the molecular
475 weights obtained by SEC should be always regarded as apparent (De Nobili and Chen, 1999).

476 The problem is complex and in the future we need to avoid any over-simplification. The actual
477 molecular size range of HS has been under debate for many years and still is. Evidence for
478 predominance of small molecular sizes is nowadays supported the most advanced techniques, as for
479 instance Fourier transform ion cyclotron resonance electrospray ionization (ESI) mass spectrometry.
480 The first step in the analysis is the formation of gas-phase ions to be selectively separated by the mass
481 analyser and, in ESI, efficiency of ion formation is deeply influenced by both sample composition
482 and preparation and experimental conditions (Piccolo et al., 2010). Applying Fourier transform ion
483 cyclotron resonance mass spectrometry (FT–ICR–MS) to a steam-exploded lignin from wheat straw
484 (D'Auria et al., 2012), did not allow to isolate fragments with a mass higher than 4534 g mol^{-1}, in
485 spite of the fact that analysis by SEC gave for the same sample a Mn and Mw of respectively 6175
486 and 28302 g mol^{-1}. It should also be noted that a certain fraction of the analyzed material reaches the
487 spectrometer in a double or triple charged state: the measured Mw of these ions should be multiplied
488 by 2 or 3, thereby exhibiting molecular weights of 2000–2500 g mol^{-1} multiplied by 2 or 3, providing
489 Mw weights of up to 7500 g mol^{-1}.

490 Some aliphatic carboxyl rich molecules do not ionize well in either positive- or negative ion
491 mode ESI or are incapable of acquiring sufficient charge to be detected such as high-MW lignin
492 degradation products (Grinhut et al., 2011) are not likely to be detected. In addition, a strong limit of
493 the validity of the MWs obtained by this technique stems from the fact that these analyses represent
494 most commonly less than 5% of the sample, while 95% of the of it are usually adsorbed on the

beginning sections of the chromatography column. This fact results in a heavy bias of the analyses towards low MWs. These two issues need to be addressed to ensure that the results obtained are properly representing distribution of MWs of the HS samples.

Although modern techniques seem to suggest that HS are relatively small, the existence of large HS molecules cannot be reasonably rejected. Spontaneous abiotic non catalysed oxidation of tannins is accompanied by polymerization and occurs at 25°C by simple exposure of these substances to atmospheric oxygen. As shown by thiolysis (depolymerization followed by HPLC analysis) and small angle X-ray scattering (SAXS), upon oxidation the MW of tannins increases indicating formation of intermolecular bonds (Poncet-Legrand et al. 2010). HS themselves can react and polymerize under the action of laccases (Cozzolino and Piccolo, 2002).

The degradation of lignin, albeit much more rapid than previously believed, is still, under field conditions, a lengthy process (Rasse et al., 2006; Bahri et al., 2008). We must not forget than most modern degradation studies, which show rapid decomposition rates, are actually carried out on solubilized lignins and not on wood pieces and fragmented plant residues as in the natural environment. The degradation of a piece of wood in a forest takes place through a complex food web, which often starts with a passage through the alkaline gut of wood feeding insects, where optimal environmental conditions are inevitably associated with the presence of specialized microbial communities which provide the necessary enzymes (Geib et al., 2008). Many of these enzymes belong to the classes described in the previous paragraphs. Even *in vitro*, oxidation of lignin by peroxidase is not just a straightforward exclusive release of simple hydrolysis products, but a complex process that results in the concomitant formation of brown large molecular weight adducts (Fig.4).

Polymerization as a central feature during laccase oxidation of lignin moieties has also been reported (Hüttermann et al., 1980; Elegir et al., 2007). As indicated earlier by Karhunen et al. (1990a, 1990b), the radicals generated by laccases undergo resonance stabilization forming different mesomeric forms that couple via intermolecular bonds forming polymers of different sizes. The increase in MW is accompanied by a decrease in phenolic groups and carboxylic groups. Several

authors have observed a similar decrease in phenolic groups (Buchert et al., 2002; Rittstieg et al., 2002; Grönqvist et al., 2005; Shleev et al., 2006). The structure of lignin is not linear, but a three-dimensional network of different types of bonds. Enzymatic hydrolysis, being fundamentally based on an uncontrolled radical attack, is not unlikely to cause concomitant detachment of partially oxidized, relatively large, structurally complex reactive fragments. Their coupling with nucleophilic groups is indeed catalyzed by the same enzymes that implement the decomposition of lignified tissues. Lignin oxidation by laccases is in fact accompanied by production of resonance stabilized radicals that easily form inter-molecular bonds and give adducts of different sizes.

The products obtained from simple phenols by oxidative coupling in the presence of laccase are not only dimers and oligomers but even macromolecular products (Sun et al. 2013).

Aliphatic polycarboxylic residues are among the likely products derived from lignin decomposition and these fragments too can be incorporated, via radical reactions into secondary synthesis products. For example, a poly(phenylenoxide) with number average molecular weight up to 18 000 was obtained from a laccase-catalyzed oxidative polymerization of syringic acid in 24h at pH 5 (Ikeda et al., 1996).

Formation of large HS molecules is therefore possible, but this process is counteracted by the action of the same enzymes that contribute to their formation and can result in bleaching and depolymerization of HS (Grinhut et al., 2011, Zavarzina et al., 2018).

7. Complementarity of current SOM models

The fate of organic inputs to soil is complex and has been successfully approached from many points of view, which apparently exclude each other, but nonetheless are all necessary to describe the intricacy of effecting factors and outcomes.

The holistic modelling approach, based on the division of the systems in pools and the measurement of fluxes linking these pools, has probably been so far the most efficient in terms of

enabling a remarkably reliable quantitative prediction of organic C decomposition and sequestration in soil. To this purpose, evolution of CO_2 from soil is considered a proxy of biological activity with respect to the C cycle and ammonification that of the N cycle. This approach considers soil microbial biomass as a single "black box" compartment, assuming a uniform common behaviour of the soil microbial community in all soils. This assumption is based on a large amount of experimental evidence that showed how the soil microbial biomass, unless under stress from lack of moisture or oxygen availability, displays, not only the same state of metabolic alertness in all soils, having an adenylate energy charge (AEC) of 0.8 and an ATP concentration of 11 mg kg^{-1} (Contin et al., 2001), but also very close SOM decomposition patterns (Jenkinson and Anayaba, 1977).

Unless heavily contaminated, soil microbial communities normally do not display any specific lack of functionality. Even if they may be not actively functioning, any functionality can be easily induced when the specific substrate, or even a similar one, is occasionally added to the soil. Although reductions in biodiversity have been detected in some cases, this does not really seem to have any effect on the rate of organic matter decomposition or on any specific step of biological transformation, as different species and even classes of microorganisms are able to perform the same function (Nannipieri et al., 2003). SOM decomposition is actually little affected by a drastic reduction in microbial biodiversity: in fact, soil fumigated with chloroform, with a much smaller microbial biomass than the corresponding non-fumigated soil (Domínguez-Mendoza et al., 2014) respires about the same amount of ^{14}C-CO_2 from labelled straw as the non-fumigated soil (Chanders et al., 2002).

At present, there is no strong evidence that the determination of the composition of microbial communities in soil might improve our capability to predict SOM decomposition or nutrient dynamics in the long term (Hirsch et al., 2009). Indeed, iterate validations of soil organic C models against long term experiments have successfully demonstrated that turnover of soil organic C can be predicted assuming a single homogeneous behaviour of the soil microbial community in widely different soils (Jones et al., 2005).

Another view, consolidated by a huge number of studies deems that all components of plant residues are eventually completely decomposed in soil within a relatively short term and therefore considers physical protection as the main affecting factor of mineralization (Torn et al., 1997; Six et al., 2002; Kalbitz et al., 2005). Surface sorption and occlusion into microaggregates are the basic mechanisms by which solubility of molecules, which could be directly taken up by microorganisms, becomes limited and readily hydrolizable substrates are made unaccessible to enzymes. In this way the concentration of DOM is indeed regulated by iron oxides surface area and silt plus clay particles content of a soil may determine the potential limit of C sequestration. Yet HS rich surface layers often form in forest soils even in the absence of the formation of organo-mineral complexes (Zanella et al., 2011; Zanella et al., 2018b). Other constraints to microbiological activity therefore must concur to allow for the formation of holorganic or prevalently organic layers. One of the possible factors is the acquisition of recalcitrance through formation of molecular structures possessing different types of chemical bonds and requiring the combined action of more than one enzyme to be hydrolyzed, while at the same time yielding little energy in return for their decomposition. A fitting example of this kind of molecule is again provided by the structure shown in Fig. 7. Recalcitrance does not imply impossibility of decomposition, but only that microorganisms, given the chance, would eventually prefer to decompose other more energetically convenient substrates.

To consider physical protection as the only cause of C sequestration in soils is prejudiced by studies on cultivated mineral soils, where mineralization is exacerbated by agricultural practices and physical protection, favored by tillage, is indeed the main process governing preservation of SOM.

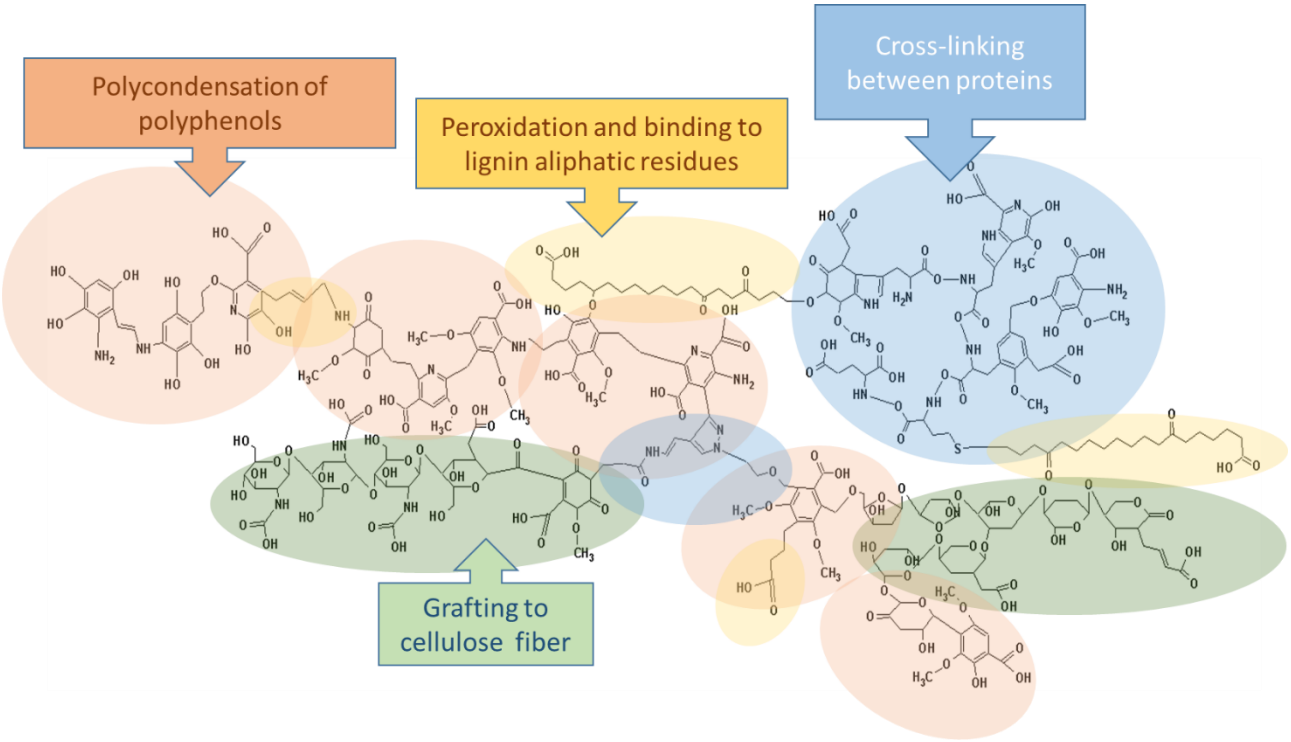

Fig. 7. Proposed macromolecular structure of a soil humic acid (HA) based on the following common characteristics: MW: 6386 Da. Elemental analysis (%) C: 53.9; N: 5.0-; H: 5.8; O: 35.1; S: 0.5. C/N: 10.7. Functional groups (cmol g^{-1}): carboxyl: 376; phenol: 188; total acidity: 564. Distribution of C% based on NMR analyses: aliphatic: 18.1; aromatic: 20.9; carbohydrates: 23.7; methoxy: 4.9; carboxylic: 8.4; keton: 4.5; phenolic: 4.2; other groups: 15.3 (Stevenson, 1994). The molecule displays the random occurrence of structures and chemical bonds expected from the reaction of PO generated radicals with a variety of SOM components.

This review shows that ample justification for the classical humification theory can be independently derived from other disciplines, that prove that re-synthesis of new complex molecules from simple plant tissues components occurs spontaneously under conditions that are normal in soil. Re-synthesis of HS is not driven by specific biological needs and does not require energy inputs. The inherent natural reactivity of small size intermediate products of decomposition and residual activity of extracellular enzymes concur to transform plant and microbial metabolites into a brown polydisperse complex mixture which, because of its innate structural complexity is less easily attacked by hydrolytic enzymes and yields a lower energy gain to decomposing microorganisms. A more recalcitrant, albeit not completely un-decomposable fraction of SOM: in one word, HS.

All current different approaches to SOM have so far fruitfully contributed to highlight different coexisting aspects of the complexity of SOM nature and dynamics. Alone, however, each of them provides just a partial overview of effecting factors and processes that contribute not only to

610 C sequestration, but ultimately to all aspects related to soil fertility, sustainability of terrestrial
611 ecosystems and contaminants fate. There is certainly a need for a unifying theory to bring together
612 all contributions into a single holistic view, but not of wishful oversimplification. One day, an all-
613 encompassing, coherent theoretical framework, some kind of SOM Theory of Everything, will
614 eventually stem from all this information, but at present we still know too little on this extremely
615 complex issue. Till that day, an open minded, humble attitude, that does not exclude contribution
616 from all types of approach, should be maintained to ease the progress of science.

617 The SCM theory might very well "facilitate communication among disciplines and the public"
618 as claimed by the authors, but this cannot be considered in itself proof of validity or reason for
619 preference in science. As a slightly misquoted, but frequently cited aphorism by H.L. Mencken says:
620 "*For every complex problem there is an answer that is clear, simple, and wrong*".
621

622 **8. Conclusions**

623 The assumption that plant and microbial metabolites will stay on in soil, without reacting, to
624 form the bulk of SOM has to be rejected, considering the enormous amount of scientific literature
625 that proves their high reactivity.

626 The secondary synthesis of humic substances does not require energy investments. We have
627 amply demonstrated in this review that what is required is simply the ubiquitous presence and
628 uncontrolled spontaneous action of enzymes that are commonly present in plant tissues and produced
629 by soil microorganisms for their own specific metabolic reasons. Even the capability of oxidized
630 phenols to undergo spontaneous abiotic oxidative coupling with other organic substrates may very
631 well lead, in itself, to the formation of molecular structures which were not originally present in plant,
632 animal or microbial residues and which are typically found in soil, but also in freshwater, oceans and
633 even aerosols: again, in one word, HS.

The passage of plant residues through the digestive tract of insects naturally exposes them to alkaline pH conditions, increasing at the same time the contact with enzymes. This represents not only an under esteemed contribution to the formation of HS, but also proof that alkaline extractants may not be as extraneous to natural conditions, as recurrently suggested.

The nature of SOM, if we acknowledge its complexity and consider the ample evidence collected by independent disciplines on the reactivity of its components, is not only non-controversial but, on the contrary, highly substantiated by new scientific evidence supporting the classic view of humification.

642 **References**

643 Adams, A., V. Kitrytė, R. Venskutonis, and N. De Kimpe. 2009. Formation and
644 characterisation of melanoidin-like polycondensation products from amino acids and lipid oxidation
645 products. Food Chem. 115:904–911.

646 Albers, C.N., G.T. Banta, O.S. Jacobsen, and P.E. Hansen. 2008. Characterization and
647 structural modelling of humic substances in field soil displaying significant differences from
648 previously proposed structures. Eur. J. Soil Sci. 59:693–705.

649 Allison, S.D. 2006. Brown ground: A soil carbon analogue for the green world hypothesis?
650 Am. Nat. 167:619–627.

651 Almendros, G., P. Tinoco, J.M. De la Rosa, H. Knicker, J.A. González-Pérez, and F.J.
652 González-Vila. 2018. Selective effects of forest fires on the structural domains of soil humic acids as
653 shown by dipolar dephasing ^{13}C NMR and graphical-statistical analysis of pyrolysis compounds. J
654 Soils Sediments 18(4):1303–1313.

655 Appel, H.M. 1994. The chewing herbivore gut lumen: Physicochemical conditions and their
656 impact on plant nutrients, allelochemicals and insect pathogens. In: E.A. Bernays, editor, Insect-plant
657 interactions. Vol. 5. CRC Press, Boca Raton, FL. p. 209–221.

658 Avneri-Katz, S., R.B. Young, A.M. McKenna, H. Chen, Y.E. Corilo, T. Polubesova, T. Borch,
659 and B. Chefetz. 2017. Adsorptive fractionation of dissolved organic matter (DOM) by mineral soil:
660 Macroscale approach and molecular insight. Org. Geochem. 103:113–124.

661 Ba, S., and V.V. Kumar. 2017. Recent developments in the use of tyrosinase and laccase in
662 environmental applications. Crit. Rev. Biotechnol. 37(7):819–832.

663 Bahri, H., D.P. Rasse, C. Rumpel, M.-F. Dignac, G. Bardoux, and A. Mariotti. 2008. Lignin
664 degradation during a laboratory incubation followed by ^{13}C isotope analysis. Soil Biol. Biochem.
665 40:1916–1922.

666 Baldrian, P. 2006. Fungal laccases – occurrence and properties. FEMS Microbiol. Rev.
667 30(2):215–242.

668 Baldrian, P., and J. Šnajdr. 2011. Lignocellulose-degrading enzymes in soils. In: G. Shukla
669 and A. Varma, editors, Soil enzymology, Soil Biology Book Ser. 22. Springer, Heidelberg. p. 167–
670 186.
671 Baxter, N.J., T.H. Lilley, E. Haslam, and M.P. Williamson. 1997. Multiple interactions
672 between polyphenols and a salivary proline-rich protein repeat result in complexation and
673 precipitation. Biochemistry 36:5566–5577.
674 Bell, N.G.A, A.A.L. Michalchuk, J.W.T. Blackburn, M.C. Graham, and D. Uhrín. 2015.
675 Isotope-filtered 4D NMR spectroscopy for structure determination of humic substances. Angew.
676 Chem. Int. Edit. 54:8382–8385.
677 Bell, N.G.A., L. Murray, M.C. Graham, and D. Uhrín. 2014. NMR methodology for complex
678 mixture 'separation'. Chem. Commun. 50:1694–1697.
679 Beveridge, T., and R.E. Wrolstad. 1997. Haze and cloud in apple juices. Crit. Rev. Food Sci.
680 37(1):75–91.
681 Bignell, D.E., and P. Eggleton. 1995. On the elevated intestinal pH of higher termites
682 (Isoptera: Termitidae). Ins. Soc. 42:57–69.
683 Bremner, J.M. 1949. Studies on soil organic matter: Part III. The extraction of organic carbon
684 and nitrogen from soil. J. Agric. Sci. 39:280–282.
685 Buchert, J., A. Mustranta, T. Tamminen, P. Spetz and B. Holmbom. 2002. Modification of
686 spruce lignans with *Trametes hirsuta* laccase. Holzforschung 56:579–584.
687 Cañas A.I., and S. Camarero. 2010. Laccases and their natural mediators: Biotechnological
688 tools for sustainable eco-friendly processes. Biotechnol. Adv. 28:694–705.
689 Cao, X., and K. Schmidt-Rohr. 2018. Abundant nonprotonated aromatic and oxygen-bonded
690 carbons make humic substances distinct from biopolymers. Environ. Sci. Technol. Lett. 5:476–480.
691 Cesco S., T. Mimmo, G. Tonon, N. Tomasi, R. Pinton, R. Terzano, G. Neumann, L.
692 Weisskopf, G. Renella, L. Landi, and P. Nannipieri. 2012. Plant-borne flavonoids released into the

693 rhizosphere: impact on soil bio-activities related to plant nutrition. A review. Biol. Fertil. Soils.
694 48:123–149.

695 Chander, K., T. Klein, U. Eberhardt, and R. Joergensen. 2002. Decomposition of carbon-14-
696 labelled wheat straw in repeatedly fumigated and non-fumigated soils with different levels of heavy
697 metal contamination. Biol. Fert. Soils 35:86–91.

698 Chaurasia, P.K., R.S.S. Yadav, and S. Yadava. 2013. A review on mechanism of laccase
699 action. Res. Rev BioSci. 7(2):66–71.

700 Chefetz, B., Y. Hadar, and Y. Chen. 1998a. Dissolved organic carbon fractions formed during
701 composting of municipal solid waste: properties and significance. Acta Hydrochim. Hydrobiol.
702 26:172–179.

703 Chefetz, B., P.G. Hatcher, Y. Hadar, and Y. Chen. 1998b. Characterization of dissolved
704 organic matter extracted from composted municipal solid waste. Soil Sci. Soc. Am. J. 62:326–332.

705 Chen Y.M., T.M. Tsao, C.C. Liu, P.M. Huang, and M.K. Wang. 2010. Polymerization of
706 catechin catalyzed by Mn-, Fe-and Al-oxides. Colloid. Surface. B. 81:217–223.

707 Cheng, G.W., and C.H. Crisosto. 1997. Iron-polyphenol complex formation and skin
708 discoloration in peaches and nectarines. J. Amer. Soc. Hort. Sci. 122:95–99.

709 Chin, Y.P., G. Aiken, and E. O'Loughlin. 1994. Molecular weight, polydispersity, and
710 spectroscopic properties of aquatic humic substances. Environ. Sci. Technol. 28(11):1853–1858.

711 Chou, T., M. Yang, S. Tseng, S.Lee, and C. Chang. 2018.Tea silkworm droppings as an
712 enriched source of tea flavonoids. J Food Drug Anal. 26(1):41–46.

713 Choudhri, M.B., and F.J. Stevenson. 1957. Chemical and physicochemical properties of soil
714 humic colloids: III. Extraction of organic matter from soils. Soil Sci. Soc. Am. J. 21:508–513.

715 Ćirić-Marjanović, G., M. Milojević-Rakić, A. Janošević-Ležaić, S. Luginbühl, and P. Walde.
716 2017. Enzymatic oligomerization and polymerization of arylamines: State of the art and perspectives.
717 Chem. Pap. 71(2):199–242.

718 Clark, T.M. 1999. Evolution and adaptive significance of larval midgut alkalinization in the
719 insect superorder Mecopterida. J. Chem. Ecol. 25(8):1945–60.
720 Contin M., A. Todd, and P.C. Brookes. 2001. The ATP concentrations in the soil microbial
721 biomass. Soil Biol. Biochem. 33:701–704.
722 Cozzolino, A., and A. Piccolo. Polymerization of dissolved humic substances catalyzed by
723 peroxidase. Effects of pH and humic composition. 2002. Org. Geochem. 33:281–294.
724 Criquet, S., S. Tagger, G. Vogt, G. Iacazio, and J. Le Petit. 1999. Laccase activity of forest
725 litter. Soil Biol. Biochem. 31:1239–1244.
726 Curtin, D., M.E. Peterson, and C.R. Anderson. 2016. pH-dependence of organic matter
727 solubility: Base type effects on dissolved organic C, N, P, and S in soils with contrasting mineralogy.
728 Geoderma 27:161–172.
729 D'Auria M., L. Emanuele, and R. Racioppi. 2012. FT–ICR–MS analysis of lignin. Nat. Prod.
730 Res. 26(15):1368–1374.
731 De Nobili, M., and Y. Chen. 1999. Size exclusion chromatography of humic substances:
732 Limits, perspectives and prospectives. Soil Sci. 164(11):825–833.
733 Dec, J., K. Haider, and J.M. Bollag. 2003. Release of substituents from phenolic compounds
734 during oxidative coupling reactions. Chemosphere 52(3):549–556.
735 Devasia S. and A. Jayakumaran Nair. 2016. Screening of potent laccase producing organisms
736 based on the oxidation pattern of different phenolic substrates Int.J.Curr.Microbiol.App.Sci. 5(5):
737 127-137.
738 Di Donato, N., H. Chen, D. Waggoner, and P.G. Hatcher. 2016. Potential origin and formation
739 for molecular components of humic acids in soils. Geochim. Cosmochim. Acta 178:210–222.
740 Dick, D.P., and P. Burba. 1999. Extraction kinetics and molecular size fractionation of humic
741 substances from two Brazilian soils. J. Braz. Chem. Soc. 10(2):146–152.
742 Dillon, R.J., and V.M. Dillon. 2004. The gut bacteria of insects: Nonpathogenic interactions.
743 Annu. Rev. Entomol. 49:71–92.

744 D'Imporzano, G., and F. Adani. 2007. The contribution of water soluble and water insoluble
745 organic fractions to oxygen uptake rate during high rate composting. Biodegradation 18:103–113.
746 Domínguez-Mendoza, C.A., J.M. Bello-López, Y.E. Navarro-Noya, A.S. de León-Lorenzana,
747 L. Delgado-Balbuena, S. Gómez-Acata, V.M. Ruíz-Valdiviezo, D.A. Ramirez-Villanueva, M. Luna-
748 Guido, and L. Dendooven. 2014. Bacterial community structure in fumigated soil. Soil Biol.
749 Biochem. 73:122–129.
750 Eichlerová, I., J. Šnajdr, and P. Baldrian. 2012. Laccase activity in soils: considerations for
751 the measurement of enzyme activity. Chemosphere 88:1154–1160.
752 Elegir, G., D. Bussini, S. Antonsson, M.E. Lindström, and L. Zoia. 2007. Appl. Microbiol.
753 Biotechnol. 77:809-817.
754 Evans, L.T. 1959. The use of chelating regents and alkaline solutions in soil organic matter
755 extractions. Eur. J. Soil Sci. 10(1):110–118.
756 Friedman, M. 1996. Food browning and its prevention: an overview. J. Agric. Food Chem.
757 44(3):631–653.
758 Fukuchi, S., A. Miura, R. Okabe, M. Fukushima, M. Sasaki, and T. Sato. 2010. Spectroscopic
759 investigations of humic-like acids formed via polycondensation reactions between glycine, catechol
760 and glucose in the presence of natural zeolites. J. Mol. Struct. 982:181–186.
761 García, C.J., R. García-Villalba, M.I. Gil, and F.A. Tomas-Barberan. 2017. LC-MS untargeted
762 metabolomics to explain the signal metabolites inducing browning in fresh-cut lettuce. J. Agric. Food
763 Chem. 65(22):4526–4535.
764 Geib S. M., T. R. Filley, P. G. Hatcher, K. Hoover J. E. Carlson, M. del Mar Jimenez-Gasco
765 A. Nakagawa-Izumi R. L. Sleighter, Ming Tien (2008) Lignin degradation in wood-feeding insects.
766 Proc. of the Nat. Ac. of Sci. 105, 12932–12937
767 Grinhut, T., N. Hertkorn, P. Schmitt-Kopplin, Y. Hadar, and Y. Chen. 2011. Mechanisms of
768 humic acids degradation by white rot fungi explored using ^{1}H NMR spectroscopy and FTICR mass
769 spectrometry. Environ. Sci. Technol. 45(7):2748–2754.

770 Grönqvist, S., L. Viikari, M.L. Niku-Paavola, M. Orlandi, C. Canevali, and J. Buchert. 2005.
771 Oxidation of milled wood lignin with laccase, tyrosinase and horseradish peroxidase. App. Microbiol.
772 Biotechnol., 67:489–494.
773 Hagerman, A.E. 2012. Fifty years of polyphenol-protein complexes. In: V. Cheynier, P. Sarni-
774 Manchado and S. Quideau, editors, Recent advances in polyphenol research. Wiley-Blackwell,
775 Oxford, UK. p. 71–97.
776 Hayes, M.H.B., and C.E. Clapp. 2001. Humic substances: considerations of compositions,
777 aspects of structure, and environmental influences. Soil Sci. 166(11):723–737.
778 Hayes, M.H.B., R.S. Swift, R.E. Wardle, and J.K Brown. 1975. Humic materials from an
779 organic soil: A comparison of extractants and of properties of extracts. Geoderma 13:231–245.
780 Hidalgo, F.J., and R. Zamora. 2000. The role of lipids in nonenzymatic browning. Grasas
781 Aceites 51:35–49.
782 Hirsch, P.R., L.M. Gilliam, S.P. Sohi, J.K. Williams, I.M. Clark, and P.J. Murray. 2009.
783 Starving the soil of plant inputs for 50 years reduces abundance but not diversity of soil bacterial
784 communities. Soil Biol. Biochem. 41:2021–2024.
785 Hofrichter, M. 2002. Review: lignin conversion by manganese peroxidase (MnP). Enzyme
786 Microb Tech. 30 454–466.
787 Huang, P.M., and A.G. Hardie. 2009. Formation mechanisms of humic substances in the
788 environment. In: N. Senesi, B. Xing and P.M. Huang, editors, Biophysico-chemical processes
789 involving natural nonliving organic matter in environmental systems. John Wiley & Sons, Hoboken,
790 NJ. p. 41–109.
791 Hurrell, R.F., and P.A. Finot. 1985. Effects of food processing on protein digestibility and
792 amino acid availability. In: J.W. Finley, and D.T. Hopkins, editors, Digestibility and amino acid
793 availability in cereals and oilseeds. American Association of Cereal Chemists, St. Paul, Minnesota.
794 p. 233–246.

Hüttermann, A., C. Herche, and A. Haars. 1980. Polymerisation of water-insoluble lignins by *Fomes annosus*. Holzforschung 34:64-66.

Ikeya, K., R.L. Sleighter, P.G. Hatcher, and A. Watanabe. 2015. Characterization of the chemical composition of soil humic acids using Fourier transform ion cyclotron resonance mass spectrometry. Geochim. Cosmochim. Ac. 153:169–182.

Jardine, P. M., J. F. McCarthy, and N. L. Weber. 1989. Mechanisms of Dissolved Organic Carbon Adsorption on Soil. Soil Sci. Soc. Am. J. 53:1378-1385.

Jenkinson, D.S., and A. Ayanaba. 1977. Decomposition of carbon-14 labeled plant material under tropical conditions. Soil Sci. Soc. Am. J. 41:912–915.

Johnson, K.S., and R.V. Barbehenn. 2000. Oxygen levels in the gut lumens of herbivorous insects. J. Insect Physiol. 46:897–903.

Jones, C., C. McConnell, K. Coleman, P. Cox, P. Falloon, D. Jenkinson, and D Powlson. 2005. Global climate change and soil carbon stocks; predictions from two contrasting models for the turnover of organic carbon in soil. Glob. Change Biol. 11:154–166.

Kaiser, K., and G. Guggenberger. 2000. The role of DOM sorption to mineral surfaces in the preservation of organic matter in soils. Org. Geochem. 31:711–725.

Kaiser, K., and W. Zech. 1997. Competitive sorption of dissolved organic matter fractions to soils and related mineral phases. Soil Sci. Soc. Am. J. 61:64–69.

Kalbitz, K., D. Schwesig, J. Rethemeyer, and E. Matzner. 2005. Stabilization of dissolved organic matter by sorption to the mineral soil. Soil Biol. Biochem. 37:1319–1331.

Karhunen, E., A. Kantelinen, and M.L. Niku-Paavola. 1990a. Mn-dependent peroxidase from the lignin-degrading white rot fungus *Phlebia radiata*. Arch. Biochem. Biophys. 279(1):25–31.

Karhunen, E., M.L. Niku-Paavola, L. Viikari, T. Haltia, R.A. van der Meer, and J.A. Duine. 1990b. A novel combination of prosthetic groups in a fungal laccase; PQQ and two copper atoms. FEBS Lett. 267(1):6–8.

820 Kelleher, B.P., and A.J. Simpson. 2006. Humic substances in soils: are they really chemically
821 distinct? Environ. Sci. Technol. 40(15):4605–4611.
822 Kellner, H., P. Luis, M.J. Pecyna, F. Barbi, D. Kapturska, D. Krüger, D.R. Zak, R. Marmeisse,
823 M. Vandenbol, and M. Hofrichter. 2014. Widespread occurrence of expressed fungal secretory
824 peroxidases in forest soils. Plos One 9:1–9.
825 Khan, M.A., K. Ueno, S. Horimoto, F. Komai, T. Someya, K. Inoue, K. Tanaka, and Y. Ono.
826 2009. CIELAB color variables as indicators of compost stability. Waste Manag. 29:2969–2975.
827 Kleber M., and J. Lehmann. 2019. Humic substances extracted by alkali are invalid proxies
828 for the dynamics and functions of organic matter in terrestrial and aquatic ecosystems. J. Environ.
829 Qual. 48:207–216.
830 Knicker, H., S. Lange, B. van Rossum, and H. Oschkinat. 2016. Dynamic Nuclear Polarization
831 (DNP) solid-state NMR spectroscopy, a new approach to study humic material? Geophysical
832 Research Abstracts. 18, EGU2016–8235.
833 Kroll, J., and H.M. Rawel. 2001. Reactions of plant phenols with myoglobin: Influence of
834 chemical structure of the phenolic compounds. J. Food Sci. 66:48–58.
835 Lagrimini, L.M. 1991. Wound-induced deposition of polyphenols in transgenic plants
836 overexpressing peroxidase. Plant Physiol. 96(2):577–583.
837 Lattanzio, V. 2003. Bioactive polyphenols: their role in quality and storability of fruit and
838 vegetables. J. Appl. Bot-Angew. Bot. 77:128–146.
839 Lehmann, J., and M. Kleber. 2015. The contentious nature of soil organic matter. Nature
840 528:61–68.
841 Leinemann, T., S. Preusser, R. Mikutta, K. Kalbitz, C. Cerli, C. Höschen, C.W. Mueller, E.
842 Kandeler, and G. Guggenberger. 2018. Multiple exchange processes on mineral surfaces control the
843 transport of dissolved organic matter through soil profiles. Soil Biol. Biochem. 118:79–90.

844 Lemke, T., U. Stingl, M. Egert, M.W. Friedrich, and A. Brune. 2003. Physicochemical
845 conditions and microbial activities in the highly alkaline gut of the humus-feeding larva of *Pachnoda*
846 *ephippiata* (Coleoptera: Scarabaeidae) Appl. Environ. Microbiol. 69(11):6650–6658.
847 Li, H., A. Guo, and H. Wang. 2008. Mechanisms of oxidative browning of wine. Food Chem.
848 108:1–13.
849 Lin, X., and D.W. Su. 2019. Research advances in browning of button mushroom (*Agaricus*
850 *bisporus*): Affecting factors and controlling methods. Trends Food Sci. Tech. 90:63–75.
851 Liers, C., T. Arnstadt, R. Ullrich, and M. Hofrichter. 2011. Patterns of lignin degradation and
852 oxidative enzyme secretion by different wood- and litter-colonizing basidiomycetes and ascomycetes
853 grown on beech-wood. FEMS Microbiol. Ecol. 78:91–102.
854 Luis, P., G. Walther, H. Kellner, F. Martin, and F. Buscot. 2004. Diversity of laccase genes
855 from basidiomycetes in a forest soil. Soil Biol. Biochem. 36:1025-1036.
856 Lundell, T.K., M.R. Mäkelä, and K. Hildén. 2010. Lignin-modifying enzymes in filamentous
857 basidiomycetes - ecological, functional and phylogenetic review. J Basic Microb. 50:5–20.
858 Martin, A.E., and R. Reeve. 1957. Chemical studies on podzolic illuvial horizons I. The
859 extraction of organic matter by organic chelating agents. Eur. J. Soil Sci. 8(2):268–278.
860 Martinez, M.V., and J.R. Whitaker. 1995. The biochemistry and control of enzymatic
861 browning. Trends Food Sci. Tech. 6(6):195–200.
862 Mattinen, M.L., K. Kruus, J. Buchert, J.H. Nielsen, H.J. Andersen, and C.L. Steffensen. 2005.
863 Laccase-catalyzed polymerization of tyrosine-containing peptides FEBS J. 272(14):3640–3650.
864 Mikolasch, A., and F. Schauer. 2009. Fungal laccases as tools for the synthesis of new hybrid
865 molecules and biomaterials. Appl. Microbiol. Biotechnol. 82(4):605–624.
866 Mishra, B.B., and S. Gautam. 2016. Polyphenol oxidases: Biochemical and molecular
867 characterization, distribution, role and its control. Enz. Eng. 5(1):141–150.
868 Morozova, O.V., G.P. Shumakovich, S.V. Shleev, and Ya.I. Yaropolov. 2007 Laccase-
869 mediator systems and their applications: A review. Appl. Biochem. Micro+. 43(5):523–535.

Nagai M., Kawata M., Watanabe H., Ogawa M. K. Saito, T. Takesawa, K. Kanda and T. Sato (2003) Important role of fungal intracellular laccase for melanin synthesis: purification and characterization of an intracellular laccase from Lentinula edodes fruit bodies. Microbiology 149, 2455–2462.

Nannipieri, P., J. Asher, M.T. Ceccherini, L. Landi, G. Pietramellara, and G. Renella. 2003. Microbial diversity and soil functions. Eur. J. Soil Sci. 54:655–670.

Nicolas, J.J., F.C. Richard-Forget, P.M. Goupy, M.J. Amiot, and S.Y. Aubert. 1994. Enzymatic browning reactions in apple and apple products. Crit. Rev. Food Sci. Nutr. 34(2):109–157.

Obeng-Ofori, D., B. Torto, P.G. Njagi, A. Hassanali, and H. Amiani. 1994. Fecal volatiles as part of the aggregation pheromone complex of the desert locust, *Schistocerca gregaria* (Forskal) (Orthoptera: Acrididae). J. Chem. Ecol. 20:2077–87.

Okuda, A., and S. Hori. 1956. Some aspects on the nature of humic acid. J. Soil Sci. Plant Nutr. 2(1):42–43.

Olk D.C., P.R Bloom, M. De Nobili, Y. Chen, D. McKnight, M. Wells, and J. Weber. 2019a. Using humic fractions to understand natural organic matter processes in soil and water: selected studies and applications. J. Environ. Qual. doi:10.2134/jeq2019.03.0100.

Olk D.C., P.R. Bloom, E.M. Perdue, D.M. McKnight, Y. Chen, A. Farenhorst, N. Senesi, Y.-P. Chin, P. Schmitt-Kopplin, N. Hertkorn, and M. Harir. 2019b. Environmental and agricultural relevance of humic fractions extracted by alkali from soils and natural waters. J. Environ. Qual. 48:217–232.

Ortner, A., D. Huber, O. Haske-Cornelius, H.K. Weber, K. Hofer, W. Bauer, G.S. Nyanhongo, and G.M. Guebitz. 2015. Laccase mediated oxidation of industrial lignins: Is oxygen limiting? Process Biochem. 50:1277–1283.

Ozdal, T., E. Capanoglu, and F. Altay. 2013. A review on protein–phenolic interactions and associated changes. Food Res. Int. 51:954–970.

Pal, S., J.-M. Bollag, and P.M. Huang. 1994. Role of abiotic and biotic catalysts in the transformation of phenolic compounds through oxidative coupling reactions. Soil Biol. and Biochem. 26(7):813–820.

Perminova, I.V., F.H. Frimmel, A.V. Kudryavtsev, N.A. Kulikova, G. Abbt-Braun, S. Hesse, and V.S. Petrosyan. 2003. Molecular weight characteristics of humic substances from different environments as determined by size exclusion chromatography and their statistical evaluation. Environ. Sci. Technol. 37(11):2477–2485.

Piccolo, A. 1988. Characteristics of soil humic extracts obtained by organic and inorganic solvents and purified by HF/HCl. Soil Sci. 146(6):418–426.

Piccolo, A., M. Spiteller, and A. Nebbioso. 2010. Effects of sample properties and mass spectroscopic parameters on electrospray ionization mass spectra of size-fractions from a soil humic acid. Anal. Bioanal. Chem. 397:3071–3078.

Poncet-Legrand, C., B. Cabane, A.B. Bautista-Ortín, S. Carrillo, H. Fulcrand, J. Pérez, and A. Vernhet. 2010. Tannin oxidation: Intra- versus intermolecular reactions. Biomacromolecules 11:2376–2386.

Rasse, D.P., M.-F. Dignac, H. Bahri, C. Rumpel, A. Mariotti, and C. Chenu. 2006. Lignin turnover in an agricultural field: from plant residues to soil-protected fractions. Eur. J. Soil Sci. 57: 530–538.

Rawel, H., S. Rohn, and J. Kroll. 2000. Reactions of selected secondary plant metabolites (glucosinolates and phenols) with food proteins and enzymes: Influence on physico-chemical protein properties, enzyme activity and proteolytic degradation. In: S.G. Pandalai, editor, Recent Research Developments in Phytochemistry. Research Signpost, Trivandrum, India. p. 115–142.

Richard-Forget, F.C., and F.A. Gauillard. 1997. Oxidation of chlorogenic acid, catechins, and 4-methylcatechol in model solutions by combinations of pear (*Pyrus communis* cv Williams) polyphenol oxidase and peroxidase: A possible involvement of peroxidase in enzymatic browning. J. Agric. Food Chem. 45:2472–2476.

Rittstieg, K., A. Suurnakki, T. Suortti, K. Kruus, G. Guebitz, and J. Buchert. 2002. Investigations on the laccase-catalyzed polymerization of lignin model compounds using size-exclusion HPLC. Enzyme Microb. Tech. 31:403–410.

Riva, S. 2006. Laccases: blue enzymes for green chemistry. Trends Biotechnol. 24(5):219–226.

Robards, K., P.D. Prenzler, G. Tucker, P. Swatsitang, and W. Glover. 1999. Phenolic compounds and their role in oxidative processes in fruits. Food Chem. 66(4):401–436.

Rodríguez Couto, S., and J.L. Toca Herrera. 2006. Industrial and biotechnological applications of laccases: A review. Biotechnol. Adv. 24:500–513.

Said-Pullicino, D., and G. Gigliotti. 2007. Oxidative biodegradation of dissolved organic matter during composting. Chemosphere 68:1030–1040.

Shao, Q., B. Yang, Q. Xu, X. Li, Z. Lu, C. Wang, Y. Huang, K. Söderhäll, and E. Ling. 2012. Hindgut innate immunity and regulation of fecal microbiota through melanization in insects. J. Biol. Chem. 287:14270–14279.

Shleev, S., P. Persson, G. Shumakovich, Y. Mazhugo, A. Yaropolov, T. Ruzgas, and L. Gorton. 2006. Interaction of fungal laccases and laccase-mediator systems with lignin. Enzyme Microb. Tech. 39:841–847.

Slabbert, N. Complexation of condensed tannins with metal ions. In Plant Polyphenols; Springer, 1992; pp 421−436.

Šmejkalová, D., and A. Piccolo. 2008 Aggregation and disaggregation of humic supramolecular assemblies by NMR diffusion ordered spectroscopy (DOSY-NMR). Environ. Sci. Technol. 42(3):699–706.

Sinsabaugh, R.L. 2010. Phenol oxidase, peroxidase and organic matter dynamics of soil. Soil Biol. Biochem. 42:391–404.

Six, J., R.T. Conant, E.A. Paul, and K. Paustian. 2002 Stabilization mechanisms of soil organic matter: Implications for C-saturation of soils. Plant Soil 241:155–176.

948 Stenson, A.C., A.G. Marshall, and W.T. Cooper. 2003. Exact masses and chemical formulas
949 of individual Suwannee River fulvic acids from ultrahigh resolution electrospray ionization Fourier
950 transform ion cyclotron resonance mass spectra. Anal. Chem. 75:1275–1274.
951 Stevenson, F.J. 1994. Humus chemistry: Genesis, composition, reactions. 2nd ed. John Wiley
952 & Sons, New York.
953 Straathof, A.L., and R.N.J. Comans. 2015. Input materials and processing conditions control
954 compost dissolved organic carbon quality. Biores. Technol. 179:619–623.
955 Sugahara, K., Y. Harada, and A. Inoko. 1979. Color change of city refuse during composting
956 process. Soil Sci. Plant Nutr. 25:197-208.
957 Sun, X., R. Bai, Y. Zhang, Q. Wang, X. Fan, J. Yuan, L. Cui, and P. Wang. 2013. Laccase-
958 catalyzed oxidative polymerization of phenolic compounds. Appl. Biochem. Biotechnol. 171:1673–
959 1680.
960 Sutton, R., and G. Sposito. 2005. Molecular Structure in Soil Humic Substances: The New
961 View. Environ. Sci. Technol. 39(23):9009–9015.
962 Thalmann, C.R. and T. Lötzbeyer. 2002. Enzymatic cross-linking of proteins with tyrosinase.
963 Eur. Food Res. Technol. 214:276–281.
964 Tomas-Barberan, F.A., J. Loaiza-Velarde, A. Bonfanti, and M.E. Saltveit. 1997. Early wound-
965 and ethylene-induced changes in phenylpropanoid metabolism in harvested lettuce. J. Am. Soc.
966 Hortic. Sci. 122(3):399–404.
967 Torn, M.S., S.E. Trumbore, O.A. Chadwick, P.M. Vitousek, and D.M. Hendricks. 1997
968 Mineral control of soil organic carbon storage and turnover. Nature 389:170–173.
969 Witayakran, S., and A.J. Ragauskas. 2009. Synthetic applications of laccase in green
970 chemistry. Adv. Synth. Catal. 351:1187–1209.
971 Wolters, V. 2000. Invertebrate control of soil organic matter stability. Biol Fertil Soils. 31:1–
972 19.

973 Wong, D.W.S. 2009. Structure and action mechanism of ligninolytic enzymes. Appl.
974 Biochem. Biotechnol. 157:174–209.
975 Wu, K., J. Zhang, Q. Zhang, S. Zhu, Q. Shao, K.D. Clark, Y. Liu, and E. Ling. 2015. Plant
976 phenolics are detoxified by prophenoloxidase in the insect gut. Sci. Rep. 5(16823). doi:
977 10.1038/srep16823.
978 Yuant, T.L. 1964. Comparison of reagents for soil organic matter extraction and effect of pH
979 on subsequent separation of humic and fulvic acids. Soil Sci. 98(2):133–141.
980 Zanella, A., B. Jabiol, J.F. Ponge, G. Sartori, R. De Waal, B. Van Delft, U. Graefe, N. Cools,
981 K. Katzensteiner, H. Hager, and M. Englisch. 2011. A European morpho-functional classification of
982 humus forms. Geoderma 164:138–145.
983 Zanella, A., B. Berg, J. F. Ponge, and R. H. Kemmers (2018). Humusica 1, article 2: essential
984 bases-functional considerations. Applied Soil Ecology 122(Part 1):22–41.
985 Zanella A. et al. (2018a) Humusica 1, article 4: Terrestrial humus systems and forms—
986 Specific terms and diagnostic horizons. Applied Soil Ecology 122 56–74.
987 Zanella A., Ponge J.F and M.J. Briones (2018b) Humusica 1, article 8: Terrestrial humus
988 systems and forms – Biological activity and soil aggregates, space-time dynamics. Applied Soil
989 Ecology 122, Part 1, January 2018, Pages 103-137
990 Zavarzina, A.G., A.V. Lisov, and A.A. Leontievsky. 2018. The role of ligninolytic enzymes
991 laccase and a versatile peroxidase of the white-rot fungus Lentinus tigrinus in biotransformation of
992 soil humic matter: Comparative in vivo study. J. Geophys. Res-Biogeo. 123:2727–2742.
993 Zdarta, J., A.S. Meyer, T. Jesionowski, and M. Pinelo. 2018. Developments in support
994 materials for immobilization of oxidoreductases: A comprehensive review. Adv. Colloid Interface
995 Sci. 258:1–20.
996 Zhang X., M.D. Do, P. Casey, A. Sulistio, G.G. Qiao, L. Lundin, P. Lillford, and S. Kosaraju.
997 2010. Chemical cross-linking gelatin with natural phenolic compounds as studied by high-resolution
998 NMR spectroscopy. Biomacromolecules 11:1125–1132.

999 Zmora-Nahum, S., O. Markovitch, J. Tarchitzky, and Y. Chen. 2005. Dissolved organic
1000 carbon (DOC) as a parameter of compost maturity. Soil Biol. Biochem. 37:2109–2116.

CHAPTER 2

In this Chapter are reported the results of an experimental investigation aimed at verifying the possible formation of artefacts during the alkaline extraction of humic substances. Three different peats at different stage of humification were extracted using four different extractants at various pH. These results are complementary to those reported in Chapter 1 and assessed the reliability to use humic substances as valid proxy to study natural organic matter.

Preliminary results were presented as an oral presentation at the 2018-2019 International Soils Meeting (6-9 January 2019, San Diego, USA).

Is alkalinity of extractants responsible of artefacts formation during humic substances extraction?

Bravo C. [1,2], Khakbaz A. [1,3], Contin M. [1], Goi D. [3], De Nobili M [1] *

[1] Department of Agricultural Food Environmental and Animal Sciences, University of Udine, via delle Scienze 208, 33100 Udine (I).

[2] Department of Life Sciences, University of Trieste, via Licio Giorgieri 5, 34128 Trieste (I).

[3] Dipartimento Politecnico di Ingegneria e Architettura, University of Udine, via delle Scienze 206, 33100 Udine, (I).

*Corresponding author: maria.denobili@uniud.it

Keywords: humic substances, peat, artefacts, alkaline extraction

Abstract

Humic substances (HS) are usually extracted from soil and sediments using alkaline solutions. The alkaline extraction procedure was recently criticized and considered prone to create artefacts. Because of the importance of humic carbon and its widespread use as a parameter for the characterization of natural organic matter, the aim of this work was to re-examine the possibility of artefacts formation during the alkaline extraction.

Sphagnum moss and peats at different stages of decomposition were extracted by both alkaline (sodium hydroxide and sodium pyrophosphate) and neutral solutions (neutral sodium pyrophosphate and water) and extracts were fractionated according to the classic solubility scheme. Whole extracts and fractions (humic acids, fulvic acids and not-humic fraction) were quantified and characterized by UV-Vis, FT-IR, EEM fluorescence spectroscopy and ^{1}H NMR.

Results showed that extraction yields vary with the extractant pH: alkaline extractants do extract more organic matter from the different substrates. Spectroscopic properties are conserved when different extractant are used. Moreover, substances extracted from sphagnum are easily shown to differ both in their solubility properties and in their spectroscopic characteristics from humic substances extracted from peat. This allowed to observe structural differences among humic substances extracted from substrates at different stages of humification. All results were coherent with the classical view of humification.

1. Introduction

Humic substances (HS) are defined as "naturally occurring materials found in or extracted from soils, sediments, and natural waters. They result from the decomposition of plant and animal residues" (MacCarthy, 2001). Studies on HS have helped to understand biochemical processes underlying several important environmental and agronomical issues and have been used for the characterization of natural organic matter (NOM) in water systems (Olk et al., 2019).

The reliability of the extraction of HS by alkaline extractants had been strongly questioned in the past decades (Waksman, 1936; Lehmann et al., 2008) and has been challenged again recently. Lehmann and Kleber (2015) rejected the classical humification model proposing the Soil Continuum Model, in which soil organic matter exists as a continuum that spans from intact plant material to highly oxidized carbon, excluding any secondary synthesis during the decomposition process. However, no experimental evidences were shown against the humic polymerization theory (Gerke, 2018). The main argument against what the authors call the "humic paradigm" (i.e. the existence of HS) is the alkaline extraction used to isolate these compounds. The alkaline extraction is considered "incomplete, selective and prone to create artefacts" (Lehmann and Kleber, 2015). It is reported that alkaline extraction "cannot distinguish between humic substances and non-humic substances" and "cannot discriminate for products of secondary synthesis" (Kleber and Lehmann, 2019). In other words, according to these authors, HS are not real compounds that form in natural environments (soil, compost, water, etc.) from decomposition of plant and animal residues, but merely artefacts of the alkaline extraction procedure. However, the fact that HS can also be extracted by neutral solvents (Hayes, 2006), was never considered in their criticism.

In the years from 1930 to 1980, extraction of HS from soil had been carried out with different extractants, including solutions of alkali (Arnold and Page, 1930), neutral salts (Choudhri and Stevenson, 1957), diluted acids (Evans, 1959) and chelating substances (Posner, 1966). By employing not alkaline extractants, HS are extracted from soil with different yields, ash content and sometimes with different chemical characteristics (Zaccone et al., 2007; Prentice and Webb, 2010; Bakina and

Orlova, 2012). Anyway, the suspect that these substances might be of a different nature compared to those extracted under alkaline conditions was never raised (Bremner, 1949; Yuant, 1964). All these works agreed on that structural differences among HS extracted from different soils are indeed more pronounced than differences observed in isolates obtained from the same soil by milder extraction procedures (Okuda and Hori, 1956; Martin and Reeve, 1957; Hayes et al., 1975).

The aim of this study was to verify whether harsh alkaline conditions are responsible for the formation of artefacts or if HS are indeed pre-existing entities which are progressively solubilized by increasing the extractant pH because of their polyphenolic, polycarboxylic nature. Two complementary approaches were pursued: 1) testing the effect of extractant pH on the composition of the extracts; 2) testing the effect of prolonged exposure to alkaline conditions on the chemical properties of extracts. Sphagnum moss and two sphagnum peat samples at different stages of decomposition were extracted using extraction conditions spanning from acid to strongly alkaline.

2. Materials and Methods

2.1 Experiment I: Extraction and characterization of extracts

Sphagnum moss and two sphagnum peat samples at different stages of decomposition (partly-humified peat and well-humified peat; Fig. S1, Supporting Information) were air dried, sieved at 2 mm and extracted by four different extractants: a) 0.5 M NaOH, pH 13.7; b) 0.1 M $Na_4P_2O_7$, pH 10.0 (A-NaPP); c) 0.1 M $Na_4P_2O_7$, pH 7.0 (N-NaPP); d) Milli-Q water, pH 5.8. All extractants had been degassed and saturated with N_2 before use to remove dissolved O_2. Extractions (40:1 extractant/sample ratio) were carried out for 4 hours in a reciprocating shaker after closing containers under bubbling nitrogen.

Extracts were centrifuged (14000 rpm, 1 h), filtered under vacuum at 0.45 μm and the final extraction pH measured in the supernatants immediately at the end of the extraction. To precipitate humic acids (HA), extracts were acidified to pH 1 with 6 M HCl. After overnight precipitation, HA

were separated by centrifugation (5000 rpm, 45 min), frozen and finally freeze-dried. Supernatants (fulvic acid fractions) were passed through a DAX-8 resin column (previously washed and equilibrated with 0.1 M HCl). The eluate, which represents the non-humic fraction (NHU, hydrophilic acids and hydrophilic neutrals), was collected and stored. The retained fulvic acids (FA) were eluted with 0.1 M NaOH and immediately neutralized to pH 7 with 6 M HCl before storage at 4°C.

Organic carbon (OC), carbon stable isotope composition ($\delta^{13}C$) and total nitrogen (TN) of peat samples and HA were determined by CHN elemental analyzer (Vario Microcube, Elementar) coupled with a stable isotope ratio mass spectrometer (Isoprime 100, Elementar). The OC of whole extracts and of their fractions was determined, after appropriate dilution and pH adjustment to neutral values, by high temperature catalytic oxidation and subsequent non-dispersive infrared spectroscopy and chemo luminescence detection (TOC-VCPN, Shimadzu).

All UV-vis spectra of extracts were recorded at pH 7 on a Cary Varian Spectrophometer using 1 cm quartz cuvettes over an interval from 220 to 700 nm (scan rate 60 nm min^{-1}). Specific absorbance (SA) was calculated by normalizing absorbance by the optical path length (cm) and C concentration (mg L^{-1}).

FTIR spectra of HA were recorded in transmission mode with a FTIR spectrum (100 PerkinElmer Spectrometer) equipped with an ATR device, over an interval from 4000 to 800 cm^{-1}, with a 4 cm^{-1} resolution. A linear baseline correction was applied to compare spectra; intensity ratios were calculated for specific pairs of bands (Inbar et al., 1989).

Fluorescence EEM measurements of extracts were conducted at pH 7 using a Cary Eclipse Fluorescence Spectrophotometer (Agilent). Excitation and emission wavelength ranges were set to 240 – 400 nm (10 nm intervals) and 280 – 550 nm (2 nm intervals), respectively. Fluorescence intensities were normalized by the C concentration in the cuvette.

The ^{1}H NMR spectra of HA were recorded on a Bruker spectrometer. Spectra were divided into the following diagnostic regions (Gigliotti et al., 2003): 0–1.7 ppm (methyl and methylene groups of methylene chains, methylene of alicyclic groups and CH_2 and CH groups at least two carbons away

from aromatic rings or polar functional groups); 1.7–3.0 ppm (protons of methyl and methylene groups α to aromatic or carboxylic acid groups); 3.0–5.0 ppm (protons α to carbon attached to oxygen groups in polysaccharides or carbohydrates); 5.0–6.5 ppm, (olefins); and 6.5–9.0 ppm, (aromatic protons). Areas of the chemical shift regions were integrated and expressed as percentages of total area (relative intensity).

2.2 Experiment II: Strong alkaline conditions- effect of time

A sample of well-humified peat was extracted by 0.5 M NaOH, 0.1 M A-NaPP and 0.1 M N-NaPP following the procedure described above, reducing the extraction time to 5 min. After filtration, the extract was divided in two equal parts: one was immediately (T_0) processed and the other was stored in the dark for 24 h (T_1) under N_2 atmosphere. Quantification and characterization of the extracted fractions were performed at T_0 and T_1. Moreover, an aliquot sample of the whole extract was taken at t =T_0 and put in a quartz cuvette, purged with N_2 and closed (to avoid contact with air). The absorbance at 465 nm was monitored for 4 h and the Vis spectrum (450 - 700 nm) was recorded at beginning and at the end of this period.

3. Results

3.1. Quantification and composition of extracts

The amount of C extracted (total extractable carbon, TEC) per unit of organic C (extraction yield, EY) depends on the extractant used and increased linearly with pH up to 10 (Fig. 1a, Table S1). A sharp increase of both TEC and NHU-C (Fig. 1b) was conversely observed when the pH was raised from 10 to 13. However, this trend was not mirrored by a corresponding increase of HA-C/TEC ratios (Fig. 1c). If strong alkaline extraction had induced the artefactual production of HA or FA, then HU-C/TEC ratios (HU-C = HA-C + FA-C) should have followed and even magnified the sharp increase displayed by TEC at the highest pH. On the contrary, the proportion of HU-C is even lower than

would be expected from a linear model (Fig. 1d). This result is coherent with an enhanced extraction of NHU-C (likely due to hydrolysis of hemicellulose and proteins), but not with an artefactual formation of HS.

As expected, the HU fraction in the two peats extracts was significantly higher than in the sphagnum moss extracts for all the extractants used.

Strongly alkaline extracts (NaOH and A-NaPP) of sphagnum moss contain substances that, similarly to HA, precipitate pH below 2 (Hayes and Clapp, 2001). However, these substances could not be directly re-solubilized in phosphate buffer (pH 7), like all other HA, but only by addition of 0.1 M NaOH. No visible trace of precipitated components was observed when HA extracted from the two peats were dissolved in phosphate buffer.

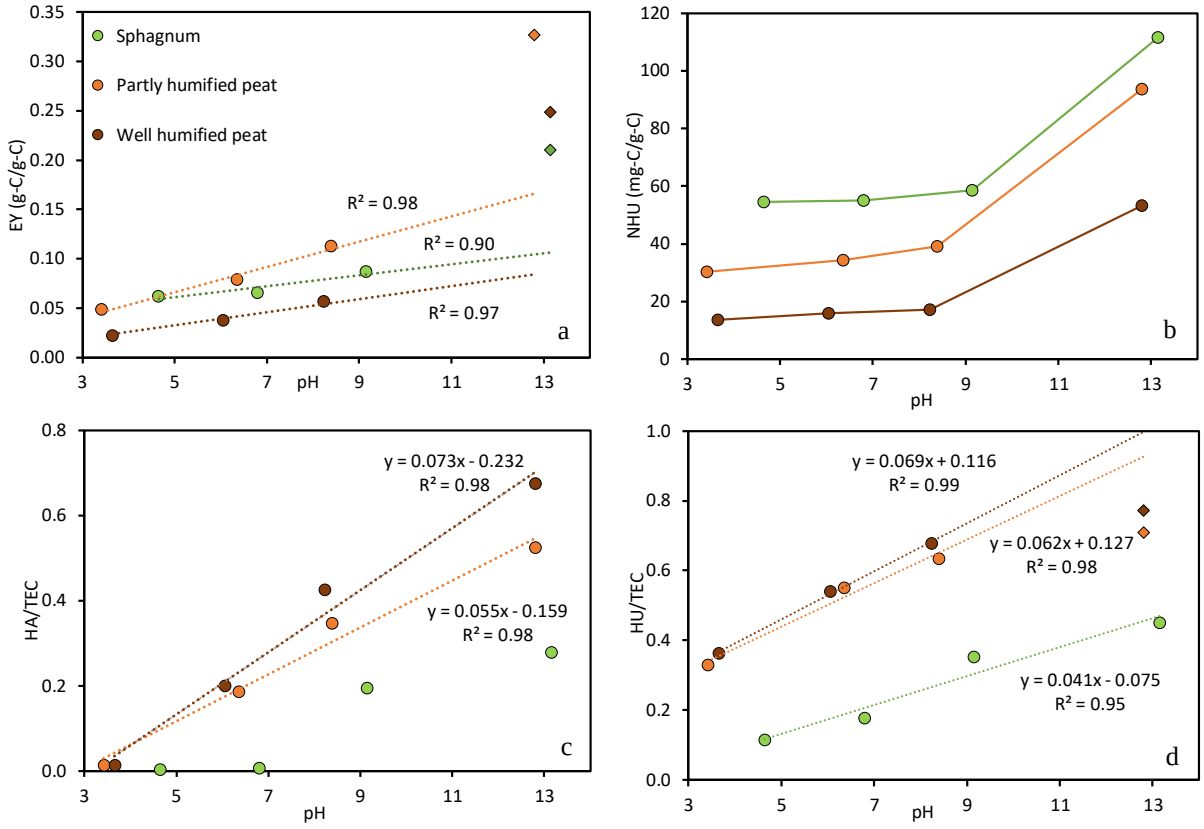

Fig 1. Trends of a) extraction yields (EY), b) not-humic carbon (NHU), c) ratio of humic acid carbon (HA) to TEC, d) ratio of humic carbon (HU) to TEC as a function of the final pH at the end of the extraction.

147 Table 1 reports the organic carbon, total nitrogen and ^{13}C content of the extracted HA. The
148 elemental and carbon isotopic composition of HA extracted from sphagnum moss was significantly
149 different compared from HA extracted from the two peats. Moreover, C/N ratios were much different
150 and closer to the C/N ratios of proteins than to those of HA.

151
152 **Table 1**. Elemental composition and ^{13}C content of the extracted humic acids (HA). Numbers in parenthesis represent
153 standard deviations from the mean.

Sample	Extractant	C (%)	N (%)	C/N	$\delta^{13}C$ (‰ vs VPDB)
Sphagnum	NaOH	50.77 (0.80)	5.86 (0.02)	8.67	-29.54 (0.02)
	A-NaPP	45.20 (0.71)	6.06 (0.01)	7.46	-29.11 (0.03)
	N-NaPP	42.07 (0.67)	5.87 (0.01)	7.17	-28.77 (0.02)
	Water	n.d.	n.d.	n.d.	n.d.
Partly-humified peat	NaOH	48.94 (0.79)	2.15 (0.01)	22.82	-26.60 (0.17)
	A-NaPP	48.78 (0.08)	2.48 (0.01)	19.71	-26.35 (0.09)
	N-NaPP	47.02 (0.81)	2.51 (0.04)	18.93	-25.65 (0.07)
	Water	46.73 (0.56)	2.96 (0.03)	15.79	-25.85 (0.10)
Well-humified peat	NaOH	48.80 (0.51)	2.22 (0.01)	21.98	-27.08 (0.01)
	A-NaPP	49.01 (0.59)	2.00 (0.04)	24.50	-27.27 (0.03)
	N-NaPP	48.35 (0.42)	2.58 (0.02)	18.74	-27.07 (0.05)
	Water	48.93 (0.35)	2.81 (0.03)	17.41	-27.21 (0.04)

154

155

156 *UV-Vis spectroscopy*

157 Although NaOH extracts are visibly darker than extracts obtained under milder pH conditions
158 (Fig. 2), the color of HS is not an artefact produced by alkalinity, but the combined effect of the
159 increased concentration of organic C (particularly HU-C) and the bathochromic shift caused by
160 dissociation of weak acid groups at increasing pH. Once spectra are normalized with respect to
161 concentration of organic C (specific absorbance, SA) and recorded at the same pH (Fig. 3), differences
162 among spectra of extracts obtained from the same material, virtually disappear in the visible region.
163 On the contrary, differences related to the degree of humification of the extracted material remain.

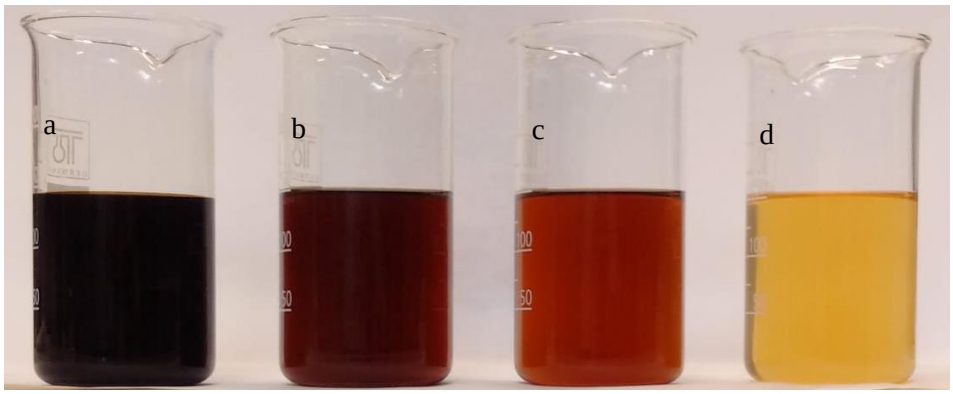

Fig 2. Total extracts from well-humified peat using a) 0.5 M NaOH (pH 13.7), b) 0.1 M A-NaPP (pH 10), c) 0.1 M N-NaPP (pH 7) and d) water (pH 5.8).

In the UV region from 220 to 240 nm, the SA of sphagnum HA extracted by NaOH is about 25% higher than that of HA extracted by milder solutions. The SA of all HA strongly increase at all wavelengths with the degree of humification of peat, whereas the shoulder at about 270-280 nm, more pronounced in the spectra of sphagnum HA (generally attributed to tryptophan residues), becomes less visible.

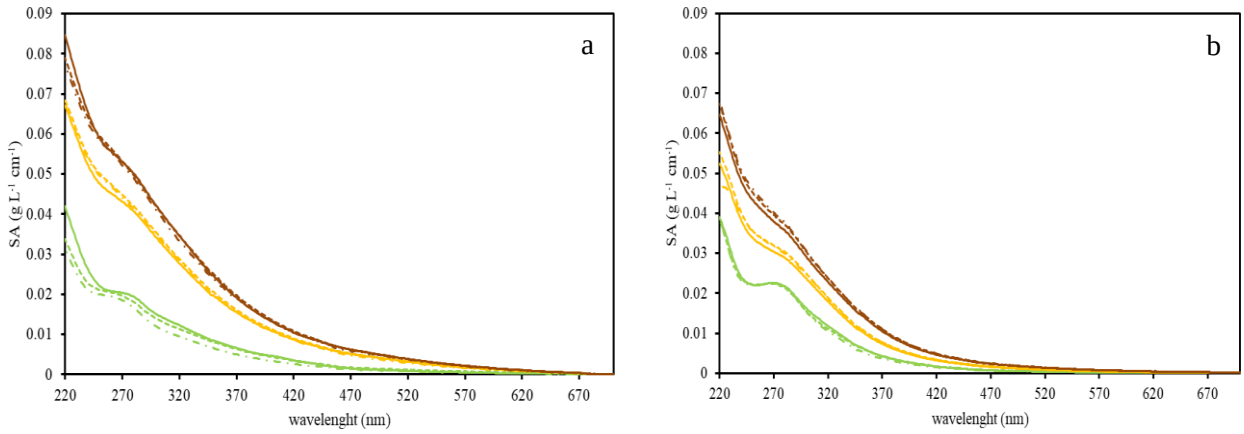

Fig. 3. Organic C normalized UV-Vis spectra from 220 to 700 nm of HA (a) and FA (b) from Sphagnum (green), partly-humified (yellow) and well-humified (brown) peat. HA and FA were extracted with 0.5 NaOH (continuous line), A-NaPP (dashed line) and N-NaPP (dash dot line). All solutions were adjusted to pH 7 before recording the spectra.

Specific absorbance at 254 nm ($SUVA_{254}$) makes possible to statistically evaluate compositional differences from UV spectra (Fig. 4). This evaluation confirmed that no significant difference existed among materials extracted from the same material by extractants of increasing alkalinity, but aromaticity of HA and FA extracted from different substrates were indeed significantly

different. At the same time there was no significant difference in aromaticity among hydrophilic fractions (NHU) isolated from all extracts: this means that the NHU fraction, contrary to the HU one, is conserved not only among extracts of different pH but also among different materials. This again is coherent with the conservation of chemical nature and absence of artefactual modifications under strongly alkaline conditions of extractant solutions.

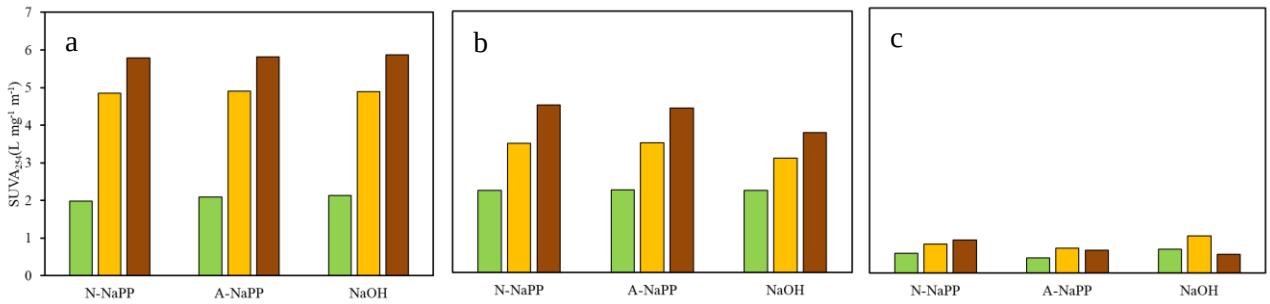

Fig 4. $SUVA_{254}$ values for a) HA, b) FA (hydrophobic acids) c) hydrophilic (not-humic) fraction extracted with neutral pyrophosphate (N-PP), alkaline pyrophosphate (A-PP) and sodium hydroxide (NaOH) from sphagnum (green bars), partly-humified peat (yellow bars) and well-humified peat (brown bars).

3.3. FT-IR spectroscopy

FT-IR spectra of the extracted HA are reported in Fig. S2. All spectra are characterized by HA typical absorption bands: a broad band at about 3280 cm^{-1} (O-H stretching vibrations); twin peaks at 2920 and 2850 cm^{-1} (asymmetric and symmetric C-H stretching of CH_2 and CH_3 groups; a shoulder at 1710 cm^{-1} (C-O stretching of carboxyl and ketonic carbonyl) merged with the more intense band at 1610 cm^{-1} (conjugated carbonyl C=O and aromatic C=C); a discrete peak at about 1515 cm^{-1} (uncondensed aromatic compounds bound to N and O atoms); two small peaks at 1450 and 1420 cm^{-1} (C-H bending of CH_2 and CH_3 groups); a band at 1215 cm^{-1} (stretching C-O and bending O-H vibrations) and stretching of carbohydrate or alcoholic C–O at 1040 cm^{-1}.

Regardless the used extractant, several spectral differences are evident between the three materials, from sphagnum to well-humified peat: a) the band at 3280 cm^{-1} became broader; b) the twin peaks at 2920 and 2850 cm^{-1} are less intense and resolute; c) the peak absorbance at 1710 cm^{-1} increased, while the ones at 1215 and 1040 cm^{-1} decreased.

Within the same material, the spectra of HA extracted by NaOH, A-NaPP and N-NaPP do not present clear differences among them. However, the HA extracted by water present the lowest 1710/1040 and 1215/2920 intensity ratios.

3.4. ^{1}H NMR spectroscopy

^{1}H NMR spectra of HA are reported in Fig. S3 and the proton distribution is summarized in Table 2. These results confirmed FT-IR evidences: in fact, well-humified peat presented the highest aromatic and lowest alkyl percentage. Moreover, the differences using different extractants are within the instrumental deviation (± 5%)

Table 2. Proton distribution percentage calculated from ^{1}H NMR spectra.

Material	Extractant	Alkyl-H	Alkyl-H	Carbohydrate-H	Olefins	Aromatic-H
		0-1.7 ppm	1.7-3.0 ppm	3.0 -5.0 ppm	5.0-6.5 ppm	6.5-9.0 ppm
Sphagnum	NaOH	41.1	20.5	24.9	6.4	7.0
	A-NaPP	45.1	20.3	23.6	4.1	6.9
Partly-HP	NaOH	34.0	19.2	28.8	6.3	11.6
	A-NaPP	33.0	21.6	26.4	6.5	12.5
	N-NaPP	30.1	21.8	28.1	6.7	13.4
Well-HP	NaOH	25.8	21.6	26.9	8.9	16.8
	A-NaPP	27.3	24.2	23.7	8.2	16.6
	N-NaPP	29.3	23.9	25.7	7.9	13.2

3.4. Fluorescence spectroscopy

EEM spectra of total extracts (Fig. S4), fulvic acids (Fig. S5) and the not-humic fraction (Fig. S6) reflect much more the effects of different humification degree of the original material than the pH of extractant solutions.

These results support the hypothesis that the alkalinity of extractants is not responsible of artefacts as claimed by Lehmann and Kleber.

3.5 Strong alkaline conditions- effect of time

To verify whether exposure of solubilized materials to harsh alkaline conditions did modify their nature, we followed the chemical characteristics of extracts of the well humified sphagnum peat

during a time course experiment. To this purpose extraction time was limited to 5 minutes, in order to start monitoring spectral characteristics as soon as possible. Extraction yields after 5 min of extraction were significantly lower than after 4 h of extraction (39, 26 and 22 % respectively for NaOH, alkaline and neutral $Na_4P_2O_7$). However, after 24 h of storage the DOC did not vary significantly, excluding any spontaneous precipitation. Also the amount humic C did not change, indicating that even at very alkaline conditions there is not creation of "artefactual" HS. In fact, if HS would merely be produced by exposure to alkaline conditions, keeping the extracts at high pH for long time should cause an appreciable increase in humic C. Moreover, the pH of the extracts did not change between T0 and T1, confirming that no decarboxylation (as also confirmed by the elemental and isotopic composition of HA) nor H^+ consuming hydrolysis reactions occurred.

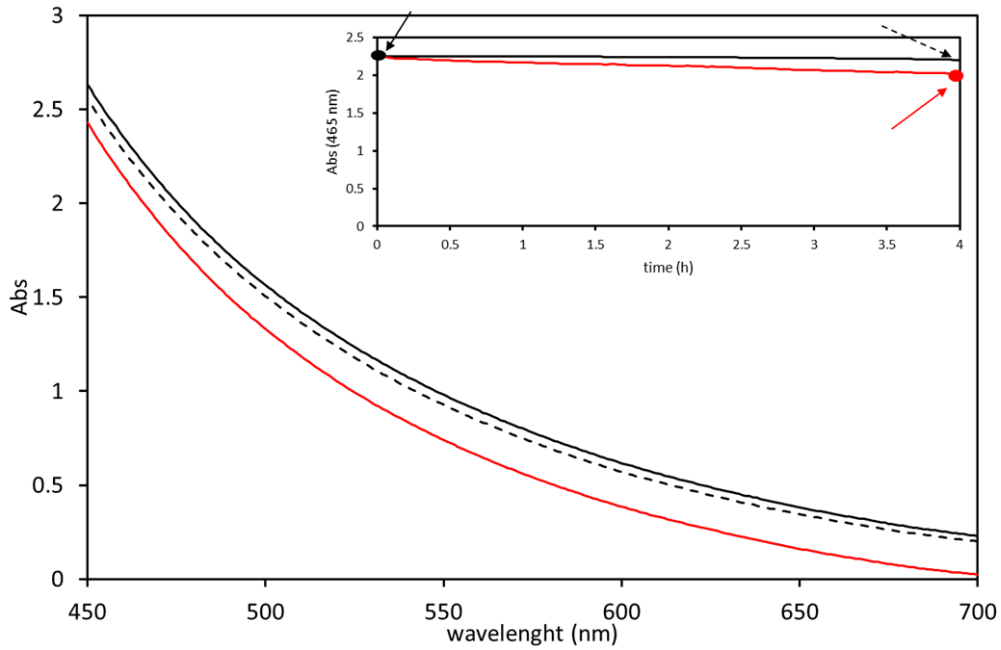

Fig 5. Vis spectrum of NaOH extract at t=0 (continuous line) and at t=4h (dotted line). The insert represents the variation of the absorbance at 465 nm for 4 h. The red curve represents the UV spectrum of the extract stored 4 h in contact with the atmospheric air.

Regarding the spectroscopic properties of extracts, UV-Vis spectra did not change appreciably between T0 and T1 (Fig. 5). This indicates that the dark color of HS is not created by the alkaline conditions and even storing the solutions at pH > 12 for 1 day at room temperature, did not result in any modification in the optical properties of extracts. Considering the NaOH extract, if the extract

had been exposed to the air during transfer to the cuvette (dashed line in Fig. 5), after 4 h there was a 2.4% decrease in absorbance at 465 nm, but no significant change in SUVA. This was reflected by an increase of the E4/E6 ratio from 6.80 to 7.34, consistent with possible hydrolysis reactions (Chen and Schnitzer, 1977). On the other side, changes in the E4/E6 ratio for the alkaline and neutral pyrophosphate extracts were lower and not significative resulting in E4/E6 variations from 6.65 to 6.69 and from 4.45 to 4.42, respectively. These changes could be explained with exposure to atmospheric O_2. In fact, by leaving the cuvette open to the air, the decrease in absorbance at 465 nm increased to 8.45 %, and consequently the E4/E6 ratio increased to 8.53. In fact, in alkaline solutions the presence of O_2 can led to decarboxylation processes. For these reasons it is important to carry out extractions under nitrogen with fully de-aerated solutions.

Table 3. Chemical and spectroscopic characteristics of extracts and HA between T0 and T1, for the 3 different extractants.

	N-NaPP		A-NaPP		NaOH	
	T0	T1	T0	T1	T0	T1
pH	6.70	6.72	9.04	9.02	12.81	12.83
TEC (mg-C/g-C)	8.03	7.94	14.69	14.85	97.36	99.21
HU (mg-C/g-C)	7.36	7.48	14.12	13.68	89.31	89.34
NHU/HU	0.11	0.10	0.08	0.09	0.12	0.12
%C of HA	48.30	47.55	47.64	47.13	48.84	48.92
%N of HA	2.14	2.08	1.69	1.67	1.96	1.93
C/N	22.57	22.86	28.19	28.22	24.98	25.34
$\delta^{13}C$ of HA	-27.02	-26.95	-27.00	-27.32	-26.88	-26.87
$SUVA_{254}$	5.15	5.27	5.42	5.33	5.38	5.30
% Arom					34.01	34.60
1605/1030 (IR)	1.40	1.39	1.35	1.35	1.36	1.36

However, EEM fluorescence confirms that changes were minor: no changes in either peaks position and intensities occurred during exposure to alkaline conditions. ATR-FTIR spectra of HA recorded at T0 and T1 practically overlapped: this is also highlighted by the ratio between absorption at 1605 cm^{-1} (aromatic C=C stretching) and that at 1030 cm^{-1} (C-O stretching of polysaccharides) did not change.

4. Conclusions

All the results are coherent with the classical humification theory, demonstrating that humic substances are not artefacts of the extraction process. In fact, humification consists in demolition and loss of labile substrates and in structural changes of the hydrophobic acid fraction. Moreover, not only spectroscopic properties are conserved when different extractant are used, but also extraction of substrates at different stages of humification allows to observe structural differences among corresponding fractions.

References

Arnold, C.W.B. and Page H.J. 1930. Studies on the carbon and nitrogen cycles in the soil. II. The extraction of the organic matter of the soil with alkali. The Journal of Agricultural Science 20:460-477.

Bakina, L.G. and Orlova N.E. 2012. Special features of humus acids extraction from soils by sodium pyrophosphate solutions of different alkalinity. Eurasian Soil Science 45:392-398.

Bremner J. M. 1949. Studies on soil organic matter: Part III. The extraction of organic carbon and nitrogen from soil. J. of Agr. Sci. 39:280-282.

Chen, Y., Senesi N. and Schnitzer M. 1977. Information provided on humic substances by the E4/E6 ratios. Soil Sci. Soc. Am. J. 41:352-358.

Choudhri, M.B. and F. J. Stevenson. 1957. Chemical and Physicochemical Properties of Soil Humic Colloids: III. Extraction of Organic Matter from Soils1. Soil Sci. Soc. Am. J. 21:508-513.

Evans L.T. 1959. The use of chelating regents and alkaline solutions in soil organic matter extractions. Eur. J. Soil Sci.

Gerke, J. 2018. Concepts and misconceptions of humic substances as the stable part of soil organic matter: a review. Agronomy 8:76.

Gigliotti, G., Macchioni, A., Zuccaccia, C., Giusquiani, P. and Businelli D. 2003. A spectroscopic study of soil fulvic acid composition after six-year applications of urban waste compost. Agronomie 23:719-724.

Hayes, M.H.B. 2006. Solvent Systems for the Isolation of Organic Components from Soils. Soil Sci. Soc. Am. J. 70:986–994.

Hayes, M.H.B and Clapp C.E. 2001. Humic substances: considerations of compositions, aspects of structure, and environmental influences. Soil Sci. 166:723-737.

Hayes, M.H.B., Swift, R.S., and Wardle R.E. Brown. 1975. Humic materials from an organic soil: A comparison of extractants and of properties of extracts. Geoderma 231-245.

Inbar, Y., Chen, Y. and Hadar, Y. 1989. Solid-state Carbon-13 Nuclear Magnetic Resonance and Infrared Spectroscopy of Composted Organic Matter. Soil Sci. Soc. Am. J. 53:1695-1701.

Kleber, M and Lehmann, J. 2019. Humic Substances Extracted by Alkali Are Invalid Proxies for the Dynamics and Functions of Organic Matter in Terrestrial and Aquatic Ecosystems. J. Environ. Qual. 48:207–216.

Lehmann, J., Solomon, D., Kinyangi, J., Dathe, L., Wirick, S. and Jacobsen, C. 2008. Spatial complexity of soil organic matter forms at nanometer scales. Nature Geosci. 1:238-242.

Lehmann, J. and Kleber, M. 2015. The contentious nature of soil organic matter. Nature.

MacCarthy, P. 2001. The principles of humic substances. Soil Sci. 166:738-751.

Martin A.E. and Reeve R. 1957. Chemical studies on podzolic illuvial horizons I. The extraction of organic matter by organic chelating agents. European J. Soil Sci. 8:268-278.

Okuda A. and Hori S. 1956. Some aspects on the nature of humic acid, Soil Sci. Plant Nutri. 2:42-43.

Olk, D.C, Bloom, P.R., De Nobili, M., McKnight, D.M., Wells, M.J.M. and Weber, J. 2019. Using Humic Fractions to Understand Natural Organic Matter Processes in Soil and Water: Selected Studies and Applications. J. Environ. Qual. doi:10.2134/jeq2019.03.0100.

Posner A.M. 1966. The humic acids extracted by various regents from a soil Part I. Yield, inorganic components and reaction curves. European J. Soil Sci. 17:65-68.

Prentice, A.J. and Webb E.A. 2010. A comparison of extraction techniques on the stable carbon-isotope composition of soil humic substances. Geoderma 155:1-9.

Waksman, S.A. 1936. Humus. Origin, chemical composition and importance in nature. Williams and Wilkins.

Yuant T.L. 1964. Comparison of Reagents for Soil Organic Matter Extraction and Effect of pH on Subsequent Separation of Humic and Fulvic Acids Soil Sci.98:133-141.

Zaccone, C., Cocozza C., D'Orazio, V., Plaza, C., Cheburkin, A. and Miano T.M. 2007. Influence of extractant on quality and trace elements content of peat humic acids. Talanta 73:820-830

CHAPTER 3

The fact that humic substances can reversibly sustain redox cycling was only demonstrated for humic acids (HA) analogues and extracted HA in solutions. Moreover, climate change could alter redox properties of HA and affect ratios of greenhouse gases emissions (CO_2:CH_4). In this work structural and electrochemical changes of natural HA brought about by biological reduction in their natural solid state were investigated.

Electrochemical analyses were performed in the laboratories of the group of Electrochemistry of the University of Udine.

Preliminary results were presented at the 19th International Conference of the International Humic Substances society (16-21 September 2018, Albena Resort, Bulgaria) and prized as best poster of the conference.

Redox behavior of humic acids after aerobic and anaerobic peat incubations

C. Bravo[a,b],* R. Toniolo[a], M. Contin[a] and M. De Nobili[a]

[a] Department of Agricultural, Food, Environmental and Animal Sciences, University of Udine, via delle Scienze 208, 33100 Udine, Italy.

[b] Department of Life Sciences, University of Trieste, Via Licio Giorgieri 5, 34128 Trieste, Italy.

* Tel. +39 0432 558642; E-mail: carlo.bravo@uniud.it

Keywords: TEA; reduction; humic acids; peat; anaerobic respiration.

Highlights:

- Humic acids undergo redox changes after aerobic/anaerobic incubation.
- 3 months of aerobic incubation do not exhaust electron donating capacity of humic acids.
- Electron transfer kinetic constant is modified by aerobic/anaerobic conditions.

Abstract

Humic acids (HA) may act as terminal electron acceptors, allowing facultative anaerobic bacteria to perform anaerobic respiration. In peatlands, extended drought periods could alter redox properties of HA affecting ratios of greenhouse gases emissions. This work investigated changes in peat HA by caused aerobic/anaerobic microorganisms, during 90 days of incubation.

Relative intensities ratios of selected FTIR bands of HA were modified. The intensities of the 1720/1025 cm^{-1} and of the 1650/1600 cm^{-1} ratios were lower in the anaerobically incubated peat HA, whereas ratios between bands typical of aromatic ring stretching increased their intensity with respect to that of C=O stretching in COOH. The number of carboxyl groups decreased as a result biological reduction, whereas that of phenolic groups increased.

Cyclic voltammetry showed that microbial activity affected the redox properties of HA. Pseudo-first order kinetic constants were 9.5 and 13.8 L s^{-1} g^{-1} for HA extracted after respectively aerobic and anaerobic incubation. Coherently, values of electron donating capacity (EDC) were significantly different and ~20 % higher after anaerobic incubation.

Incubation of peat under conditions that strongly accelerate oxidative processes did not cause exhaustion of the original electron donating capacity of HA, which seemed to be only marginally affected (~10 %).

Alterations in hydrology of peat deposits might therefore have only minor effects on the actual in situ availability of organic TEA and is possible that no substantial alterations will occur in future CO_2 to CH_4 emissions ratios from peatlands.

1. Introduction

About 10% of the global natural emissions of methane (54 Tg y^{-1}) originates in bogs and tundra soils (Mikaloff Fletcher et al., 2004). As a consequence of global warming, in the next decades peatlands are expected to release larger amounts of greenhouse gases (CO_2 and CH_4) (Davidson and Jansen, 2006). They will therefore contribute to the scarcely known feedback mechanisms that may hamper our capability to predict climate change. The temperature dependence of organic C decomposition has been extensively investigated and modelled (Ise and Moorcroft, 2006), but mechanisms affecting the CO_2:CH_4 emission ratio during peat decomposition are not fully understood (Keller and Bridgham, 2007; Ye et al., 2012). Considering that CH_4 has a global warming potential 25 times that of CO_2, it is important to understand which factors may be important in affecting emission ratios from peatlands.

In peatlands, facultative anaerobic bacteria may perform anaerobic respiration during which different terminal electron acceptors (TEAs) are reduced in place of the missing oxygen (Bridgham et al., 2013). Following depletion of inorganic TEAs, hydrogenotrophic methanogenesis becomes the main pathway for organic matter decomposition. The higher energy yield of this type of metabolism compared to methanogenesis, provides the thermodynamic justification for the higher CO_2 to CH_4 production. However, peatlands are naturally poor in inorganic TEAs such as nitrate and iron (Vile et al., 2003; Keller and Bridgham, 2007), so CO_2:CH_4 production ratios higher than one can only be sustained by humic substances (HS) (Galand et al., 2010). In fact, HS can act as organic TEAs and are contained in large amount in peat (Lovley et al., 1996; Cervantes et al., 2000, Keller et al., 2009, Klupfel et al., 2014). Keller and Takagi (2013) had demonstrated that the reduction of organic TEAs accounted for a significant fraction of the CO_2 released from a bog soil during anaerobic respiration, whereas CH_4 was not produced until the electron-accepting capacity of the organic TEAs was exhausted. Keller et al. (2009) proved that the addition of HA extracted from wetland soils alters the ratio of CO_2:CH_4 produced during anaerobic laboratory incubations. Moreover, HA and HA analogs

have been proved to inhibit methane production in different types of peatlands by various mechanisms (Ye et al. 2016).

About 270–370 Pg of C, nearly one-third of the world's soil carbon, are sequestered in peatlands and most of them accumulated below the water table, where organic matter decomposition is restricted by lack of oxygen and inorganic TEAs (Drake et al., 2009; Bridgham et al., 2013). Unfortunately, because of the greater incidence and length of drought periods induced by climate change, peatlands will increasingly suffer fluctuations of their water table which will enforce the onset of aerobic conditions in deeper sections of their profile. Therefore, the redox properties of organic matter might be altered, affecting the availability of TEAs during ensuing periods of flooding and, in the long term, the emission ratio of CO_2 to CH_4 (Ise et al, 2008; Gao et al., 2018).

The aim of this work is to investigate the chemical-physical modifications that humic acids undergo when peat is subjected to a change from anaerobic to aerobic conditions due to the fluctuations of the water table, in order to highlight potential modifications of their redox state. Previous studies investigated the effects of the addition of model organic TEAs, HA and biological reduction of solid phase organic matter (Gao et al., 2018) on emissions from peat. However, no studies have so far been directly addressed to evaluate HA extracted after aerobic or anaerobic incubation.

Biological oxidation/reduction, by aerobic/anaerobic microorganisms, of peat HA in their natural solid state were performed by subjecting a sample of sphagnum peat to intense biological oxidative or reductive conditions during a 90-day incubation experiment in mesocosms. Structural changes of HA were investigated by ATR-FTIR spectroscopy and quantitative determination of acid functional groups, while electrochemical effects were characterized and quantified by cyclic voltammetry and coulometry.

2. Materials and methods

2.1 Experiment layout

Lithuanian sphagnum peat (characteristics are reported in the Supporting Information) was sieved at 2 mm and incubated in mesocosms under either fully aerobic (40% WHC, continuous insufflation of air) and anaerobic (submerged under water previously purged with N_2 for 90 minutes and kept under N_2 atmosphere) conditions. Mesocosms were kept in the dark in a thermostatic cell at 25 °C for 90 days. A scheme of the experimental layout is reported in Fig. 1. Each mesocosm contained an amount of peat corresponding to 100 g of dry weight which had been thoroughly mixed just before incubation with 3 g of ground poplar litter (to boost biological activity) and 1 g of either an aerobic or anaerobic soil (as natural inoculum). In the case of the anaerobic treatment, all operations were carried out under N_2 in an anoxic glove box.

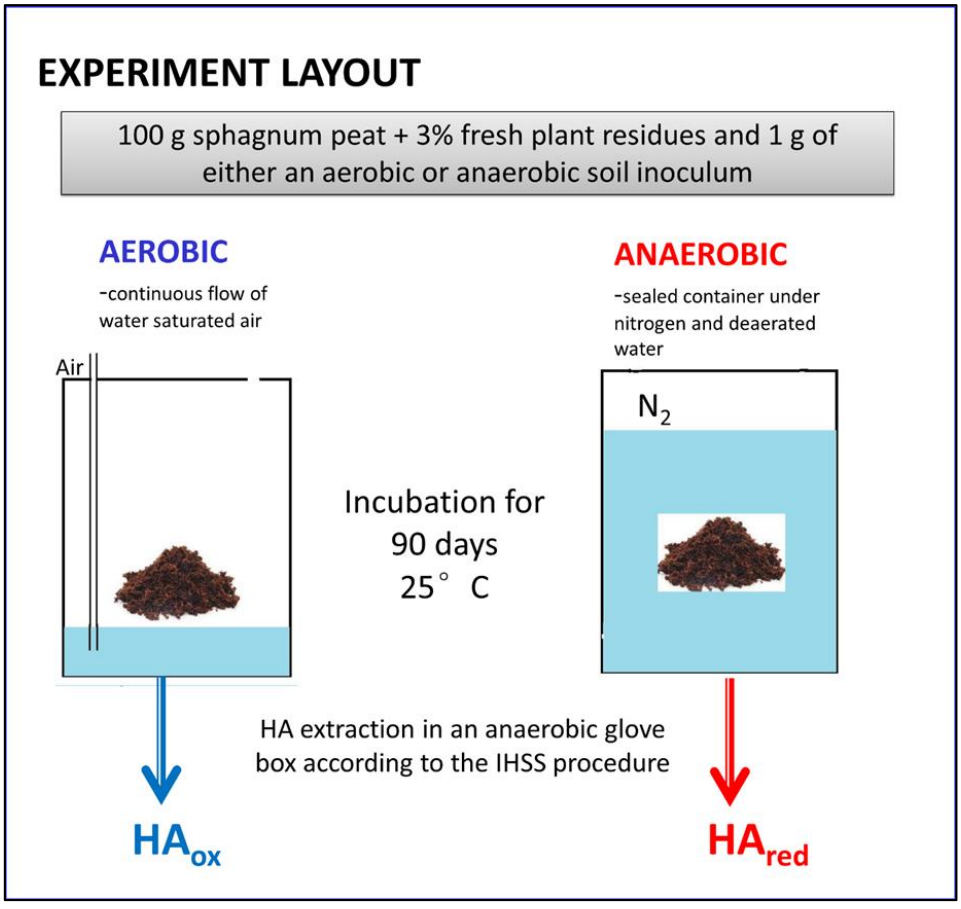

Fig. 1. Representation of the experimental layout.

96 *2.2 HA extraction*

97 At the end of the incubation, HA_{ox} (from aerobic incubation) and HA_{red} (from anaerobic
98 incubation) were extracted in an anoxic glovebox following the procedure recommended by the IHSS.
99 Briefly, extractions were carried out using 0.1 M NaOH (previously deoxygenated and N_2-saturated)
100 for 4 h at 1:20 peat/solution ratio. Suspensions were centrifuged (14000 rpm for 30 min) and
101 supernatants were filtered through 0.2 um cellulose filters and acidified to pH 1 using 6 M HCl to
102 allow HA precipitation. After washing with Milli-Q water, HA were frozen and then freeze-dried.
103 HA were extracted also from a not incubated peat sample ($HA_{not\text{-}inc}$).

104

105 *2.3 HA characterization*

106 Organic carbon (%OC), total nitrogen (%N) and carbon stable isotope composition ($\delta^{13}C$) of
107 the original peat and extracted HA were determined with a CHN elemental analyzer (Vario
108 Microcube, Elementar) coupled with a stable isotope ratio mass spectrometer (Isoprime 100,
109 Elementar).

110 Titration of acidic groups was carried out under N_2 according to Barack and Chen (1992) with
111 a Mettler Memo titrator DL 50.

112 UV-Vis spectra of HA were recorded using a Cary Varian Spectrophotometer in 1 cm quartz
113 cuvettes over a wavelength interval from 220 to 800 nm at a scan rate of 60 nm min^{-1}. Each spectrum
114 was normalized by the OC concentration of the sample.

115 FTIR spectra were recorded with a FT-IR Spectrum 100 (PerkinElmer) spectrometer equipped
116 with a universal ATR (attenuated total reflectance) sampling device containing a diamond/ZnSe
117 crystal. The spectra were recorded at room temperature in transmission mode over a wavenumber
118 interval from 4000 to 500 cm^{-1} (30 scans at a resolution of 4 cm^{-1}). Triplicate runs of each sample
119 were averaged to obtain an average spectrum. A background spectrum of air was scanned under the
120 same instrumental conditions before each series of measurements. Intensity ratios (R) were calculated
121 for specific pairs of bands (Inbar et al., 1989).

122 *2.4 Electrochemical experiments*

123 The electrochemical mediator 2,2'-Azinobis (3-ethylbenzothiazoline-6-sulfonic acid)
124 diammonium salt (ABTS) was obtained from Sigma-Aldrich (St. Louis, USA). HA stock solutions
125 were prepared by dissolving a certain amount of HA in 0.1 M phosphate buffer (pH 7.0), previously
126 N_2-saturated. All solutions used were prepared using high purity water (18 MΩ resistivity, Milli-Q
127 Corp.).

128 Cyclic voltammograms (CVs) were recorded by a 430A CHI electrochemical analyzer in 0.1
129 M phosphate buffer (pH 7.0) solutions (10-12 mL) using a 3 mm diameter glassy carbon (GC) disk
130 working electrode, an Ag/AgCl reference electrode and a Pt wire auxiliary electrode. The working
131 electrode was cleaned after each CV using 1.0 and 0.05 μm aluminum oxide on polishing pads,
132 thoroughly rinsed with Milli-Q water and dried. The cathodic and anodic vertex potentials were fixed
133 at Eh = -0.1 V and +0.7 V (scan rate 0.010 V s^{-1}, unless stated differently). CVs were collected in the
134 presence of either ABTS (3-90 μM) or HA (0.2-2.0 g L^{-1}), and in the presence of both 3 or 60 μM
135 ABTS and HA (0.05 to 3.5 g L^{-1}).

136 Mediated Electrochemical Oxidation (MEO) measurements were carried out, under anoxic
137 atmosphere and continuous solution stirring, in a bulk electrolysis cell containing a macro GC WE
138 polarized to E = 0.423 V, an Ag/AgCl reference electrode and a Pt wire auxiliary electrode (separated
139 by a porous glass frit). ABTS was used as electrochemical mediator to shuttle electrons from electron
140 donating moieties in HA to the WE (Aeschbacher et al. 2010). After oxidation of a 0.20 mM ABTS
141 solution (0.1 M phosphate buffer, pH 7), small aliquots of HA (0.4 mg), were spiked into the
142 electrochemical cell. Oxidative currents were automatically integrated by a digital current integrator
143 (Model 731, Amel) to quantify the EDC of HA.

144

145 *2.5 Statistics*

146 All CVs and MEO measurements were replicated at least three times, while other analyses
147 were performed in double and reported in tables and figures as mean ± standard error (SE). Difference

between treatments was considered significant at $p < 0.05$. Regression analysis, test of significance of the correlation coefficient, and analysis of parallelism were carried out by R software (Miller and Miller 2010; Development Core Team 2018).

3. Results and discussion

3.1 Structural changes

Organic carbon, total nitrogen and carbon stable isotope composition ($\delta^{13}C$) of HA extracted before and after aerobic and anaerobic incubations ($HA_{not\text{-}inc}$, HA_{red}, HA_{ox}) are reported in the Supporting Information (Table S1).

Incubations, under either aerobic or anaerobic conditions, did not substantially alter the UV-Vis spectra of HA compared to those extracted from the not-incubated peat (Fig. S1). In fact, each spectrum showed a monotonical decrease of the specific absorbance (SA) with increasing wavelengths and a shoulder around 270-280 nm (generally attributed to absorption by tryptophan residues). However spectral parameters reveal that HA underwent some selective structural changes. Although $SUVA_{254}$ values did not display significant differences ($p > 0.17$) among the three samples, a bathochromic shift of UV absorption (at 254 nm) towards higher (5 nm) wavelengths was displayed by HA_{ox}. This shift is compatible with oxidation of hydroquinones groups during aerobic incubation. On the other hand, the hypsochromic (3 nm) shift which occurred after anaerobic incubation in HA_{red} is probably associated with the reduction of quinones, which results in a decrease of the electron delocalization in aromatic structures.

Moreover, the E_{445}/E_{665} ratio of HA_{ox} (5.83) was significantly higher than HA_{red} (5.52, $p < 0.04$) and $HA_{not\text{-}inc}$ (5.49, $p < 0.03$), confirming that some oxidative depolymerization probably occurred during aerobic incubation.

ATR FTIR spectra of HA extracted from non-incubated, aerobically and anaerobically incubated peat did not display major structural changes (Fig. S2). All HA exhibited a peak in the

region around 3400 cm^{-1} (assigned to OH stretching), broadened by intermolecular hydrogen bonding and/or H-bonded OH attributed to phenolic groups and similar weak absorption bands associated with aliphatic C-H. The band due to C=O stretching in carboxyls (1720 cm^{-1}), overlapped with the band at 1650 cm^{-1} which could be attributed to aromatic C=C, C=O and/or C=O of conjugated ketones or to C=N amide I stretching. Absorption at 1600 cm^{-1} is related to aromatic skeleton vibrations. The band at 1230 cm^{-1}, assigned to O-C-C ester linkage of carboxylic and phenolic acid, C–O stretch of COOH and CH twisting, was more intense in the spectrum of $HA_{not\text{-}inc}$ and less intense in the spectrum of HA_{ox}. The same occurred for the band at 1033 cm^{-1} which is ascribed to ortho-substituted OH stretching, C-C-O of primary alcohols. ATR FTIR spectra of $HA_{not\text{-}inc}$ displayed intermediate absorption between HA_{red} and HA_{ox}.

Significative changes were highlighted by calculating the relative intensities ratios of selected bands. The 1720/1025 cm^{-1} intensity ratio is related to variations in sorption by C=O of COOH with respect to C-O of carbohydrates and the 1650/1600 cm^{-1} to presence of quinones in aromatic structures. Both ratios were lower in the HA_{red} extracted from the anaerobically incubated peat HA,

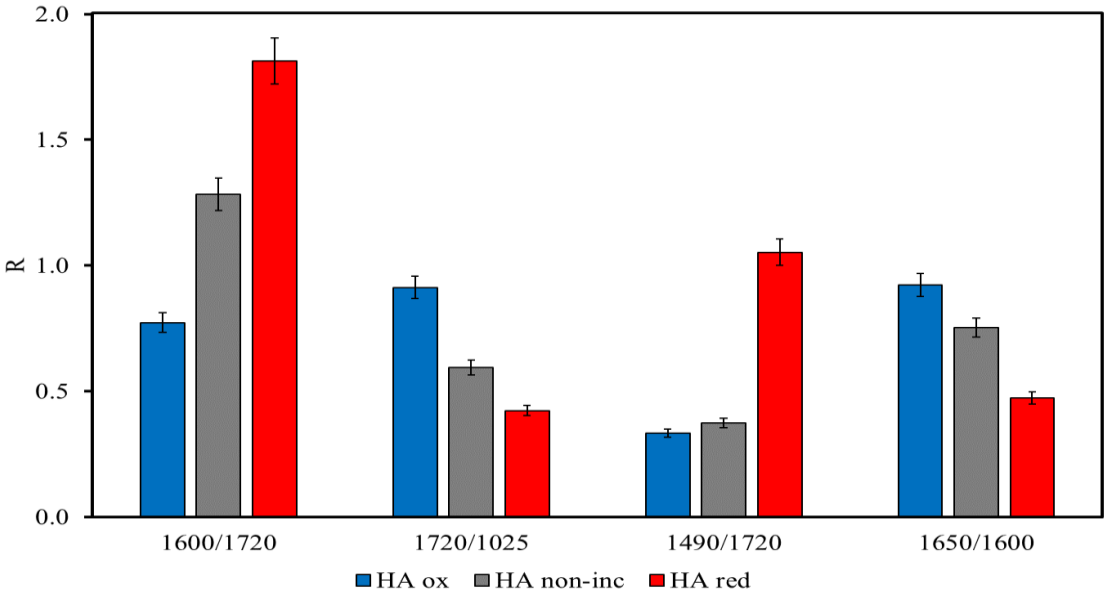

Fig. 2. Intensity ratios of selected absorption peaks in FTIR spectra of HA extracted from not incubated peat ($HA_{not\text{-}inc}$, grey bars) and from anaerobically (HA_{red}, red bars) or aerobically (HA_{ox}, blue bars) incubated peat.

whereas ratios between bands typical of aromatic ring stretching increased their intensity with respect to that of C=O stretching in COOH. As expected, in all cases $HA_{not\text{-}inc}$ displayed intermediate structural characteristics between HA_{ox} and HA_{red} (Fig. 2).

Direct titration of carboxyl groups allowed quantitative determination of the number of strong and weak acid groups: HA_{ox} and HA_{red} respectively contained 10.91 and 7.95 mmol COOH g^{-1}HA-C, and 3.64 and 5.45 mmol (phenolic OH) g^{-1} HA-C. Therefore, the number of carboxyl groups decreased in HA after anaerobic incubation, as shown by FTIR spectra: a likely result of direct or shuttle mediated biological reduction, whereas that of phenolic groups increased.

Handerson-Hasselbach elaboration of titration data (Fig. 3) also allows to determine average pKa at α=0.5. HA_{red} displayed an average pKa of 5.70 which shows they are weaker than most aliphatic acids, whereas those of HA_{ox} are on the contrary stronger and typical of substituted aromatic acids.

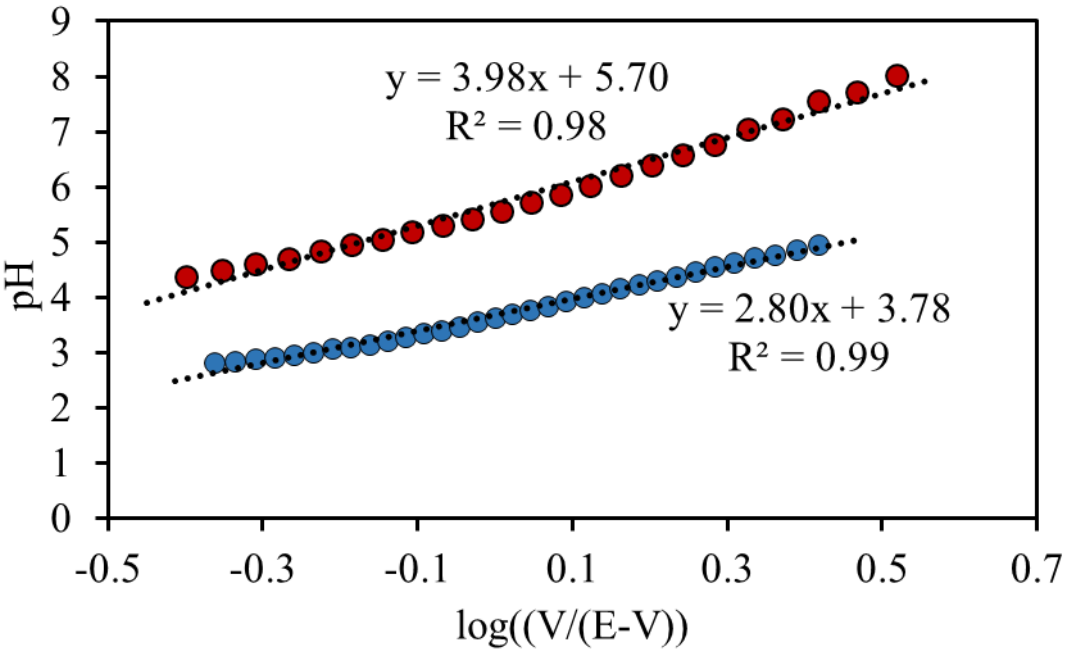

Fig. 3. Henderson-Hasselbach plot of HA extracted from aerobically (blue symbols) and anaerobically (red symbols) incubated peat.

3.2 Electron transfer properties

Compared to background, the CVs of HA_{ox} and HA_{red} solutions showed higher oxidative currents during anodic scanning, at potentials above +0.3 V, demonstrating that HA can be directly oxidized at the GC-WE (Fig. 4a and 4b).

The absence of any clearly defined peak indicated that electron exchange involved an extensive range of oxidizable moieties (Aeschbacher et al., 2012). These likely consist of closely related functional groups, whose reactivity is influenced by differences in their structural environment, resulting in a wide distribution of overlapping redox potentials (Nurmi and Tratnyek, 2002).

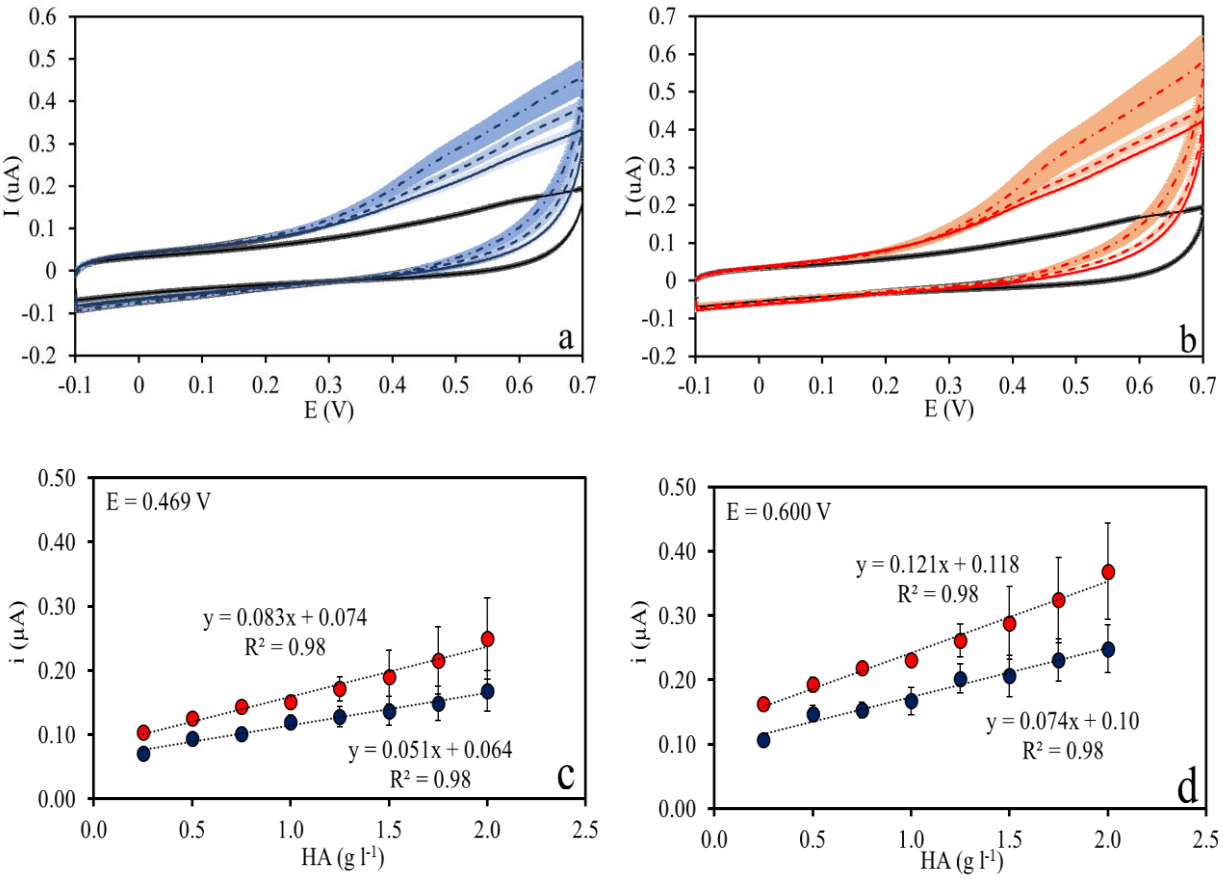

Fig. 4. a and b. Cyclic voltammograms of HA_{ox} (**a**) and HA_{red} (**b**) solutions at different concentrations (0.25 – 1.50 gl^{-1}). Black traces represent the background electrolyte. **c and d**. Linear correlation between anodic current at 0.469 V (**c**) and 0.600 V (**d**) versus HA_{ox} (blue symbols) and HA_{red} (red symbols) concentrations.

On the other hand, the featureless CVs of HA not only suggests the lack of defined oxidation or reduction potentials, but also a sluggish electron transfer from the oxidizable moieties in HA to the

WE. Furthermore, electrode passivation by surface-active fractions of HA occurs at a relatively high concentration of HA (> 1.0 g l^{-1}). This leads to lower reproducibility and larger standard errors when the concentration of HA in the electrochemical cell exceeds this concentration.

A linear correlation was found between HA concentration and current intensities measured at 0.469 and 0.600 V (Fig. 4c and 4d). In both cases, HA_{red} presented a significantly higher slope ($p < 0.004$) compared to HA_{ox}. Microbial reduction therefore increased in the HA_{red} the number of electrons that can be directly transferred from HA to the WE.

To further characterize the electrochemical behavior of microbially reduced and oxidized HA and calculate pseudo first order kinetic constants of electron transfer, the 2,2'-azino-bis(3-ethylbenzthiazoline-6-sulfonic acid) diammonium salt (ABTS) was used to mediate the electron transfer from electron donating moieties in HA to the WE (Aeschbacher et al., 2012).

The ABTS showed a reversible charge transfer process and obeyed the Randles-Sevcik law as confirmed by the linear correlations found between the oxidative peak current (i_p) and the concentration ($R^2 = 1.00$) and $v^{1/2}$ ($R^2 = 1.00$) (Fig. S3). The difference in the reduction potentials E_h of anodic and cathodic peak currents was 0.061 ± 0.002 V, confirming the diffusive nature of the process.

The catalytic currents registered in the presence of both ABTS (60 µM) and HA were higher than when only one component was present in the solution (Fig. S4). In fact, at the boundary layer the WE oxidizes the ABTS to the $ABTS^{\cdot+}$; the radical cation is then chemically reduced by HA and regenerates the non-radical reduced form, ABTS, which is again oxidized at the WE:

$$ABTS \rightleftarrows ABTS^{\cdot+} + 1e^-$$

$$ABTS^{\cdot+} + HA \rightarrow ABTS + HA^{\cdot}$$

The catalytic peak currents increased linearly with the concentration of HA up to 0.5 g L^{-1}. To calculate the pseudo-first order kinetic constant (k_f) it is necessary to reach the stationary state, where the homogeneous regeneration reaction (i.e. $ABTS^{\cdot+}$ reduction by HA) occurs quantitatively

during the potential sweep. When these conditions apply, the voltammetric response is no longer a peak but assumes a sigmoidal shape and no backward (anodic) peak is found. These conditions were reached at an ABTS concentration of 3 µM (Fig. 5 and S5). The k_f constants for HA_{ox} and HA_{red} were calculated as suggested by Nicholson (1965):

$$k_f = (0.4463\ \frac{i_{lim}}{i_d})^2\ \frac{nFv}{RT[HA]}$$

where i_{lim} is the plateau current, i_d is the peak current when only ABTS is present in solution, n is the number of e^- involved in the reaction (in this case 1), F is Faraday's constant (96,487 C mol^{-1}), v is the scan rate (0.010 V s^{-1}), R is the ideal-gas constant (8.31 J), T is the absolute temperature (298 K) and [HA] is the concentration of HA_{ox} or HA_{red} (g L^{-1}) which allows reaching of the stationary state (indicated by arrows in Fig. 5b). The calculated values were 9.5 and 13.8 L s^{-1} g^{-1} for HA_{ox} and HA_{red}, respectively. This indicated that, compared to HA_{ox}, HA_{red} can donate electrons faster (~30 %) to the radical form $ABTS^{\cdot+}$. Compared to HA_{red}, HA_{ox} therefore possess electron donating groups which are more sterically challenged and for this reason better protected from oxidation. On the other hand, for the same reason, they must concomitantly possess exposed electron accepting groups, which correspond to the ones reduced during anaerobic incubation.

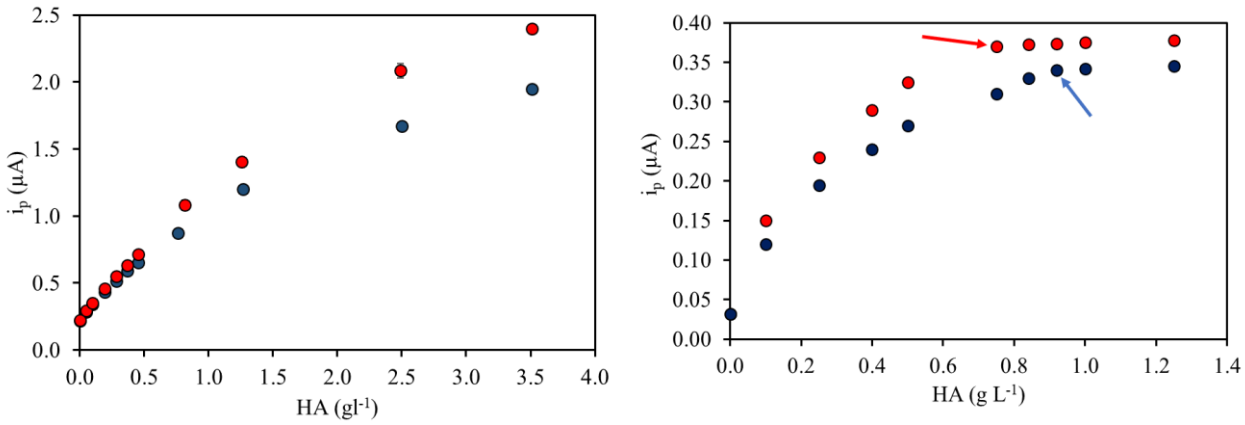

Fig. 5. Dependency of the oxidative peak current (i_p) on HA_{ox} (blue symbols) and HA_{red} (red symbols) concentration when 60 µM (**a**) or 3 µM (**b**) ABTS is present in solution. In b arrows indicate the considered point for k_f calculation.

3.3 Quantitative effects

The quantitative effects of the aerobic/anaerobic incubation on the EDC of HA were quantified by MEO (Fig. 6). The charge response in the presence of both $ABTS^{\cdot+}$ and HA is directly proportional to the number of electrons, n_{e^-} (mol) transferred from HA to $ABTS^{\cdot+}$:

$$n_{e^-} = \frac{Q}{F}$$

where Q is the integrated charge (C) and F is the Faraday constant. The EDC ($mmol_{e^-}\ g_{HA}^{-1}$) of HA_{ox} and HA_{red} were calculated at different times by normalizing n_{e^-} to the mass of the sample.

MEO results clearly differentiated the quantitative effects of the aerobic and anaerobic incubations and confirmed the redox-active role of HA. The EDC values of HA_{ox} and HA_{red} were significantly different ($p<0.05$) and ~20 % higher after anaerobic incubation (Table 1).

The fact that peat HA exposed to a biologically active oxic environment still displays a substantial residual EDC is not surprising. Peat forms in anoxic environments and in its natural state all its components can be assumed to be in reduced conditions. Albeit subject to oxidation during excavation and further on during aerobic incubation, some residual ECD may persist in the absence of suitable electron acceptors. Moreover, sterical hindrance of reduced groups in HA_{ox}, probably contributes to their preservation in oxic environments.

Table 1. Electron donating capacity values ($mmol_{e^-}\ g_{HA}^{-1}$) of HA_{ox} and HA_{red} obtained from MEO at different times after the spike of HA in the cell. Values in parentheses indicate standard deviation of three replications.

	20 min	60 min	90 min
HA_{ox}	1.64 (0.05)	2.46 (0.08)	2.75 (0.09)
HA_{red}	1.96 (0.06)	3.12 (0.08)	3.47 (0.10)
HA_{ox}/HA_{red}	0.84	0.79	0.79

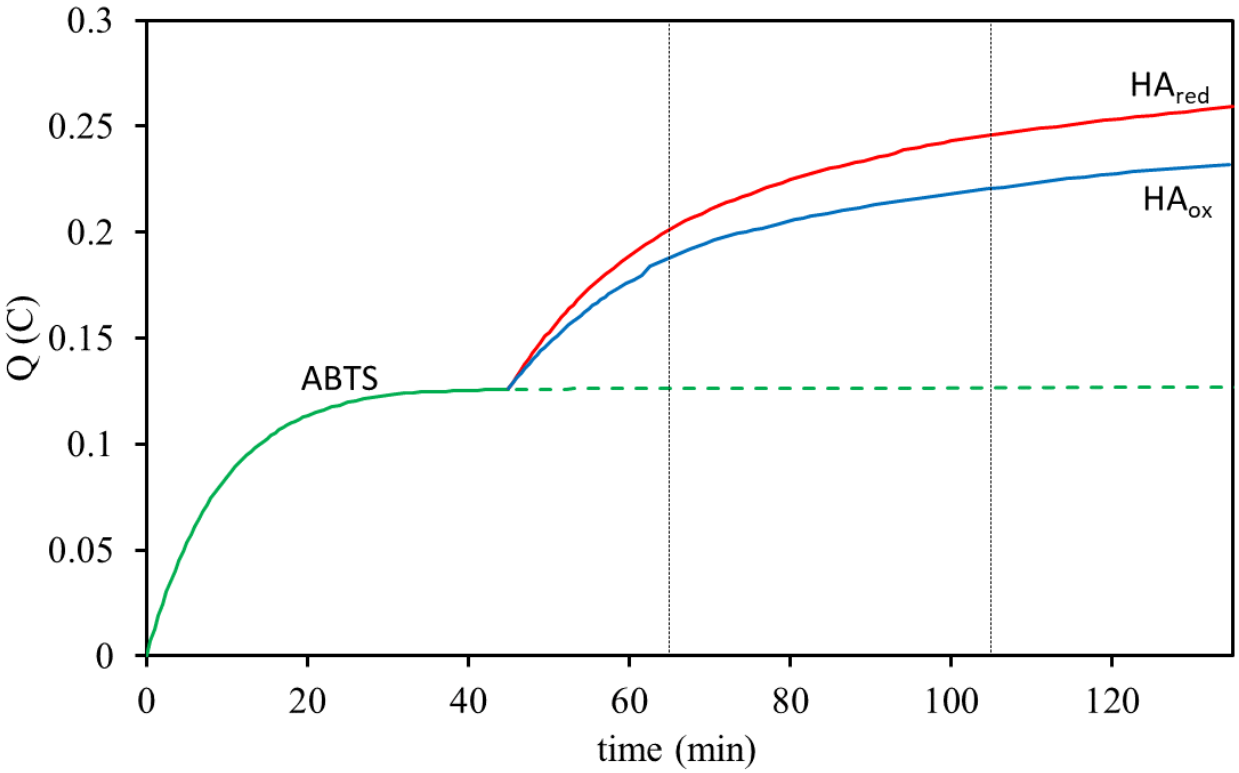

285 **Fig. 6.** Oxidative charge responses to a spike of ABTS (green line, spike added at time = 0) and to spikes of HA_{ox} (blue
286 line) and HA_{red} (red line) added to the ABTS solution after 65 minutes.
287

288 ## 4. Conclusions

289 This experiment confirmed that, even in their natural solid state, HA undergo chemical-
290 physical and structural changes that are coherent with their role as TEAs when exposed to the action
291 of facultative anaerobes, even in the absence of soluble inorganic redox carriers.

292 Incubation of peat for 90 days under conditions that strongly accelerate oxidative processes
293 (25°C, air insufflation, optimal humidity and substrate boosted biological activity) did not cause
294 exhaustion of the original EDC capacity of HA, which seemed to be only marginally affected. This
295 means, on one side, that drought periods lasting 3 months or less will not result in large alterations of
296 the overall availability of TEA during subsequent flooding. On the other side, the original EDC of
297 HA extracted from the not-incubated peat (that however had been excavated and air dried) seemed to
298 be close to saturation (~90%). This is confirmed by the fact that their EDC was not substantially

299 modified by incubation under strict anaerobic conditions with boosted biological activity. This
300 suggests that the EDC of peat are not readily modifiable by transient environmental conditions.

301 Climatic changes which may alter the hydrology of peat deposits might therefore have only
302 minor effects on the actual in situ availability of organic TEA. As a consequence, it is possible that
303 no substantial alterations will occur in future emissions ratios of CO_2 to CH_4 from peatlands unless
304 other factors may be involved in directing methanogenesis through different metabolic pathways, or
305 influence the efficiency of facultative anaerobes.

306 In fact, although quantitative changes might be relatively small, kinetic factors could
307 potentially impact microbial control on peat redox environment as electron transfer rates are
308 significantly modified by incubation under either aerobic or anaerobic conditions.

References

Aeschbacher, M., Graf, C., Schwarzenbach, R.P., Sander, M., 2012. Antioxidant properties of Humic Substances. Environ. Sci. Technol. 46, 4916-4925.

Aeschbacher, M., Sander, M., Schwarzenbach, R.P., 2010. Novel electrochemical approach to assess the redox properties of humic substances. Environ. Sci. Technol. 44, 87-93.

Barak, P., Chen, Y., 1992. Equivalent radii of humic macromolecules from acid-base titration. Soil Sci. 152, 184-195.

Bridgham, S.D., Cadillo-Quiroz, H., Keller, J.K., Zhuang, Q., 2013. Methane emissions from wetlands: biogeochemical, microbial, and modeling perspectives from local to global scales. Global Change Biology. 19, 1325-1346.

Cervantes, F.J., van der Velde, S., Lettinga, G., Field, J.A., 2000, Competition between methanogenesis and quinone respiration for ecologically important substrates in anaerobic consortia. FEMS Microbiology Ecology. 34, 161-171.

Davidson, E.A., Janssens, I.A., 2006. Temperature sensitivity of soil carbon decomposition and feedbacks to climate change. Nature. 440, 166-169.

Drake, H.L., Horn, M.A., Wüst, P.K., 2009. Intermediary ecosystem metabolism as a main driver of methanogenesis in acidic wetlands soil. Environmental Microbiology Reports. 1, 307-318.

Galand, P.E., Yrjälä, K., Conrad, R., 2010. Stable carbon isotope fractionation during methanogenesis in three boreal peatland ecosystems. Biogeosciences. 7, 3893-3900.

Gao, C., Sander, M., Agethen, S., Knorr, K.H., 2018. Electron accepting capacity of dissolved and particulate organic matter control CO_2 and CH_4 formation in peat soils. Geochim. Cosmochim. Acta. https://doi.org/10.1016/j.gca.2018.11.004

Inbar, Y., Chen, Y., Hadar, Y., 1989. Solid-state carbon-13 nuclear magnetic resonance and infrared spectroscopy of composted organic matter. Soil Sci. Soc. Am. J. 53, 1695-1701.

Ise, T., Moorcroft, P.R., 2006. The global-scale temperature and moisture dependencies of soil organic carbon decomposition: An analysis using a mechanistic decomposition model. Biogeochemistry. 80, 217–231.

Ise, T., Dunn, A.L., Wofsy, S.C., Moorcroft, P.R., 2008. High sensitivity of peat decomposition to climate change through water-table feedback. Nature Geoscience. 1, 763-766.

Keller, J.K., Bridgham, S.D. 2007. Pathways of anaerobic carbon cycling across an ombrotrophic-minerotrophic peatland gradient. Limnol Oceanogr. 52, 96-107.

Keller, J.K., Weisenhorn, P.B., Megonigal, J.P. 2009. Humic acids as electron acceptors in wetland decomposition. Soil Biol. Biochem. 41, 1518-1522.

Keller, J.K., Takagi, K.K. 2013. Solid-phase organic matter reduction regulates anaerobic decomposition in bog soil. Ecosphere. 4, 1-10.

Klüpfel, L., Piepenbrock, A., Kappler, A., Sander, M., 2014. Humic substances as fully regenerable electron acceptors in recurrently anoxic environments. Nature Geosci. 7, 195-200.

Lovley, D.R., Coates, J.D., Blunt-Harris, E.L., Phillips, E.J.P., Woodward, J.C., 1996. Humic substances as electron acceptors for microbial respiration. Nature. 382, 445–448.

Mikaloff Fletcher, S.E., Tans, P.P., Bruhwiler, L.M., Miller, J.B., Heimann, M., 2004. CH_4 sources estimated from atmospheric observations of CH_4 and its $^{13}C/^{12}C$ isotopic ratios: 1. Inverse modeling of source processes. Global Biogeochem. Cycles. 18, GB4004.

Miller, J.C., Miller, J.N., 2010. Statistics and chemometrics for analytical chemistry, 6th edn. Pearson, Harlow.

Nicholson, R.S., 1965. Theory and application of cyclic voltammetry for measurement of electrode reaction kinetics. Anal. Chem. 37, 1351-1355.

Nurmi, J.T., Tratnyek, P.G., 2002. Electrochemical properties of natural organic matter (NOM), fractions of NOM, and model biogeochemical electron shuttles. Environ. Sci. Technol. 36, 617-624.

R Development Core Team, 2018. R: A language and environment for statistical computing. R Foundation for Statistical Computing, Vienna, Austria.

Vile, M.A., Bridgham, S.D., Wieder, R.K., 2003. Response of anaerobic carbon mineralization rates to sulfate amendments in a boreal peatland. Ecological Applications. 13, 720-734.

Ye, R., Jin, Q., Bohannan, B., Keller, J.K., Bridgham, S.D., 2014. Homoacetogenesis: A potentially underappreciated carbon pathway in peatlands. Soil Biol. Biochem. 68, 385-391.

Ye, R., Keller, J.K., Jin, Q., Bohannan, B.J.M., Bridgham, S.D. 2016. Peatland types influence the inhibitory effects of a humic substance analog on methane production. Geoderma. 2016, 131-140.

CHAPTER 4

After verifying in Chapter 3 that humic acids can be directly oxidized/reduced by microorganisms, in this Chapter the mechanisms involved in the electron donating reactions concerning humic acids were evaluated. Different analytical techniques (EPR, cyclic voltammetry, coulometry and ABTS decolorization assay) were applied, and the obtained results were consistent among them.

Electrochemical analyses were performed in the laboratories of the group of Electrochemistry of the University of Udine. EPR analysis were performed in the laboratories of Embrapa Instrumentation Center. The author acknowledges the financial support provided by Research Traineeship TRA 2019-2 from the International Humic Substances Society.

Electron donating capacity of humic substances in relation to fast electron shuttling mechanisms at environmentally meaningful pH

C. Bravo[a,b],* R. Toniolo[a], M. Contin[a], L. Martin-Neto[c], O. R. Nascimento[d] and M. De Nobili[a]

[a] Department of Agricultural, Food, Environmental and Animal Sciences, University of Udine, via delle Scienze 208, 33100 Udine, Italy.

[b] Department of Life Sciences, University of Trieste, Via Licio Giorgieri 5, 34128 Trieste, Italy.

[c] Embrapa Instrumentação Agropecuária, CP 741, 13560-970 São Carlos-SP (BR).

[d] Institute of Physics of São Carlos (IFSC), University of São Paulo, CP 369, 1356970 São Carlos-SP (BR).

* Tel. +39 0432 558642; E-mail: carlo.bravo@uniud.it

Keywords: humic substances; ABTS, electron shuttling, kinetics

Abstract

Humic substances (HS) contain moieties, mostly quinones and phenols groups, covering a wide range of reduction potentials which can be used by the microbial community as terminal electron acceptors. Reduced HS exert also antioxidant functions, affecting the fate of reactive oxidants and preventing oxidative damage to biological membranes and molecules.

To quantitative estimate the electron donating capacity (EDC) of HS, the 2,2'-azino-bis(3-ethylbenzothiazoline-6-sulfonic acid) (ABTS) has been widely used. The two most common techniques used are the ABTS decolorization assay and mediated electrochemical oxidation.

An essential parameter that should be considered in every kinetic study is the time allowed to complete the reaction. However, it is not clear yet what is the time of reaction that should be chosen in order to obtain environmentally meaningful EDC values for HS.

To serve as suitable electron shuttles between facultative anaerobic bacteria and soil components HS should be able to accept electrons and transfer them relatively quickly: otherwise the micro-environment around microbial cells would become easily depleted in extracellular electron acceptors, polarizing the medium and blocking energy production from anaerobic respiration in a short time.

In this work, EPR spectroscopy, cyclic voltammetry and ABTS decolorization were used to investigate the kinetics of redox exchange between ABTS and HS in order to understand the mechanisms involved.

We found evidence of a two-stage mechanism of electron exchange which comprises both a fast and a slow transfer process and propose that these two stages might have different environmental roles.

1. Introduction

Humic substances (HS) are considered ubiquitous in both terrestrial and aquatic environments (Gaffney et al., 1996) and originate from the spontaneous reactions that take place, during the decomposition of natural organic matter, among the reactive intermediate products released in the process. Due to their recalcitrance, they often accumulate in soil (Filip and Tesarova, 2004) where they are involved in several biogeochemical processes, like carbon sequestration (McLeod et al., 2011), metal complexation (Zhang et al., 2015) and pollutant sorption (Schwarzenbach et al., 1990).

In environments such as peatlands and submerged soils, where oxygen is periodically not available for the microbial respiration, HS can act as terminal electron acceptors (TEAs) (Lovley et al., 1999; Klupfel et al., 2014), reducing methanogenesis (Heitmann et al., 2007). In fact, HS contain moieties covering a wide range of reduction potentials (Aeschbacher et al., 2011) which can be used by the microbial community. In these environments HS exert also antioxidant functions, affecting the fate of reactive oxidants (Aeschbacher et al., 2012) and preventing oxidative damage to biological membranes (Kulikova et al., 2005) and molecules (Tarasova et al., 2015). The redox activity of HS is mostly provided by quinones and phenols (Scott et al., 1998; Nurmi and Tratnyek, 2002).

The ability of HS to act as TEAs and antioxidants is strongly connected to their electron donating capacity (EDC), defined as the number of electrons ($mmol_{e^-}$) that can be donated per gram of HS. To quantitative estimate the EDC of HS, the redox mediator 2,2'-azino-bis(3-ethylbenzothiazoline-6-sulfonic acid) (ABTS) has been widely used. The two most common techniques used are the ABTS decolorization assay (Re et al., 1999) and mediated electrochemical oxidation (Aeschbacher et al., 2010).

An essential parameter that should be considered in every kinetic study is the time allowed to complete the reaction. However, it is not clear yet what is the time of reaction that should be chosen in order to obtain environmentally meaningful EDC values for HS. Klein et al. (2018) examined long term kinetics profiles of the scavenging activity of HS towards the ABTS radical by way of a Trolox equivalent antioxidant capacity (AOC) approach using the decolorization assay. They proposed that,

considering the slow kinetics displayed by HS, their end point EDC should be determined only after investigating the kinetic profile of the reaction, which may take several hours to reach the end point.

To serve as suitable electron shuttles between facultative anaerobic bacteria and soil components, HS should be able to accept electrons and re-oxidize relatively quickly: otherwise the micro-environment around microbial cells would become easily depleted in extracellular electron acceptors, polarizing the medium and blocking energy production from anaerobic respiration in a short time.

The aim of this work is to investigate the redox mechanism between ABTS and HS using EPR spectroscopy, cyclic voltammetry and the ABTS decolorization assay.

2. Materials and methods

2.1 Solutions

For the decolorization assay and EPR analyses, the oxidized ABTS radical ($ABTS^{\cdot+}$, Fig. 1) was chemically generated at pH 4.8 (in 0.1 M citrate buffer) and 7.0 (in 0.1 M phosphate buffer), following the method proposed by Re et al. (1999). Briefly, 38.4 mg of ABTS (7.0 mM) were dissolved in 10 ml of buffer and 6.6 mg of potassium persulfate ($K_2S_2O_8$, 2.45 mM final concentration) were added. The mixture was let in the dark at room temperature for 16 h before use.

Stock solutions (0.5 g L^{-1}) of Suwannee River Standard fulvic acids (SRFA) were prepared in 0.1 M citrate buffer (pH 4.8) and 0.1 M phosphate buffer (pH 7.0).

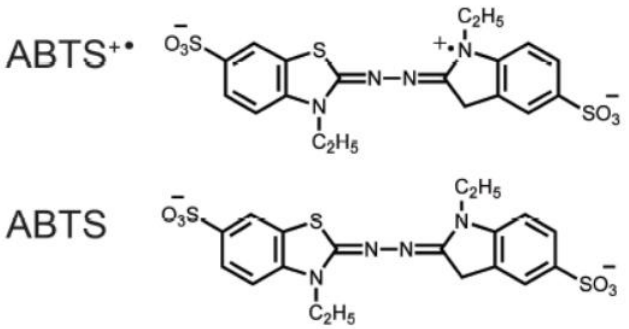

Fig. 1. Structure of the radical $ABTS^{\cdot+}$ and the parent ABTS.

2.2 ABTS decolorization assay

The Vis spectrum of the radical $ABTS^{\cdot+}$ displays an absorbance maximum at 734 nm, while the parent form does not absorb in the visible region (Fig. S1, Supporting Information). Within the range of $ABTS^{\cdot+}$ concentrations used in this study, the linear correlation (Walpen et al., 2016) between the concentration of the radical and its absorbance (A) at 734 nm (data not shown) was used to calculate the molar extinction coefficient ($\varepsilon = 15000\ mol^{-1}\ L\ cm^{-1}$).

Addition of increasing amounts of electron donating substances to an $ABTS^{\cdot+}$ solution causes the fading of the blue color, which typically accompanies the reduction of the radical to the parent form

The $ABTS^{\cdot+}$ stock solution was diluted to an initial absorbance of 0.7 at 734 nm (corresponding to a concentration of 46.67 µM). Then, spikes of SRFA (various final concentrations) were added to the spectrophotometric cell, mixed and the absorbance decrease at 734 nm was monitored for 9 min. One test was also performed monitoring the reaction for 72 h.

The self-decay of the radical was also monitored and for short periods of time (< 10 min) $ABTS^{\cdot+}$ can be considered stable. Prior to each analysis, the spectrum of a properly diluted $ABTS^{\cdot+}$ sample was recorded to measure the initial absorbance ($t = 0$, A_0). The stability of the radical was verified through proper time course registration of absorbance at 734nm.

Due to experimental limitations (mixing and opening/closing of the cell compartment of the spectrophotometer), it was not possible to record the initial absorbance decrement right after the addition of the SRFA spike, but recordings started after 15 seconds.

2.2 EPR

EPR analysis were performed at room temperature in a Cary Varian (E-109) spectrometer operating at X-band (9.5 GHz). All the analysis were performed in liquid using a 150 µL quartz flat cell containing inside a crystal of Cr(III)MgO (g = 1.9797) as paramagnetic marker.

The $ABTS^{\cdot+}$ stock solution was diluted before measurement in order to obtain an optimal signal intensity. Variable amounts of an SRFA stock solution (0.5 g L^{-1}) were then vigorously mixed with 300 µL of the $ABTS^{\cdot+}$ diluted solution in an Eppendorf tube and 150 µL of the mixture were transferred to the EPR flat cell, which was collocated in the resonance cavity. Measurements started precisely 1 min after mixing. In the presence of SRFA, the radical cation $ABTS^{\cdot+}$ is reduced to the non-radical form ABTS, which does not present EPR signal (data not shown).

At first, the course of the reaction was followed in two ways: a) EPR spectra were recorded over time, simulated using a Gaussian model and the calculated area was plotted against time. In this way each point of the curve corresponded to one single spectrum. b) the reaction was followed continuously fixing the magnetic field to the positive maximum of the $ABTS^{\cdot+}$ and measuring the relative intensity during the course of the reaction. Fig. S2 shows that the two methods did not present significant differences. For this reason, the method b) was applied to all the other cases. The relative concentration of $ABTS^{\cdot+}$ (c_{rel}) at a precise mixing time was calculated as:

$$c_{rel} = \left[\frac{I}{I_0}\right]_t,$$

where I is the signal intensity after adding SRFA and I_0 is the reference sample (only $ABTS^{\cdot+}$) (Brezova et al., 2009). The EPR signal of HS in the range of concentrations used during the experiments was negligible compared to the signal of $ABTS^{\cdot+}$ (<0.5 %) and therefore not considered in the calculations.

2.3 Cyclic voltammetry

Cyclic voltammograms (CVs) were recorded in a three-electrode cell (3 mm diameter glassy carbon working electrode, Ag/AgCl reference electrode, Pt counter electrode) containing solutions of i) Minnesota Peat HA (MPHA), Minnesota Peat FA (MPFA), Suwannee River FA (SRFA) (from the International Humic Substances Society); ii) ABTS (3-220 µM); iii) ABTS (60 µM) plus HA or FA (0.05-0.50 g L^{-1}). To determine the pseudo-first order kinetic constant k_f (Nicholson, 1965), CVs of

ABTS (3 or 60 µM) solutions were measured in the presence of increasing amounts of SFRA till a constant anodic peak current ($i_{p,a}$) was reached. All solutions were prepared in 0.1 M phosphate buffer (pH 7). The voltammetric cell was purged with nitrogen before recording each CV. The cathodic and anodic vertex potentials were fixed at Eh = -0.1 V and +0.7 V (scan rate 0.010 V s^{-1}). The working electrode was cleaned after each CV using 1.0 and 0.05 µm aluminum oxide on polishing pads, thoroughly rinsed with Milli-Q water and dried. The cleaning procedure was necessary to avoid any underestimation of the cathodic currents (Fig. S3).

3. Results and discussion

3.1 Cyclic voltammetry

CVs of solutions containing only SRFA were featureless, but displayed higher cathodic currents compared to the background (Fig. S3). This suggests a sluggish electron transfer from HS to the working electrode. Compared to FA, HA have a higher passivation effect on the WE.

For this reason, as suggested by Aeschbacher et al. (2012), ABTS was used to mediate the electron transfer from oxidable moieties in HA to the WE:

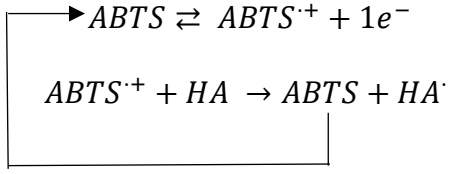

An exhaustive voltammetric characterization of the mediator ABTS is reported in Scott et al. (1993).

In the presence of increasing concentration of HS, the catalytic anodic peak current ($i_{p,a}$) of ABTS increased linearly up to 0.5 g L^{-1} (insert in Fig. 2), showing that the radical had been proportionally reduced. Addition of different types of HS resulted in significantly different slopes of $i_{p,a}$ versus HS concentration regression models. This indicates that HS of different origin, present a different capacity to reduce the $ABTS^{\cdot+}$ and therefore EDC, namely in the order MPHA > MPFA > SRFA.

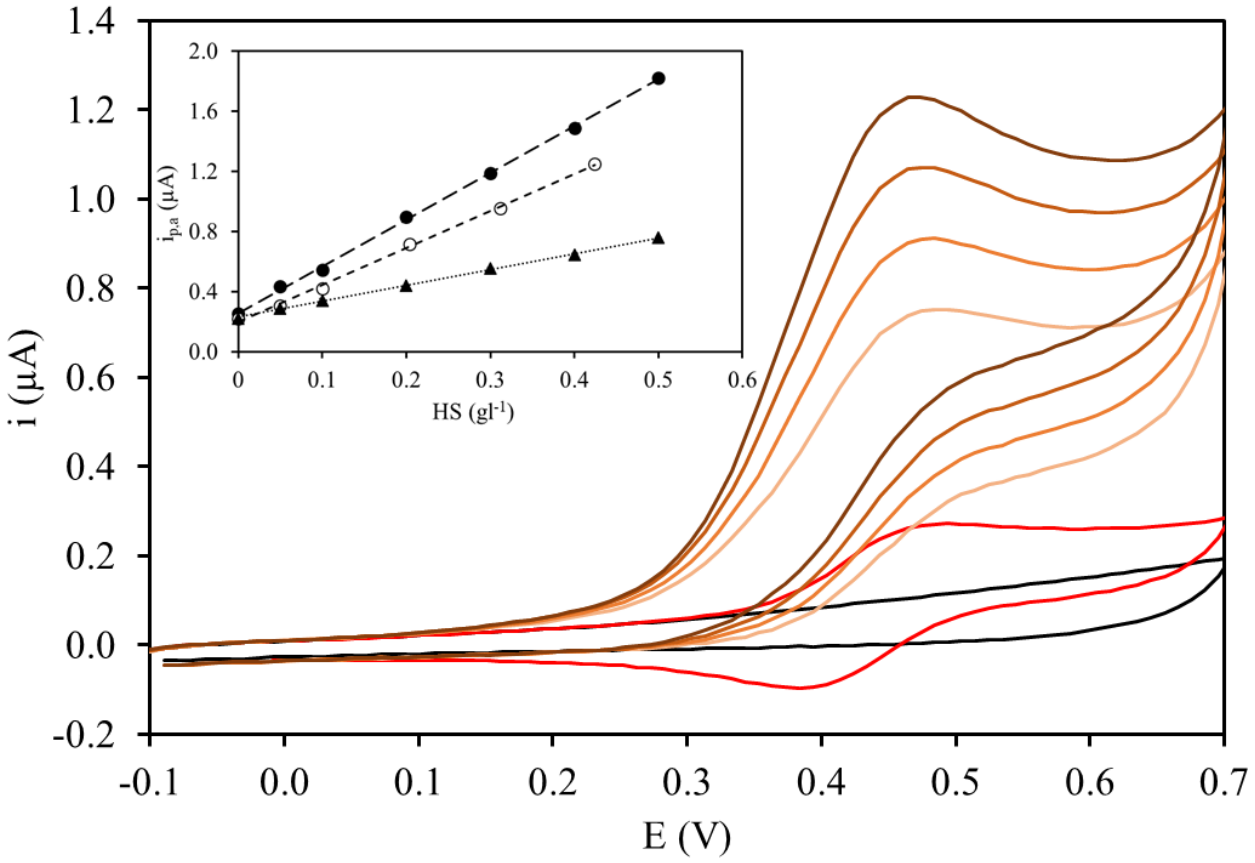

160 **Fig. 2.** Cyclic voltammograms (CVs) of solutions containing only: the background electrolyte (black trace); 60 µM
161 ABTS (red trace) and both ABTS and SRFA (0.2-0.5 gL^{-1}). The insert shows the linear dependency of the oxidative
162 peak current ($i_{p,a}$) on SRFA (▲), MPFA (○) and MPHA (●) concentration.
163

164 By increasing the concentration of HS in the electrochemical cell, while maintaining constant
165 that of $ABTS^{\cdot+}$, a stationary state is eventually reached, at which the homogeneous step (i.e. $ABTS^{\cdot+}$
166 reduction by SRFA in solution) occurs quantitatively and therefore $i_{p,a}$ current does not vary anymore
167 upon addition of HS. In the presence of an excess amount of HS, as shown for SRFA (Fig. 3) the
168 reaction can be considered of pseudo-first order. Under these pure kinetic conditions, the plateau
169 current is proportional to the root square of the pseudo-first order kinetic constant k_f (Nicholson,
170 1965). The calculated k_f values, for 3 or 60 µM ABTS, were respectively 2.61 ± 0.11 and 2.50 ± 0.12
171 L s^{-1} g^{-1}. The fact that these two values were not significantly different ($p<0.05$) confirms the
172 reliability of the method.

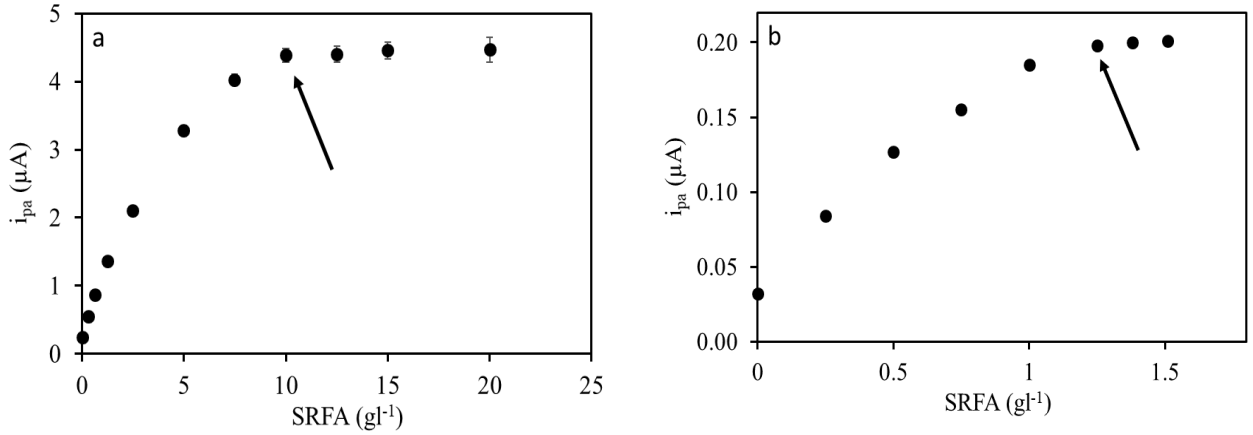

Fig. 3. Dependency of oxidative peak current ($i_{p,a}$) on SRFA concentration recorded in the presence of 3 (**a**) and 60 (**b**) µM ABTS. Arrows indicate the point at which the plateau current was reached.

3.2 ABTS decolorization assay

The time course of the relative concentration of $ABTS^{\cdot+}$ (c_{rel}) remaining in the cell after addition of increasing quantities of SRFA is reported in Fig. 4. Recording the decrease of A_{734} it is possible to visualize that the initial rapid reduction of $ABTS^{\cdot+}$ (0-15 s) is followed by a much slower, but steady decline in the concentration of the radical. The reduction reaction does not apparently reach a stable endpoint: not only a defined transfer of electrons from SRFA to $ABTS^{\cdot+}$ was not achieved within the time allowed for the experiment (9 minutes), but even prolonging the reaction time to 72 hours did not result in complete stabilization. The same trend was found also for the other types of HS, both at acid and neutral pH (data not shown).

This behavior differs from that displayed by strong model antioxidants such as Trolox: the electron exchange with $ABTS^{\cdot+}$ is fast and the stable end-point is reached in less than one minute, Fig. 5), the same results are obtained by coulometry (data not shown).

The EDC of SRFA, expressed as $mmol_{e^-}\ g_{SRFA}^{-1}$, was calculated considering the decrease in absorbance at 734 nm measured 30 s after the addition of the SRFA spike in the cell ($\Delta A = A_{30} - A_0$). Since the decrease in absorbance corresponds to the reduction of $ABTS^{\cdot+}$ to ABTS, and the process is monoelectronic, it is possible to calculate the µmol of e^- transferred from SRFA to $ABTS^{\cdot+}$:

$$\mu mol_{e^-} = \frac{\Delta Abs}{\varepsilon} * 10^6 * \frac{V_{cell}}{10^3}$$

where V_{cell} is the volume of the solution after the addition of SRFA and 10^6 and 10^3 are conversion factors. To calculate the EDC it is just necessary to normalize the transferred µmol of e^- to the mass of SRFA in the cell:

$$EDC = \mu mol_{e^-}/mg_{SRFA} = mmol_{e^-}\ g_{SRFA}^{-1}$$

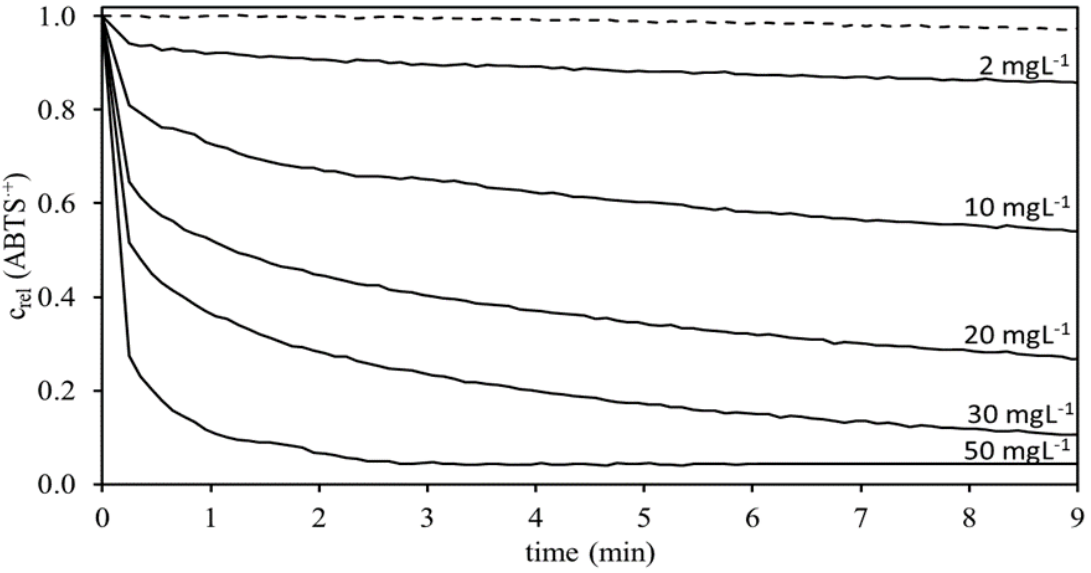

Fig. 4. Time trend of the decrease in the concentration of ABTS$^{\cdot+}$ (expressed as relative concentration compared to t_0), corresponding to the reduction of ABTS$^{\cdot+}$ to ABTS, after the addition of increasing amounts of SRFA. Dotted line represents the auto-decay of ABTS$^{\cdot+}$.

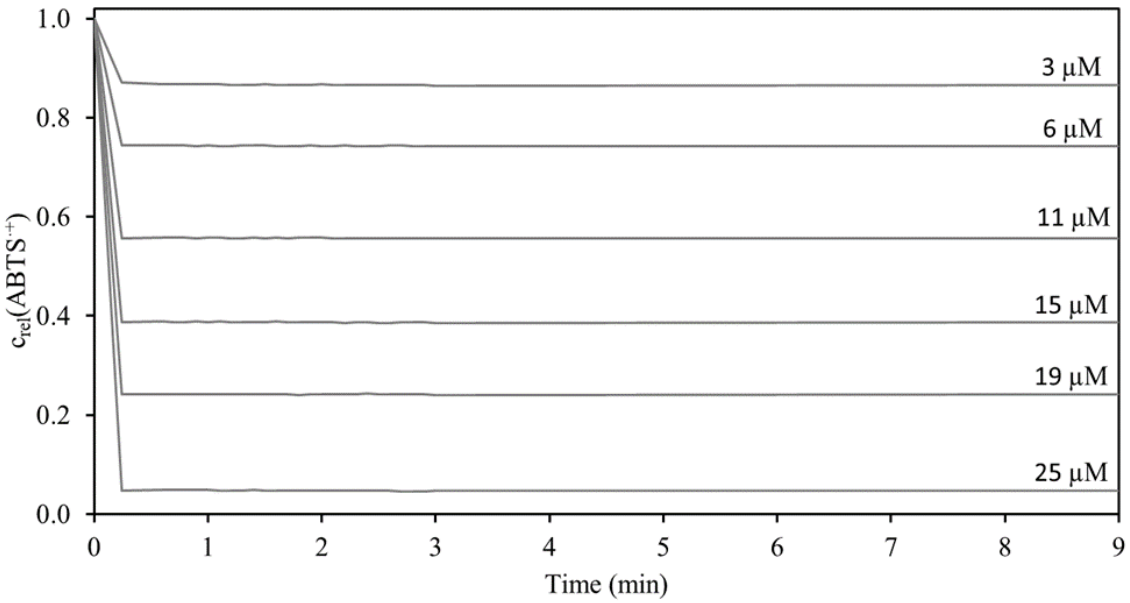

Fig. 5 Time trend of the decrease in the concentration of ABTS$^{\cdot+}$ (expressed as relative concentration compared to t_0), corresponding to the reduction of ABTS$^{\cdot+}$ to ABTS, after the addition of increasing amounts of Trolox.

As shown in Fig. 4 and Fig. 5, for the same amount of time (we considered 30s), higher concentrations of SRFA (or Trolox) in the cell lead to a higher reduction of $ABTS^{\cdot+}$ to ABTS and consequently the $ABTS^{\cdot+}$ concentration decreases (Fig. 6). Accordingly, for definition, the EDC (calculated after 30 seconds of reaction, EDC_{30}) is the slope of the curve obtained interpolating the experimental points. Also in this case the trends are different: i), for SRFA (Fig. 6a) it assumes a negative exponential trend (for low concentration of SRFA (< 10 mg L^{-1}) the correlation is linear). Considering a linear model (red dotted line in the figure), at high concentrations of SRFA there is and under-reduction of the radical $ABTS^{\cdot+}$ and, consequently, an under-estimation of the EDC_{30} value; ii) for the Trolox the correlation is linear, no matter the concentration; iii) in both cases, once the radical $ABTS^{\cdot+}$ is completely reduced, adding in the cell higher concentration of antioxidant (>60 mg L^{-1} for SRFA and >25 µM for Trolox) does not create a different situation.

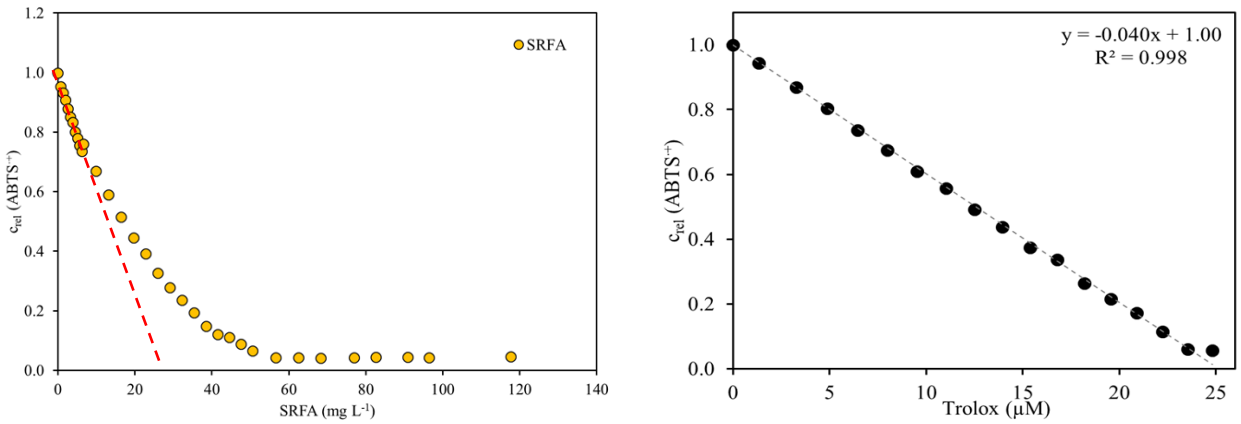

Fig. 6. Relative concentration of $ABTS^{\cdot+}$, measured after 30 seconds of reaction, versus the SRFA (a) and Trolox concentration

3.3 EPR

The EPR spectrum of $ABTS^{\cdot+}$ presents a complex hyperfine (due to electron spin interaction with nuclear spin) and superhyperfine (due to electron spin interaction with close nuclear spins) overlapping of signals (Fig. 7a). Increasing the modulation amplitude from 0.2 to 1.0 G, the spectrum become a broad Lorentzian singlet and the maximum positive intensity can be easily detected (Fig.

7b). The spectrum is centered at g = 2.0050 ± 0.0002, displaying an intermediate value between those reported by Scott et al. (1993) and Osorio et al. (2011).

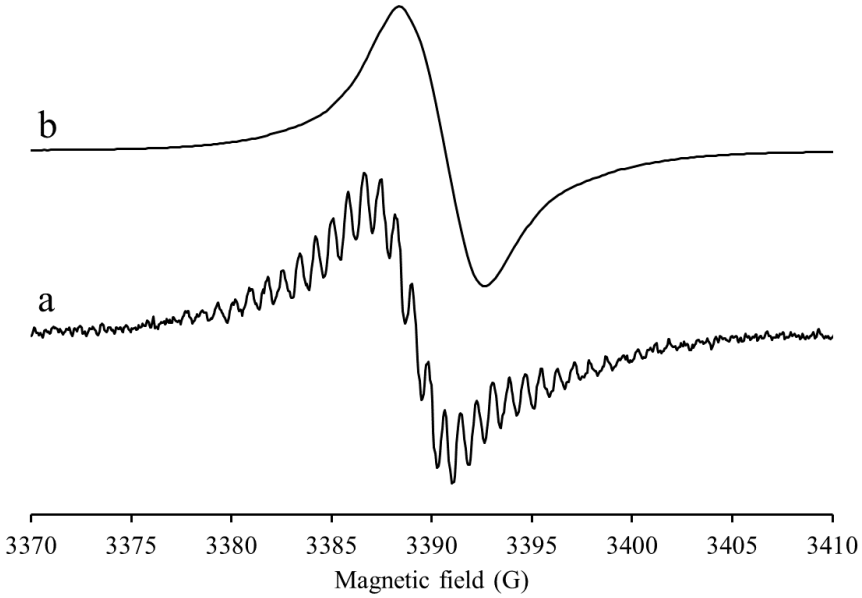

Fig. 7. EPR spectrum of $ABTS^{\cdot+}$ at modulation amplitude of 0.2 (**a**) and 1.0 G (**b**). In spectrum **a** lines are caused from the hyperfine and superhyperfine structures.

Fig. 8 shows the decrease of the relative $ABTS^{\cdot+}$ concentration at pH 4.8 after the addition of SRFA at three different concentrations (0.06, 0.12 and 0.18 g L^{-1}). The EPR signal of $ABTS^{\cdot+}$ rapidly decrease within a short time period and then the reaction between the radical and SRFA continued more slowly, without reaching a stable endpoint. The same trend was found also for the other tested HS, in both acid and neutral pH solution (data not shown).

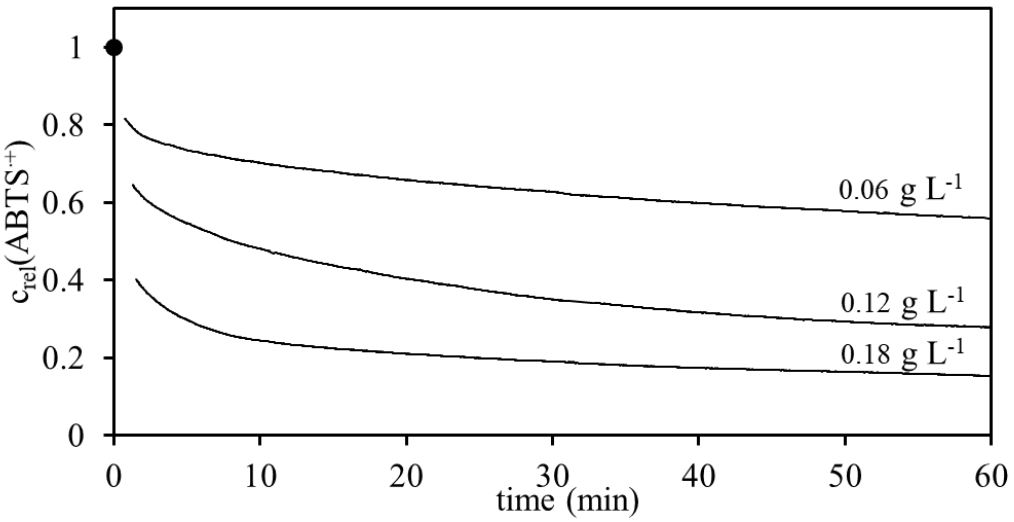

Fig. 8. Relative concentration (c_{rel}) of $ABTS^{\cdot+}$ after the addition of SRFA at different final concentrations (0.06, 0.12 and 0.18 g L^{-1}). The black point indicates the c_{rel} at t_0.

The reaction between $ABTS^{\cdot+}$ and SRFA is also pH depending. Under the same experimental conditions (same $ABTS^{\cdot+}$/SRFA initial ratio), the radical cation is more intensely reduced at pH 7 compared to pH 4.8 (Fig. S5). This could be explained considering that at higher pH i) phenolic groups are more dissociated and ii) their molecular conformation is more expanded, with the consequent enhancement exposure of reactive functional groups.

3.4 Data modeling

The experimental curves of the time trend of the decrease in the concentration of $ABTS^{\cdot+}$ after the addition of different amounts of SRFA (Fig. 5) can be plotted considering the total $ABTS^{\cdot+}$ concentration in the cell (μM instead of c_{rel}, Fig. S6).

The experimental curves were modeled (OriginLab software) considering two first order reactions and one residual term ($[ABTS]_{res}$):

$$[ABTS]_t = [ABTS]_1 * e^{-k_1 t} + [ABTS]_2 * e^{-k_2 t} + [ABTS]_{res}$$

where k_1 and k_2 are kinetic constants (min^{-1}), t is expressed in min and the $ABTS^{\cdot+}$ concentration is expressed in μM.

Results of the simulated parameters, upon the initial concentration ratios of antioxidants SRFA to $ABTS^{\cdot+}$ are reported in Fig. 9. They evidenced the presence of two different mechanisms, with two different kinetic constants ($k_1 > k_2$) until the radical is in excess compared to SRFA. In the opposite case, the fast reaction step predominates.

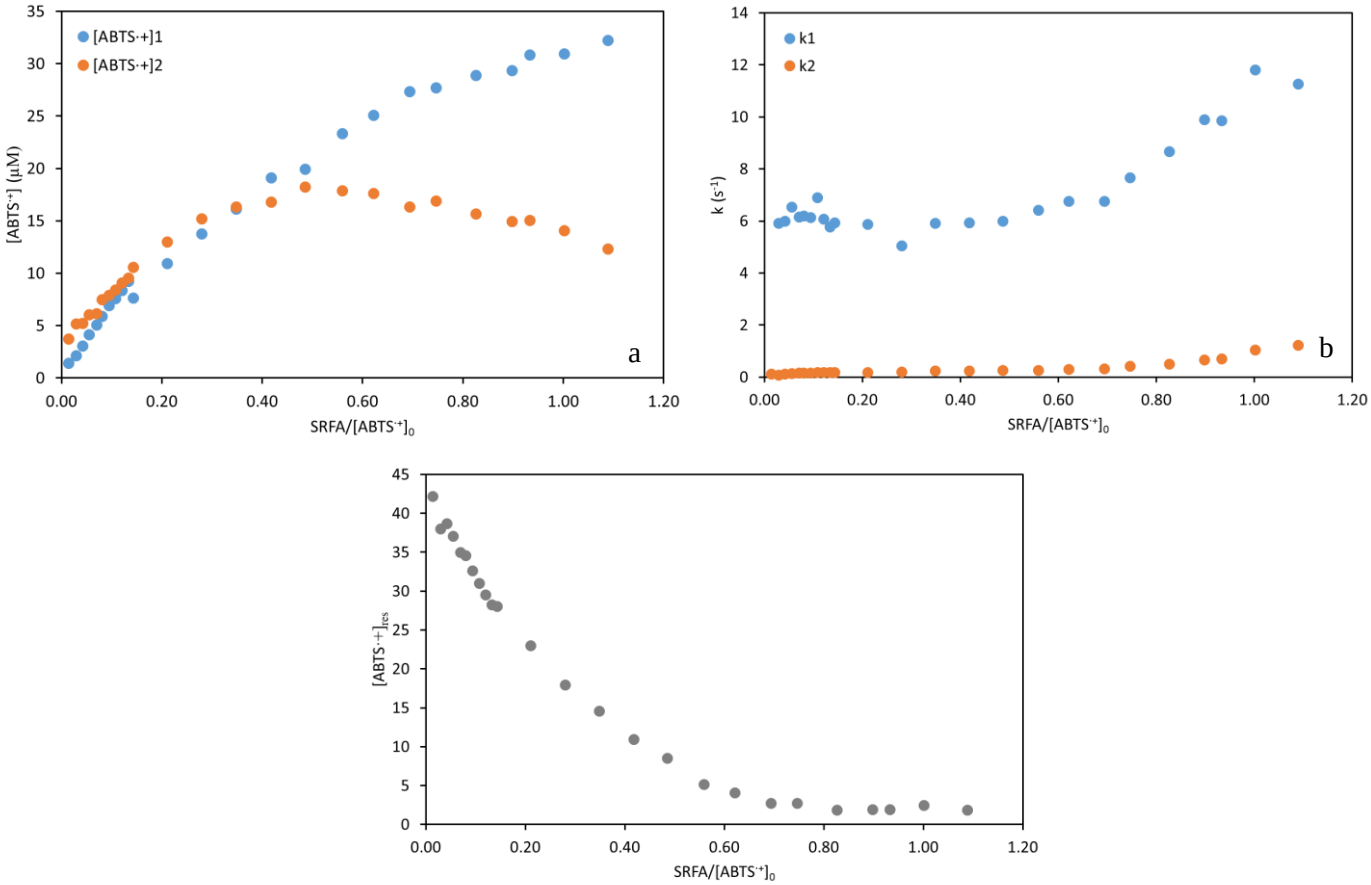

Fig. 9. Simulated parameters plotted against the initial concentration ratios SRFA/$ABTS^{\cdot+}$: **a.** $[ABTS^{\cdot+}]_1$ and $[ABTS^{\cdot+}]_2$; **b.** k_1 and k_2; **c.** $[ABTS^{\cdot+}]_{res}$.

4. Conclusions

This study demonstrated that different mechanisms are involved during the reduction of the mediator ABTS operated by humic substances. Some hypothesis can be made: i) the EDC of humic substances depends on the accessibility of reducing sites that can donate electrons; ii) there are mechanism that involve both the transfer of e^- and H^+ with different kinetics, iii) some secondary reactions can be established and kinetics of various order can overlap.

Considering the fast redox reactions that occur in soils and sediments, long reactions time when the $ABTS^{\cdot+}$ is used to calculate the electron donating capacity of humic substances are probably not environmentally relevant. However further studies are needed to better understand the possible mechanisms (and the environmental implications) involved in the slow reactions.

References

Aeschbacher M., Sander M., Schwarzenbach R. P. (2010) Novel electrochemical approach to assess the redox properties of humic substances. Environ. Sci. Technol. 44:87-93.

Aeschbacher M., Vergari D., Schwarzenbach R. P., Sander M. (2011) Electrochemical analysis of proton and electron transfer equilibria of the reducible moieties in humic acids. Environ. Sci. Technol. 45:8385-8394.

Aeschbacher M., Graf C., Schwarzenbach R. P., Sander M. (2012) Antioxidant properties of Humic Substances. Environ. Sci. Technol. 46:4916-4925.

Brezova V., Slebodova A., Stasko A. (2009) Coffee as a source of antioxidants: An EPR study. Food Chemistry 114:859-868.

Filip Z., Tesarova M. (2004) Microbial degradation and transformation of humic acids from permanent meadow and forest soils. Int. Biodeterior. Biodegrad. 54:225-231.

Gaffney J.S. Marley N.A. Clarks S.B. Humic and fulvic acids and organic colloidal materials in the environment. In: Gaffney J.S., editor; Marley N.A., editor; Clarks S.B., editor. Humic and Fulvic Acids: Isolation, Structure, and Environmental Role. American Chemical Society; Washington, DC: 1996. pp. 2–16

Heitmann T., Goldhammer T., Beer J., Blodeau C. (2007) Electron transfer of dissolved organic matter and its potential significance for anaerobic respiration in a northern bog. Global Change Biology 13:1771-1785.

Lovley D. R., Fraga J. L., Coates J.D., Blunt-Harris E. L. (1999) Humics as an electron donor for anaerobic respiration. Environmental Microbiology 1:89-98.

Klein O. I., Kulikova N. A., Filimonov I. S., Koroleva O. V., Konstantinov A. I. (2018) Long-term kinetics study and quantitative characterization of the antioxidant capacities of humic and humic-like substances. J. Soils Sediments 18:1355-1364.

Klüpflel L., Piepenbrock A., Kappler A., Sander M. (2014) Humic substances as fully regenerable electron acceptors in recurrently anoxic environments. Nature Geoscience 7:195-200.

Kulikova N., Stepanova E., Koroleva O. (2005) Mitigating activity of humic substances: direct influence on biota. In: Perminova I.V., Hatfield K., Hertkorn N. (eds) Use of humic substances to remediate polluted environments: from theory to practice. NATO Science series (Series IV: earth and environmental series), vol. 52. Springer, Dordrech.

Mcleod E., Chmura G. L., Bouillon S., Salm R., Björn M., Duarte C. M., Lovelock C. E., Schlesinger W. H., Silliman B. R. (2011) A blueprint for blue carbon: toward an improved understanding of the role of vegetated coastal habitats in sequestering CO_2. Front. Ecol. Environ. 9:552-560.

Nicholson RS (1965) Theory and application of cyclic voltammetry for measurement of electrode reaction kinetics. Anal. Chem. 37:1351-1355.

Nurmi J. T., Tratnyek P. G. (2002) Electrochemical properties of natural organic matter (NOM), fractions of NOM, and model biogeochemical electron shuttles. Environ. Sci. Technol. 36:617-624.

Osorio C., Carriazo J. G., Almanza O. (2011) Antioxidant activity of corozo (*Bactris guineensis*) fruit by electron paramagnetic resonance (EPR) spectroscopy. Eur. Food Res. Technol. 233:103-108.

Re R., Pellegrini N., Proteggente A., Pannala A., Yang M., Rice-Evans C. (1999) Antioxidant activity applying an improved ABTS radical cation decolorization assay. Free Radical Biology & Medicine 26:1231-1237.

Schwarzenbach R. P., Stierli R., Lanz K., Zeyer J. (1990) Quinone and iron porphyrin mediated reduction of nitroaromatic compounds in homogeneous aqueous solution. Environ. Sci. Technol. 24:1566-1574.

Scott S. L., Chen W. J., Bakac A., Espenson J. H. (1993) Spectroscopic parameters, electrode potentials, acid ionization constants, and electron exchange rates of the 2,2’-Azinobis(3-ethylbenzothiazioline-6-sulfonate) radicals and ions. J. Phys. Chem. 97:6710-6714.

Scott D. T., McKnight D. M., Blunt-Harris E. L., Kolesar S. E., Lovley D. R. (1998) Quinone moieties act as electron acceptors in the reduction of humic substances by humics-reducing microorganisms. Environ. Sci. Technol. 32:2984-2989.

Tarasova A. S., Stom D. I., Kudryasheva N. S. (2015) Antioxidant activity of humic substances via bioluminescent monitoring in vitro. Environ Monit Assess 187:89.

Zhang W., Zheng J., Zheng P., Tsang D. C. W., Qui R. (2015) The roles of humic substances in the interactions of phenanthrene and heavy metals on the bentonite surface. J. Soils Sediments 15:1463-1472.

CHAPTER 5

Humic acids are particularly important in aquatic environments, being recognized as redox active components of natural organic matter. In this work the contribution of autochthonous versus terrestrial carbon sources to HA was investigated in the Marano and Grado Lagoon (Northern Adriatic Sea, Italy).

This article was the result of the collaboration between the university of Udine, the university of Trieste and the Oceanographic institute of the university of Sao Pãulo (BR). This article was already published in the Journal of Soils and Sediments (https://doi.org/10.1007/s11368-019-02457-6).

Journal of Soils and Sediments
https://doi.org/10.1007/s11368-019-02457-6

SEDIMENTS, SEC 2 • PHYSICAL AND BIOGEOCHEMICAL PROCESSES • RESEARCH ARTICLE

Terrestrial-marine continuum of sedimentary natural organic matter in a mid-latitude estuarine system

Carlo Bravo[1,2] · Christian Millo[3] · Stefano Covelli[4] · Marco Contin[1] · Maria De Nobili[1]

Received: 20 February 2019 / Accepted: 4 September 2019

Abstract

Purpose Humic acids (HA) have several environmental roles, but are particularly important in aquatic environments, being recognized as redox active natural organic matter (NOM) components. We examined NOM in recent sediments of a low-energy coastal environment which is free from inputs of dissolved terrestrial HA as their solubility is suppressed by bonding with Ca^{2+} ions. Our aim is to investigate the contribution of autochthonous versus terrestrial C sources to HA and their fractions along a river-coastal lagoon transect.

Materials and methods Surface sediments were collected along the Aussa River (R), in the central basin of the Marano and Grado Lagoon (L) and within a secluded lagoon fish farm (FF). Extractable NOM components were obtained by extracting sediments first with 0.5 M NaOH (free NOM) and then with 0.1 M NaOH plus 0.1 M $Na_4P_2O_7$ (bound NOM). Extracts were separated into non-humic and humic fractions by solid phase chromatography. Organic carbon (C_{org}), total nitrogen (N_{tot}), $\delta^{13}C$, and $\delta^{15}N$ were determined with an Isotope Ratio Mass Spectrometer (Thermo Scientific Delta V Advantage) coupled with an Elemental Analyzer (Costech Instruments Elemental Combustion System). Fourier-transform infrared (FTIR) spectra were recorded with a FT-IR100 PerkinElmer Spectrometer. UV-vis spectra were recorded at pH 7 by a Varian Cary Spectrophotometer.

Results and discussion Both NOM and HA display typical traits of terrestrial origin in river sediments and of a more marine (algal) origin in lagoon and fish farm sediments. This trend is evident in free HA, whereas bound HA seem more influenced by terrestrial inputs. A larger proportion (60–70%) of non-humic C was extracted by NaOH in all samples. Bound HA differ from free HA for their C/N ratios, which are higher and vary within a much narrower range. The changes in HA's ^{13}C isotopic composition, FTIR spectra, and spectroscopic parameters ($SUVA_{254}$, S_R, and aromaticity) highlight a progressive mixing of terrestrial and marine substrates that either undergo in situ humification or are transported as materials sorbed onto suspended mineral particles.

Conclusions Our results highlight the existence of a complex, but continuous pattern of terrestrial and marine contributions to C sequestration and humification even in transitional environments where allochthonous humic C inputs are restricted due to insolubilization of humic substances by Ca^{2+}. Along the examined transect, the NOM and free and bound HA appear well differentiated. Terrestrial inputs contribute to the bound HA fraction via transported mineral particles in all the samples, no matter the environment encountered.

Keywords Humic acids · Lagoon · Natural organic matter · Sediments · Stable isotopes

Responsible editor: Nives Ogrinc

Electronic supplementary material The online version of this article (https://doi.org/10.1007/s11368-019-02457-6) contains supplementary material, which is available to authorized users.

✉ Carlo Bravo
carlo.bravo@uniud.it

[1] Department of Agricultural, Food, Environmental and Animal Sciences, Via delle Scienze 206, 33100 Udine, Italy

[2] Department of Life Sciences, University of Trieste, Via Licio Giorgieri 5, 34128 Trieste, Italy

[3] Oceanographic Institute, University of Sao Paulo, Praça do Oceanográfico 191, Sao Paulo 05508-900, Brazil

[4] Department of Mathematics and Geosciences, University of Trieste, Via Weiss 2, 34128 Trieste, Italy

Published online: 11 September 2019

1 Introduction

Coastal lagoons are highly productive transitional environments which act as an active interface between terrestrial and marine ecosystems, sustaining biodiversity and carrying out several invaluable ecosystem services (Aliaume et al. 2007). In particular, they are significant sinks of organic carbon (Tesi et al. 2007; McLeod et al. 2011) and play an important role in the global carbon cycle (Chmura et al. 2003). Accumulation of natural organic matter (NOM) in lagoon sediments is the result of a complex intermixing of organic materials from allochthonous and autochthonous sources, including dissolved and particulate river NOM (Otero et al. 2003; Andersson et al. 2018), marine NOM brought in by tidal currents, and organic materials produced in situ (Faganeli et al. 1981; Goñi et al. 2003; Berto et al. 2013). Humic substances (HS) are the major refractory components of NOM (Powlson et al. 2013). They consist of polydisperse heterogeneous mixtures of molecules which are formed during the decay of plant, animal, and microbial remains. They either derive from recalcitrant plant components (polyketides, which for energetic reasons are not readily utilized as substrates by microorganisms (Schnitzer and Monreal 2011)), from abiotic chaotic reactions of polyphenols with intermediate decomposition products, or from microbial metabolites (Stevenson 1982). All of these processes, which contribute to the gradual biochemical stabilization of organic C (C_{org}) and finally to C sequestration, imply that NOM develops an increasing phenolic character during humification.

In spite of their importance in the global C cycle and of their widely recognized ecological functions, the study of HS is not widespread in coastal environmental science. Yet they are particularly important in aquatic environments, because they possess imbedded quinones or quinone-like moieties which are well-known redox active NOM components (Ratasuk and Nanny 2007) and can act as reversible electron shuttles in the reduction of iron oxides (Lovley et al. 1998; Wolf et al. 2009; Roden et al. 2010; Klüpfel et al. 2014).

The stabilization of NOM against microbial decomposition also occurs by means of physical protection and chemical stabilization, due to insolubilization and Ca^{2+} binding (Six et al. 2002). In fact, sorption of NOM components, including humic acids (HA), on mineral surfaces is one of the main drivers of C sequestration and, in upland soils, a direct relationship exists between abundance of fine particles (silt and clay) and the amount of protected C (Scott et al. 1996; Six et al. 2002).

Sequential extraction of NOM, firstly by a solution of sodium hydroxide and then by an alkaline solution of pyrophosphate (able to disrupt cationic bridges), successfully highlights trends in terrestrial C stabilization caused by contrasting soil management practices (Olk et al. 1995; De Nobili et al. 2008). Sorption of HA on mineral particles is environmentally important as it modifies surface properties and interactions with hydrophobic contaminants, potentially toxic metals (Zhang et al. 2015) and ions (Wang et al. 2016). At the same time, the composition and humification degree of NOM affect the mobility of pesticides and emerging organic pollutants (Souza et al. 2016).

So far, most of the studies dealing with HS in estuaries and lagoons have focused on dissolved humic substances or have examined the sequestration of C_{org} in tidal sediments that receive dissolved organic carbon (DOC)–rich waters where the solubility of HA is not suppressed by the flocculation capacity of Ca^{2+} ions (Fooken and Liebezeit 2000; Uher et al. 2001; Mao et al. 2007). Under these circumstances, upon mixing of river waters with marine waters, dissolved terrestrial HA carried to the sea by rivers precipitate because of increasing salinity, masking in situ humification trends (Sholkovitz 1976). Concentration of Ca^{2+} ions regulates DOC leaching from most mineral soils (Kerr and Eimers 2012). However, in catchments where percolating water is constantly at equilibrium with calcite, solubility of humic substances is permanently depressed. The waters of the Marano and Grado Lagoon have concentrations of Ca^{2+} ions at saturation levels, because not only incoming freshwaters and sea water, but also the brackish waters of the lagoon itself are in equilibrium with calcium carbonate–rich sediments. Therefore, the Marano and Grado Lagoon does not receive inputs of allochthonous dissolved humic materials, nor does it contain a high concentration of dissolved humic C. It therefore represents an ideal environment to study in situ humification pathways of transitional environments, which can either operate on autochthonous organic residues or on transported organo-mineral and organic materials of either terrestrial or marine origin.

Besides being the third major transitional water body in the Mediterranean Sea, the Marano and Grado Lagoon is considered one of the best preserved (Petranich et al. 2017). The lagoon has been protected by the Ramsar Convention since 1971 and it is included in the "Natura 2000" network as a Site of Community Importance (SCI – IT3320037). The lagoon is at the same time an area of great economic importance, mainly due to fish farming and clam farming, with 55 fish farms covering an area of about 15% of the basin (De Vittor et al. 2012). Human activities date back to Roman times and, over the centuries, have caused typical morphological and sedimentological changes (Fontolan et al. 2012).

The aim of this work is to investigate the contribution of terrestrial versus marine sources of NOM and in particular of the organic C sequestered in HA along a transect which represents a gradual transition from river to marine conditions in a low-energy coastal environment, where HA solubility is suppressed by a relatively high Ca^{2+} content. To this purpose, surface sediments, representing the present state of the sedimentary processes, were sampled in this transitional environment, spanning from freshwater to mesohaline and from

polyhaline to euhaline water body types. To fully represent autochthonous sources, sediment samples were also taken from a secluded lagoon sector, which comprises a fish farm. The relative contribution of terrestrial versus marine HA is relevant for the geochemical characterization of transitional environments. In fact, humification of lignified plant residues of terrestrial origin can lead to HA which have a much higher phenolic character and can therefore be expected to be more redox active than HA derived from autochthonous sources (Ratasuk and Nanny 2007; Rimmer and Abbott 2011). For this reason, the origin and structure of HA could have a potential impact on the participation of NOM to the redox chemistry of sediments.

2 Materials and methods

2.1 Study area and sampling

The Marano and Grado Lagoon covers an area of approximately 160 km^2 extending for about 35 km, between the Tagliamento and Isonzo River estuaries, with an average width of 5 km. The lagoon is separated from the Adriatic Sea by a series of barrier islands spaced by tidal inlets. Tidal fluxes are semi-diurnal with a mean and spring tidal range of respectively 65 and 105 cm (Gatto and Marocco 1993). A regularly dredged channel, 8-m deep, separates the western sector, characterized by conspicuous inputs of fresh waters (mean rivers' discharge estimation of 81.5 $m^3\ s^{-1}$) and few areas above sea level, from the eastern sector which presents shallow waters and complex channel networks (Marocco 1995). Nutrient levels set the lagoon in the "medium eutrophication" category (Acquavita et al. 2015). The salinity gradient varies from very low (2–7) close to the Aussa River mouth to a maximum of 36 registered in summer at the tidal inlets (Brambati 1996).

The Aussa River is the main fluvial input to the central sector of the lagoon. It originates from karst springs located in the southern part of the coastal plain and joins the Corno River close to the mouth. Its total discharge varies from 8 to 20 $m^3\ s^{-1}$ (Covelli et al. 2009). Its hydrological basin covers about 60 km^2 and is characterized by several tributaries, drainage channels, and irrigation ditches.

The Valle Noghera fish farm, examined in this study, is the most extended of the all Marano and Grado Lagoon fish farms, covering an area of 220 ha, and it is located near the barrier islands of the Porto Buso basin (Ferrarin et al. 2010). Its ponds are isolated from the open lagoon by a perimetric embankment and the water exchange is automatically regulated by four sluice gates to maintain a constant water level. Gilt-head bream (*Sparus auratus*), bass (*Dicentrarchus labrax*), and gray mullet (*Mugil cephalus*) fish species are currently bred following an intensive practice with the use of industrial feed.

Surface sediments (0–2 cm) were collected in May 2015 using a stainless steel Van Veen grab, along the main axis of the Aussa River (R), in the central basin of the Marano and Grado Lagoon (L) and within the selected fish farm (FF) (Fig. 1). Geographical coordinates of sites are reported in Table 1. At each sampling site, three sediment subsamples were collected within an area of about 12 m^2 and pooled together to obtain a representative sample. After sampling, sediments were transferred into pre-cleaned bottles, transported to the laboratory and stored at −4 °C.

2.2 Analysis of sediments

A laser granulometer (Malvern Mastersizer 2000) was used for grain-size analyses; samples were previously treated with H_2O_2 for 48 h to remove organic matter and then wet-sieved through a 2-mm sieve.

Organic carbon (C_{org}) and total nitrogen (N_{tot}) of bulk sediments and HA (free and bound) were determined by an Elemental Analyzer (Costech Instruments Elemental Combustion System). The C_{org} was determined in bulk sediments, previously lyophilized and homogenized, after removing carbonates with 1 M HCl (Nieuwenhuize et al. 1994). Carbon and nitrogen stable isotope compositions in NOM ($\delta^{13}C_{NOM}$; $\delta^{15}N_{NOM}$) and HA fractions ($\delta^{13}C_{HA}$; $\delta^{15}N_{HA}$) were measured with an Isotope Ratio Mass Spectrometer (Thermo Scientific Delta V Advantage) coupled with the Elemental Analyzer (Costech Instruments Elemental Combustion System). Isotopic results were expressed in the usual δ notation in parts per mil (‰) versus the relative international standard: Vienna Pee Dee Belemnite (V-PDB) for carbon and atmospheric air for nitrogen. The analytical precision was < 0.1‰ and < 0.2‰ for $\delta^{13}C$ and $\delta^{15}N$, respectively, based on the standard deviations of replicate analyses ($n = 6$) of certified reference materials (caffeine IAEA 600 and L-glutamic acid USGS 40).

2.3 Sequential extraction and separation of non-humic and humic NOM

Non-humic (NH) extractable NOM and free and bound HA were obtained through a sequential extraction procedure (De Nobili et al. 2008) extracting air-dried and sieved sediments, firstly with 0.5 M NaOH (free HA and free NH) and then with 0.1 M NaOH plus 0.1 M $Na_4P_2O_7$ (bound HA and bound NH). Both extractions were carried out at 1:10 sediment/extractant ratios by shaking suspensions for 1 h under an inert atmosphere (N_2) to avoid oxidation in alkaline conditions. To separate the solid residues, suspensions were centrifuged (14,000 rpm for 20 min) and supernatants filtered through 0.2-μm cellulose filters. Free and bound HA were precipitated from the respective solutions with 96% H_2SO_4 at pH 1, allowed to settle overnight and then separated by centrifugation. After washing the

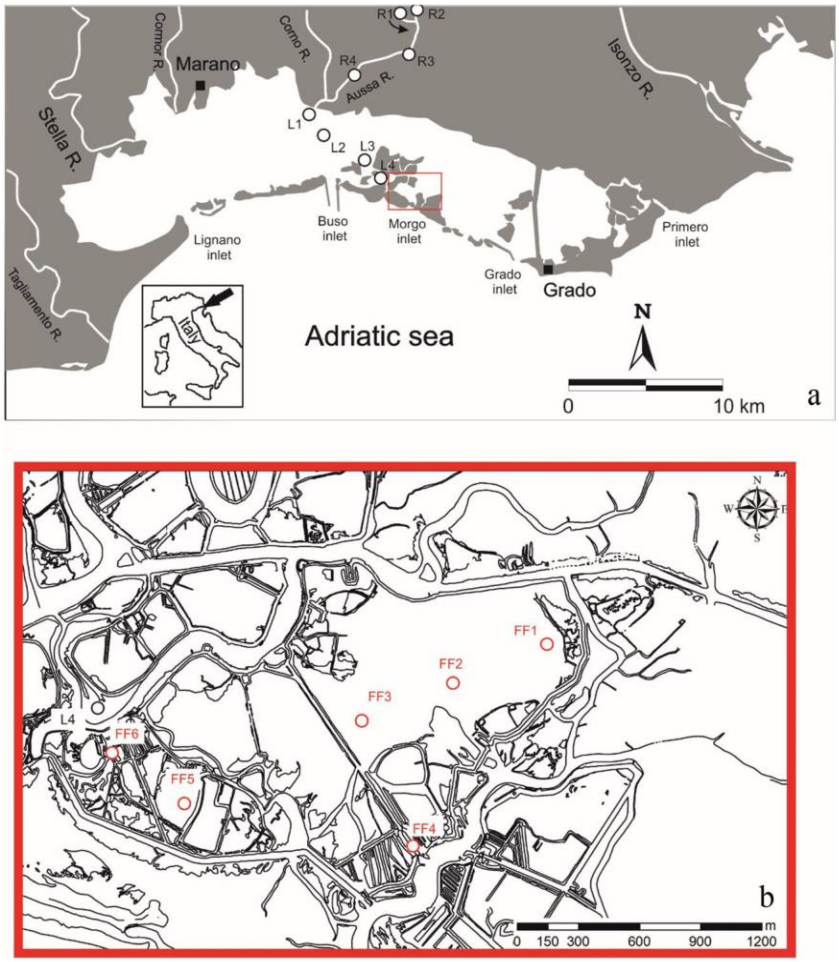

Fig. 1 Geographical location of the Marano and Grado Lagoon and of the sampling sites along the examined transect (**a**). Location of sampling sites within the fish farm (**b**)

precipitate with acidified water, HA were dialyzed against reagent grade water and checked against contamination by marine salts (Cl^- controlled with $AgNO_3$). Finally, HA were frozen and freeze-dried. The ash content, determined using 20 mg of freeze-dried HA in a muffle furnace at 550 °C for 4 h, was less than 4% in all samples.

The non-humic fraction of extractable NOM was separated from the humic (i.e., phenolic) fraction by solid phase chromatography (De Nobili and Petrussi 1988). Briefly, at first, 25 ml of filtrated sediment extract was acidified at pH < 2 with 96% H_2SO_4. Then the suspension was fed onto a 4 cm^3 column of insoluble polyvinylpyrrolidone (PVP), previously washed and equilibrated with 0.005 M H_2SO_4. The eluate, which represents the non-humic fraction, was collected in a 50-ml volumetric flask and diluted to volume with 0.005 M H_2SO_4. The retained humic fraction was eluted with 0.5 M NaOH and collected in a 25-ml volumetric flask. The organic carbon of the extracts was determined, after appropriate dilution and pH adjustment to neutral values, by high temperature catalytic oxidation and subsequent non-dispersive infrared spectroscopy and chemoluminescence detection (TOC-VCPN, Shimadzu).

2.4 Characterization of HA

Attenuated reflectance Fourier-transform infrared (ATR-FTIR) spectra were recorded with a FTIR spectrum (100 PerkinElmer Spectrometer) equipped with an ATR device, over an interval from 4000 to 500 cm^{-1}, with a 4 cm^{-1} resolution. A linear baseline correction was applied to compare spectra; the attribution of the main absorption bands was done according to Filip et al. (1988) and Giovanela et al. (2004). Intensity ratios were calculated for specific pairs of bands (Inbar et al. 1989).

All UV-vis spectra were recorded at pH 7 on a Cary spectrophotometer (Varian) in 1-cm quartz cuvettes and scanned from 200 to 600 nm. Specific absorbance (SA), calculated normalizing absorbance by the optical path length (cm) and the C concentration (mg l^{-1}), was plotted against the energy of radiation (eV).

E_{465}/E_{665} ratios were determined according to Chen et al. (1977). Calculation of aromaticity from UV-vis spectral data was carried out as presented by Roccaro et al. (2015), according to the following formulas:

$$\text{Arom}\ (\%) = 527 \times \text{SUVA}_{254} + 2.8 \quad (1)$$

Table 1 Geographic coordinates of sampling sites and granulometric composition, organic C (C_{org}), and total nitrogen (N_{tot}) content of sediments

Station	Latitude N	Longitude E	Sand %	Silt %	Clay %	C_{org} g kg^{-1}	N_{tot} g kg^{-1}	C/N
R1	45° 48′ 13.55″	13° 17′ 46.61″	26.9	68.1	5.0	57.6	4.8	11.9
R2	45° 48′ 27.55″	13° 18′ 16.38″	30.3	66.0	3.7	55.1	5.3	10.5
R3	45° 46′ 59.85″	13° 18′ 6.30″	15.7	76.7	7.7	35.4	4.2	8.5
R4	45° 46′ 6.58″	13° 15′ 37.90″	5.6	83.5	10.9	19.8	2.7	7.4
L1	45° 45′ 3.24″	13° 14′ 13.26″	30.9	61.5	7.6	7.5	1.1	6.6
L2	45° 44′ 30.49″	13° 14′ 37.50″	42.1	50.6	7.3	4.4	0.9	4.8
L3	45° 43′ 29.82″	13° 16′ 28.86″	14.3	78.3	7.4	15.3	2.0	7.6
L4	45° 42′ 52.44″	13° 17′ 7.98″	12.7	77.6	9.7	16.1	2.4	6.8
FF1	45° 43′ 4.02″	13° 18′ 50.16″	18.2	75.3	6.5	18.4	3.1	5.9
FF2	45° 42′ 57.30″	13° 18′ 24.72″	22.7	72.8	4.5	12.7	1.9	6.6
FF3	45° 42′ 51.78″	13° 18′ 13.62″	16.4	76.6	7.0	15.0	2.0	7.4
FF4	45° 42′ 32.16″	13° 18′ 23.82″	15.2	76.1	8.6	18.5	2.8	6.7
FF5	45° 42′ 39.66″	13° 17′ 30.12″	34.8	62.5	2.7	36.0	5.5	6.6
FF6	45° 42′ 45.12″	13° 17′ 17.76″	16.6	78.8	4.6	25.1	3.9	6.5

where $SUVA_{254}$ is the specific UV absorbance at 254 nm (l cm^{-1} mg^{-1});

$$\text{Arom}\ (\%) = 0.057 \times \varepsilon_{280} + 3.0 \quad (2)$$

where ε_{280} is the molar absorptivity at 280 nm (l m^{-1} mol^{-1}).

The slope ratio dimensionless parameter (S_R) was obtained calculating the ratio of the slope of the wavelength region 275–295 nm to that of the 350–400 nm wavelength region (Helms et al. 2008).

2.5 Statistics

All measurements were analytically replicated three times, based on oven-dried sediment and reported in tables and figures as mean ± standard error of the mean (SE). Kruskal-Wallis one-way analyses of variance and Mann-Whitney test were applied to compare C/N ratios. Difference between treatments was considered significant at $p < 0.05$. Regression analysis, test of significance of the correlation coefficient, and analysis of parallelism were carried out by R software (Miller and Miller 2010; Development Core Team 2018).

3 Results

3.1 Sediment and NOM characteristics

Grain-size composition, C_{org}, and N_{tot} contents of surface sediment samples are reported in Table 1. River sediments show a slight downstream enrichment in fine mineral particles, with clay contents increasing from 5.0% in the sampling station R1 to 10.9% at the river mouth (site R4). Sediments collected at the sampling sites L1 and L2, located near the inner lagoon coastline, but along the flanks of a periodically dredged channel in direct connection with the open sea, are much coarser and show 30.9 and 42.1% of sand, respectively. However, silt is the predominant grain-size fraction in all the three sections of the transect.

Accumulation of NOM increases with distance from the nearest tidal inlet, following a linear trend (Fig. 2). The strongest accumulation of NOM occurs in the freshwater section of the Aussa River: with a maximum (57.6 g C_{org} kg^{-1}) at the most upstream sampling site (site R1). Within the lagoon, the C_{org} content of surface sediments is relatively low (7.5–16.1 g C_{org} kg^{-1}), but larger values are found within the fish farm (12.7–36.0 g C_{org} kg^{-1}). Total nitrogen (N_{tot}) concentrations range from 1.1 to 5.5 g N kg^{-1} and follow a similar decreasing trend. However, average C/N ratios of NOM in

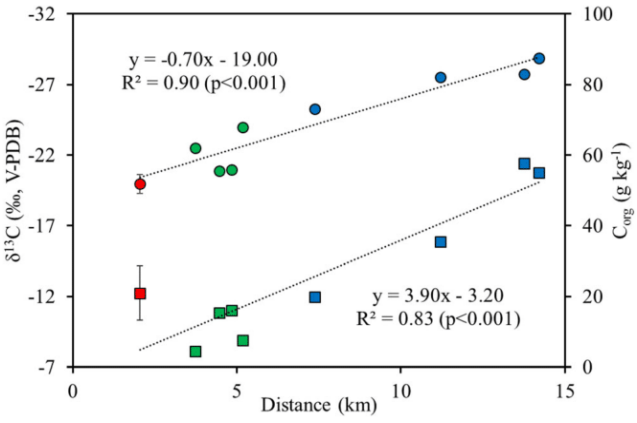

Fig. 2 Changes in C_{org} content (squares) and $\delta^{13}C$ values (circles) of sediment NOM along the sampling transect as a function of the distance (km) from the nearest lagoon inlet: river (blue symbols), lagoon (green symbols), and fish farm (red symbols). Fish farm values are given as a mean of all 6 sampling points; error bars indicate standard deviation

river sediments (Fig. 3) display values (average 9.6 ± 2.0) typical of well-humified soil NOM, whereas in lagoon and fish farm sediments, they display significantly lower values (on average C/*N* = 6.4 ± 1.1 and 6.6 ± 0.5, respectively).

The NOM also displays a linearly decreasing trend matching a progressive ^{13}C enrichment, moving along the transect from the mainland sites to the inner lagoon. In fact, the C_{org} of sediments becomes progressively less depleted in ^{13}C at decreasing distances from the nearest lagoon inlet and displays less negative $\delta^{13}C$ values (Fig. 2) which range from − 28.9‰ at R1 to an average of − 20.1 ± 0.7‰ in the secluded environment of the fish farm.

No clear trend is observed for $\delta^{15}N$ values. The ranges of $\delta^{15}N$ values of river and lagoon sediments practically overlap, with average $\delta^{15}N$ values of respectively 4.9 ± 0.6‰ and 5.1 ± 0.3‰. However, river and lagoon sediments are both significantly enriched in ^{15}N compared with those of the fish farm ($\delta^{15}N = 3.3 \pm 0.7$‰).

3.2 Amount and composition of extractable C_{org}

On average, total extractable C_{org} is about 21% of the C content of sedimentary NOM. In all samples, a larger proportion (58–72%) of non-phenolic, i.e., non-humic C_{org} (NH-C), was extracted during the first step of the sequential extraction (free C_{org}) compared with that extracted in the subsequent step (28–42%) (bound C_{org}). This indicates that the hydrophobic and aromatic humic fraction is preferentially bound to mineral surfaces by formation of cationic bridges compared with the more polar NH-C fraction. In fact, bound HA can only be solubilized by the action of $Na_4P_2O_7$, which complexes calcium and disrupts this kind of bonds (Olk et al. 1995). Overall, more humic C was extracted from river than from lagoon and fish farm sediments during both extractions. Moreover, bound HA are more abundant than free HA in all sediments (Fig. S1, Electronic Supplementary Material - ESM). The fraction of C_{org} stabilized in sediments as HA (free + bound) varies along the different sections of the transect. On average, only 6.7% of C_{org} is present in river sediments as carbon sequestered in free + bound HA. Carbon contained in HA is even lower in lagoon and fish farm sediments (5.9 and 3.9%, respectively).

While there is no relationship between total extractable C_{org} (C-extr) and the amount of free humic C in lagoon and fish farm sediments, a strong linear relationship ($R^2 = 0.93$, $p < 0.001$) exists between C-extr and bound humic C (Fig. 4). The carbon present in free HA represents a constant and relatively small part of the total extractable C_{org} in lagoon and fish farm sediments, whereas it increases linearly going upstream in river samples.

3.3 C/N ratios of free and bound HA

Bound HA well differentiate from free HA on the basis of their C/N ratios (Fig. 5) which are significantly higher than those of free HA. In all sediments, C/N ratios of bound HA vary within a narrow range and do not display any significant difference among the examined sections of the transect. On the contrary, river free HA are significantly different from fish farm free HA but not from lagoon free HA.

3.4 UV-vis spectroscopic parameters of free and bound HA

Specific absorbance (SA) spectra of free and bound HA are reported in the supplementary material (Fig. S2 - ESM). The values of SA at low wavelengths are stronger for river free HA (0.12 to 0.06 SA at 230 nm (5.39 eV)) and decrease in lagoon and fish farm sediments HA, ranging from 0.06 to 0.04 and from 0.07 to 0.035, respectively. Free HA spectra are characterized by a shoulder at 280 nm (4.43 eV). By contrast, the UV-vis spectra of bound HA are mostly featureless and, once again, display a much lower variability among the different transect sections. Only the spectra of bound HA extracted from fish farm sediments, albeit having comparable SA at low wavelengths, display a strong similarity with the free HA extracted from the same sediments. Spectral parameters of free and bound HA are reported in Table 2. Specific UV absorbances at 254 and 280 nm (i.e., $SUVA_{254}$ and ε_{280}) are commonly used to compare humic substances of different

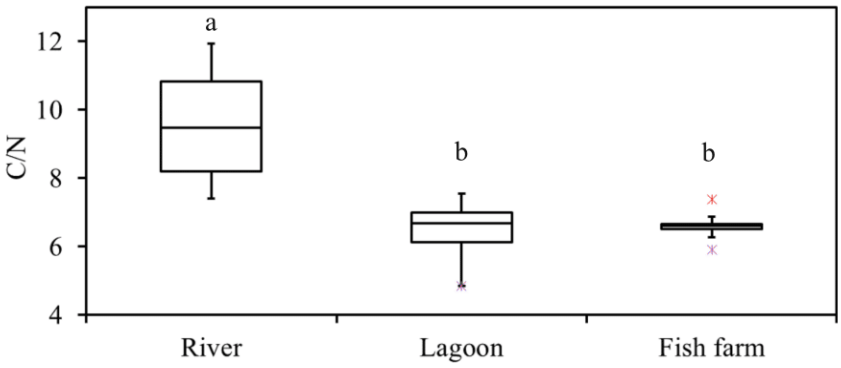

Fig. 3 C/N ratios of NOM in sediments from the three different environments along the transect: river, lagoon, and fish farm. The line within the box marks the median and the boundaries of the box indicate the 25th and 75th percentiles. Whiskers indicate the minimum and maximum; asterisks indicate outliers

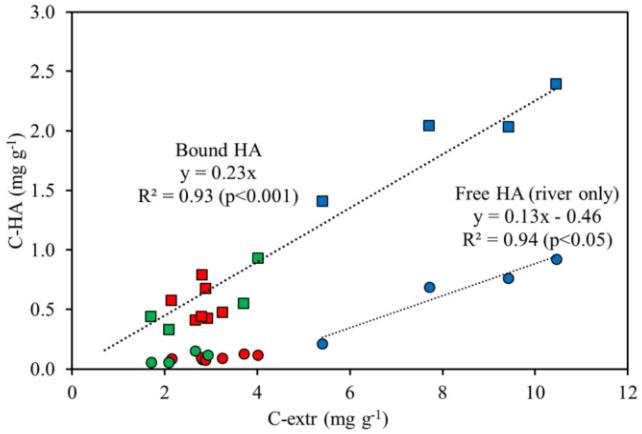

Fig. 4 Bound C-HA (squares) and free C-HA (circles) as a function of total extractable C_{org} (C-extr) in river (blue symbols), lagoon (green symbols), and fish farm (red symbols) sediments

origin (Peuravuori and Pihlaja 1997; Croué et al. 2000). Both $SUVA_{254}$ and ε_{280} of free HA reveal a relatively low contribution of aromatic structures, as well as their significant decrease passing from river to lagoon and fish farm sediments. Aromaticity values calculated from these parameters are consistent to one another and indicate a lower degree of aromaticity in the structure of lagoon and fish farm HA. Except free and bound river HA, which are not significantly different, in lagoon and fish farm samples, bound HA have a stronger aromatic character than the corresponding free HA.

The E_{465}/E_{665} ratio is also often considered linked to aromaticity, but in this case, there is no match with the aromaticity trend displayed by both $SUVA_{254}$ and ε_{280}. Furthermore, the E_{465}/E_{665} ratio was demonstrated to be better related to molecular size (Chen et al. 1977) than to aromaticity, and the decreasing E_{465}/E_{665} ratio would therefore indicate a progressive increase of molecular size from river to lagoon and fish farm free HA. Similarly to all the other spectroscopic parameters, the E_{465}/E_{665} ratio points out a closer similarity among bound HA in the different environments considered in this study. The slope ratio parameter (S_R), which was also found to be inversely related to molecular size (Helms et al. 2008), correlates positively with the E_{465}/E_{665} ratio and points out a clear increase in the average molecular weight of free HA fractions, whereas bound HA are again characterized by a much lower variability and do not display any definite trend.

3.5 Isotopic composition of HA

Stable C and N isotopic compositions do not allow discrimination between free and bound HA, but separate HA into distinct groups depending on their origin (Fig. 6). The HA of fish farm sediments are, however, less depleted in ^{13}C than river HA ($\delta^{13}C = -19.7 \pm 0.5‰$ and $-27.0 \pm 1.8‰$, respectively) and less enriched in ^{15}N compared with lagoon HA ($\delta^{15}N = 2.8 \pm 0.4‰$ and $5.1 \pm 0.3‰$, respectively). The other two groups differ only on the basis of their $\delta^{13}C$ values, with the river samples displaying the strongest ^{13}C depletion.

Both the NOM and HA of river sediments are more depleted in ^{13}C than lagoon sediments and the latter are less depleted than fish farm samples. The different nature of free HA in fish farm sediments from that of river and lagoon sediments is confirmed by the significant difference between both the slope and the intercept of their respective linear regression models of free HA and NOM $\delta^{13}C$ (Fig. S3 - ESM). Contrary to free HA, bound HA extracted from fish farm sediments fit a regression line that is not significantly different from that fitting river and lagoon samples.

3.6 FTIR spectra of HA

Average FTIR spectra of HA are reported in Fig. 7, while individual spectra are reported in the Supplementary Material (Fig. S4 - ESM).

All FTIR spectra exhibit the same typical bands, albeit with different intensities: O–H or N–H stretch around 3400–

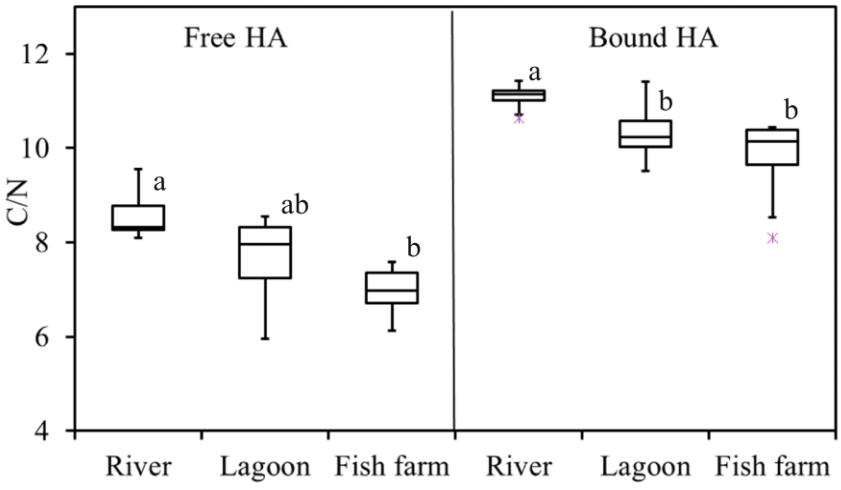

Fig. 5 C/N ratios of free HA and bound HA extracted from riverine, lagoon, and fish farm sediments. The line within the box marks the median concentration and the boundaries of the box indicate the 25th and 75th percentiles. Whiskers indicate the minimum and maximum; asterisks indicate outliers

Table 2 Average UV-vis spectroscopic parameters of free and bound HA. Values in parenthesis represent standard deviations

		E_{465}/E_{665}	S_R	$SUVA_{254}$	ε_{280}	Arom (%)	
				$l\ m^{-1}\ mg^{-1}$	$l\ cm^{-1}\ mol^{-1}$	from $SUVA_{254}$	from ε_{280}
Free HA	River	10.2 (2.1)	2.0 (0.3)	5.8 (1.6)	55 (15)	5.9 (0.8)	6.1 (0.9)
	Lagoon	6.5 (1.5)	0.5 (0.3)	3.7 (0.3)	32 (3)	4.7 (0.2)	4.9 (0.2)
	Fish farm	4.7 (0.9)	0.4 (0.1)	3.2 (0.5)	28 (6)	4.5 (0.2)	4.7 (0.3)
Bound HA	River	7.8 (1.3)	0.7 (0.1)	5.1 (0.4)	52 (5)	5.5 (0.2)	5.9 (0.3)
	Lagoon	6.6 (1.6)	1.0 (0.1)	5.6 (1.0)	57 (8)	6.0 (0.3)	6.2 (0.5)
	Fish farm	6.8 (0.7)	0.9 (0.2)	4.84 (1.4)	45 (16)	5.3 (0.7)	5.6 (0.9)

3300 cm^{-1}, aliphatic C–H stretching at 2930 cm^{-1}, carboxyl and ketonic carbonyl stretching at 1710 cm^{-1}, only visible as a shoulder merged with the much more intense 1650–1620 cm^{-1} (conjugated carbonyl C=O and aromatic C=C) absorption band. Absorption due to CH_2 bending, OH deformation, and C–O stretching of phenolic groups is visible in the region 1485–1400 cm^{-1}, C–O stretching and O–H deformation of COOH groups around 1200 cm^{-1} and stretching of carbohydrate or alcoholic C–O at 1040 cm^{-1}. However, free and bound HA spectra of river, lagoon, and fish farm samples are also well distinct, as well as the free and bound fractions extracted from the same sediment sample. The bound HA spectra qualitatively show the same bands of free HA, with some shifts and variations in intensity. However, these bands are broader and not well resolved, pointing out an increasing molecular complexity accompanied by a stronger contribution of intra and intermolecular H bonds. These features are coherent with the trends suggested by E_{465}/E_{665} and S_R values. Furthermore, there is a more intense absorption in the part of the spectrum related to functional groups of polysaccharides (1300–1150 cm^{-1}) and cellulose. In the spectra of bound HA, the 3600–3000 cm^{-1} region is more typical of intramolecular H-bonded phenolic groups which is coherently coupled with a stronger intensity of absorption at 1740 cm^{-1} by uncoupled C=O in xylanes (Rodrigues et al. 1998).

Stretching bands of C–H in methylene and methyl groups are more pronounced in bound HA, as indicated by the lower absorbance ratios of the 2930 cm^{-1} band with respect to the 1640 cm^{-1} band (Fig. S5 - ESM), indicating that hydrophobicity might be one of the driving forces promoting adsorption of bound HA to solid mineral surfaces.

On the contrary, the spectra of free HA are characterized by a larger contribution of secondary amides, testified by the combination of stronger N–H stretching bands at 3300–3250 cm^{-1} accompanied by weak bands at 3100 cm^{-1}, which are an overtone of the amide II band due to coupling of N–H bending and C–N stretching at 1530 cm^{-1}. A broad N–H wagging adsorption also appears at 750–650 cm^{-1}.

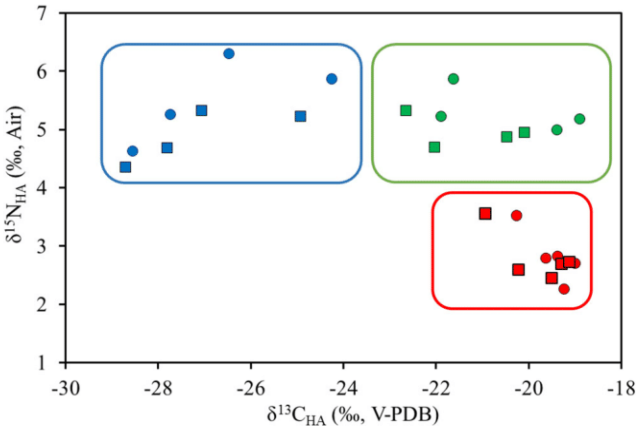

Fig. 6 C and N isotopic composition biplot of river (blue), lagoon (green), and fish farm (red) free (circles) and bound (squares) HA

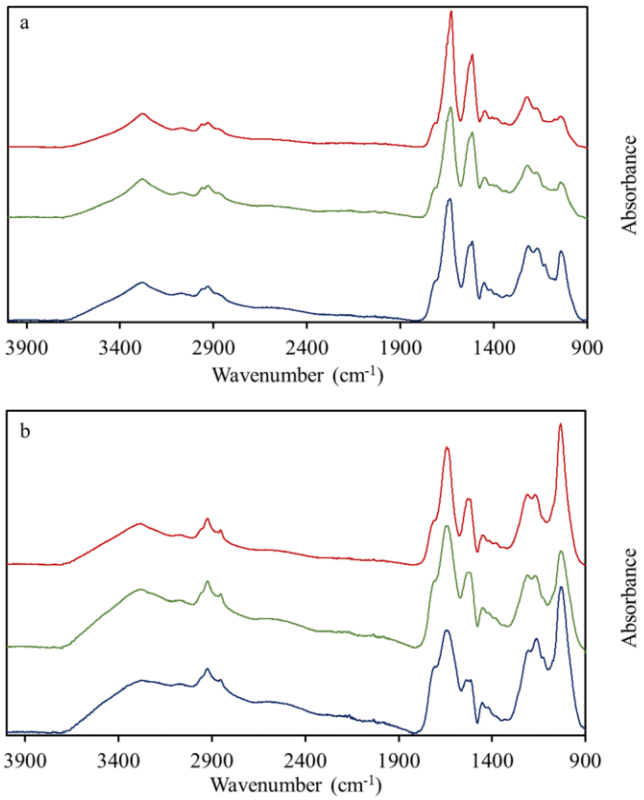

Fig. 7 Average FTIR spectra of free (**a**) and bound (**b**) HA from river (blue), lagoon (green), and fish farm (red)

These features are less marked in the river free HA, where the main bands of the spectrum (1164, 1039, and 858 cm^{-1}) highlight a strong contribution (C–O stretching and O–H bending absorption bands) of cellulose. On the other hand, the spectra of free HA extracted from the fish farm present the most intense bands at 1630 and 1516 cm^{-1}, which indicates a stronger contribution of amide groups. The aliphatic group stretching (2930 cm^{-1}) is weaker but relatively more intense than the nearby broad OH stretching. Lagoon free HA show an intermediate spectrum.

4 Discussion

Along the examined transect, the C_{org} content of sediments decreases from the mainland to the inner lagoon, showing a much higher potential of C sequestration of terrestrial versus tidal sediments. Tidal wetlands are considered important for C sequestration (Chmura et al. 2003), but allochthonous DOC inputs may substantially influence the overall C balance (Otero et al. 2003).

In most estuaries and lagoons, dissolved humic substances of terrestrial origin, which precipitate along with the salinity gradient, may represent a significative C addition to coastal sediments (Fox 1983; Kim et al. 2018), masking autochthonous contributions and in situ humification trends. The Marano and Grado Lagoon exclusively receives inputs from watersheds that, being in equilibrium with calcium carbonate–rich soils and sediments, may carry little dissolved NOM and, in particular, do not contain dissolved humic C. This situation is reflected by the fact that, in the river sediments stored, C density decreases from 0.03 inland to 0.01 g C cm^{-3} approaching the mouth of the river, displaying lower, but still comparable values with salt marsh average C densities (0.039 ± 0.003 g cm^{-3}) calculated by Chmura et al. (2003). Conversely, within the Marano and Grado Lagoon, values range between 0.004 and 0.008 g C cm^{-3} and are also much lower than those reported by van Ardenne et al. (2018) for lagoon sediments receiving dissolved NOM (0.021–0.030 g C cm^{-3}). This strongly differentiates the lagoons of the northern Adriatic Sea from most of the study sites of the transitional environments where the composition and accumulation of NOM have been studied.

In calcium-rich soils, the larger part of the refractory C stored in the humic C pool is bound to mineral surfaces by cationic Ca^{2+} bridges (Olk et al. 1998; Six et al. 2002; De Nobili et al. 2008). This is also true for the sediments examined in this study. The trend displayed by free HA in Fig. 4 may result from a lower tendency of lagoon and fish farm HA to be sorbed to mineral surfaces because of their lower aromatic character and stronger polarity, which is expected to favor solvation by water molecules.

The aromaticity of HA in the examined samples was calculated using two independent alternative formulas: both show a well-defined drop in aromatic moieties passing from the free HA of river sediments to lagoon and fish farm HA. On the contrary, bound HA appear to preserve most of their chemical and spectroscopic characteristics. Besides the relative lack of variability in C/N ratios, bound HA display, in fact, similar $SUVA_{254}$, aromaticity, E_{465}/E_{665} and spectral slope ratios (Table 2), as well as a much lower variability of intensity ratios for the most representative FTIR bands (Fig. S5 - ESM). The fact that their composition is much less affected by local environmental conditions is confirmed by the trend displayed by S_R values of free and bound HA with respect to the yearly salinity average (Ferrarin et al. 2010) of water at each sampling point (Fig. 8). This parameter, in fact, follows a strong inverse relationship ($R^2 = 0.96$, $p < 0.001$) with salinity in free HA, but a weak reverse trend ($R^2 = 0.39$, $p < 0.05$) in bound HA, confirming the autochthonous origin of free HA and the conservative nature of bound HA.

Analysis of $\delta^{13}C$ values has been recently shown to allow discrimination of upland river sediment versus streambed sediment due to marine algal contributions (Mahoney et al. 2019). On the contrary, $\delta^{15}N$ analysis does not allow discrimination of sediment sources due to the overlapping of nitrogen isotope composition of algae with that of upland sediments. In this work, the $\delta^{13}C$ values of both free and bound HA of river sediments do not overlap with the ones of bound HA from lagoon and fish farm sites (Fig. 6), confirming a contribution of inputs from autochthonous sources. The similarity displayed by bound HA throughout the transect cannot

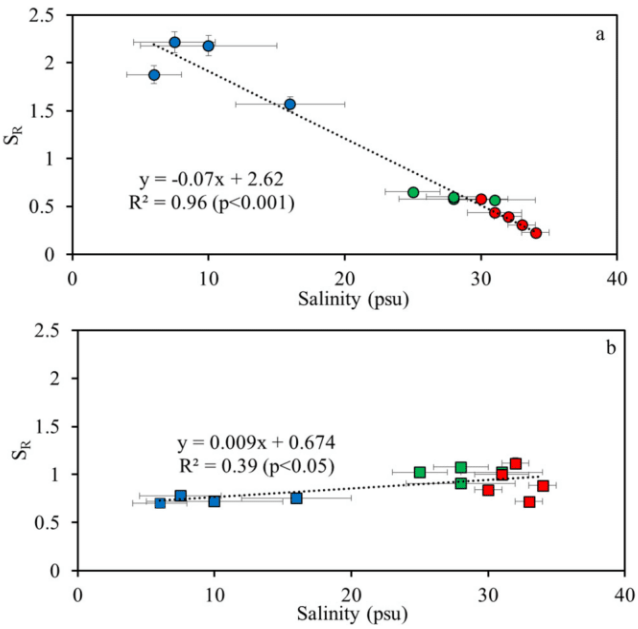

Fig. 8 Slope ratio (S_R) values of free (**a**) and bound (**b**) HA from river (blue), lagoon (green), and fish farm (red) plotted against yearly average salinity of water

therefore only be driven by continuously decreasing terrestrial contributions, but must concomitantly derive from the action of similar forcing mechanisms (e.g., selection due to solubility or hydrophobicity) which favor the selective sorption of humified autochthonous substrates. Contrary to terrestrial soils (Six et al. 2002), the fraction of C sequestered in this form is not related to the amount of fine mineral particles in the sediments, possibly due to the large inputs of fine particles in all the sediments examined.

In all sediments, the ^{13}C depletion of free and bound HA is highly correlated with the $\delta^{13}C$ of sediments NOM (Fig. S3 - ESM). The least square linear regression model shows that in river and lagoon sediments free HA-C is about 17% more depleted in ^{13}C than sediment NOM. Conversely, $\delta^{13}C$ values of free HA in fish farm sediments fit to a line with significantly different intercept and slope ($p < 0.02$) and appear to be 50% less depleted than NOM.

The $\delta^{13}C$ depletion values of bound HA do not differ from the corresponding $\delta^{13}C$ values of NOM. This may imply a lower degree of transformation of bound HA confirming the selective preservation of organic substrates bound to minerals (Six et al. 2002). The larger values and much lower variability displayed by C/N ratios of bound HA support this hypothesis and the hypothesis that this fraction may contain a larger proportion of organic components of terrestrial origin carried into the lagoon by suspended mineral particles. Their mixed origin is confirmed by FTIR spectra. In fact, the spectra show a relatively lower contribution of amide structures and a prevalence of bands covering adsorption ranges that originate from typical structural features inherited from wooden plant residues. Bound HA also display a stronger degree of similarity among their spectra, again suggesting a possible mixed origin, as confirmed by the much lower variability of absorption ratios of the main FTIR bands (Fig. S5 - ESM).

Contrary to the normal trend observed in terrestrial and lacustrine (Lehmann et al. 2002) environments, isotopic fingerprints of bound HA would apparently indicate that, along the examined transect, ^{13}C depletion did not occur during early sedimentary diagenesis (Fig. S3). This means that bound HA of recent sediments do not ostensibly undergo structural modifications implying extensive breaking of C–C bonds. In fact, a concomitant loss of the more easily decomposable components of plant residues, such as cellulose and hemicelluloses (that are less depleted in ^{13}C than lignin), would have further contributed to produce more negative $\delta^{13}C$ values in the HA of river sediments. At the same time, the lower ^{13}C depletion of NOM in secluded fish farm sediments is not accompanied by any change in $\delta^{13}C$ values of HA. Isotopic C signatures therefore confirm that, along the examined transect, the decomposition of allochthonous organic matter of surface sediments is accompanied by in situ C_{org} accumulation, reflecting the existence of a continuum of increasing marine contribution. Isotopic composition of sediment NOM is therefore not only determined by occurrence of bond breaking reactions or physico-chemical fractionation processes, but also depends on the mixing of NOM originating from terrestrial and marine sources. In fact, the $\delta^{13}C$ values of phytoplankton usually range between − 19 and − 23‰, those of benthic diatoms between − 14 and − 18‰, and those of algae from − 12 to − 21‰ (Ogrinc et al. 2005; Vizzini et al. 2005; Tesi et al. 2007).

Accumulation of materials derived from these sources must have increasingly contributed to the C_{org} pool of recent sediments along the river-lagoon transect, with bound HA fractions following the same trend of free HA, but to a lesser extent. This explains the clear separation of river sediments from those of the lagoon and fish farm in the $\delta^{13}C$–$\delta^{15}N$ biplot (Fig. 6).

The Marano and Grado Lagoon is a medium eutrophication environment, where phytoplankton biomass, albeit increasing in the innermost part of the lagoon, is not correlated with the distribution of nutrients (Acquavita et al. 2015). This probably depends on the high rates of water interchange with the open sea, which occurs through the three main inlets (Ferrarin et al. 2009).

Isotopic N composition of free and bound HA of fish farm sediments, which are formed in a more eutrophic and closed environment, is significantly more depleted in ^{15}N, rather than HA extracted from lagoon and river sediments, which conversely display similar $\delta^{15}N$ values in line with data reported by Mahoney et al. (2019). This suggests incorporation of ^{15}N-depleted organic materials from in situ bacterial or algal growth in fish farm HA. As observed by Wada et al. (1980), this is a common cause of dilution of ^{15}N in these environments. In fact, depletion in ^{15}N could have only derived from nitrogen fixation, confirming the strong contribution of algal sedimentation to fish farm HA. Indeed, dystrophy caused by imbalance of the phosphorus to nitrogen ratio, which could be particularly severe in a fish farm, often promotes the growth of cyanobacteria (Viarioli et al. 2008). Anthropogenic N sources increase $\delta^{15}N$ in coastal ecosystems (McClelland et al. 1997; McClelland and Valiela 1998) by increasing nitrate inputs. In fact, the primary form of dissolved inorganic nitrogen in the Marano and Grado Lagoon is nitrate (Aquavita et al. 2015). However, the uptake of nitrate would be immediately reflected in the N isotopic fingerprint of plant or algae, resulting in ^{15}N enrichment. In the fish farm, nutrient inputs from fish feed and deposition of feces may be larger than the contribution from terrestrial nitrate. The isotopic composition of fish feed ($\delta^{13}C = -27.47$‰ and $\delta^{15}N = 9.55$‰), which is however used only in some parts of the farm, rules out a significant contribution of this source to the fish farm sediment NOM and HA.

The organic matter of fish farm sediments displays peculiar features also in the bound HA fraction. This is not surprising considering that fish farms are closed environments where sedimentation of suspended allochthonous materials is minimized since tidal fluxes are controlled by sluice gates regulated by fish farmers.

5 Conclusions

Along the examined transect, HA extracted from recent sediments form a sort of compositional continuum from the river down to the lagoon and fish farm. Our results point out a complex but continuous pattern of terrestrial and marine contributions to C sequestration and humification in this lagoon environment, where the chemistry of fresh and salt water bodies is dominated by their equilibrium with $CaCO_3$-rich sediments. Although HA solubility is completely depressed by Ca^{2+} ions, humic materials of terrestrial origin still contribute to C_{org} sequestered in sediments due to transport and sedimentation of allochthonous organo-mineral particles, which bear a large fraction of bound HA. The continuum highlighted by $\delta^{13}C$ values derives from these inputs and from a progressive mixing of terrestrial and marine substrates that undergo in situ humification.

The NOM and free HA of sediments appear well differentiated, varying from typical HA of terrestrial origin in the river sediments, to HA of algal origin in the fish farm. By contrast, HA bound to mineral particles through cationic bridges appear to preserve most of their traits and, in particular, their more pronounced aromatic character. Considering that quinone groups are the active redox groups in HA, bound HA inputs may have important consequences on the geochemistry of iron and sulfur in similar environments.

Acknowledgments Elisa Petranich, Stefano Cirilli, and Stefano Sponza from the University of Trieste are warmly acknowledged for their technical assistance during sampling operations. We are grateful to Claudio Furlanut for his valuable support and kind hospitality at the fish farm during field work.

Funding information This study was partially supported by the University of Trieste (Finanziamento di Ateneo per progetti di ricerca scientifica - FRA 2014, ref. Stefano Covelli).

References

Acquavita A, Aleffi IF, Benci C, Bettoso N, Crevatin E, Milani L, Tamberlich F, Toniatti L, Barbieri P, Licen S, Mattassi G (2015) Annual characterization of the nutrients and trophic state in a Mediterranean coastal lagoon: the Marano and Grado Lagoon (northern Adriatic Sea). Reg Stud Mar Sci 2:132–144

Aliaume C, Do Chi T, Viaroli P, Zaldívar JM (2007) Coastal lagoons of Southern Europe: recent changes and future scenarios. Trans Wat Monogr 1:1–12

Andersson A, Brugel S, Paczkowska J, Rowe OF, Figueroa D, Kratzer S, Legrand C (2018) Influence of allochthonous dissolved organic matter on pelagic basal production in a northerly estuary. Estuar Coast Shelf Sci 204:225–235

Berto D, Rampazzo F, Noventa S, Cacciatore F, Gabellini M, Bernardi Aubry F, Girolimetto A, Boscolo Brusà R (2013) Stable carbon and nitrogen isotope ratios as tools to evaluate the nature of particulate organic matter in the Venice lagoon. Estuar Coast Shelf Sci 135:66–76

Brambati A (1996) Metalli pesanti nelle lagune di Marano e Grado: piano di studio finalizzato all'accertamento della presenza di eventuali sostanze tossiche persistenti nel bacino lagunare di Marano e Grado e al suo risanamento. Regione Autonoma Friuli-Venezia Giulia, Servizio Idraulica, Trieste

Chen Y, Senesi N, Schnitzer M (1977) Information provided on humic substances by E4/E6 ratios. Soil Sci Soc Am J 41:352–358

Chmura GL, Anisfeld SC, Cahoon DR, Lynch JC (2003) Global carbon sequestration in tidal, saline wetland soils. Glob Biogeochem Cycles 17:1111

Covelli S, Acquavita A, Piani R, Predonziani S, De Vittor C (2009) Recent contamination of mercury in an estuarine environment (Marano lagoon, Northern Adriatic, Italy). Estuar Coast Shelf Sci 82:273–284

Croué JP, Korshin GV, Leenheer J, Benjamin MM (2000) Isolation, fractionation and characterization of natural organic matter in drinking water. AWWARF, Denver, CO

De Nobili M, Petrussi F (1988) Humification index (HI) as evaluation of the stabilization degree during composting. J Ferment Technol 66: 577–583

De Nobili M, Contin M, Mathieu N, Randall EW, Brookes PC (2008) Assessment of chemical and biochemical stabilization of organic C in soils from the long-term experiments at Rothamsted (UK). Waste Manag 28:723–733

De Vittor C, Faganeli J, Emili A, Covelli S, Predonzani S, Acquavita A (2012) Benthic fluxes of oxygen, carbon and nutrients in the Marano and Grado Lagoon (northern Adriatic Sea, Italy). Estuar Coast Shelf Sci 113:57–70

R Development Core Team (2018) R: A language and environment for statistical computing. R Foundation for Statistical Computing, Vienna, Austria

Faganeli J, Fanuko N, Malej A, Stegnar P, Vokovic A (1981) Primary production in the Gulf of Trieste (North Adriatic). Rapp Comm Int Merc Medit 27:69–71

Ferrarin C, Umgiesser G, Scroccaro I, Mattassi G (2009) Hydrodynamic modelling of the lagoons of Marano and Grado, Italy. Geo Eco Mar 15:13–19

Ferrarin C, Umgiesser G, Bajo M, Bellafiore D, De Pascalis F, Ghezzo M, Mattassi G, Scroccaro I (2010) Hydraulic zonation of the lagoons of Marano and Grado, Italy. A modelling approach. Estuar Coast Shelf Sci 87:561–572

Filip Z, Alberts JJ, Cheshire MV, Goodman BA, Bacon JR (1988) Comparison of salt marsh humic acid with humic-like substances from the indigenous plant species Spartina Alterniflora (Loisel). Sci Total Environ 71:157–172

Fontolan G, Pillon S, Bezzi A, Villalta R, Lipizer M, Triches A, D'Aietti A (2012) Human impact and the historical transformation of saltmarshes in the Marano and Grado Lagoon, northern Adriatic Sea. Estuar Coast Shelf Sci 113:41–56

Fooken U, Liebezeit G (2000) Distinction of marine and terrestrial origin of humic acids in North Sea surface sediments by absorption spectroscopy. Mar Geol 164:173–181

Fox LE (1983) The removal of dissolved humic acid during estuarine mixing. Estuar Coast Shelf Sci 16:431–440

Gatto F, Marocco R (1993) Morfometria e geometria idraulica dei canali della laguna di Grado (Friuli-Venezia Giulia). Geogr Fis Din Quaternaria 16:107–120

Giovanela M, Parlanti E, Soriano-Sierra EJ, Soldi MS, Sierra MMD (2004) Elemental composition, FT-IR spectra and thermal behavior of sedimentary fulvic and humic acids from aquatic and terrestrial environments. Geochem J 38:255–264

Goñi MA, Teixeira MJ, Perkey DW (2003) Sources and distribution of organic matter in a river-dominated estuary (Winyah Bay, SC, USA). Estuar Coast Shelf Sci 57:1023–1048

Helms JR, Stubbins A, Ritchie JD, Minor EC, Kieber DJ, Mopper K (2008) Absorption spectral slopes and slope ratios as indicators of molecular weight, source, and photobleaching of chromophoric dissolved organic matter. Limnol Oceanogr 53:955–969

Inbar Y, Chen Y, Hadar Y (1989) Solid-state carbon-13 nuclear magnetic resonance and infrared spectroscopy of composed organic matter. Soil Sci Soc Am J 53:1695–1701

Kerr JG, Eimers MC (2012) Decreasing soil water Ca^{2+} reduces DOC adsorption in mineral soils: implications for long-term DOC trends in an upland forested catchment in southern Ontario, Canada. Sci Total Environ 427-428:298–307

Kim J, Cho H, Kim G (2018) Significant production of humic fluorescent dissolved organic matter in the continental shelf waters of the northwestern Pacific Ocean. Sci Rep 8:4887

Klüpfel L, Piepenbrock A, Kappler A, Sander M (2014) Humic substances as fully regenerable electron acceptors in recurrently anoxic environments. Nat Geosci 7:195–200

Lehmann MF, Bernasconi SM, Barbieri A, McKenzie JA (2002) Preservation of organic matter and alteration of its carbon and nitrogen isotope composition during simulated and in situ early sedimentary diagenesis. Geochim Cosmochim Acta 66:3573–3584

Lovley DR, Fraga JL, Blunt-Harris EL, Hayes LA, Phillips EJP, Coates JD (1998) Humic substances as a mediator for microbially catalyzed metal reduction. Acta Hydrochim Hydrobiol 26:152–157

Mahoney DT, Al Aamery N, Fox JF, Riddle B, Ford W, Wang YT (2019) Equilibrium sediment exchange in the earth's critical zone: evidence from sediment fingerprinting with stable isotopes and watershed modeling. J Soils Sediments 19:3332–3356

Mao JD, Tremblay L, Gagné JP, Kohl S, Rice J, Schmidt-Rohr K (2007) Humic acids from particulate organic matter in the Saguenay Fjord and the St. Lawrence Estuary investigated by advanced solid-state NMR. Geochim Cosmochim Acta 71:5483–5499

Marocco R (1995) Sediment distribution and dispersal in the northern Adriatic lagoons (Marano and Grado paralic system). J Geol 57: 77–89

McClelland JW, Valiela I (1998) Linking nitrogen in estuarine producers to land-derived sources. Limnol Oceanogr 43:577–585

McClelland JW, Valiela I, Michener RH (1997) Nitrogen-stable isotope signatures in estuarine food webs: a record of increasing urbanization in coastal watersheds. Limnol Oceanogr 42:930–937

McLeod E, Chmura GL, Bouillon S, Salm R, Björk M, Duarte CM, Lovelock CE, Schlesinger WH, Silliman BR (2011) A blueprint for blue carbon: toward an improved understanding of the role of vegetated coastal habitats in sequestering CO_2. Front Ecol Environ 9:552–560

Miller JC, Miller JN (2010) Statistics and chemometrics for analytical chemistry, 6th edn. Pearson, Harlow

Nieuwenhuize J, Maas YEM, Middelburg JJ (1994) Rapid analysis of organic carbon and nitrogen in particulate materials. Mar Chem 45: 217–224

Ogrinc N, Fontolan G, Faganeli J, Covelli S (2005) Carbon and nitrogen isotope compositions of organic matter in coastal marine sediments (the Gulf of Trieste, N Adriatic Sea): indicators of sources and preservation. Mar Chem 95:163–181

Olk DC, Cassman KG, Fan TWM (1995) Characterization of two humic acid fractions from a calcareous vermiculitic soil: implications for the humification process. Geoderma 65:195–208

Olk DC, Cassman KG, Mahieu REW (1998) Conserved chemical properties of young humic acid fractions in tropical lowland soil under intensive irrigated rice cropping. Eur J Soil Sci 49:337–349

Otero E, Culp R, Noakes JE, Hodson RE (2003) The distribution and $\delta^{13}C$ of dissolved organic carbon and its humic fraction in estuaries of southeastern USA. Estuar Coast Shelf Sci 56:1187–1194

Petranich E, Acquavita A, Covelli S, Emili A (2017) Potential bioaccumulation of trace metals in halophytes from salt marshes of a northern Adriatic coastal lagoon. J Soils Sediments 17:1986–1998

Peuravuori J, Pihlaja K (1997) Molecular size distribution and spectroscopic properties of aquatic humic substances. Anal Chim Acta 337: 133–149

Powlson D, Smith P, De Nobili M (2013) Soil organic matter. In: Gregory PJ, Nortcliff S (eds) Soil conditions and plant growth. Blackwell Publishing Ltd, UK, pp 86–131

Ratasuk N, Nanny MA (2007) Characterization and quantification of reversible redox sites in humic substances. Environ Sci Technol 41:7844–7850

Rimmer DL, Abbott GD (2011) Phenolic compounds in NaOH extracts of UK soils and their contribution to antioxidant capacity. Eur J Soil Sci 62:285–294

Roccaro P, Yan M, Korshin GV (2015) Use of log-transformed absorbance spectra for online monitoring of the reactivity of natural organic matter. Water Res 84:136–143

Roden EE, Kappler A, Bauer I, Jiang J, Paul A, Stoesser R, Konishi H, Xu H (2010) Extracellular electron transfer through microbial reduction of solid-phase humic substances. Nat Geosci 3:417–421

Rodrigues J, Faix O, Pereira H (1998) Determination of lignin content in Eucalyptus globulus wood using FTIR spectroscopy. Holzforschung 52:46–50

Schnitzer M, Monreal CM (2011) Quo vadis soil organic matter research? A biological link to the chemistry of humification. Adv Agron 113: 143–217

Scott NA, Cole CV, Elliott ET, Huffman SA (1996) Soil textural control on decomposition and soil organic matter dynamics. Soil Sci Soc Am J 60:1102–1109

Sholkovitz ER (1976) Flocculation of dissolved organic and inorganic matter during the mixing of river water and seawater. Geochim Cosmochim Acta 40:831–845

Six J, Conant RT, Paul EA, Paustian K (2002) Stabilization mechanisms of soil organic matter: implications for C-saturation of soils. Plant Soil 241:155–176

Souza SO, Silva MD, Santos JCC, de Oliveira LC, do Carmo JB, Botero WG (2016) Evaluation of different fractions of the organic matter of peat on tetracycline retention in environmental conditions: in vitro studies. J Soils Sediments 16:1764–1775

Stevenson FJ (1982) Humus chemistry: genesis, composition, reactions. John Wiley, New York

Tesi T, Miserocchi S, Goñi MA, Langone L, Boldrin A, Turchetto M (2007) Organic matter origin and distribution in suspended particulate materials and surficial sediments from the western Adriatic Sea (Italy). Estuar Coast Shelf Sci 73:431–446

Uher G, Hughes C, Henry G, Upstill-Goddard RC (2001) Non-conservative mixing behavior of colored dissolved organic matter in a humic-rich, turbid estuary. Geophys Res Lett 28:3309–3312

Van Ardenne LB, Jolicouer S, Bérubé D, Burdick D, Chmura GL (2018) The importance of geomorphic context for estimating the carbon stock of salt marshes. Geoderma 330:264–275

Viarioli P, Bartoli M, Giordani G, Naldi M, Orfanidis S, Zaldivar JM (2008) Community shifts, alternative stable states, biogeochemical controls and feedbacks in eutrophic coastal lagoons: a brief overview. Aquat Conserv 18:S105–S117

Vizzini S, Savona B, Caruso M, Savona A, Mazzola A (2005) Analysis of stable carbon and nitrogen isotopes as a tool for assessing the environmental impact of aquaculture: a case study from the western Mediterranean. Aquacult Int 13:157–165

Wada E, Goldber ED, Horibe Y, Saruhashi K (1980) Nitrogen isotope fractionation and its significance in biogeochemical processes occurring in marine environments. In: Goldberg ED, Horibe Y, Saruhashi K (eds) Isotope marine chemistry. Uchida Rokakuho, Tokyo, pp 375–398

Wang H, Zhu J, Fu Q, Hong C, Hu H, Violante A (2016) Phosphate adsorption on uncoated and humic acid-coated iron oxides. J Soils Sediments 16:1911–1920

Wolf M, Kappler A, Jiang J, Meckenstock RU (2009) Effects of humic substances and quinones at low concentrations on ferrihydrite reduction by Geobacter metallireducens. Environ Sci Technol 43: 5679–5685

Zhang W, Zheng J, Zheng P, Tsang DCW, Qiu R (2015) The roles of humic substances in the interactions of phenanthrene and heavy metals on the bentonite surface. J Soils Sediments 15:1463–1472

CHAPTER 6

The aim of this work was to quantify the electron donating capacity of humic acids extracted from saltmarshes soils of the Marano and Grado Lagoon. Then other geochemical characteristics of humic acids were investigated in order to understand their influence on the redox properties of humic acids.

EPR and ^{13}C NMR analyses were performed in the laboratories of Embrapa Instrumentation Center. The author acknowledges the financial support provided by Research Traineeship TRA 2019-2 from the International Humic Substances Society.

Preliminary results were presented as an oral presentation at the 17th International Conference on Chemistry and the Environment (16-20 June 2019, Thessaloniki, Greece).

Electron donating properties of humic acids in saltmarsh soils

C. Bravo[a,b],* R. Toniolo[a], C. Millo[c], M. Contin[a], L. Martin-Neto[d] and M. De Nobili[a]

[a] Department of Agricultural Food Environmental and Animal Sciences, University of Udine, via delle Scienze 208, 33100 Udine (I).

[b] Department of Life Sciences, University of Trieste, via Licio Giorgieri 5, 34128 Trieste (I).

[c] Oceanographic Institute, University of Sao Paulo, praça do Oceanografico 191, 05508-900 São Paulo (BR).

[d] Embrapa Instrumentação Agropecuária, CP 741, 13560-970 São Carlos-SP (BR).

*corresponding author: carlo.bravo@uniud.it

Keywords: Humic acid, EPR, ABTS, saltmarshes

Abstract

In saltmarsh soils, humic acids (HA) are involved in numerous redox processes. The electron donating capacity (EDC) of HA, defined as the capacity to donate electrons by reduced functional groups, depends on the presence in their molecular structure of phenolic and quinone groups. In transitional environments, such as saltmarshes, it may strongly depend on contributions of terrestrial or marine organic matter.

The aim of this work was to quantify the EDC of HA extracted from saltmarsh. Three saltmarshes belonging to the Marano and Grado Lagoon (Italy) and located along a geographical gradient. Various sampling points were then selected from each based on the vegetation cover. A specific sequential extraction methodology was used for the isolation of humic acids linked or not to the mineral matrix.

This allowed to identify the close dependence of the two HA fractions with the biogeochemical characteristics of the soil. Moreover, the geochemical characteristics of soils and humic acids are strongly related to the electron donating capacity of HA, and should be taken in account when redox processes are studied in transitional environments.

1. Introduction

In natural wetlands and submerged soils, humic acids (HA) are involved in numerous redox processes (Keller et al., 2009; Klupfel et al., 2014) and can promote Fe reduction via electron shuttling (Volker et al. 1997; Bauer and Kappler, 2009). HA can be used by facultative anaerobic bacteria as terminal electron acceptors during anaerobic respiration (Lovley et al., 1996) providing energy to microorganisms to grow. HA also act as redox mediators which can shuttle electrons not only to oxidized metals and metalloids (Palmer et al., 2006; Van der Zee and Cervantes, 2009; Lee et al. 2019) but also to oxidized organic contaminants, such as azo dyes, polyhalogenated compounds and nitroaromatics (Kappler and Haderlein, 2003).

The electron donating capacity (EDC) of HA, defined as the capacity of a molecule to donate electrons, depends on the presence in its molecular structure of phenolic and quinone groups, which act as major reducible moieties in HA (Ratasuk and Nanny, 2007). In transitional environments it may strongly depend on the relative inputs of terrestrial or marine organic matter (Ferreira et al.2013, Bravo et al. 2019).

The chemical characteristics of HA extracted from recent sediments along a mainland to sea transect across the Grado and Marano Lagoon (Bravo et al. 2019) highlighted contributions from a progressive mixing of terrestrial and marine substrates that undergo in situ humification. In this environment, where HA are made insoluble by Ca^{2+} ions, humic materials of terrestrial origin derive mainly from transport and sedimentation of allochthonous organo-mineral particles, which bear a large fraction of bound HA. Contrary to sediments, however, saltmarshes accumulate a larger amount of organic matter derived from autochthonous plants residues and are subjected to alternating redox conditions caused by more or less intense tide water flooding caused by their position above the mean sea level.

In soils and sediments, HA are mostly extracted using both alkaline (sodium hydroxide, NaOH) and chelating (sodium pyrophosphate, $Na_4P_2O_7$) solutions. Sodium hydroxide solubilizes molecules by causing the ionization of acidic functional groups, thereby increasing their polarity and

56 solubility in water. However, even concentrated NaOH solutions cannot solubilize HS bound to
57 minerals by way of cationic bridges. Alkaline sodium pyrophosphate solutions, on the other hand, are
58 also able to break the cationic bridges with the mineral components. By performing a sequential
59 extraction with the two types of extractants, it is possible to obtain two different categories of HA,
60 which have different environmental implications. The HA extracted by NaOH are defined free HA,
61 while the one extracted by $Na_4P_2O_7$ are defined bound HA. Free HA are less occluded and preserved
62 by the mineral phase of the soil/sediment, reflecting more recent and local inputs of organic matter in
63 sediments. In a previous work (Bravo et al., 2019) we demonstrated that, in lagoon environments,
64 bound HA present more terrestrial characteristics (e.g. higher aromaticity) compared to the free HA.
65 The aim of this work was to quantify the EDC of free and bound HA extracted from saltmarsh
66 soils of the Marano and Grado Lagoon (northern Adriatic Sea) which differ for vegetation cover,
67 height above the mean sea level and distance from the open sea, and to link their EDC to their
68 geochemical characteristics and local soil conditions.
69

70 **2. Material and methods**

71 *2.1 Soil sampling area*

72 The Marano and Grado Lagoon (approximately area of 160 km^2) is located in the northern
73 part of the Adriatic Sea, extending for 35 km from the Tagliamento and Isonzo River estuaries with
74 an average width of 5 km. A complete and extensive description of the Lagoon and its saltmarshes is
75 reported in Fontolan et al. (2012).
76 Surface soils (0-20 cm) were sampled following a gradient of decreasing altitude above the
77 mean sea level (a.m.s.l.) in three saltmarshes of the western sector of the Lagoon (Fig. 1). The sampled
78 areas included i) a high saltmarsh, the Allacciante di Marano (AM) which is a mainland fringing
79 saltmarsh with consistent river influences; ii) a low saltmarsh, the Allacciante di San Andrea (ASA),

where dredging operations influenced the natural process of soil formation and iii) a back-barrier saltmarsh, the Barena di Martignano (BM), where the influence of the open sea predominates.

To obtain a representative sample, at each sampling point three undisturbed soil cores were collected in PVC tubes (d= 12 cm) which were pushed into the soil and dug out from one side. The tubes were brought back to the laboratory within a few hours. After measuring the Eh, the upper 2-10 cm were separated from the rest of the soil and pooled together to measure soil characteristics and extract HA. Soil natural humidity was preserved during the sampling phase, and the contact with air was avoided. Once transported to the laboratory, soil samples were frozen and then freeze-dried to maintain unaltered the original conditions.

Geographical coordinates, dominant plant species, soil altitude., pH and selected soil characteristics are reported in Table 1.

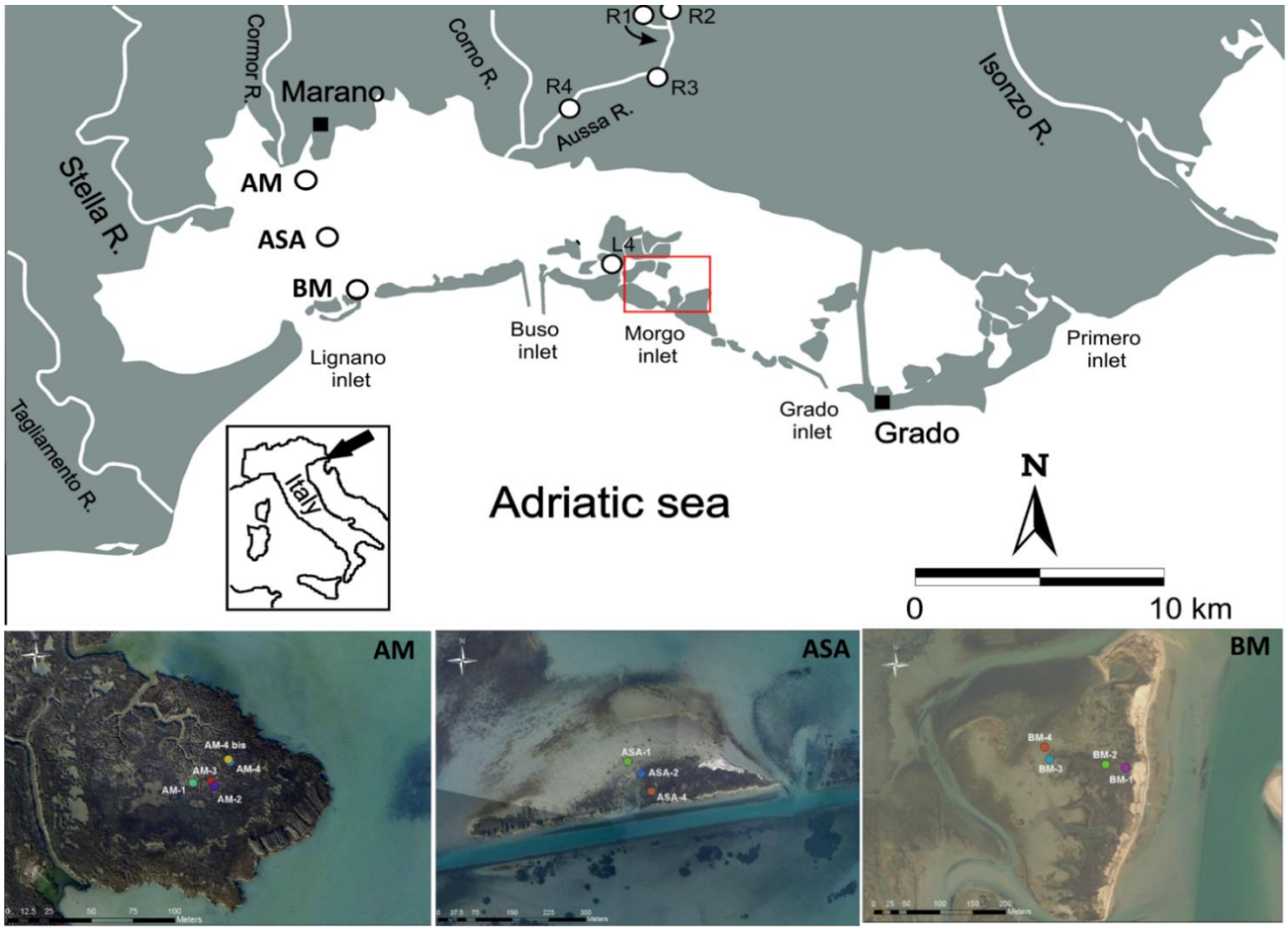

Fig. 1. Geographical location of the Grado and Marano Lagoon, of the three saltmarshes and of the sampling points within each saltmarsh.

2.2 Extraction and characterization of HA

Extraction of HA from soils was carried out under N_2 flux, first with 0.5 M NaOH (free HA) for 1h and then with 0.1 M $Na_4P_2O_7$ plus 0.1 M NaOH (bound HA) for another hour (De Nobili et al., 2008). Soil extracts were centrifuged (14000 rpm for 20 min) and supernatants were filtered using 0.2 μm cellulose filters. Free and bound HA were precipitated at pH 1 with 6 M HCl, separated by centrifugation, dialyzed against ultrapure water (until Cl^- free), frozen and then freeze-dried.

Organic carbon (C_{org}), total nitrogen (N_{tot}) and stable isotope composition ($\delta^{13}C$) of carbon in bulk soils and HA (free and bound) were determined by a Costech Instruments Elemental Combustion System elemental analyzer, coupled with an Isotope Ratio Mass Spectrometer (Thermo Scientific Delta V Advantage).

UV-Vis spectra of HA were recorded after dissolving HA in phosphate buffer (0.1 M, pH 7) using a Cary Varian Spectrophotometer in 1 cm quartz cuvettes over a wavelength interval from 220 to 800 nm at a scan rate 60 nm min^{-1}.

FTIR spectra were recorded with a FT-IR Spectrum 100 (PerkinElmer) spectrometer equipped with a universal ATR (attenuated total reflectance) sampling device containing a diamond/ZnSe crystal. The spectra were recorded at room temperature in transmission mode over a wavenumber interval from 4000 to 500 cm^{-1} (30 scans at a resolution of 4 cm^{-1}). Triplicate runs of each sample were averaged to obtain an average spectrum. A background spectrum of air was scanned under the same instrumental conditions before each series of measurements. Intensity ratios (R) were calculated for specific pairs of bands (Inbar et al., 1989).

The organic radical content of HS was measured using a Bruker EMX EPR spectrometer operating at X-band (9.5 GHz). About 40 mg of sample (equivalent to 10 mm in height) were placed in a 3.5 mm quartz tubes. Each sample was analyzed at room temperature in duplicate and the results are reported in n° spins g_{HS}^{-1} ± standard deviation. Other instrumental parameters were: center field 3410 G, sweep width 160 G, sweep time 60 s, microwave power 0.2 mW, modulation amplitude 1 G, receiver gain 10^4. The number of scans varied from 1 to 9 in function of the signal to noise ratio of

each sample. The microwave power of 0.2 mW was chosen after performing the power saturation curve (Fig. S1). Quantification of radicals was performed by the secondary standard method, using a Cr(III)MgO (g = 1.9797) as paramagnetic marker (permanently placed in the resonance cavity) calibrated with strong pitch reference (Bruker) of known free radical content.

The CPMAS ^{13}C NMR spectra of HA were obtained with an Advance III HD (Bruker) spectrometer operating at 400 MHz. Other instrumental parameters were: contact time 1 ms, delay time 1s, spinning speed of 10 KHz and 8192 scans for each sample. Semiquantification of chemical regions was performed according to Ferreira et al. (2013).

Electron donating capacity (EDC) of HA was determined using the 2,2'-azinobis-(3-ethylbenzothiazolinesulfonic acid) radical cation ($ABTS^{\bullet+}$) decolorization assay. $ABTS^{\bullet+}$ was generated according to Re et al. (1999) in 0.1 M citrate buffer (pH 4.79) and in 0.1 M phosphate buffer (pH 7.00). For spectrophotometric measurements, the $ABTS^{\bullet+}$ solution was diluted to an initial absorbance of 0.70 at 734 nm. After adding spikes (20, 50, 100, 200, 300, 400 μL) of 0.5 g L^{-1} HA solutions, the decrease in absorbance at 734 nm was measured continuously for 18 min. The EDC, expressed as $mmol_e\text{-}\ g_{HA}^{-1}$, was calculated considering the decrease in absorbance measured 30 s after addition of HA.

3. Results and discussion

All soils are characterized by relatively large contents of calcium carbonate, spanning from 30 to more than 70%, because of accumulation of sedimentary silt and sand derived from limestones. Their pH is therefore neutral to alkaline. The soils are subject to regular inundation during high tide: yearly average hydroperiods vary according to the soil's height a.m.s.l., from about 20 hours in the lower saltmarsh to 2-4 hours per day in the higher saltmarsh. E_h values of the examined soils reflect the length and frequency of flooding (Fig. 2) and span from strongly anoxic to sub-oxic conditions.

However, soils of finer textural class, such as those of the AM saltmarsh, have most of their fine pores permanently filled by the capillary rise. Moreover, redox conditions depend also on their intensity of biological activity.

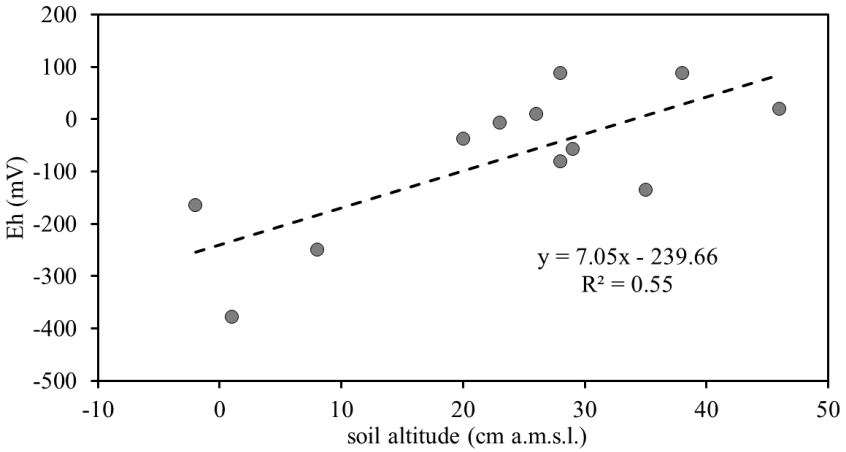

Fig. 2. Redox conditions of soils as a function of soil altitude.

The amount of C_{org} present in soils (Table 1) decreases from the innermost high saltmarsh (AM), located near a river estuary, toward the outer barrier saltmarsh (BM), the nearest to the open sea. The amounts of free and bound HA decrease accordingly to C_{org} (Fig. S2). At the same time, $\delta^{13}C$ values become less negative, reflecting the decreasing contribution of terrestrial inputs (Ogrinc et al., 2005). The three saltmarshes also differ for their average height above the mean sea level and plotting the $\delta^{13}C$ of SOM against the height of the sampling point a well-defined sigmoidal curve is obtained (Fig. 3).

The isotopic ^{13}C signature of SOM in soils that are located 30 cm and more above a.m.s.l. shows depletion levels typical of terrestrial environments, whereas in soils that are positioned at a lower level in the saltmarsh, SOM becomes progressively less depleted and reaches a more or less constant ^{13}C depletion level below 20 cm above a.m.s.l.

The isotopic signature of free and bound HA strictly follows that of SOM: linear regressions yields slopes were not significantly different than 1 (R^2=0.99, Fig. S3). Similarly to what observed in sediments (see Chapter 5), C/N ratios of bound soil HA are higher than those of free HA extracted from the same saltmarsh (Fig. 4) and confirm the larger contribution from sedimentary materials of

terrestrial origin to bound HA (Bravo et al. 2019). This is confirmed by $SUVA_{254}$ values which are higher for bound than for free HA (Table 2).

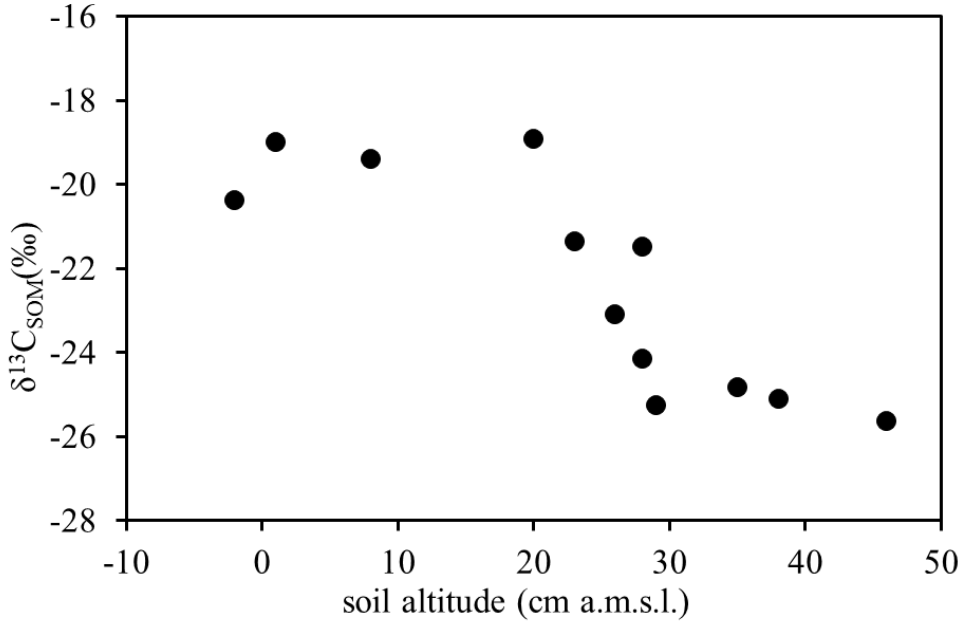

Fig. 3. Isotopic depletion of ^{13}C in SOM, as a function of height above mean sea level (a.m.s.l.) of the sampling points.

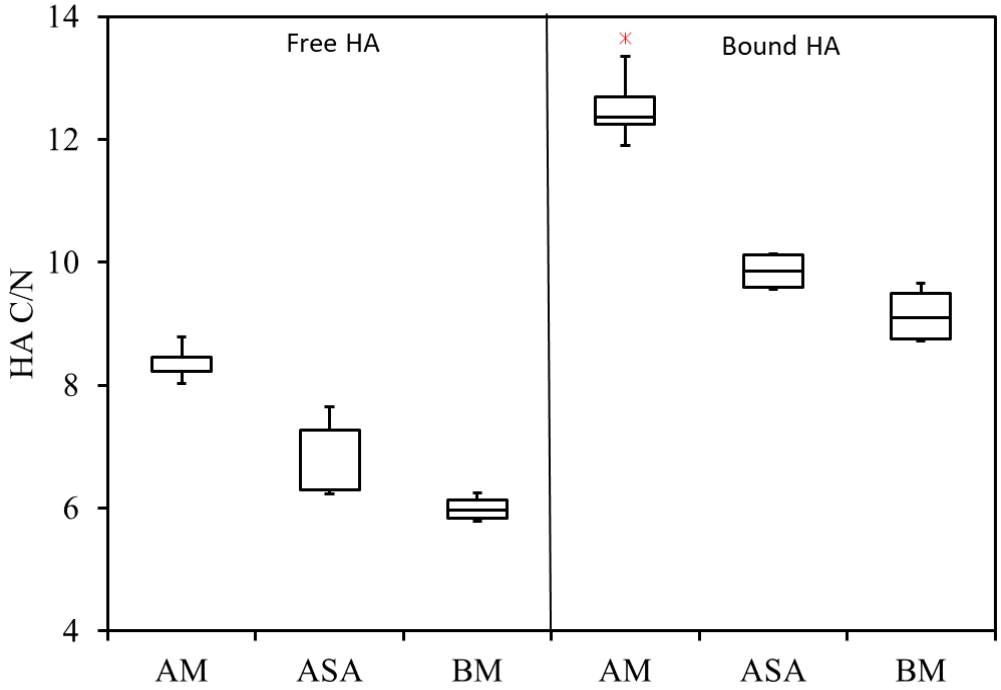

Fig. 4 Box plot of C/N ratio values of free and bound HA in the three saltmarshes. The line within the box marks the median concentration and the boundaries of the box indicate the 25th and 75th percentiles. Whiskers indicate the minimum and maximum concentrations, excluding outliers.

171 **Table 1.** Location of sampling points, dominant vegetation cover and characteristics of soils.

Station	Latitude N	Longitude E	Dominant plant species	Altitude cm a.m.s.l.	pH	$CaCO_3$ %	Eh mV	C_{org} %	N_{tot} %	$\delta^{13}C$ ‰ vs V-PDB	C/N
AM1	45°44'38.19	13°9'7.51"	*Juncus maritimus*	46	7.3	36.0	20	4.48	0.40	-25.6	11.1
AM2	45°44'35.50"	13° 9'4.99"	*Sarcocornia fruticosa*	29	7.5	34.0	-57	4.85	0.43	-25.3	11.3
AM3	45°44'34.80"	13° 9'5.85"	*Limonium narbonense*	38	7.4	32.2	121	4.94	0.41	-25.1	12.2
AM4	45°44'34.02"	13° 9'6.16"	*Puccinellia festuciformis*	37	7.4	34.1	-135	6.01	0.50	-24.8	12.0
ASA1	45°43'40.45"	13°10'15.89"	*Spartina maritima*	-1	7.5	46.2	89	1.57	0.17	-19.0	9.3
ASA2	45°43'41.29"	13°10'14.67"	*Sarcocornia fruticosa*	38	7.7	42.6	-378	3.12	0.32	-18.9	9.8
ASA3	45°43'41.94"	13°10'14.28"	*Puccinellia festuciformis*	28	7.4	43.0	-38	4.81	0.44	-21.4	10.9
ASA4	45°43'42.50"	13°10'14.03"	*Aster tripholium*	42	7.3	43.0	-6	4.78	0.45	-21.5	10.6
BM1	45°42'55.74"	13°10'33.01"	*Salicornia patula*	26	7.6	84.5	-81	0.43	0.05	-23.1	9.1
BM2	45°42'57.67"	13°10'32.35"	*Limonium narbonense*	48	6.9	49.8	11	0.82	0.09	-24.1	9.1
BM3	45°42'59.99"	13°10'32.17"	*Spartina maritima*	8	7.8	66.7	-250	0.50	0.07	-19.4	7.1
BM4	45°43'3.56"	13°10'30.91"	*Seagrasses*	2	8.9	73.6	-165	0.75	0.10	-20.4	7.5

172

173 **Table 2.** Geochemical parameters of free and bound HA extracted from the three examined saltmarshes.

Station	Free HA							Bound HA						
	C_{org} [a]	N_{tot} [a]	$\delta^{13}C$ [b]	C/N	$SUVA_{254}$ [c]	spins [d]	EDC [e]	C_{org} [a]	N_{tot} [a]	$\delta^{13}C$ [b]	C/N	$SUVA_{254}$ [c]	spins [d]	EDC [e]
AM1	51.99	6.48	-25.87	8.02	2.70	3.48	0.88	51.63	4.34	-25.60	11.90	3.21	4.05	1.08
AM2	50.04	6.03	-25.31	8.30	2.15	2.37	0.73	51.29	4.15	-25.38	12.36	2.55	2.83	0.75
AM3	49.51	5.64	-25.48	8.78	3.07	3.57	0.83	53.32	3.91	-25.71	13.65	4.05	4.60	1.13
AM4	48.97	5.87	-24.35	8.34	1.43	1.01	0.61	50.04	4.05	-24.32	12.36	2.02	2.49	0.69
ASA1	44.28	7.01	-19.40	6.32	1.28	1.17	0.61	48.55	5.06	-19.16	9.59	2.37	2.18	0.72
ASA2	45.74	7.34	-19.05	6.23	0.83	0.75	0.59	49.62	5.19	-18.86	9.56	1.71	1.75	0.58
ASA3	48.68	6.37	-21.56	7.64	2.38	3.23	0.83	52.35	5.17	-21.35	10.14	3.09	3.43	0.91
ASA4	46.21	6.48	-21.85	7.13	0.85	0.68	0.55	49.47	4.89	-21.45	10.12	2.02	1.91	0.61
BM1	53.36	8.76	-22.54	6.09	1.59	2.23	0.64	56.21	5.96	-22.86	9.44	2.74	3.06	0.74
BM2	50.04	8.02	-24.19	6.24	0.65	0.50	0.52	53.15	6.10	-24.14	8.71	2.58	3.45	0.91
BM3	50.94	8.81	-19.05	5.78	1.58	1.73	0.69	51.02	5.28	-18.48	9.66	2.78	3.67	0.83
BM4	52.67	9.01	-20.40	5.85	n.d.	n.d.	n.d.	54.17	6.18	-19.95	8.77	n.d.	n.d.	n.d.

174 Units of measure are: [a] = %, [b] = ‰ vs V-PDB, [c] = $L\ mg^{-1}\ m^{-1}$, [d] = $g \times 10^{17}$, [e] = $mmol_{e-}\ g_{HA}^{-1}$

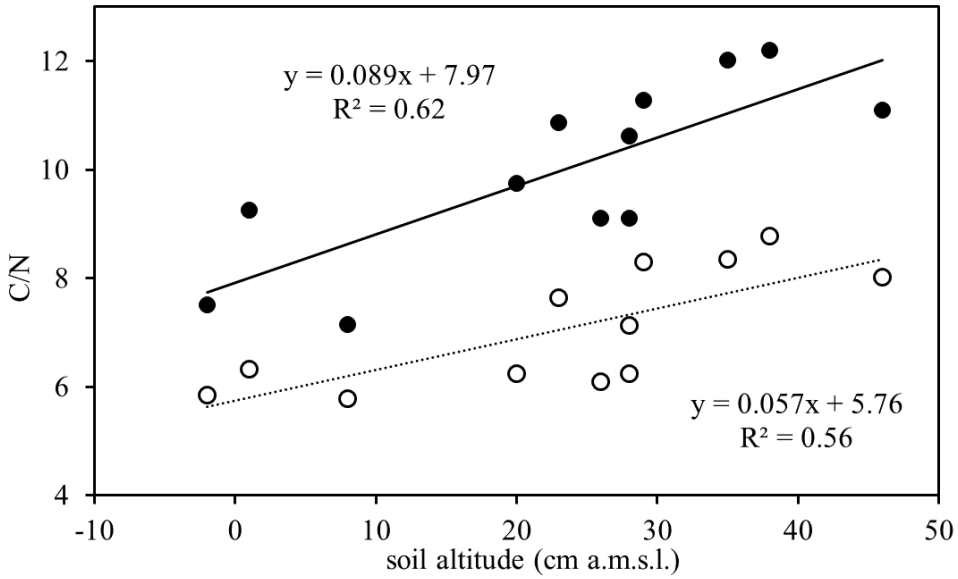

175 **Fig. 5.** C/N values of SOM (black symbols) and free HA (open symbols) as a function of soil surface height above
176 mean sea level at sampling point.
177

178 At the same time C/N values tend to increase linearly with the mean height above sea level in
179 the transition from the mainland to the open sea both in SOM and in free HA (Fig. 5), whereas the
180 trend is less significant for bound HA.

181 All ATR FTIR spectra of free (Fig. S4) and bound (Fig. S5) HA exhibited the typical bands
182 of soil HA (Giovanela et al., 2004) and namely: a broad adsorption around 3280 cm^{-1} (H-bonded OH
183 and N-H stretching), 2920-2940 cm^{-1} (aliphatic C–H stretching), 1720 cm^{-1} (C=O stretching of
184 carboxyls), 1640-1630 cm^{-1} (C=C vibrations in aromatic rings, H-bonded C=O stretching of quinone
185 and/or conjugated ketone and amide groups (amide I band), 1515 m^{-1}(aromatic ring breathing, amide
186 II band), 1400 cm^{-1}(O–H deformation, CH_3 bending, C–O stretching of phenolic OH, antisymmetric
187 stretching of aryl esters), 1250 cm^{-1}(C–O stretching and OH deformation of COOH, C–O stretching
188 of aryl-esters). Absorption bands around 1150 cm^{-1} and 1030 cm^{-1} can be assigned to C-O and C-C
189 stretching vibrations of pyranose rings in algal polysaccharides and to alcoholic C–O–H groups.
190 However, the relative intensities of these bands vary and display a somewhat regular trend for free
191 HA. The 1720 cm^{-1} band of C=O stretching in COOH progressively decreases in intensity in the HA
192 extracted from saltmarshes nearer to the sea, while the 1640 cm^{-1} band of the AM saltmarsh HA shifts
193 to 1632 and 1628 cm^{-1} in free HA of the ASA and BM saltmarshes. This band and the 1514 cm^{-1}

194 band, typically connected to amides, display a maximum intensity in free HA from the ASA
195 saltmarsh, which is situated at the centre of the lagoon.

196 The 1030 cm^{-1} band of C-O stretching in carbohydrates, increases continuously with the
197 distance from the mainland and reaches maximum intensity in free HA from the BM saltmarsh,
198 nearest to the sea.

199 Bound HA were characterized by a more intense absorption in the region typical of CH_2
200 stretching vibrations, indicating a stronger hydrophobic nature, at the same time, Amide I and II bands
201 are less pronounced in bound HA and the 1720 cm^{-1} carboxyl C=O stretching is not apparently
202 influenced by closer proximity to the open sea. With the exception of the HA extracted from the ASA
203 saltmarsh, bound HA do not seem to be affected by either the frequency and length of inundation or
204 the vegetation type and display a much lower structural variability than free HA.

205 Solid state ^{13}C-NMR spectra support structure assessment from ATR- FTIR data (Table 3).
206 Bound HA display stronger signals in the aliphatic region (0-110 ppm) with a particular intense signal
207 at about 30 ppm, which can be attributed to C in methylene groups. This lowers the Arom/Alkyl ratios
208 of bound HA. Conversely, carboxyls are more abundant in free HA and N-alkyl to O-alkyl ratios
209 increase in free HA from lower saltmarshes, while, at the same time the Arom/Alkyl ratio decreases.
210 Methoxyls decrease in free HA with distance from the mainland.

211 However, soil HA, contrary to sediment HA, reflect more strongly contributions from
212 autochthonous vegetation and position in the landscape (soil altitude). This is more evident in free
213 HA, whereas bound HA also bear evidence of a substantial contribution from sedimentary terrestrial
214 materials. The results of the analysis of the SOM and free and bound HA from the sampled soils
215 highlight the action of a geographical gradient along the three saltmarshes, which mirrors, in part,
216 results obtained in the analysis of sediments taken from a similar transect within the same lagoon
217 (Bravo et al. 2019).

Table 3. ^{13}C-CP MASS NMR estimation of structural composition of HA in the different saltmarshes. Areas represent the mean of all sampled sites.

	Chemical shift region (ppm)							
	0-45 Alkyl-C	45-60 N-alkyl/methoxyl C	60-110 O-alkyl C	110-160 Aromatics	160-185 Carboxyl C	185-245 Carbonyl C	N-alkyl/O-alkyl	Arom/Alkyl
Free HA								
AM	31.6	19.4	16.4	20.9	9.8	1.9	0.8	0.7
ASA	32.3	18.6	16.8	19.8	10.6	1.8	0.9	0.6
BM	32.3	17.8	18.6	20.3	10.2	1.7	1.1	0.6
Bound HA								
AM	34.2	16.4	18.8	20.7	8.1	2	1.2	0.6
ASA	36.4	16.7	18.5	18.4	8.5	1.5	1.1	0.5
BM	40.8	15.1	17.6	15.3	9.3	1.8	1.2	0.4

Semiquinone type free radicals (SFR) are more abundant in the AM saltmarsh, which is nearer to the mainland and more abundant in bound HA (Fig. 6). Spin concentrations of both free and bound HA is highly related to their $SUVA_{254}$ value (Fig. S6) and therefore to the aromaticity of HA molecules (R^2= 0.95).

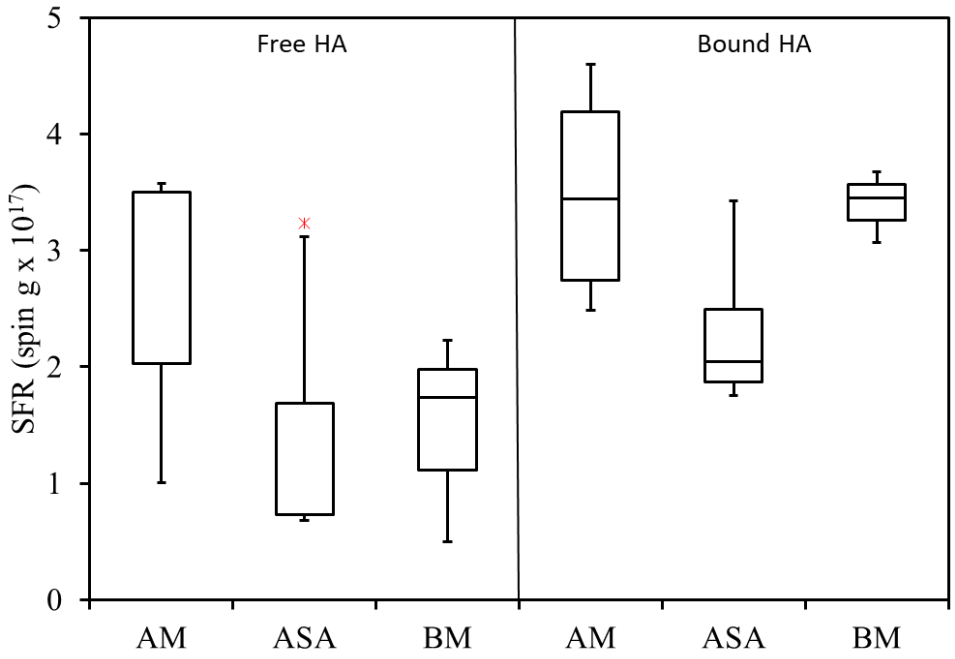

Fig. 6. Box plot of semiquinone type free radicals concentration in free and bound HA. The line within the box marks the median concentration and the boundaries of the box indicate the 25th and 75th percentiles. Whiskers indicate the minimum and maximum concentrations, excluding outliers.

The course of the reaction between the radical cation $ABTS^{\cdot+}$ and HA had the same trend as the ones shown in Chapter 3 (for peat HA) and Chapter 4 (for Suwannee River fulvic acids). Since for soil redox reactions fast times are more relevant (Chapter 4), the time considered for the EDC calculation was 30 s (Fig. S7). EDC values (Table 2) followed a decreasing trend moving from the more terrestrial saltmarsh (AM) to the more marine one (BM). Moreover, bound HA showed higher EDC values (~ 20%) compared to free HA. This could be explained considering that bound HA generally present a higher degree of aromaticity (as indicated by higher $SUVA_{254}$ values) and molecular complexity. Radicals in HA are thought to be very reactive in redox reactions (Senesi et al., 1977; Oniki and Takahama, 1994): in fact, the EDC of HA showed a linear correlation with spin concentration (Fig. 7). However, in this case, bound and free HA fit different linear equations.

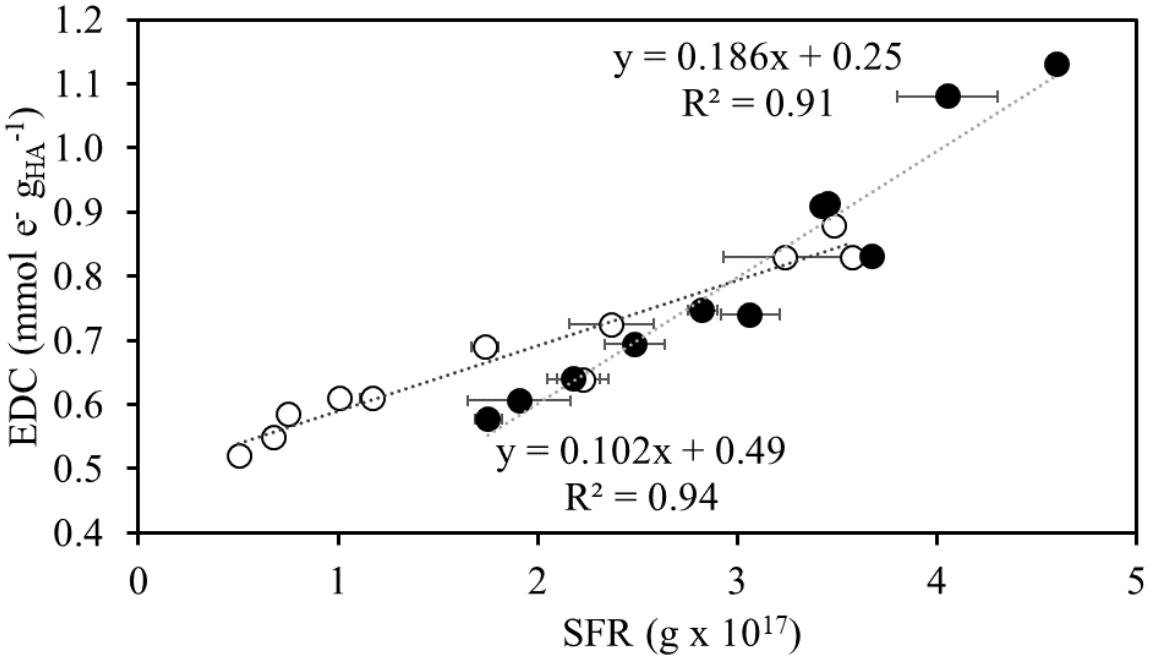

Fig. 7. Linear correlation between electron donating capacity (EDC) at the semiquinone type free radicals concentration of free (empty circles) and bound (black circles) HA.

4. Conclusions

The analytical techniques used in this work provided an exhaustive characterization of the soil organic matter and of its humified fractions in three adjacent saltmarshes with different sedimentary and transformation processes. Free and bound HA faithfully reflect the composition of SOM. The geographical location of the saltmarshes and the height of the soil above the main sea level seems to be the factors that most influences the chemical and structural characteristics of SOM along the studied transect.

The results obtained in this work confirmed the importance of the contributions of aromatic structures of terrestrial origin for the EDC capacity of HA in transitional environments. Moreover, the electron donating capacity of HA is strongly related to the geochemical characteristics of soils. These should be taken in account when redox processes are studied in transitional environments. It was also shown that bound HA present higher EDC values compared to the free one.

References

Bauer I., Kappler A. (2009) Rates and extent of reduction of Fe(III) compounds and O_2 by humic substances. Environ. Sci. Technol. 43:4902-4908.

Bravo C., Millo C., Covelli S., Contin M., De Nobili M. (2019) Terrestrial-marine continuum of sedimentary natural organic matter in a mid-latitude estuarine system. Journal of Soils and Sediments. https://doi.org/10.1007/s11368-019-02457-6.

De Nobili M., Contin M., Mahieu N., Randall E. W., Brookes P. C. (2008) Assessment of chemical and biochemical stabilization of organic C in soils from the long-term experiments at Rothamsted (UK). Waste Management 28:723-733.

Ferreira F. P., Vidal-Torrado P., Otero X. L., Buurman P., Martin-Neto L., Boluda R., Macias F. (2013) J Soils Sediments 13:253-264.

Fontolan G., Pillon S., Bezzi A., Villalta R., Lipizer M., Triches A., D'Aietti A (2012) Human impact and the historical transformation of saltmarshes in the Marano and Grado Lagoon, northern Adriatic Sea. Estuar. Coast. Shelf Sci 113:41-56.

Giovanela M., Parlanti E., Soriano-Sierra E. J, Soldi M. S., Sierra M. M. D. (2004) Elemental composition, FT-IR spectra and thermal behavior of sedimentary fulvic and humic acids from aquatic and terrestrial environments. Geochem. J. 38:255–264.

Inbar, Y., Chen, Y. and Hadar Y. (1989) Solid-state Carbon-13 Nuclear Magnetic Resonance and Infrared Spectroscopy of Composted Organic Matter. Soil Sci. Soc. Am. J. 53:1695-1701.

Kappler A., Haderlein S. B. (2003) Natural Organic Matter as Reductant for Chlorinated Aliphatic Pollutants. Environ. Sci. Technol. 37:2714-2719.

Keller J. K., Weisenhorn P. B., Megonigal J. P. (2009) Humic acids as electron acceptors in wetland decomposition. Soil Biol. Biochem. 41:1518:1522.

Klüpflel L., Piepenbrock A., Kappler A., Sander M. (2014) Humic substances as fully regenerable electron acceptors in recurrently anoxic environments. Nature Geoscience 7:195-200.

279 Lee S., Roh Y., Koh D. (2019) Oxidation and reduction of redox-sensitive elements in the
280 presence of humic substances in subsurface environments: A review. Chemosphere 220:86-97.

281 Lovley D. R., Coates J. D., Blunt-Harris E. L., Phillips E. J. P., Woodward J. C. Humic
282 substances as electron acceptors for microbial respiration. Nature 382:445-448.

283 Ogrinc N., Fontolan G., Faganeli J., Covelli S. (2005) Carbon and nitrogen isotope
284 compositions of organic matter in coastal marine sediments (the Gulf of Trieste, N Adriatic Sea):
285 indicators of sources and preservation. Mar. Chem. 95:163-181.

286 Oniki T., Takahama U. (1994) Effects of reaction time, chemical reduction, and oxidation on
287 esr in aqueous solutions of humic acids. Soil Sci. 158:204-210.

288 Palmer N. E., Freudenthal J. H., von Wandruszka R. (2006) Reduction of arsenates by humic
289 materials Environ. Chem. 3:131-136.

290 Ratasuk N., Nanny M. A. (2007) Characterization and quantification of reversible redox sites
291 in humic substances. Environ. Sci. Technol. 41:7844-7850.

292 Re R., Pellegrini N., Proteggente A., Pannala A., Yang M., Rice-Evans C. (1999) Antioxidant
293 activity applying an improved ABTS radical cation decolorization assay. Free Radical Biology &
294 Medicine 26:1231-1237.

295 Senesi N., Chen Y., Schnitzer M. (1977) The role of free radicals in the oxidation and
296 reduction of fulvic acid. Soil Biol. Biochem. 9:397-403.

297 Van der Zee F. P., Cervantes F. J. (2009) Impact and application of electron shuttles on the
298 redox (bio)transformation of contaminants: A review. Biotechnology Advances 27:256-277.

299 Voelker B., Morel F. M. M, Sulzberger B. (1997) Iron Redox Cycling in Surface Waters:
300 Effects of Humic Substances and Light. Environ. Sci. Technol. 31:1004-1011.

FUTURE RESEARCH PERSPECTIVES

Starting with the results obtained so far during these three years, I am continuing the study of the geochemical and redox dynamics of humic substances in transitional environments, with a special focus on their interactions with potentially toxic metals (project “Stable isotope characterization of humic acids and retention capacity for Pb and other metals in the Cananéia-Iguape coastal system (Sao Paulo – Brazil)”) through the collaboration between the University of Udine (I), the University of Trieste (I) and the Oceanographic Institute of the University of Sao Paulo (BR). The identified study areas are the Marano and Grado Lagoon (Italy) and the Cananéia-Iguape coastal system (Brazil): both are microtidal ecosystems affected, to a different degree, by potentially toxic metals contamination. Compared to the Marano and Grado Lagoon, the Cananéia-Iguape system is characterized by a much larger input of humified DOM carried by the brown freshwater bodies. The Cananéia–Iguape coastal system is located in the southern coast of Sao Paulo state (Brazil), acknowledged by UNESCO as Biosphere Reserve of the Atlantic Rainforest. It is 110 km long, consisting of four brackish channels (Mar Pequeno, Mar de Cananéia, Mar de Cubatao and Trapandè Bay) behind a barrier island (Comprida Island), with narrow inlets at the southern and northern ends (Cananéia and Icapara Inlets) (Fig.1).

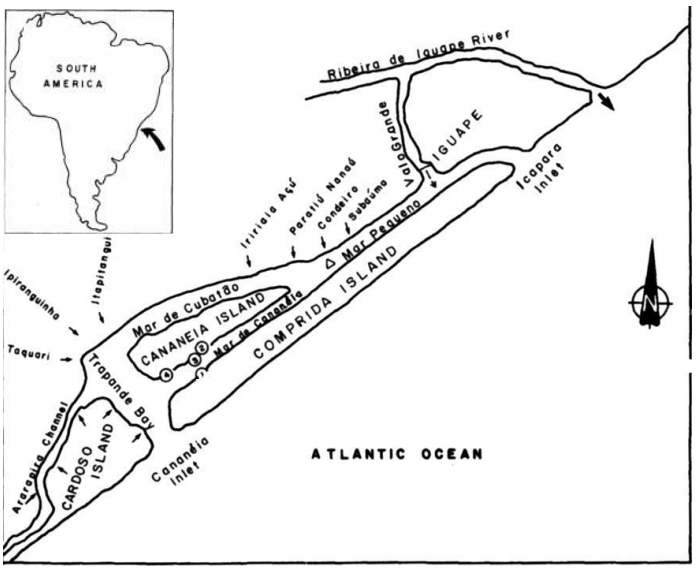

Fig. 1 Schematic view of the Cananéia-Iguape coastal system (adapted from ref [1])

Tides are semidiurnal, with a mean tidal amplitude of 0.82 m. The vegetal cover is characterized by the presence of salt marshes and mangroves on the margins of the water bodies, that are coloured by humic acids[1]. The Ribeira de Iguape River is the greatest contributor of terrestrial material to the system, mainly in its central and northern portions. The artificial channel "Valo Grande", built in the 19th century, connects the River with the lagoon system next to Iguape City and became the preferential river pathway (70% of the flux). On the other hand, the southern part presents limited freshwater inputs. Due to Au, Ag, Zn, and Pb mining activities that took place in the upstream regions of the Ribeira de Iguape River since the 17th century, the system become the final destination of contaminated sediments[2].

Materials and methods

Already performed. The sampling of surficial sediments (Fig. 2) has been performed in August 2019, on the Research Vessel "Albacora" using a stainless steel Van Veen grab. In each station, at least three sediment samples were collected and pooled together to obtain a representative sample. After sampling, sediments were transferred into pre-cleaned bottles, transported to the laboratory, frozen and finally freeze-dried.

Grain-size analyses were performed with a laser granulometer (Malvern Mastersizer 2000), after removing organic matter with H_2O_2 for 48h. Organic carbon (OC), total nitrogen (N_{tot}) and carbon and nitrogen stable isotope composition ($\delta^{13}C$ and $\delta^{15}N$) of bulk sediments were measured, after removing carbonates, with an Isotope Ratio Mass Spectrometer (Thermo Scientific Delta V Advantage) coupled with the Elementar Analyzer (Costech Instruments Elemental Combustion System).

[1] Schaeffer-Novelli, Y., De Souza Lima Mesquita, H., Cintron-Molero, G. (1990) The Cananeia Lagoon estuarine system, Sao Paulo, Brazil. Estuaries 13:193-203.

[2] Mahiques, M.M., Figueira, R.C.L., Salaroli, A.B., Alves, D.P.V., Goncalves, C. (2013) 150 years of anthropogenic metal input in a biosphere reserve: the case study of the Cananeia-Iguape coastal system. Environmental Earth Sciences 68:1073-1087.

Total Hg in sediments was determined by an automatic mercury analyzer (DMA-80, Milestone). Accuracy of results was verified using the PACS-2 standard as reference material.

Free and mineral-bound humic acids (HA) were sequentially extracted, freeze-dried and weighted using the procedure descripted in Chapter 5. In addition, also fulvic acids (FA) were isolated from the same sediments.

Planned. Spectroscopic (FT-IR, UV-Vis, ^{13}C NMR, EEM Fluorescence) and carbon and nitrogen stable isotopes analyses will be performed on the extracted HA and FA. Moreover, the metal content (Pb, Cu, Zn and As) of sediments, HA and FA will be measured using Inductively Coupled Plasma – Optical Emission Spectrometry (ICP-OES, Optima 8000, PerkinElmer). Electrochemical analysis will be performed in order to determine the redox properties (e.g. the electron donating capacity) and evaluate the metal chelating and transformation potential of HA and FA.

Fig. 2. Location of the sampling points.

Preliminary results

Preliminary results are summarized in Table 1. A low content of carbonates is present in all sediments (mean value of 3.7 ± 3.0 %). Sand is the predominant grain-size fraction in almost all samples. The distribution of the organic carbon concentration (0.2-4.2 %) and HS in sediments do not follow a clear geographical trend, as a consequence of the complex dynamics inside the lagoon. Carbon stable isotope values ($\delta^{13}C$) showed more negative values in the northern sector of the lagoon (up to -28.3 ‰ in station 16), due to more terrestrial inputs of OM. In the southern part, where the influence of marine inputs of OM is higher, $\delta^{13}C$ values became less negative (-24.0 ‰ in station Barra Nova).

Table 1. Geographic coordinates and depth of sampling sites; $CaCO_3$, C_{org}, N_{tot} content, C stable isotopes and granulometric composition, Hg and HS content of sediments.

Station	Latitude	Longitude	Depth	$CaCO_3$	C_{org}	N_{tot}	$\delta^{13}C$	Sand	Silt	Clay	Hg	Free HA	Bound HA	FA
	S	W	m	%	%	%	‰ vs V-PDB	%	%	%	mg kg^{-1}	mg g^{-1}	mg g^{-1}	mg g^{-1}
BN-borda	25°14'59.10"	48°3'0.72"	0.2	6.4	3.04	0.22	-24.0	33.8	62.2	3.9	0.09	1.85	5.73	3.40
16A	25°11'37.56"	47°59'57.60"	6.6	3.4	0.67	0.03	-27.0	67.4	30.4	2.2	0.03	0.26	0.73	0.69
15	25°10'29.64"	48° 1'35.46"	5.7	8.0	0.60	0.05	-26.7	60.4	36.9	2.7	0.08	0.10	0.92	0.74
14A	25° 7'20.46"	48° 1'7.26"	10.2	3.4	0.72	0.06	-27.3	38.8	55.9	5.3	0.13	0.01	0.19	0.32
12	25° 4'25.74"	47°58'51.78"	10.7	0.1	1.94	0.17	-25.9	43.0	54.0	3.0	0.09	1.15	4.30	3.41
7A	24°59'54.96"	47°53'50.16"	11.6	4.0	0.94	0.08	-26.2	45.3	51.1	3.6	0.17	0.46	1.00	0.93
I	24°57'33.18"	47°53'36.18"	12.2	3.9	0.73	0.08	-26.6	48.3	48.6	3.1	0.12	1.58	1.64	1.52
T4	24°57'51.00"	47°51'51.06"	10.7	2.9	0.79	0.04	-25.3	57.3	39.0	3.7	0.04	0.60	0.75	0.73
6	24°54'10.92"	47°48'29.04"	6.4	0.9	-	0.01	-	95.4	4.6	0.0	0.08	0.12	0.14	0.21
D	24°48'58.08"	47°41'44.82"	3.4	4.5	2.59	0.24	-27.5	7.8	85.7	6.6	0.20	9.23	2.56	3.09
C	24°47'37.44"	47°40'21.06"	3.1	5.2	2.65	0.21	-28.3	16.3	77.2	6.5	0.20	6.56	2.74	2.48
B	24°46'6.78"	47°38'34.50"	2.8	5.2	2.41	0.18	-28.0	17.1	76.7	6.2	0.18	5.90	1.82	2.24
Barra	25° 3'41.10"	47°54'32.34"	7.8	-	-	-	-	100.0	0.0	0.0	0.01	0.01	0.05	-
8	25° 1'16.92"	47°55'16.14"	13.8	11.5	3.73	0.31	-26.3	40.2	56.2	3.6	0.18	2.72	3.37	3.90
Porto	25° 0'41.34"	47°55'26.70"	9.8	6.8	1.24	0.07	-26.5	47.8	48.5	3.8	0.09	0.34	0.71	0.44
CUB2	24°55'0.19"	47°52'35.40"	4.8	1.3	-	0.01	-	97.5	2.5	0.0	0.03	0.17	0.37	0.52
CUB4	25° 1'12.60"	47°58'56.82"	2.8	5.1	1.10	0.10	-26.8	54.3	42.9	2.9	0.05	0.45	0.72	1.20
CUB-M	25° 1'80.30"	47°59'52.90"	0.2	-	-	-	-	39.3	58.1	2.6	0.08	3.76	7.83	3.62
CUB5	25° 2'0.66"	48° 0'49.56"	6.2	4.9	1.10	0.10	-25.6	45.2	51.5	3.3	0.06	0.47	1.15	1.10
RR	24°40'27.26"	47°34'56.21"	9.0	-	-	-	-	62.8	32.7	4.5	0.05	1.22	0.73	0.71
IVG	24°42'44.93"	47°33'48.35"	3.7	0.5	-	-	-	97.2	2.8	0.0	0.03	0.06	0.04	0.13

APPENDIX

CHAPTER 2: Supporting Information……..……..……xi

CHAPTER 3: Supporting Information……...…….…..……..xviii

CHAPTER 4: Supporting Information…….……...……..…..…..…..xxvii

CHAPTER 5: Supporting Information…….……..…..…..xxvii

CHAPTER 6: Supporting Information…….……..……..…xxxvii

CHAPTER 2: SUPPORTING INFORMATION

Is alkalinity of extractants responsible of artefacts formation during humic substances extraction?

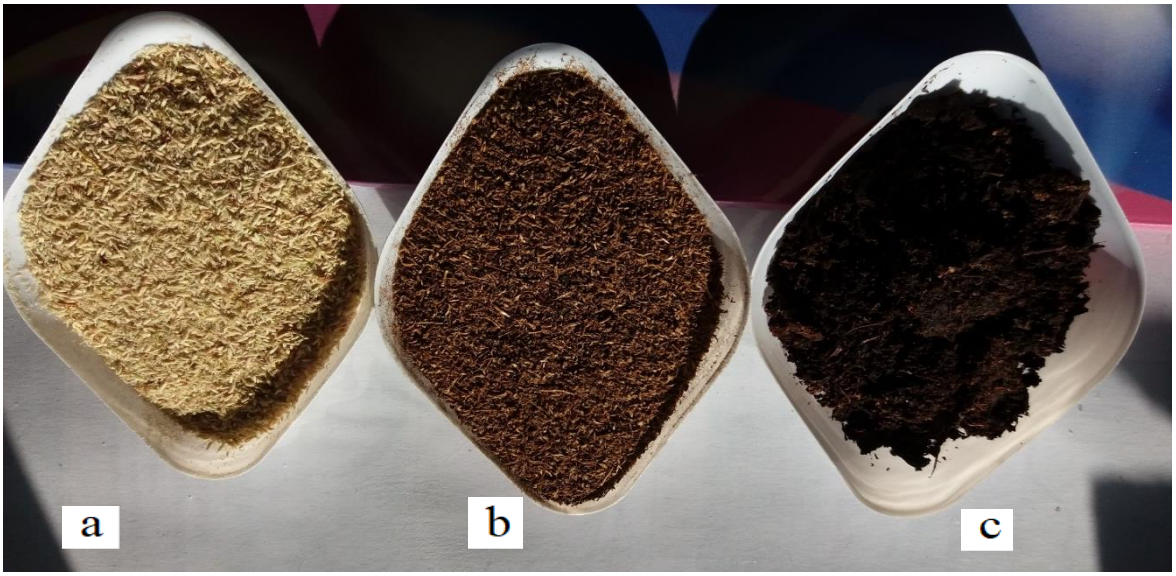

Fig. S1 Samples of **a.** sphagnum moss; **b.** partly-humified peat; **c.** well-humified peat.

Sphagnum moss was collected in an Eriophoetum-Sphagnum blanket bog (Mount Tuglia, Italy). Soil particles and impurities were manually removed after drying the sample.

The selected partly-humified peat was a White Sphagnum peat (Kekkilä, Finland), pH 3.6, Von Post index H=1.5.

The selected well-humified peat was a Blonde acid Sphagnum peat (Lithuania), pH 3.5, Von Post index = 4.

Elemental composition and ^{13}C content of the raw materials were:

	C (%)	N (%)	C/N	$\delta^{13}C$ (‰)
Sphagnum moss	42.8	1.0	41.6	-27.4
Partly-humified peat	45.2	0.8	56.0	-25.6
Well-humified peat	45.9	1.1	41.7	-26.8

Table S1 Extraction yields of total extractable carbon (TEC), humic carbon (HU), not-humic carbon (NHU) and HU/TEC and NHU/TEC ratios for the three materials investigated.

		Extractant			
		NaOH	A-NaPP	N-NaPP	Water
TEC (mg-C/g-C)	Sphagnum	210.50	86.91	65.79	62.09
	Partly-humified peat	326.62	112.81	78.72	48.22
	Well-humified peat	248.31	56.98	37.12	21.79
HU (mg-C/g-C)	Sphagnum	94.75	30.65	11.69	7.18
	Partly-humified peat	231.77	71.60	43.41	15.89
	Well-humified peat	191.62	38.67	20.10	7.94
NHU (mg-C/g-C)	Sphagnum	111.63	58.60	55.14	54.58
	Partly-humified peat	93.86	39.18	34.26	30.30
	Well-humified peat	53.30	17.18	15.81	13.51
HU/TEC	Sphagnum	0.45	0.35	0.18	0.12
	Partly-humified peat	0.71	0.63	0.55	0.33
	Well-humified peat	0.77	0.68	0.54	0.36
NHU/TEC	Sphagnum	0.53	0.67	0.84	0.88
	Partly-humified peat	0.29	0.35	0.44	0.63
	Well-humified peat	0.21	0.30	0.43	0.62

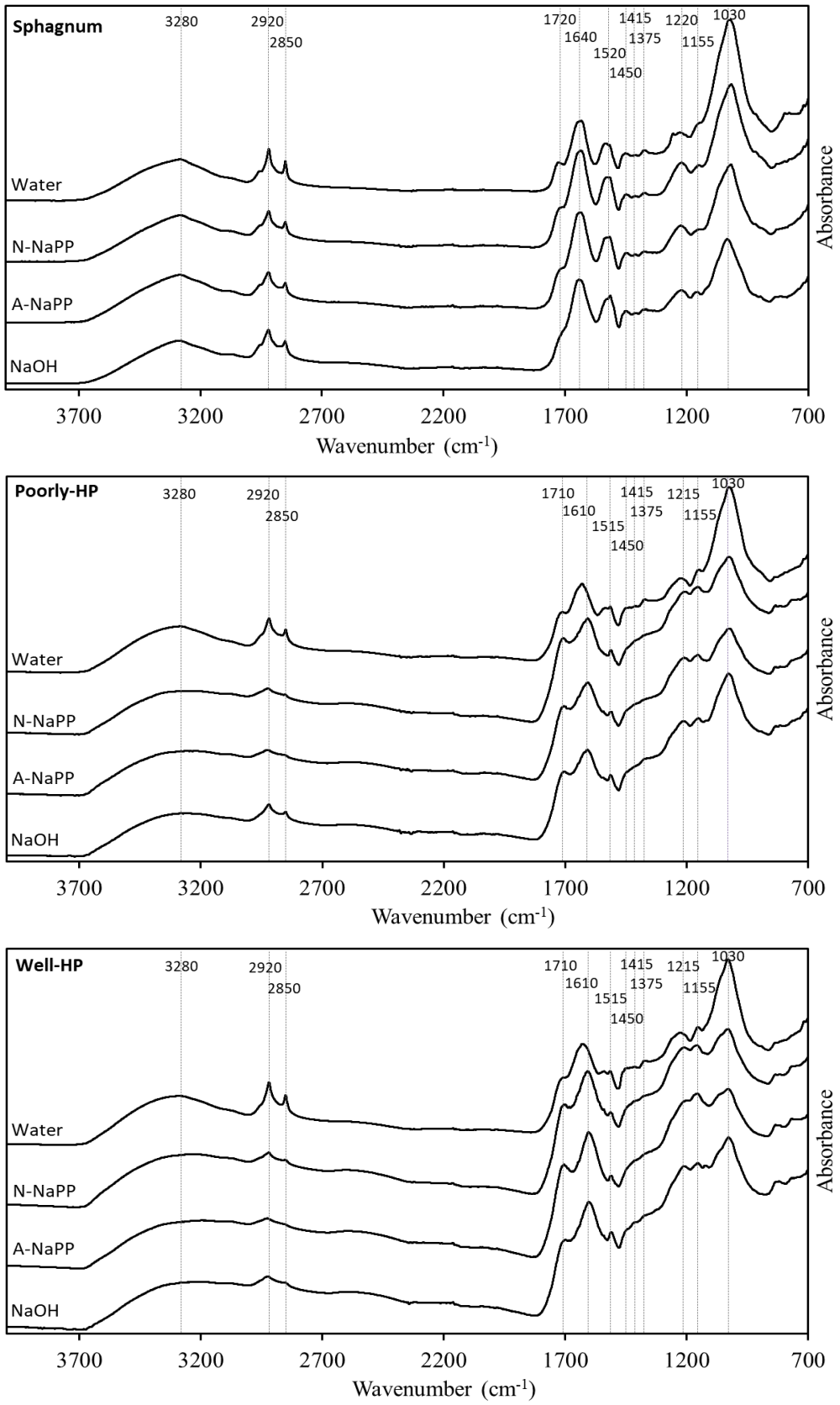

Fig. S2 FT-IR spectra of HA extracted from sphagnum, partly-humified and well-humified peat using different extractants.

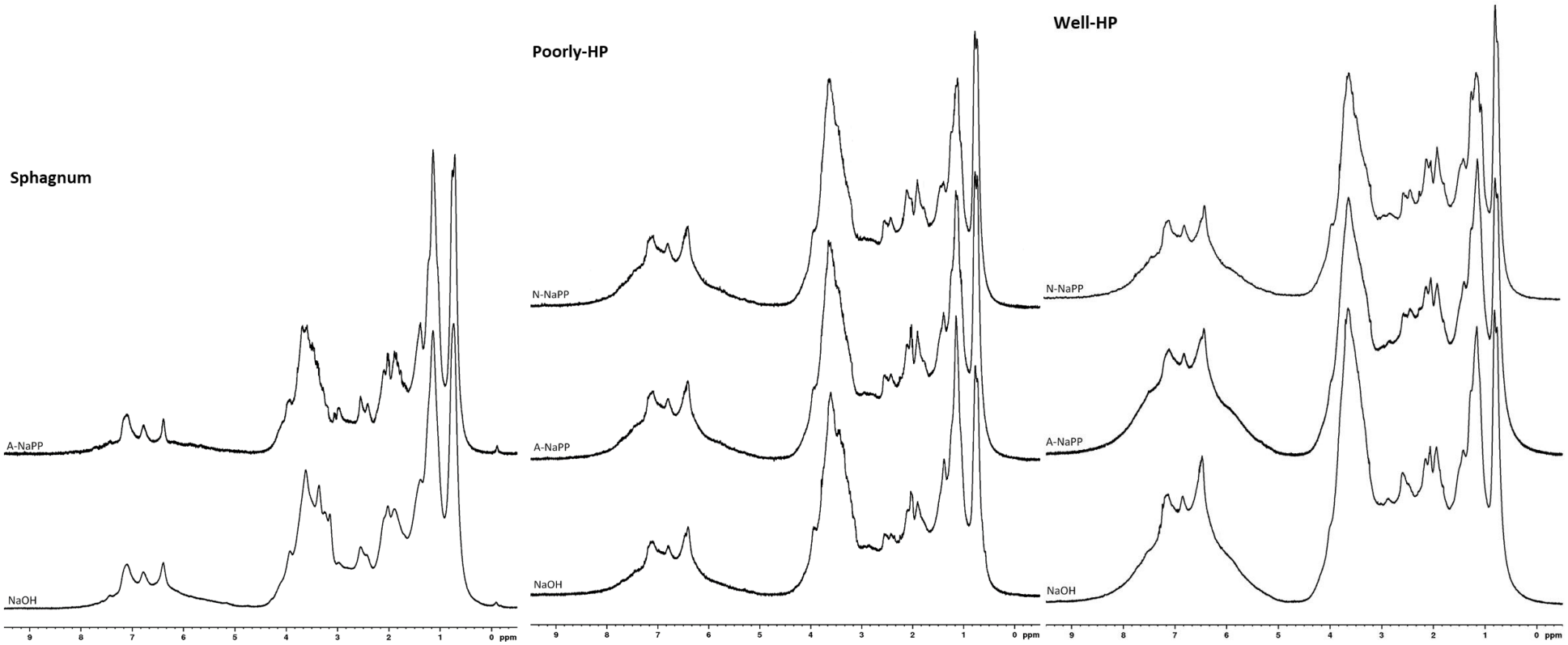

Fig. S3 ^{1}H NMR spectra of HA extracted from sphagnum, partly-humified and well-humified peat using different extractants.

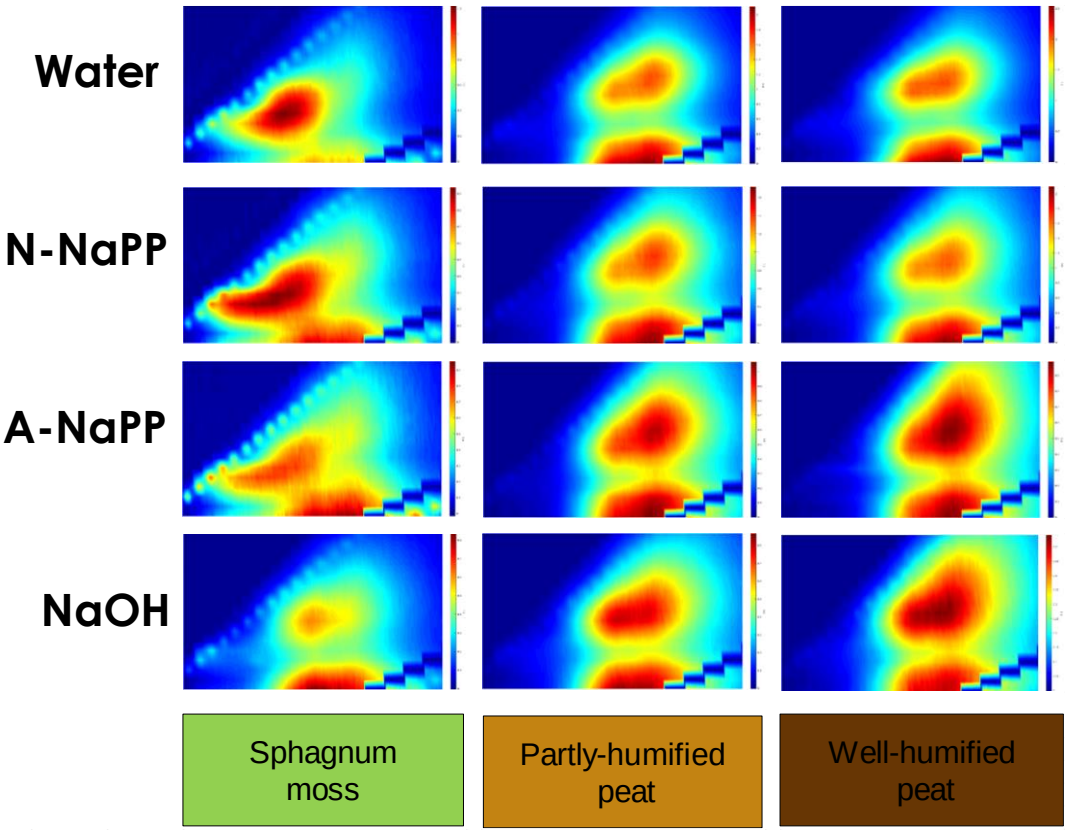

Fig. S4 Fluorescence excitation-emission matrix spectra of total extracts.

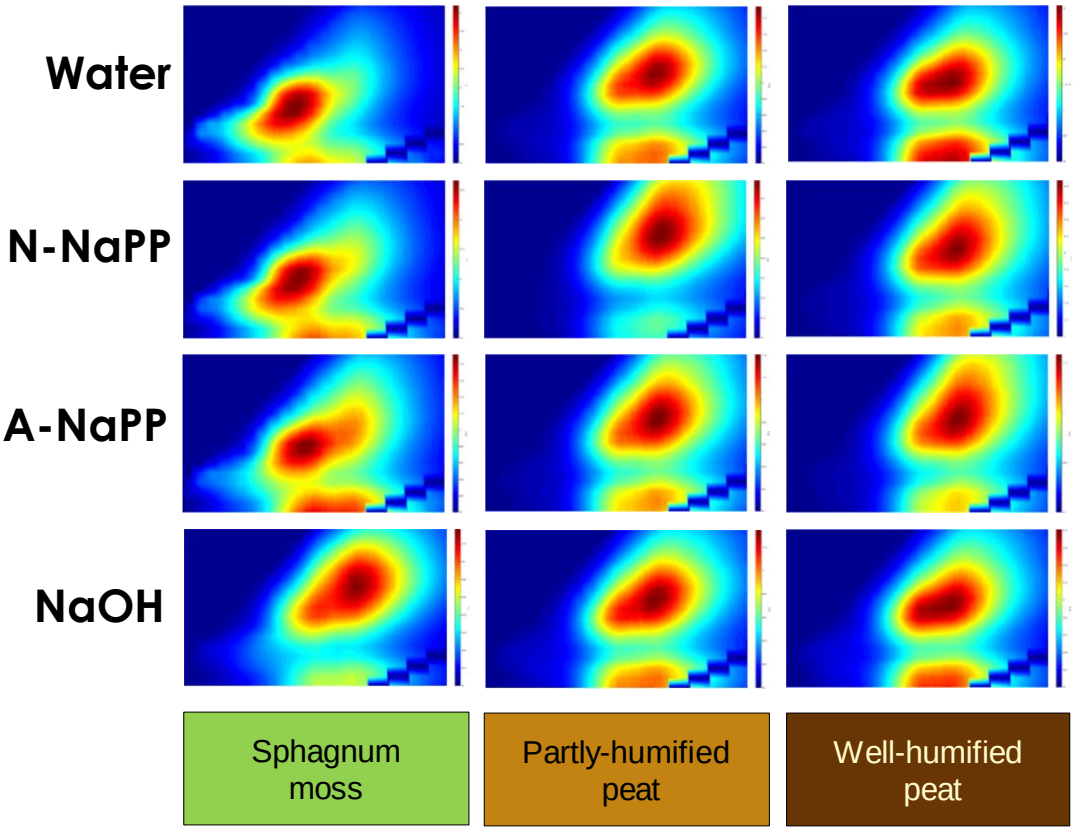

Fig. S5 Fluorescence excitation-emission matrix spectra of fulvic acids.

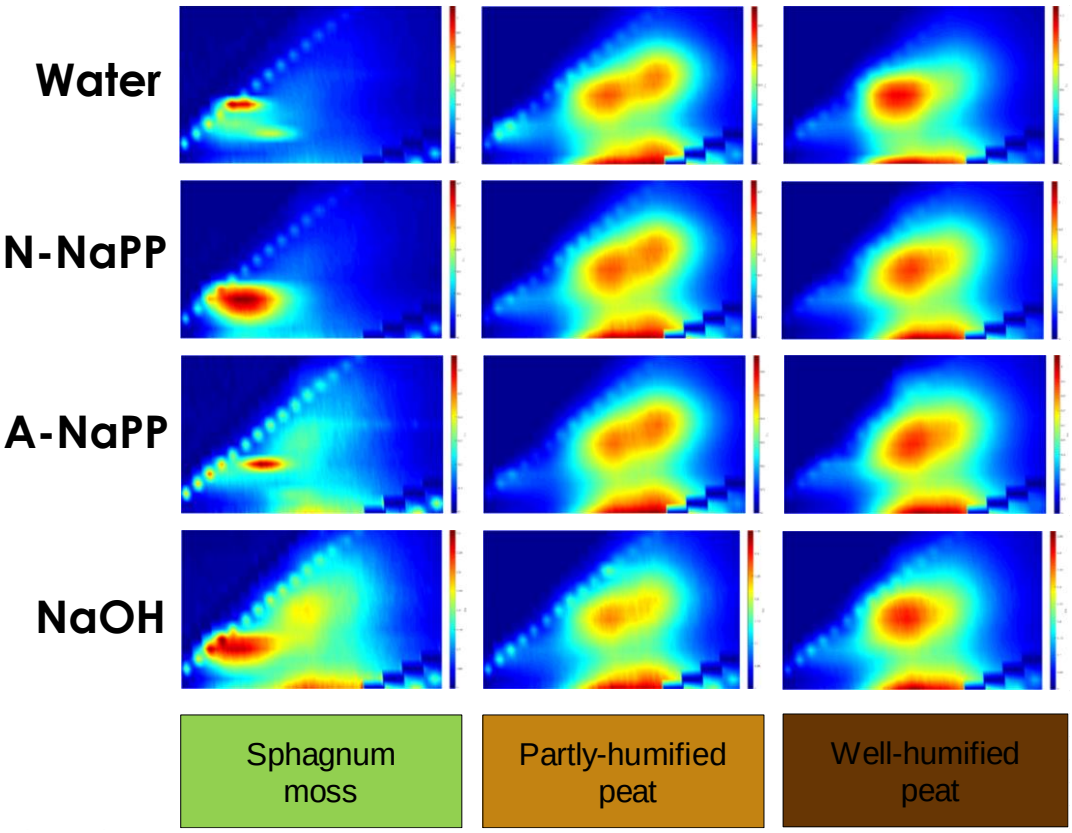

Fig. S6 Fluorescence excitation-emission matrix spectra of the not-humic fraction.

CHAPTER 3: SUPPORTING INFORMATION

Modification of peat humic acids induced by their use as terminal electron acceptors in a mesocosm incubation experiment

Peat Characterization. The peat used in this study is an acid sphagnum peat (pH 3.7), moderately decomposed (Von Post index H=4-5) where the structure of the plant remains is quite indistinct although it is still possible to recognize certain features. The measured water-holding capacity (WHC) is 675%. Other measured parameters are: Organic Carbon (OC) 45.86 ± 1.00 %, Total Nitrogen (N) 1.10 ± 0.06 %, OC/N ratio 41.7, carbon stable isotope composition ($\delta^{13}C$) -27.04 ± 0.05.

Table S1 Organic Carbon (OC), total Nitrogen (N) and carbon stable isotope composition ($\delta^{13}C$) of the extracted HA ($HA_{not\text{-}inc}$, HA_{red}, HA_{ox}).

	OC (%)	N (%)	C/N	$\delta^{13}C$ (‰ vs V-PDB)
$HA_{not\text{-}inc}$	48.80 ± 0.51	2.22 ± 0.01	22.0	-27.08 ± 0.01
HA_{red}	48.84 ± 0.02	1.96 ± 0.02	25.0	-26.98 ± 0.03
HA_{ox}	48.92 ± 0.02	1.93 ± 0.00	25.3	-26.97 ± 0.04

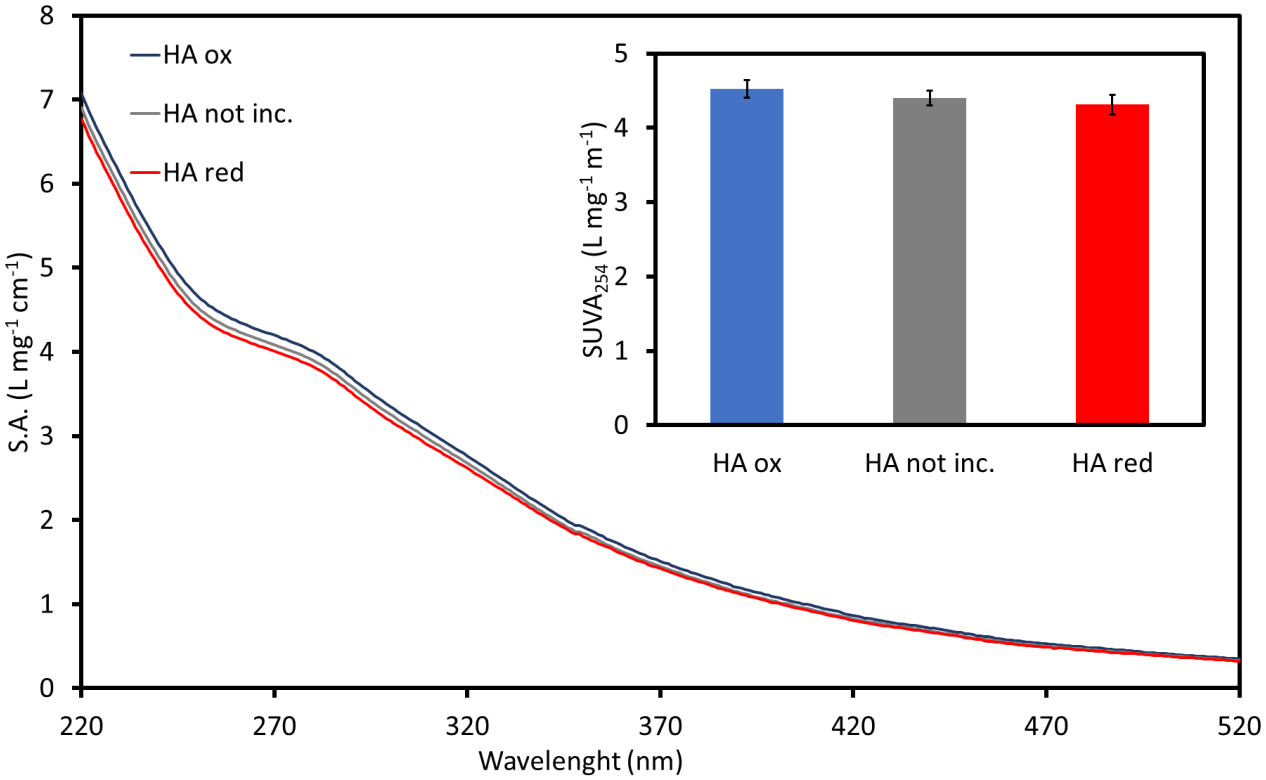

Fig. S1 Organic Carbon normalized UV-Vis spectra of HA_{ox} (blue trace), HA_{red} (red trace) and $HA_{not-inc}$ (grey trace). The insert represents the $SUVA_{254}$ values.

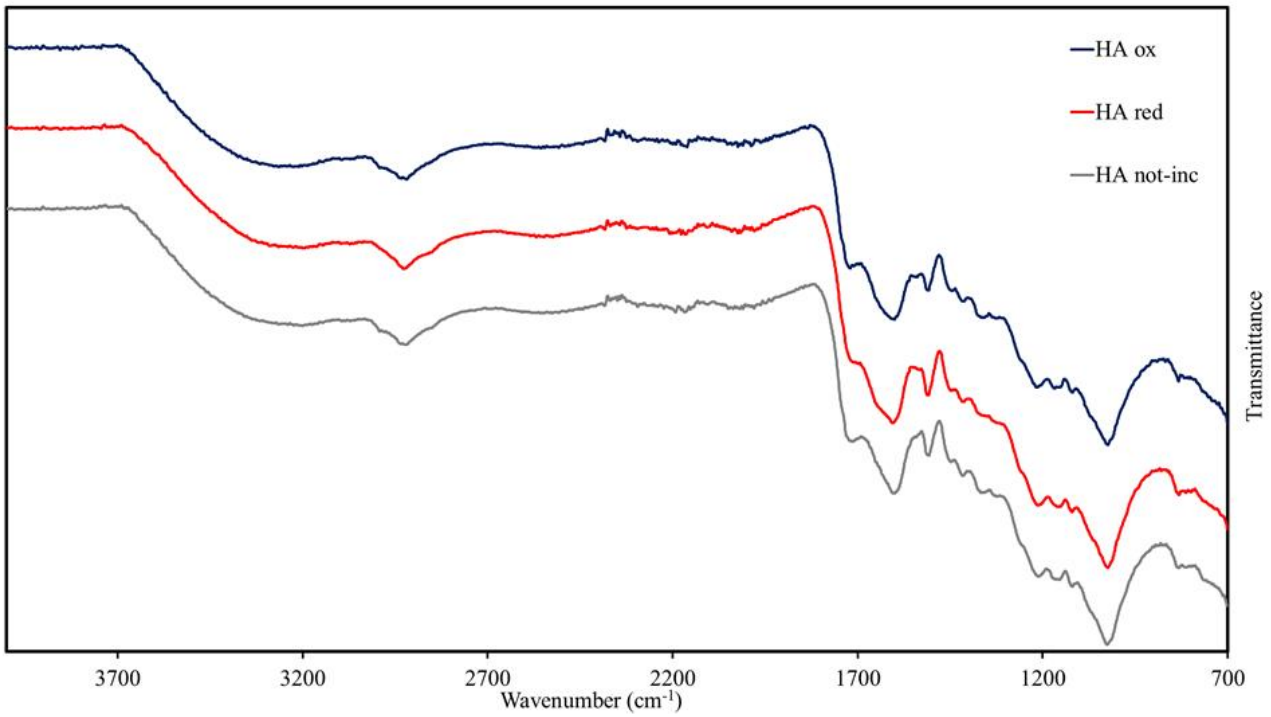

Fig. S2 FTIR spectra of HA_{ox} (blue trace), HA_{red} (red trace) and $HA_{not-inc}$ (grey trace).

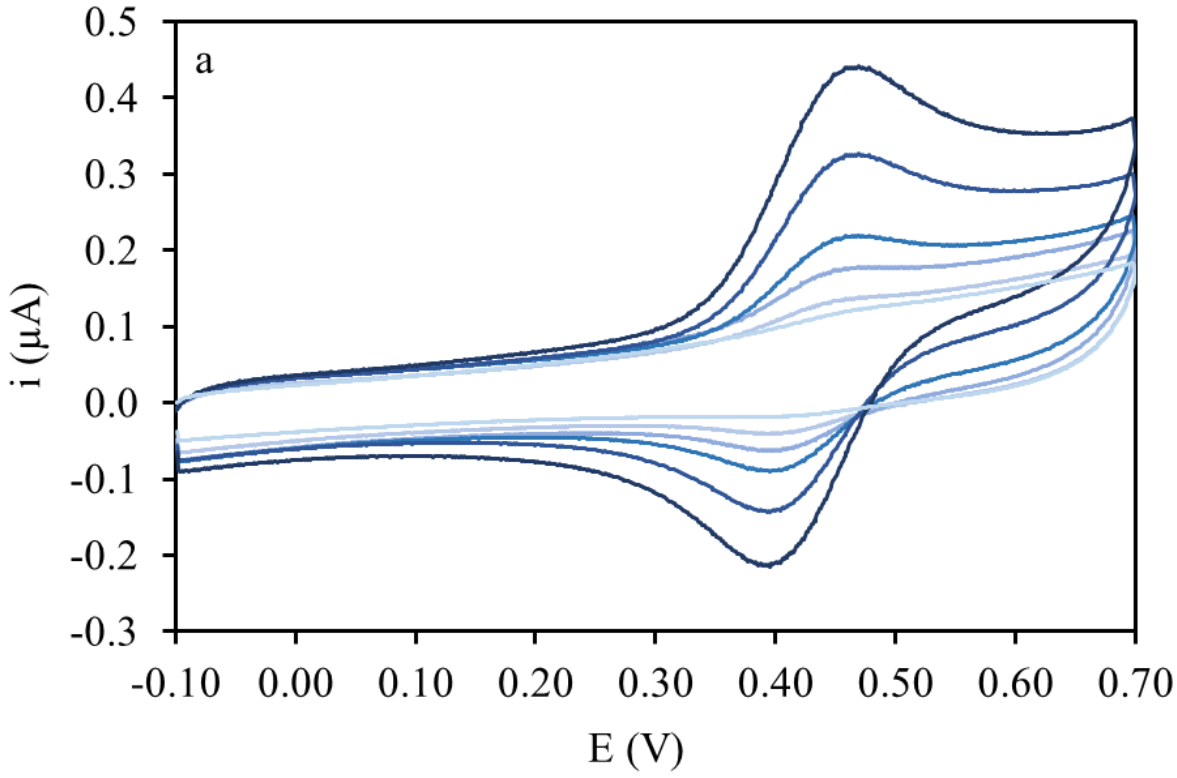
a
0.5
0.4
0.3
0.2
0.1
0.0
-0.1
-0.2
-0.3
i (µA)
-0.10
0.00
0.10
0.20
0.30
0.40
0.50
0.60
0.70
E (V)

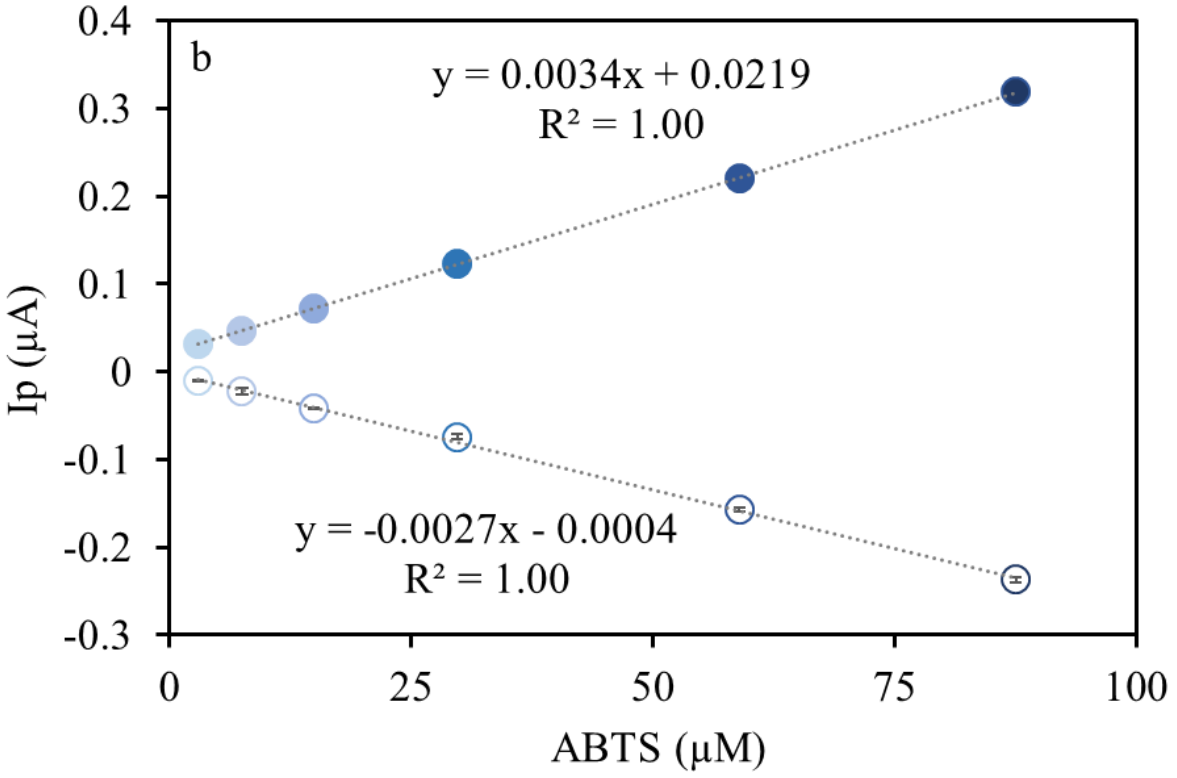
b
y = 0.0034x + 0.0219
R² = 1.00
y = -0.0027x - 0.0004
R² = 1.00
0.4
0.3
0.2
0.1
0
-0.1
-0.2
-0.3
Ip (µA)
0
25
50
75
100
ABTS (µM)

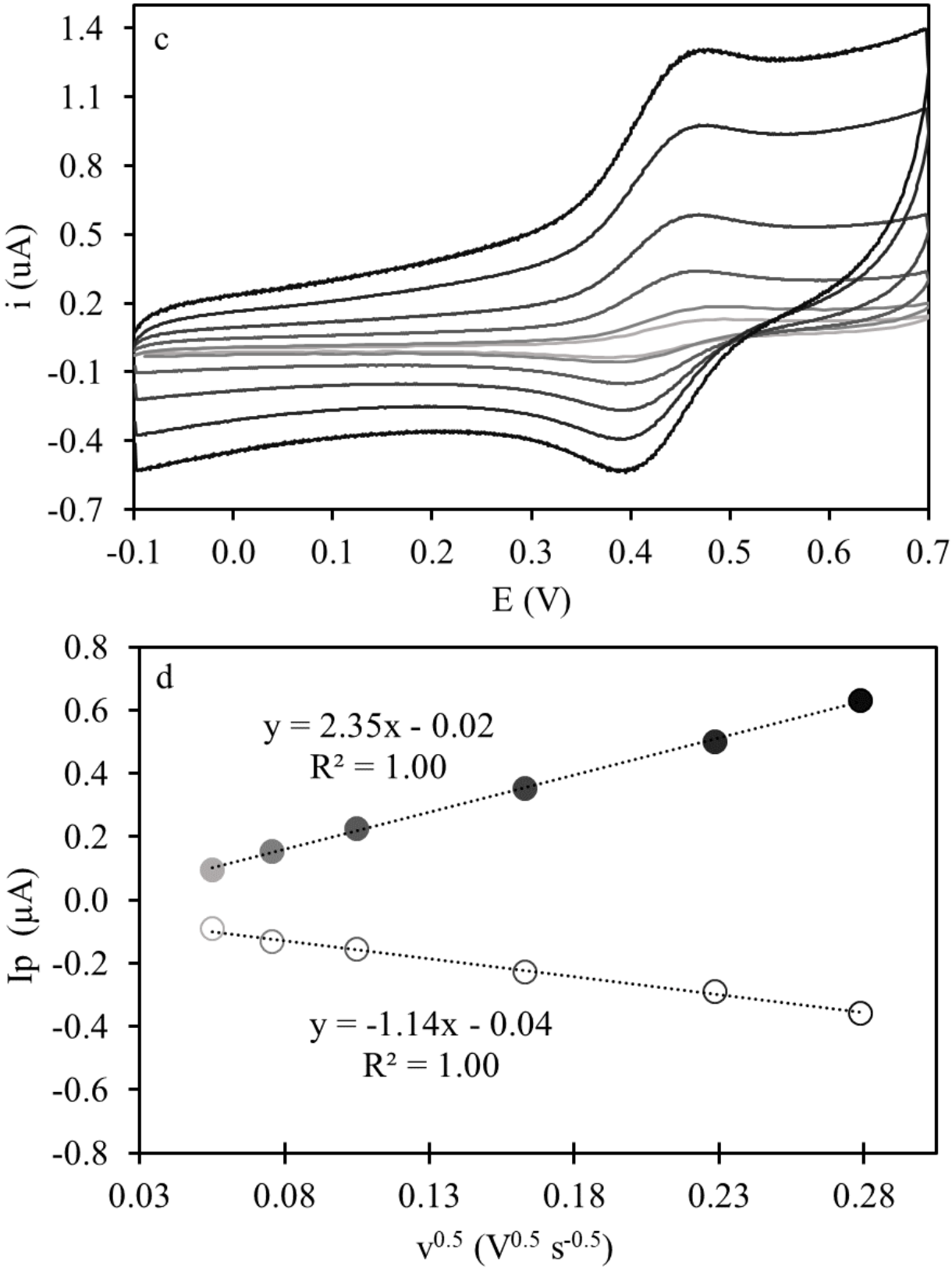

Fig. S3 a. Cyclic voltammograms of 2,2'-azino-bis(3-ethylbenzothiazoline-sulfonic acid) (ABTS) at different concentrations from 3 to 80 µM (scan rate v = 0.010 V s^{-1}). **b.** Linear correlation between anodic (filled symbols) and cathodic (empty symbols) peak currents versus the ABTS concentration. **c.** Cyclic voltammograms of ABTS (60 µM) at different scan rates from 0.0025 to 0.075 V s^{-1}. **d.** Linear correlation between anodic (filled symbols) and cathodic (empty symbols) peak currents versus the square root of the scan rate.

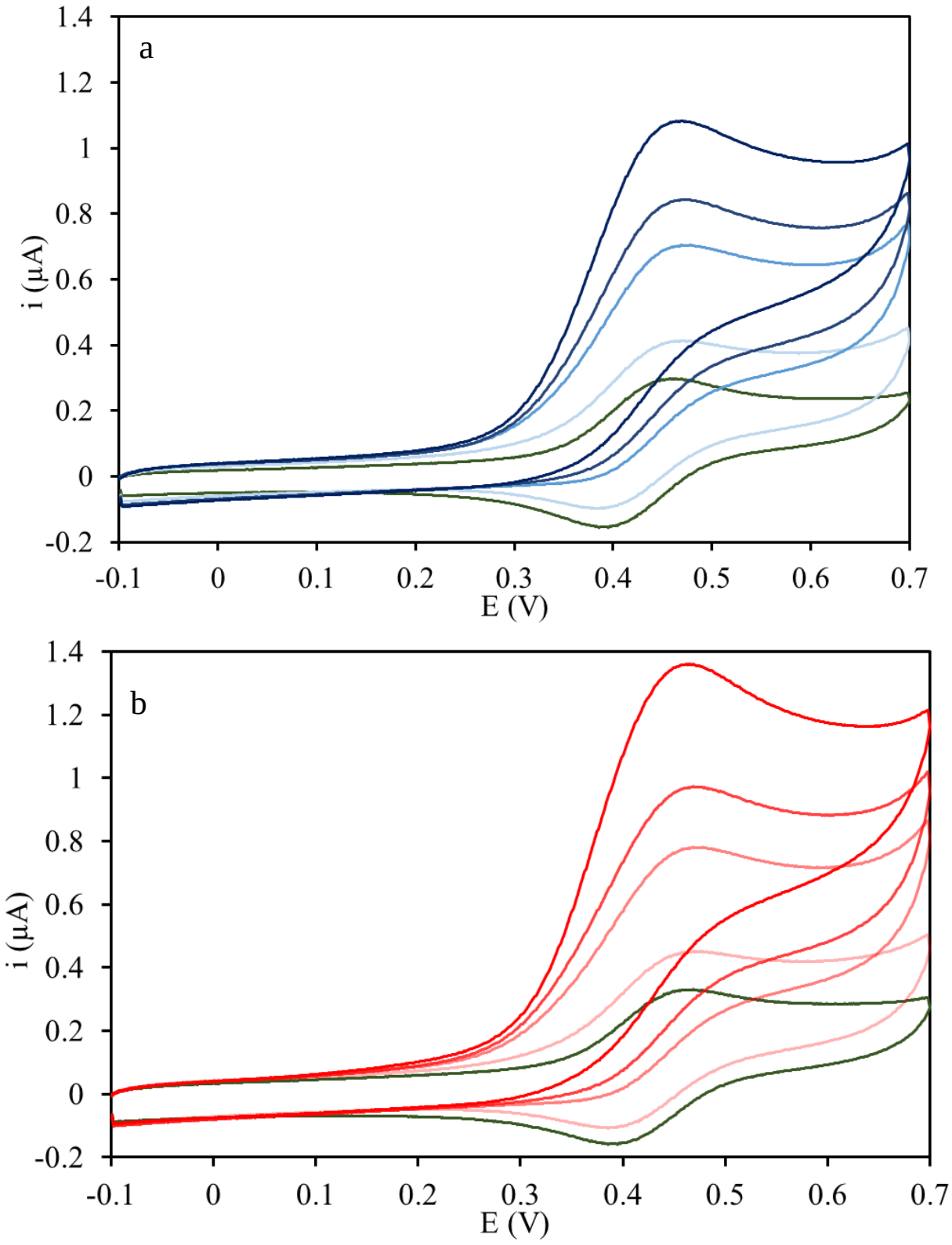

Fig. S4 Cyclic voltammograms of solutions containing only 2,2'-azino-bis(3-ethylbenzothiazoline-sulfonic acid) 60 µM (ABTS, green line) and both ABTS and HA_{ox} (**a**) and HA_{red} (**b**).

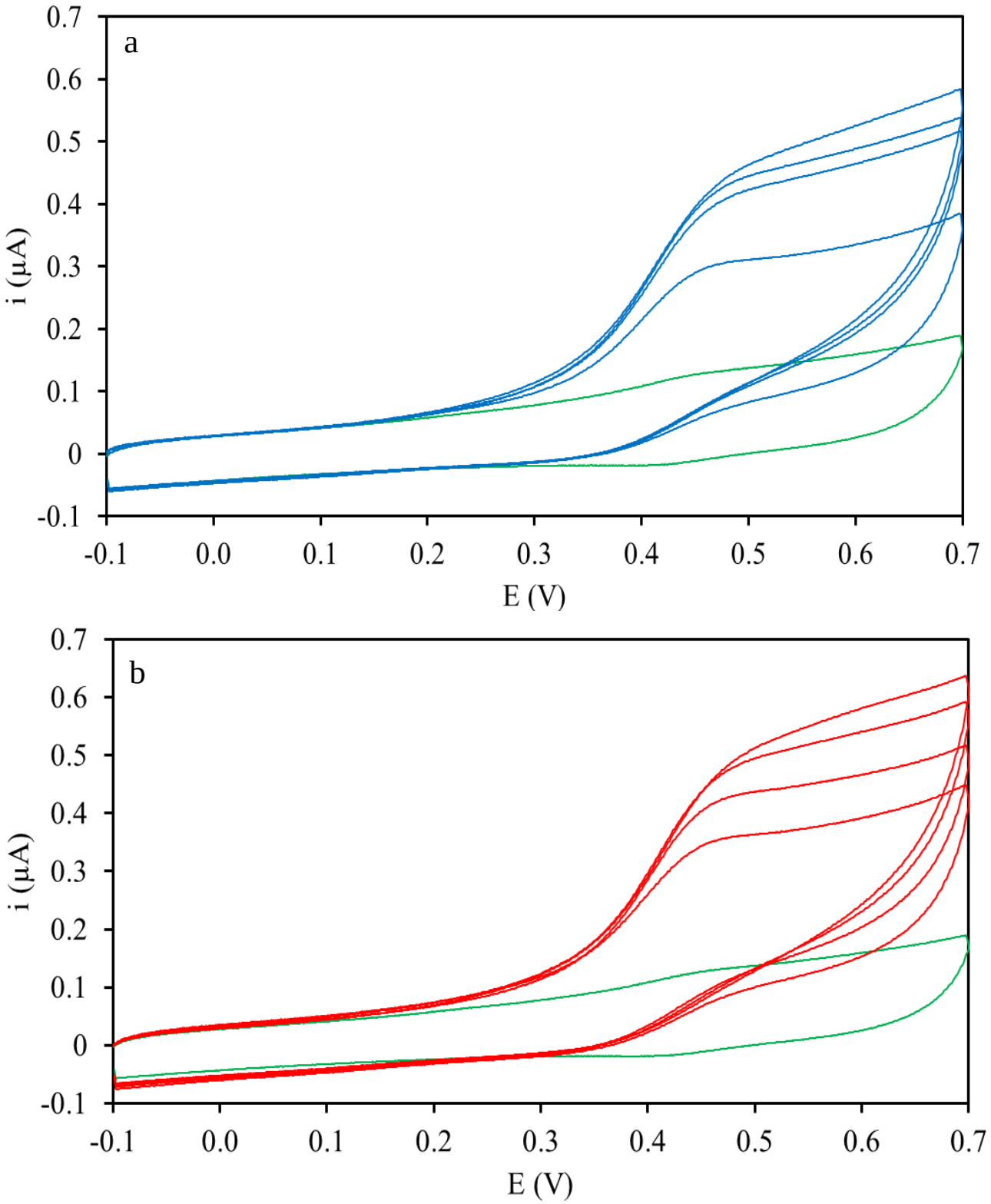

Fig. S5 Cyclic voltammograms of solutions containing only 2,2'-azino-bis(3-ethylbenzothiazoline-sulfonic acid) 3 µM (ABTS, green line) and both ABTS and HA_{ox} (**a**) and HA_{red} (**b**).

CHAPTER 4: SUPPORTING INFORMATION

Electron donating capacity of humic substances in relation to fast electron shuttling mechanisms at environmentally meaningful pH

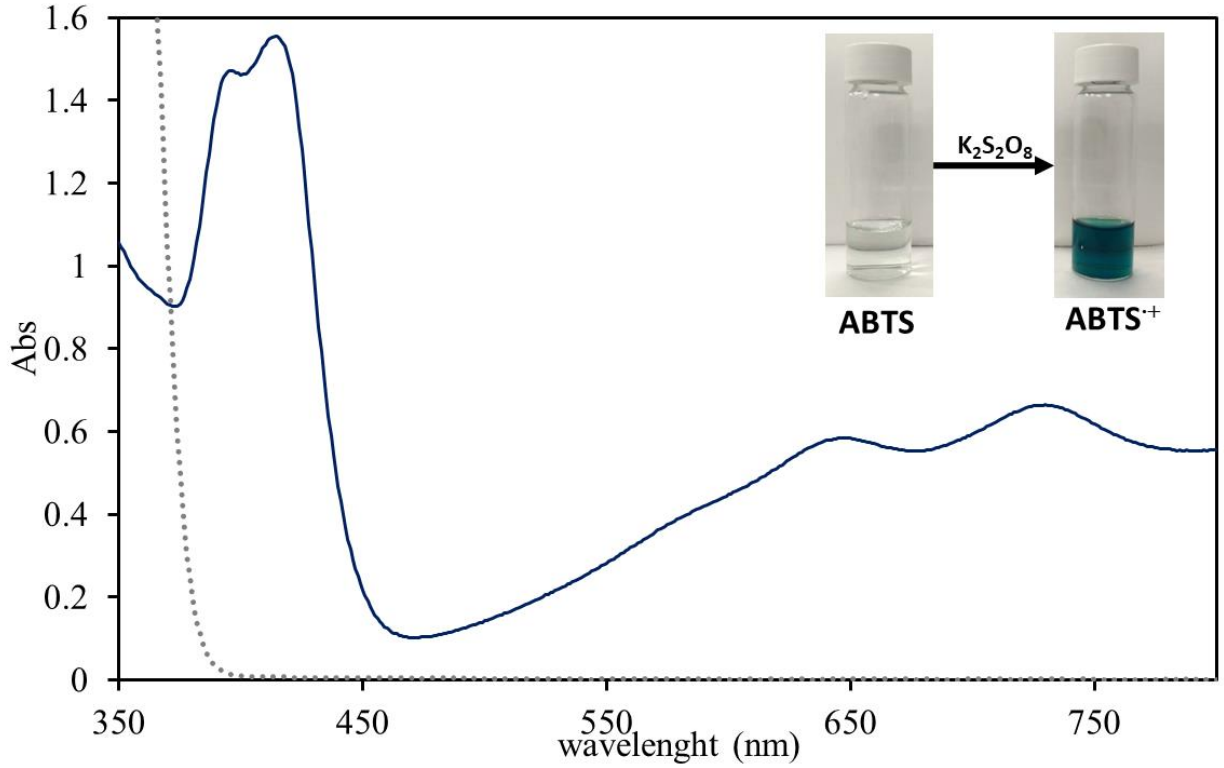

Fig. S1 Vis spectra of ABTS (•••) and its radical cation $ABTS^{\cdot+}$ (—).

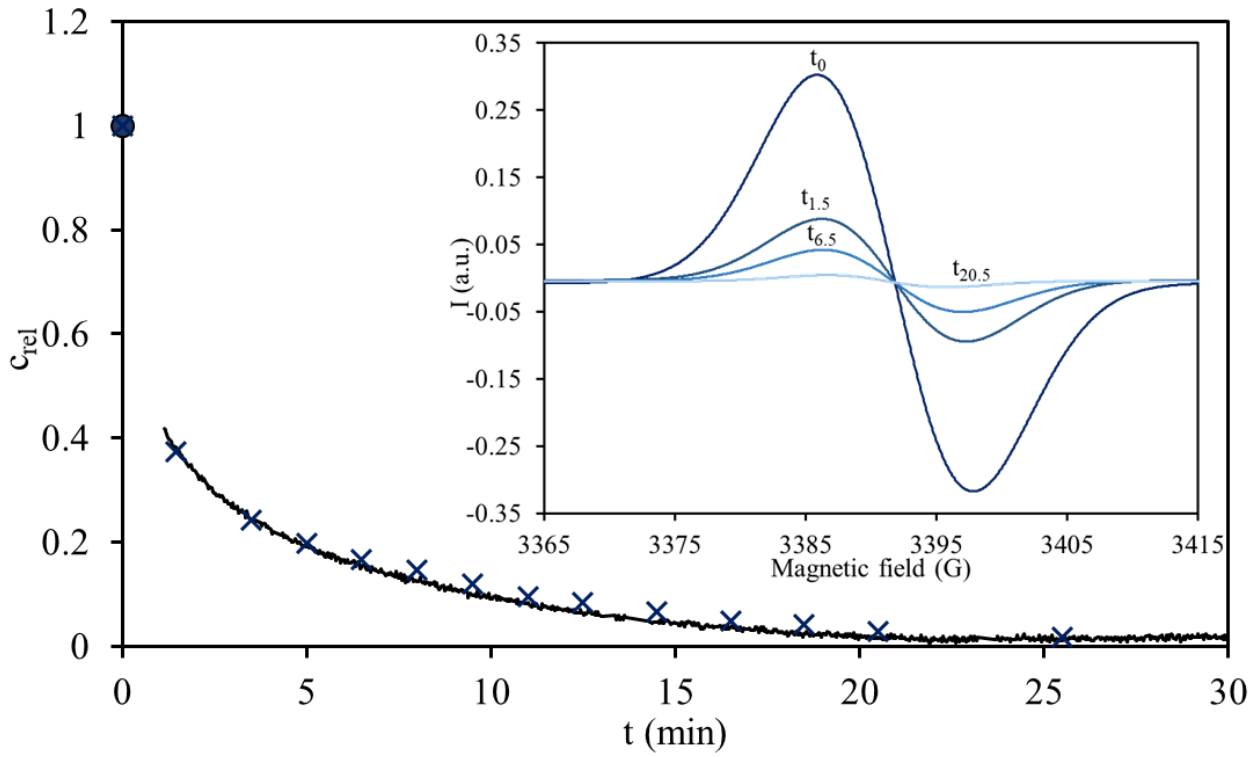

Fig. S2 Time course of the reaction between $ABTS^{\cdot+}$ and SRFA followed by double integration of the EPR signal area (insert) at different reaction times (X symbols) and continuously measurement of the intensity at the positive peak (3386 G in this case) over the time (black curve). The intensities are expressed as relative concentration (c_{rel}) respect to the signal of the $ABTS^{\cdot+}$ prior the addition of SRFA.

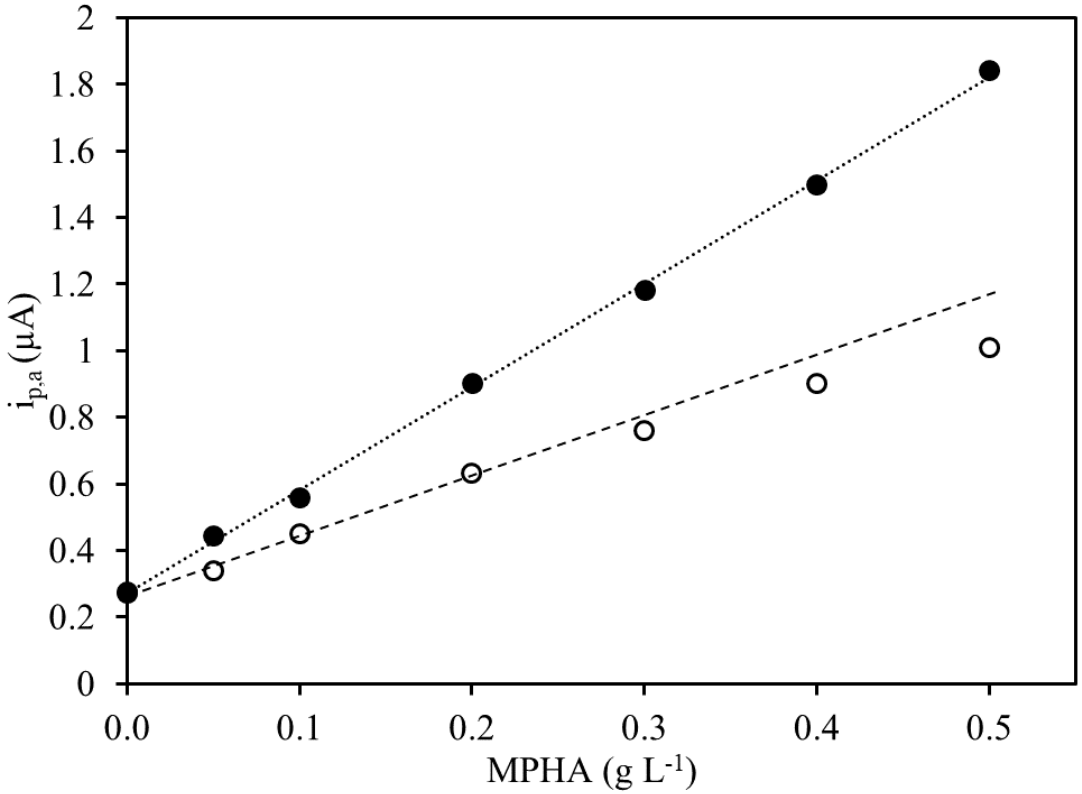

Fig. S3 Anodic peak current ($i_{p,a}$) measured from cyclic voltammograms of solutions containing 60 µM ABTS on MPHA at increasing concentrations, with (●) or without (○) cleaning the electrode before each scan.

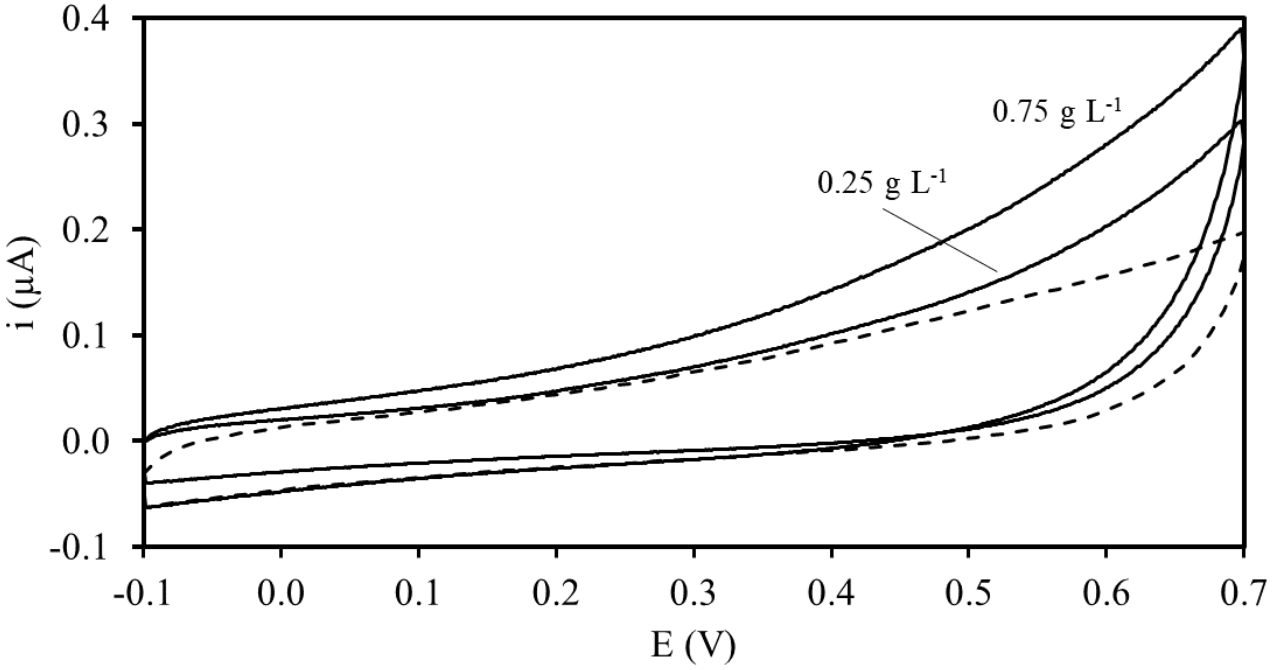

Fig. S4 Cyclic voltammograms (CVs) of SRFA solutions at 0.25 and 0.75 g L^{-1}. Dotted CV represents the background electrolyte.

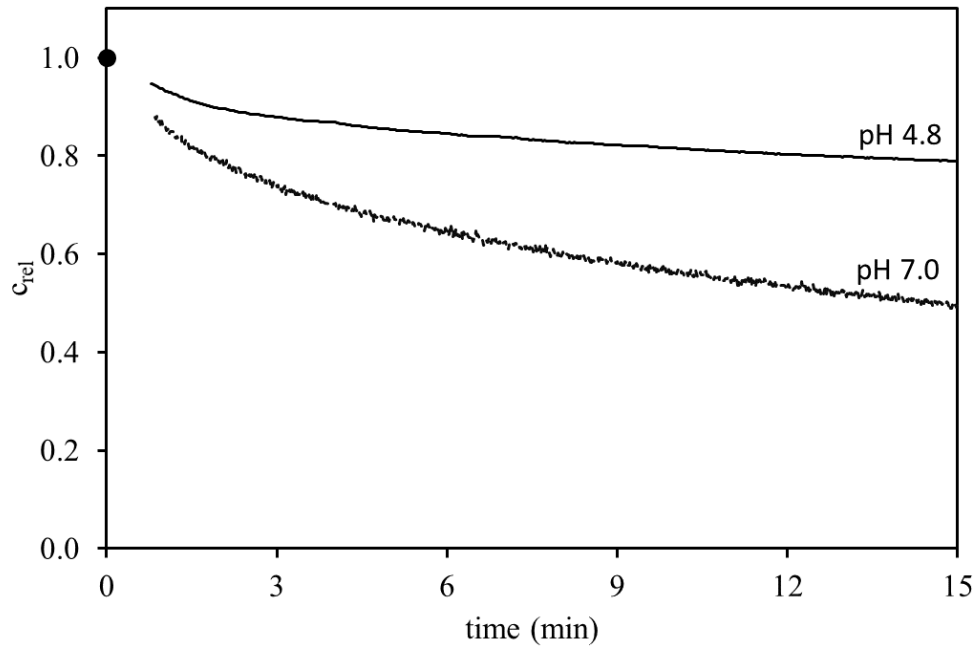

Fig. S5 Relative concentration (c_{rel}) of $ABTS^{\cdot+}$ after the addition of SRFA at different pH (4.8 and 7.0). The black point indicates the c_{rel} at t_0.

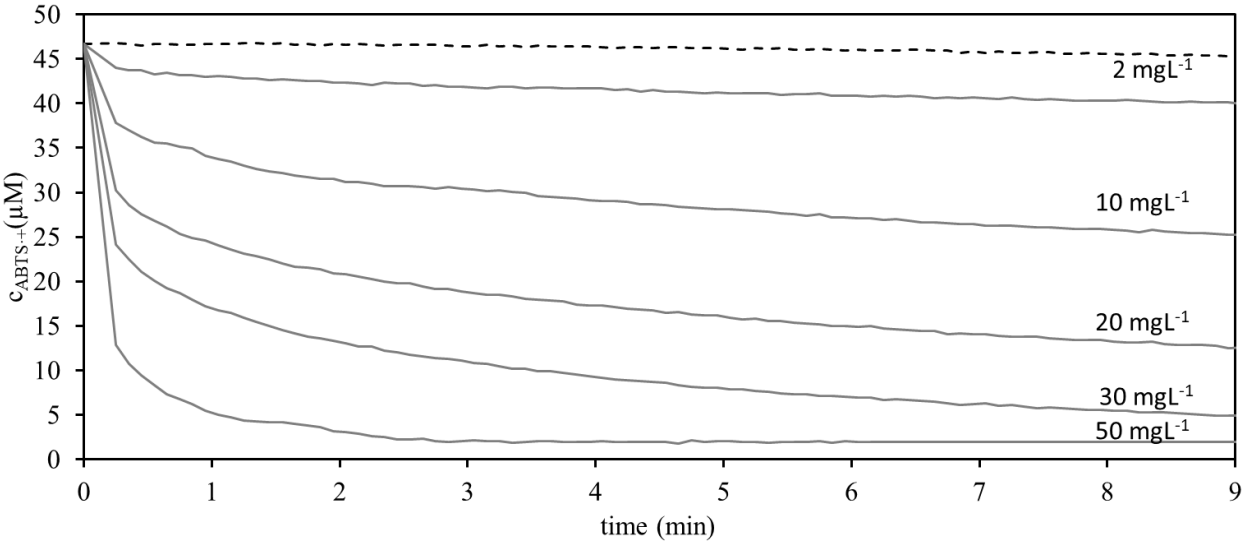

Fig. S6. Time trend of the decrease in the concentration of $ABTS^{\cdot+}$ (μM), corresponding to the reduction of $ABTS^{\cdot+}$ to ABTS, after the addition of increasing amounts of SRFA. Dotted line represents the auto-decay of $ABTS^{\cdot+}$.

CHAPTER 5: SUPPORTING INFORMATION

SEDIMENTS, SEC 2 • PHYSICAL AND BIOGEOCHEMICAL PROCESSES • RESEARCH ARTICLE

Terrestrial-marine continuum of sedimentary natural organic matter in a mid-latitude estuarine system

Carlo Bravo[1,2] • Christian Millo[3] • Stefano Covelli[4] • Marco Contin[1] • Maria De Nobili[1]

Received: 20 February 2019 / Accepted: 4 September 2019

Responsible editor: Nives Ogrinc

[1]Department of Agricultural, Food, Environmental and Animal Science, University of Udine, Via delle Scienze 206, 33100 Udine, Italy

[2]Department of Life Sciences, University of Trieste, Via Licio Giorgieri 5, 34128, Trieste, Italy

[3]Oceanographic Institute, University of Sao Paulo, Praça do Oceanográfico 191, 05508-900 Sao Paulo, Brazil

[4]Department of Mathematics and Geosciences, University of Trieste, Via Weiss 2, 34128 Trieste, Italy

✉ Carlo Bravo

carlo.bravo@uniud.it

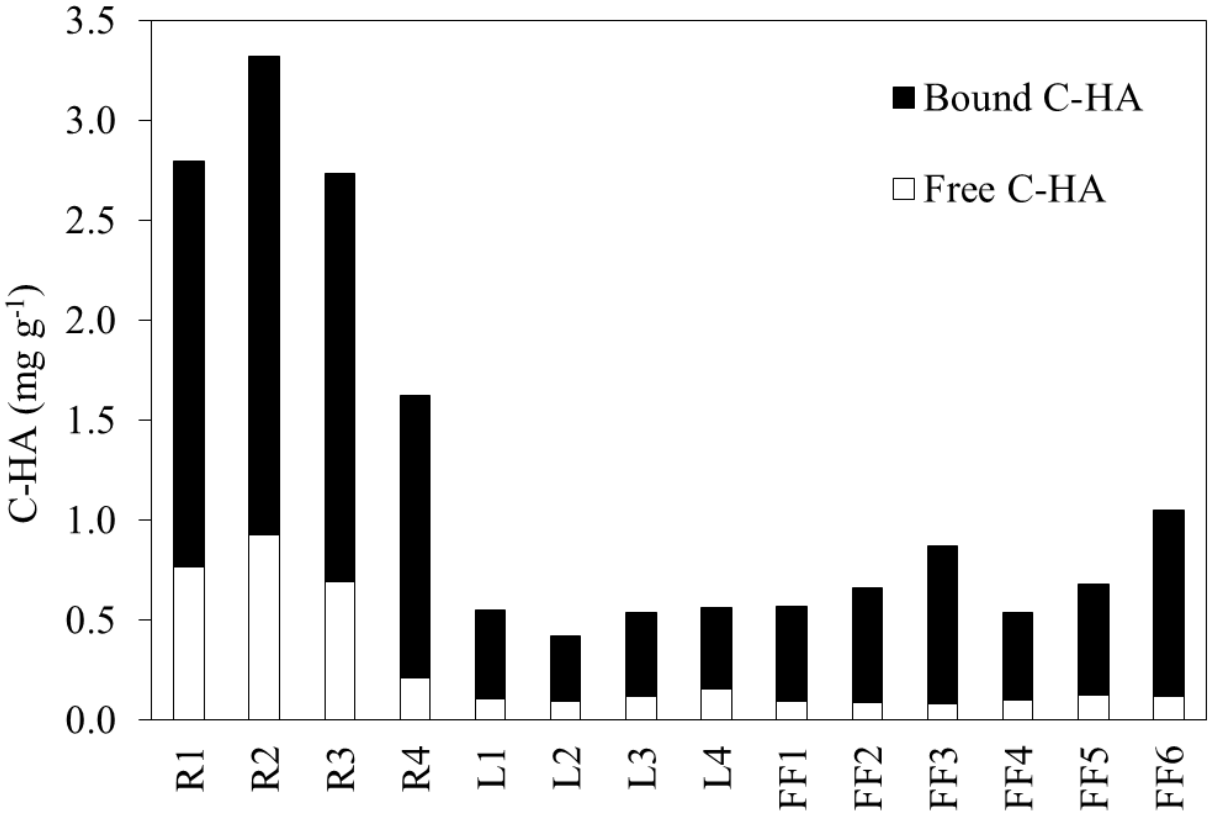

Fig. S1 Amount of free and bound humic C (C-HA) extracted from the three different environments along the transect: river (R), lagoon (L) and fish farm (FF).

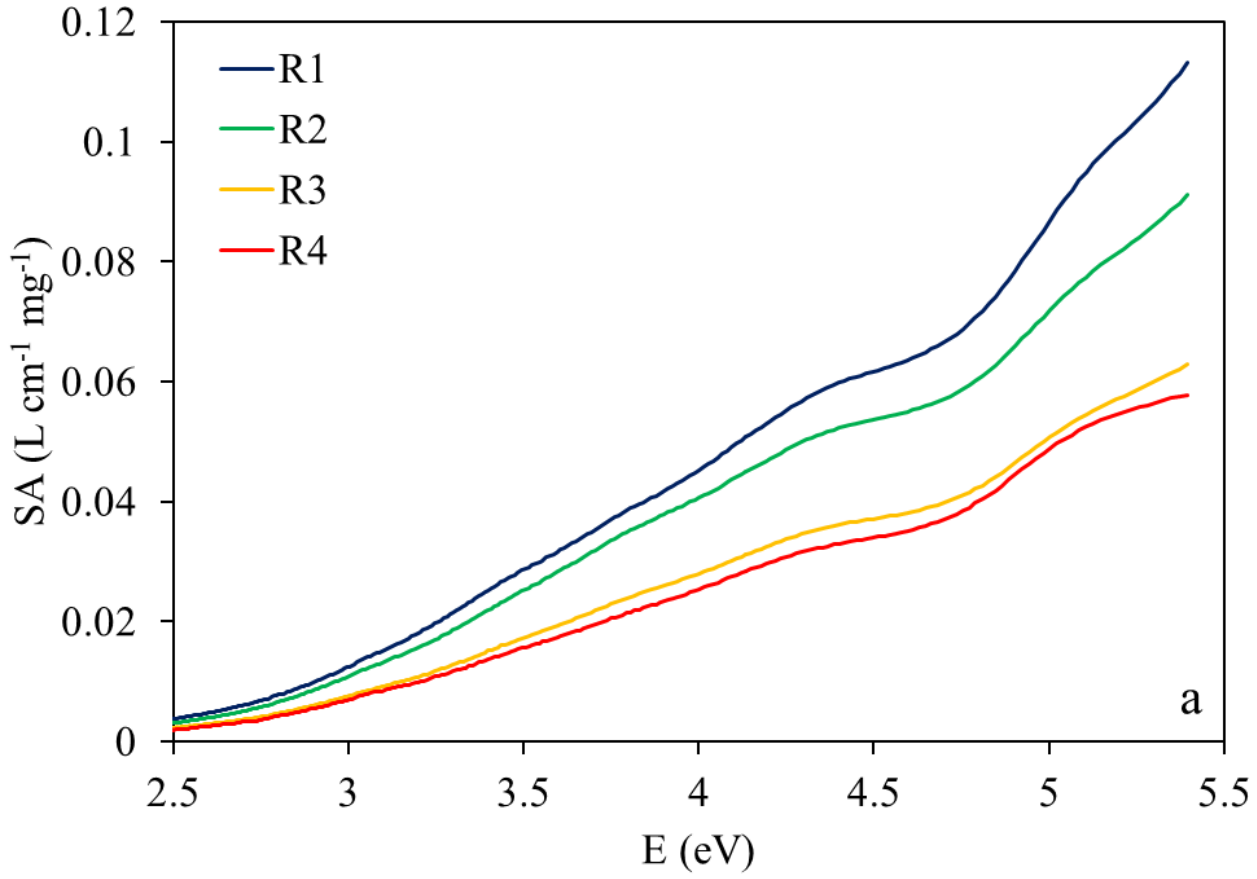
0.12
0.1
0.08
0.06
0.04
0.02
0
SA (L cm-1 mg-1)
R1
R2
R3
R4
a
2.5
3
3.5
4
4.5
5
5.5
E (eV)

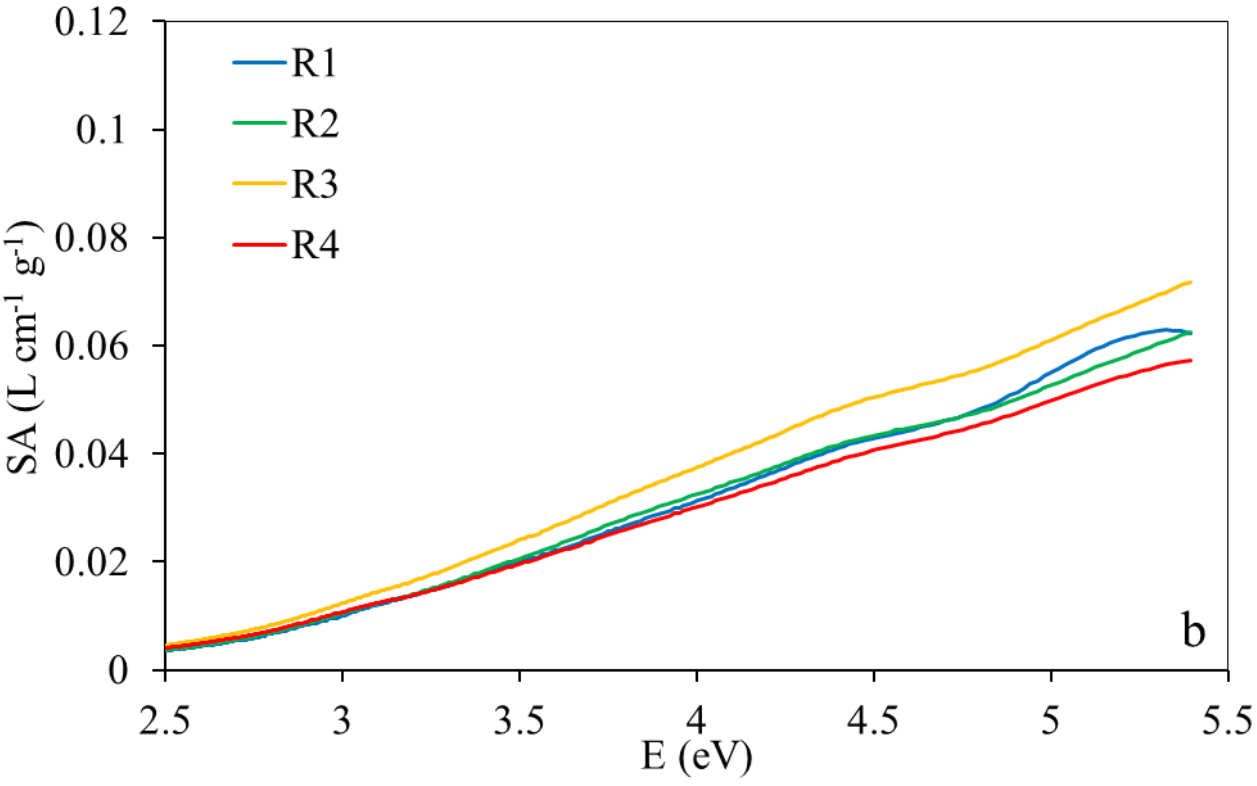
0.12
0.1
0.08
0.06
0.04
0.02
0
SA (L cm-1 g-1)
R1
R2
R3
R4
b
2.5
3
3.5
4
4.5
5
5.5
E (eV)

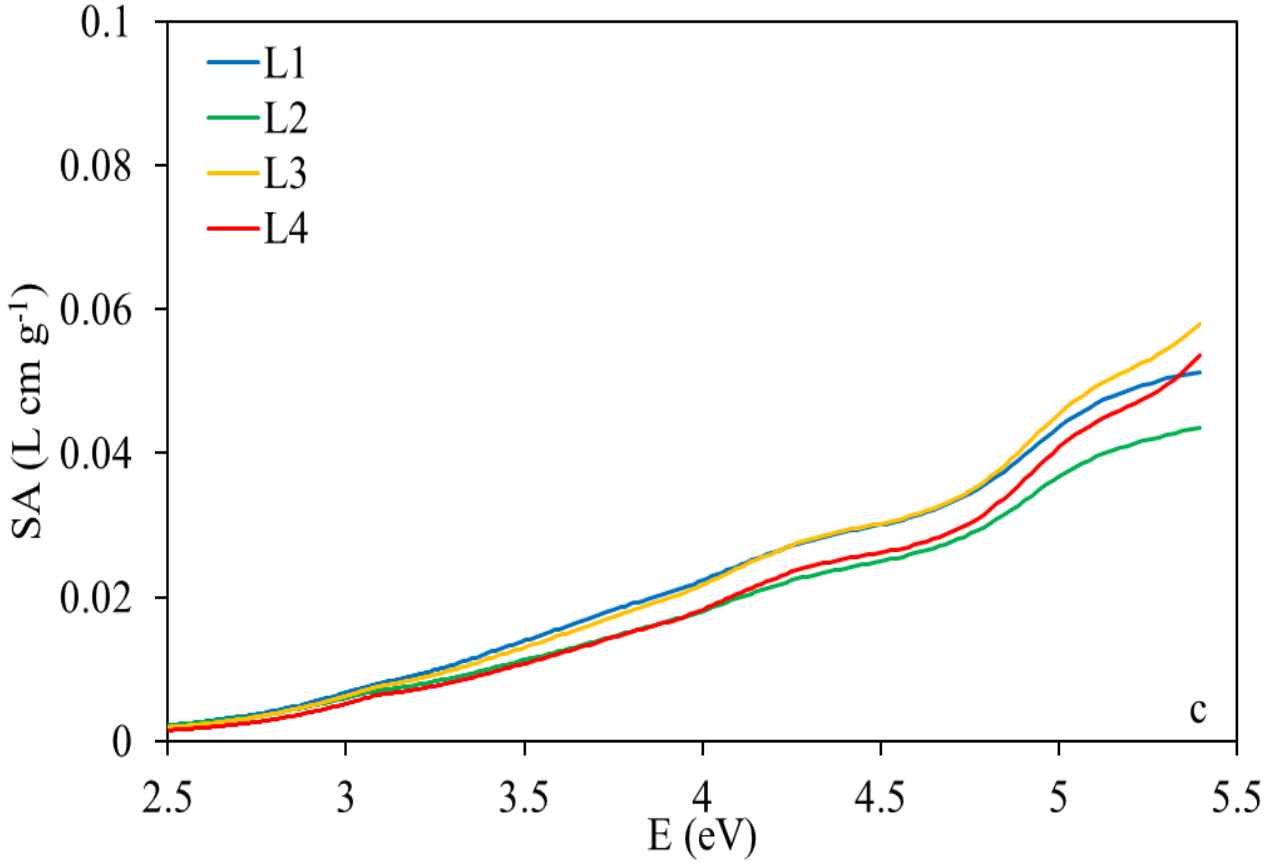
0.1
0.08
0.06
0.04
0.02
0
SA (L cm g-1)
L1
L2
L3
L4
c
2.5
3
3.5
4
4.5
5
5.5
E (eV)

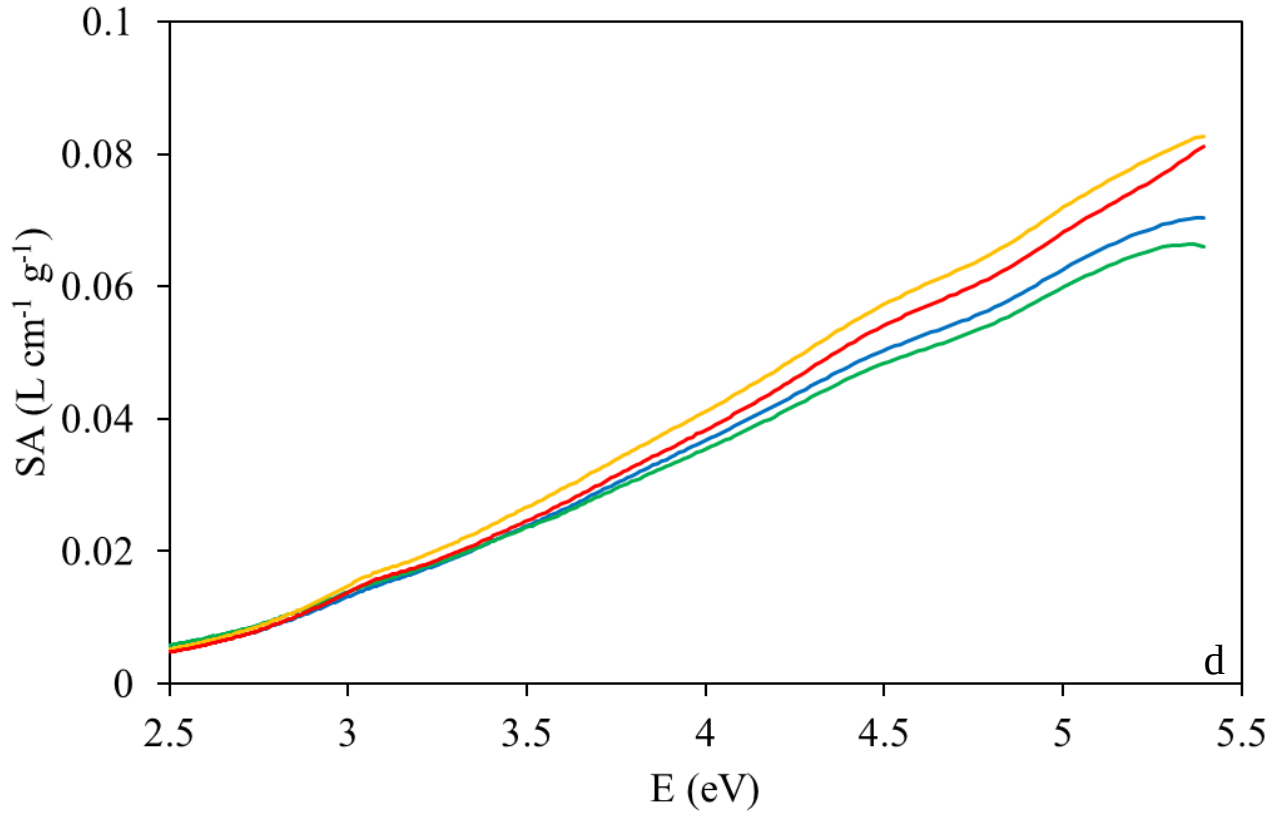
0.1
0.08
0.06
0.04
0.02
0
SA (L cm-1 g-1)
d
2.5
3
3.5
4
4.5
5
5.5
E (eV)

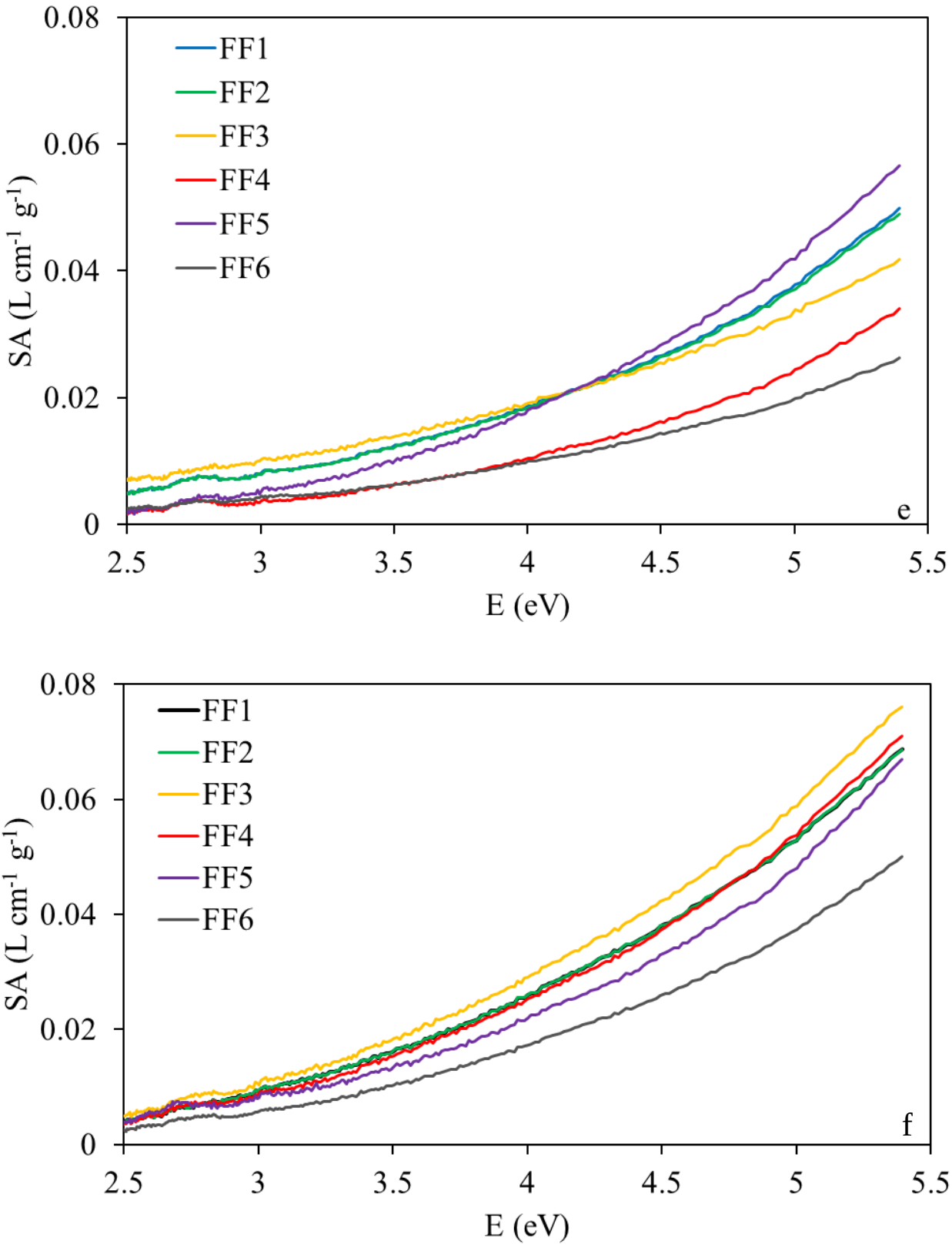

Fig. S2 UV-vis specific absorbance spectra of HA: river free HA (a), river bound HA (b), lagoon free HA (c), lagoon bound HA (d), fish farm free HA (e), fish farm bound HA (f).

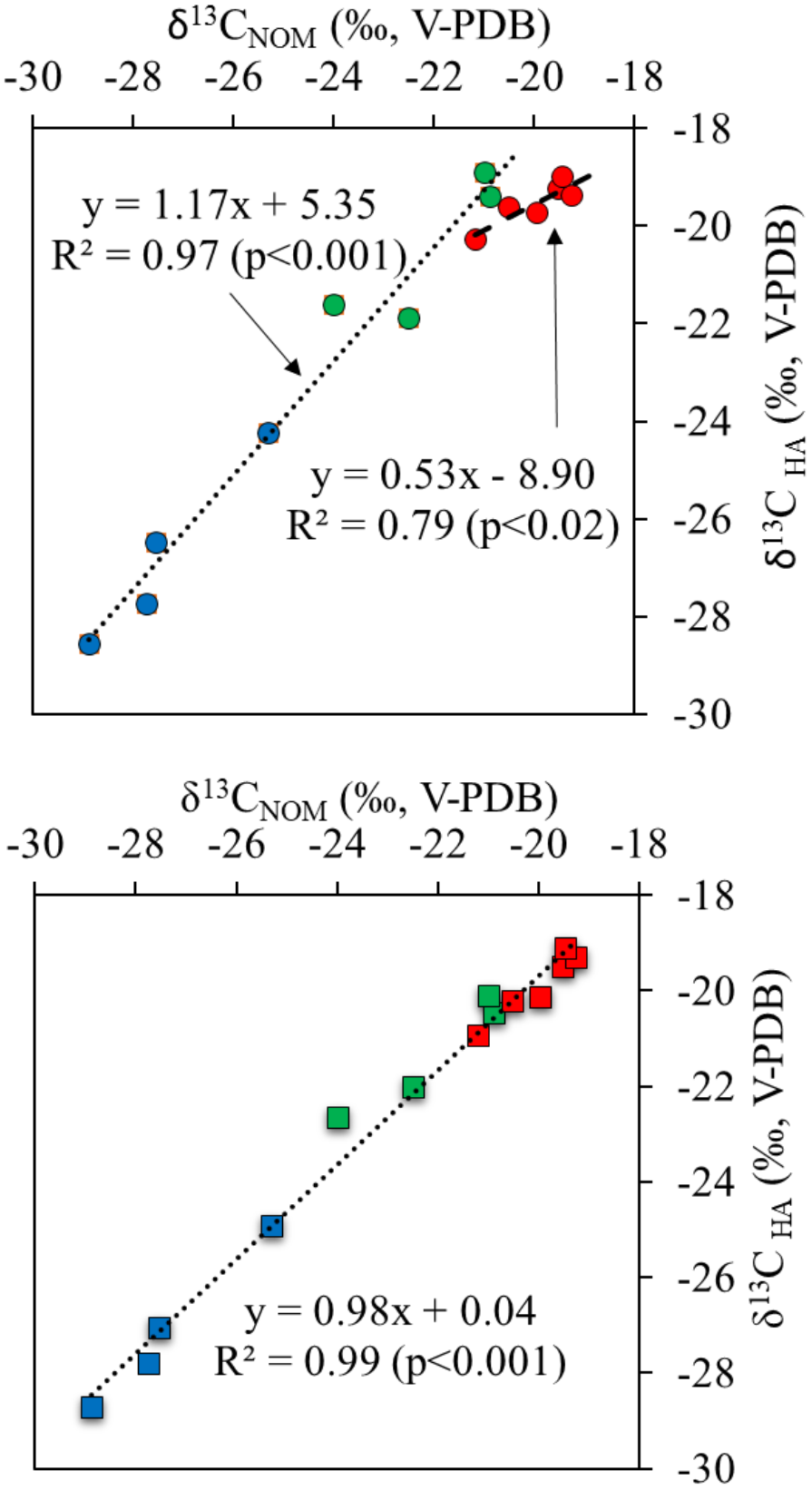

Fig. S3 Linear regression models of ^{13}C depletion of free (above) and bound (below) HA extracted from river (blue), lagoon (green) and fish farm (red) sediments versus ^{13}C depletion of NOM.

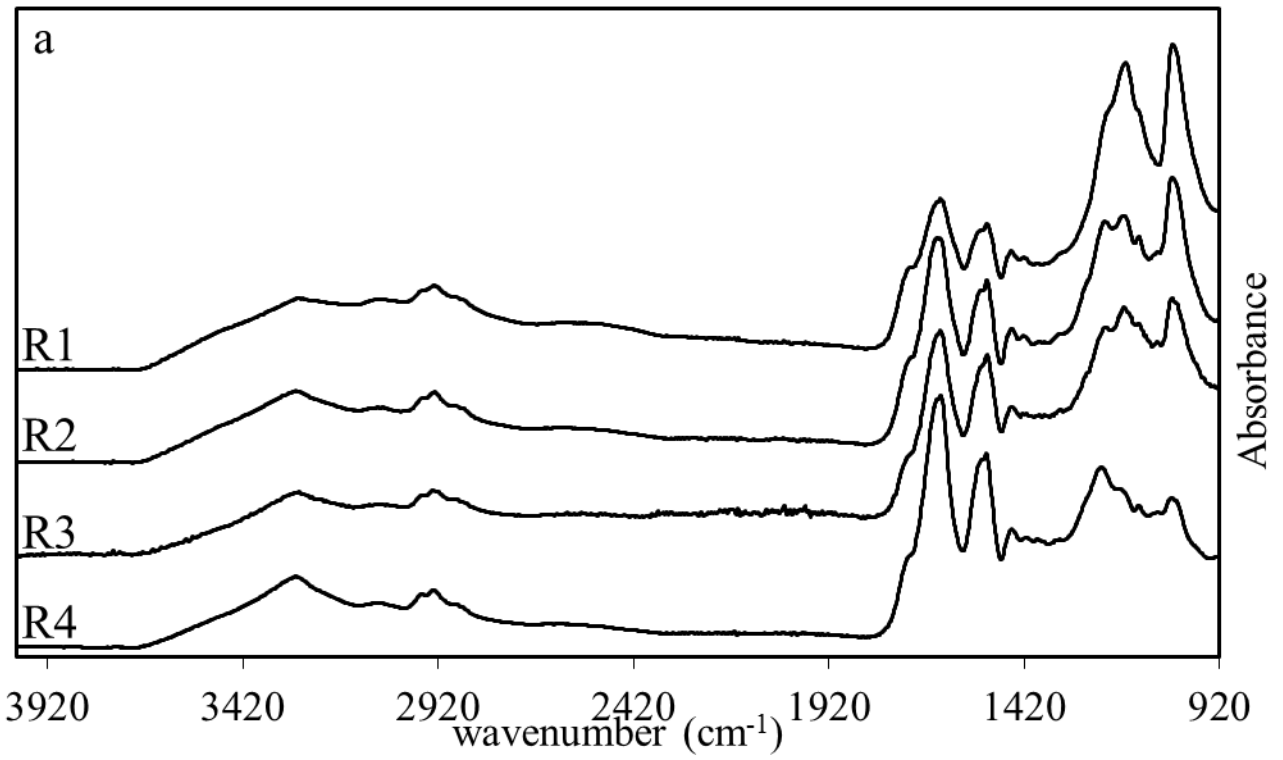
a
R1
R2
R3
R4
Absorbance
3920
3420
2920
2420
1920
1420
920
wavenumber (cm-1)

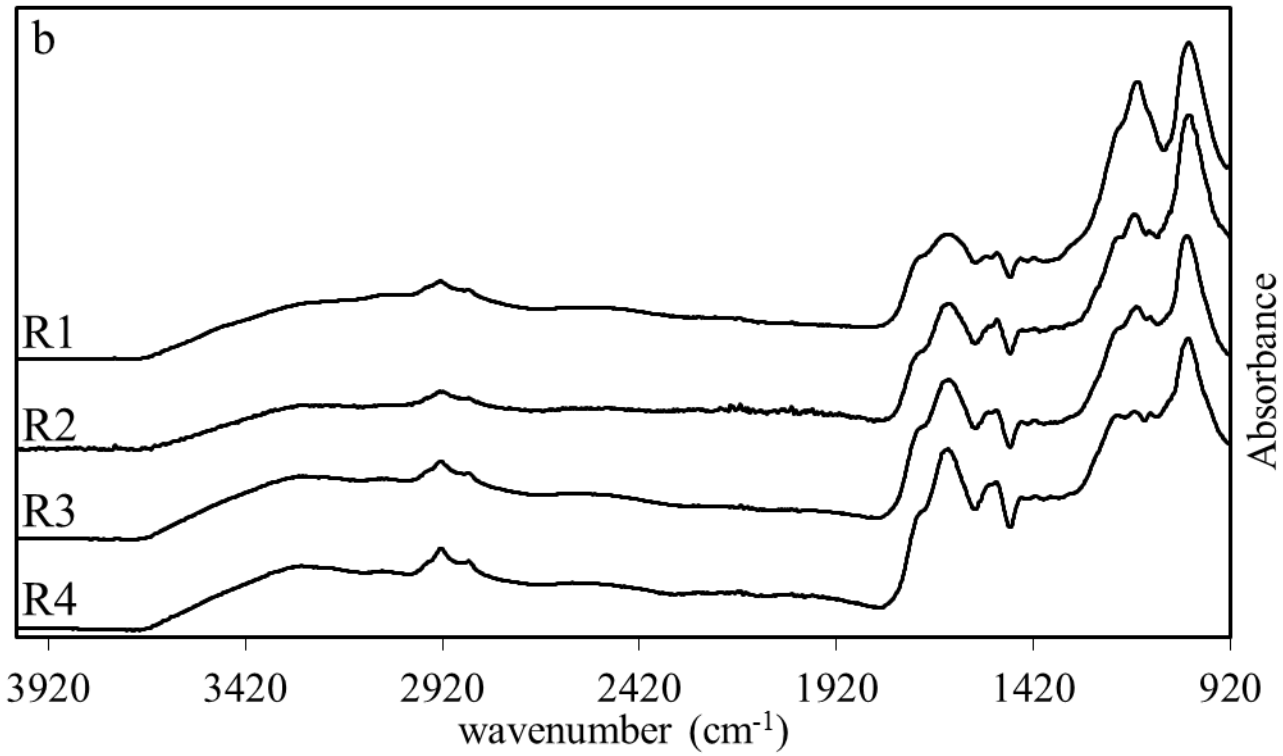
b
R1
R2
R3
R4
Absorbance
3920
3420
2920
2420
1920
1420
920
wavenumber (cm-1)

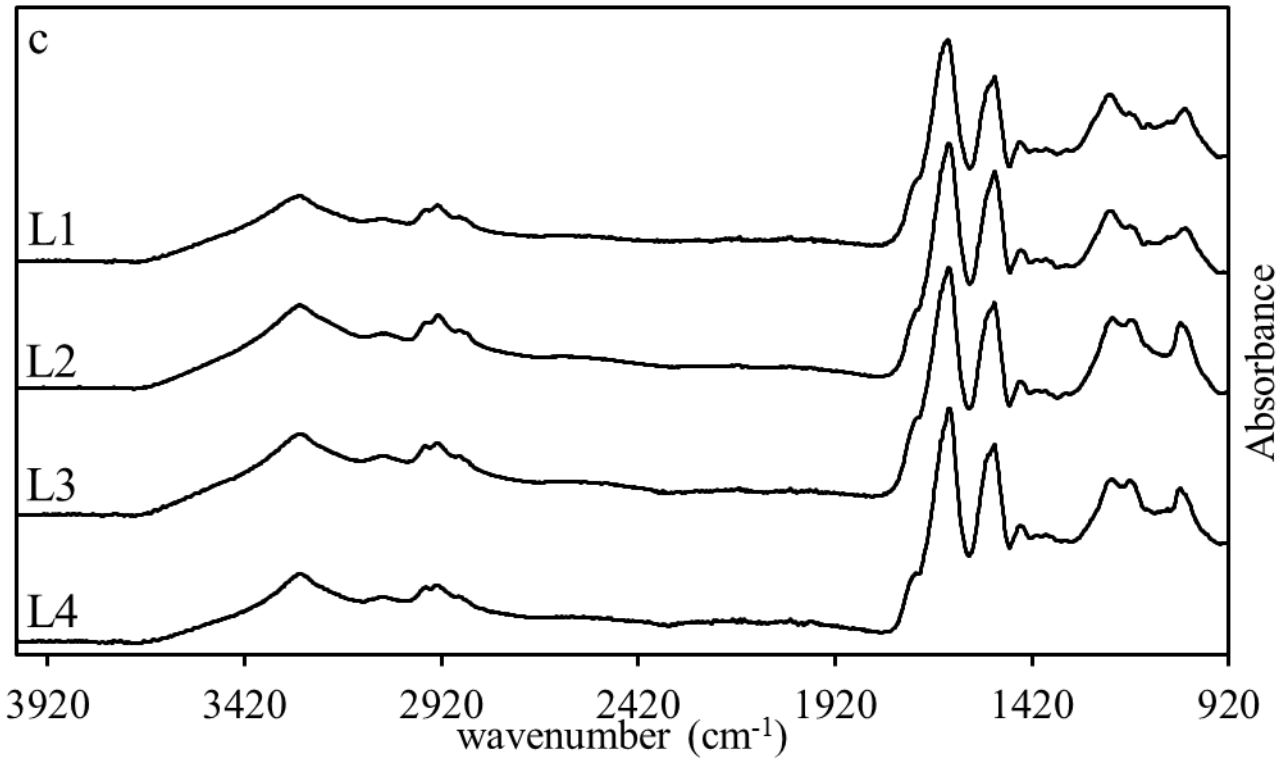
c
L1
L2
L3
L4
Absorbance
3920
3420
2920
2420
1920
1420
920
wavenumber (cm-1)

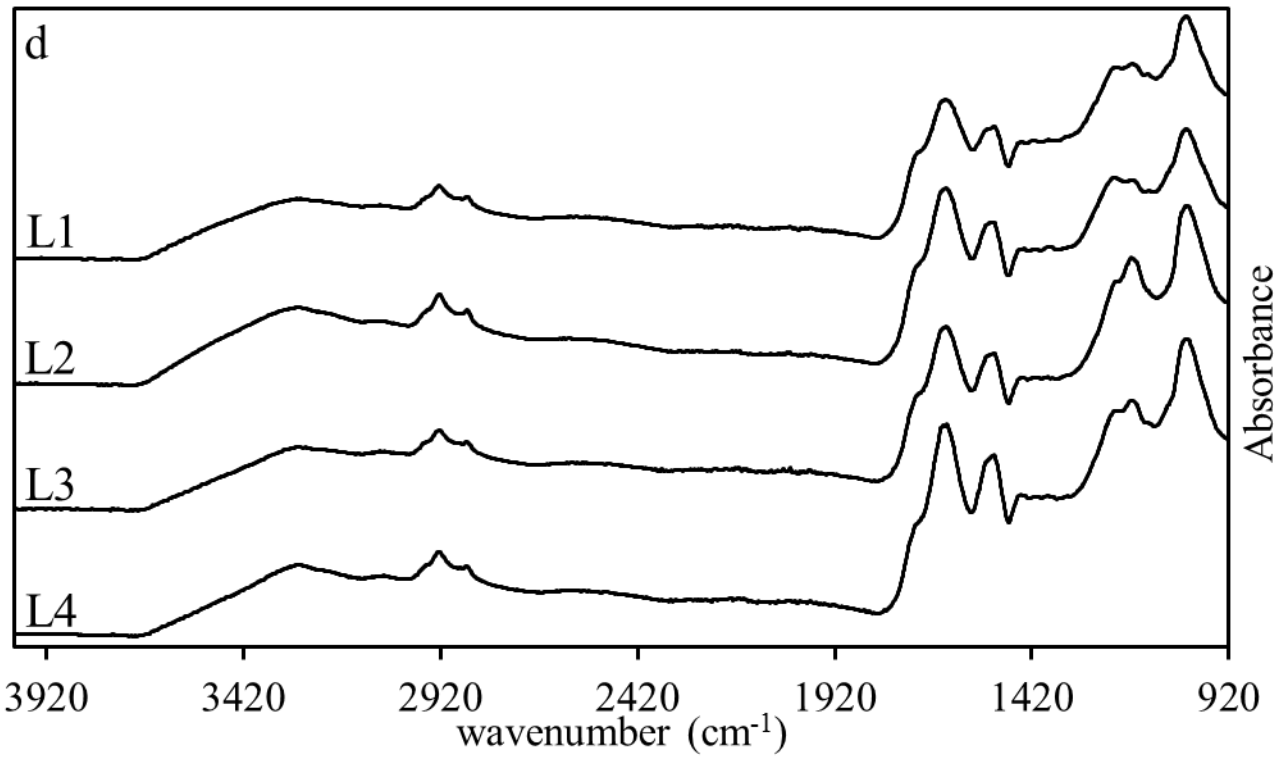
d
L1
L2
L3
L4
Absorbance
3920
3420
2920
2420
1920
1420
920
wavenumber (cm-1)

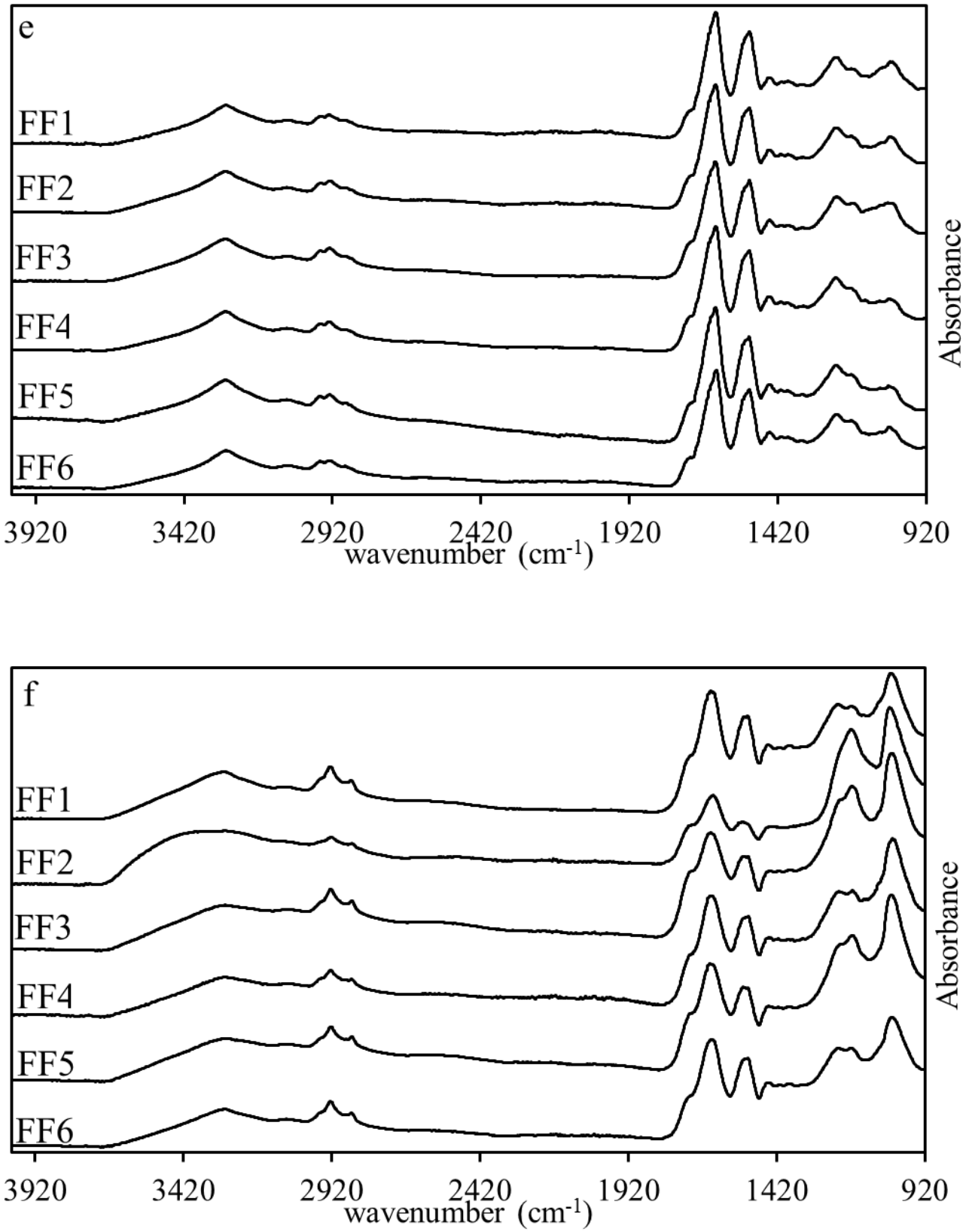

Fig. S4 FTIR spectra of HA: river free HA (a), river bound HA (b), lagoon free HA (c), lagoon bound HA (d), fish farm free HA (e), fish farm bound HA (f).

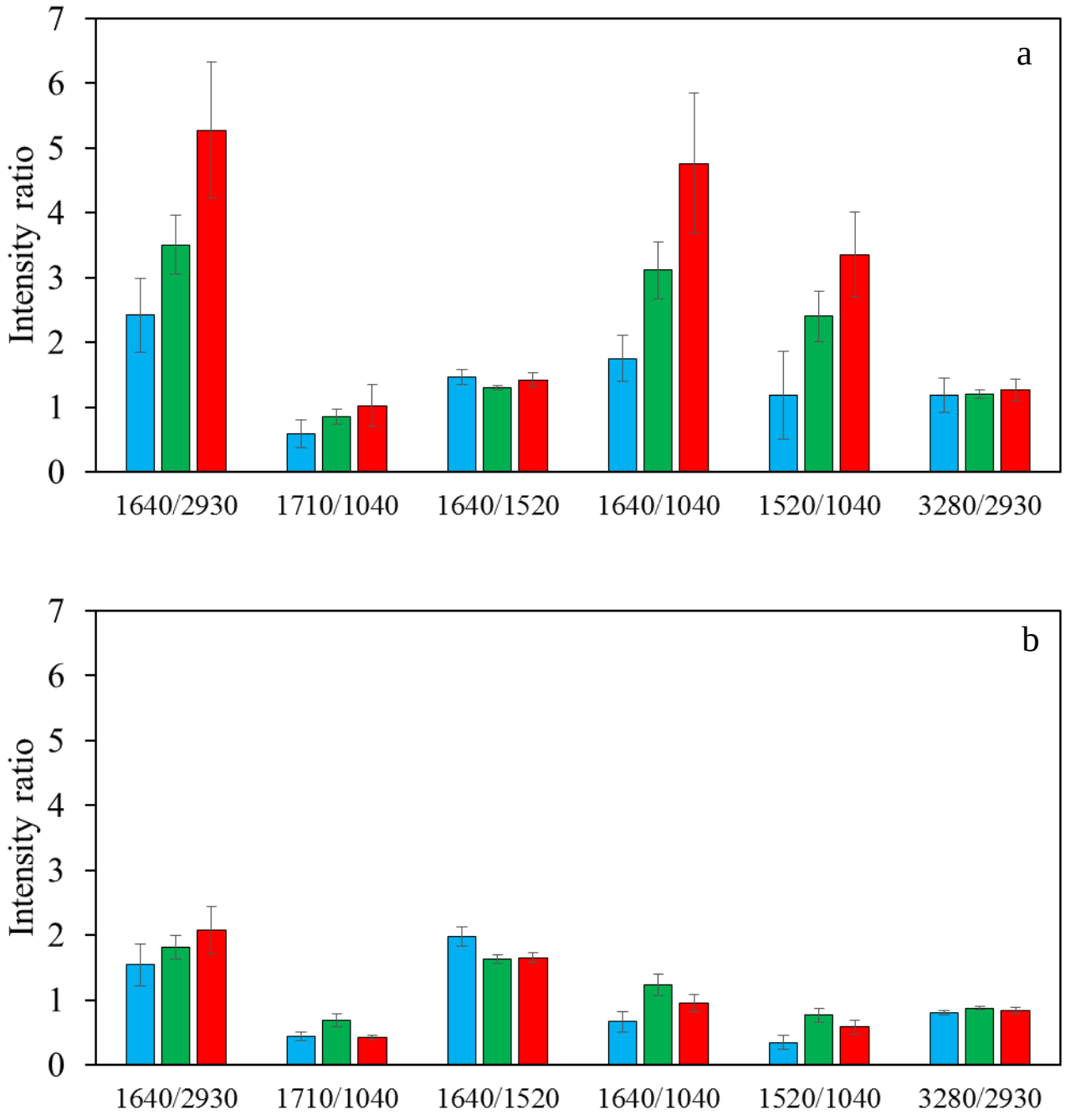

Fig. S5 Intensity ratios of the most representative FTIR bands of free (a) and bound (b) HA extracted from river (blue), lagoon (green), fish farm (red).

CHAPTER 6: SUPPORTING INFORMATION

Electron donating properties of humic acids in saltmarshes soils

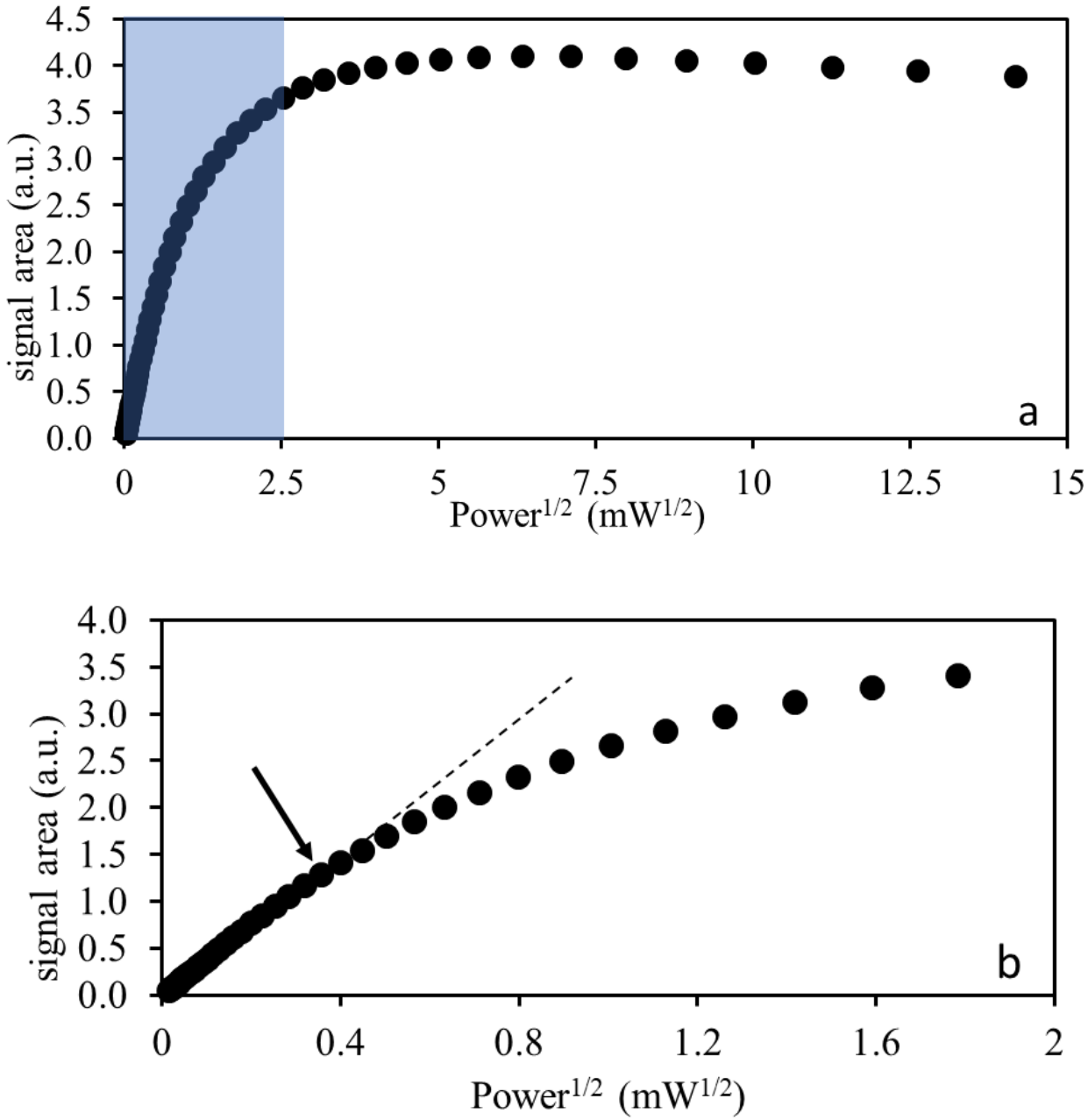

Fig. S1 a. EPR saturation curve (performed using the sample AM3 bound HA), where the area of the signal is plotted against the root square of the microwave power. Plot **b** is the zoom of the blue part of plot **a.** The arrow indicates the last point considered for the linear fitting and consequently, the microwave power used for the experiments.

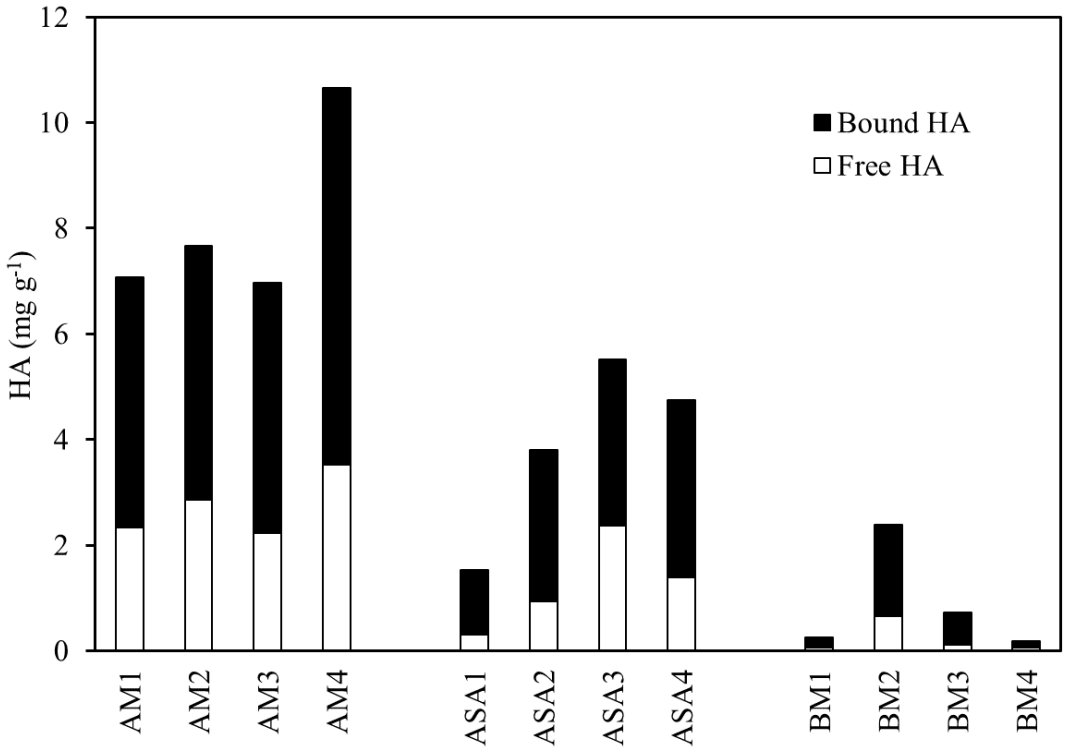

Fig. S2 Amount of free and bound humic acids extracted from the three different saltmarshes.

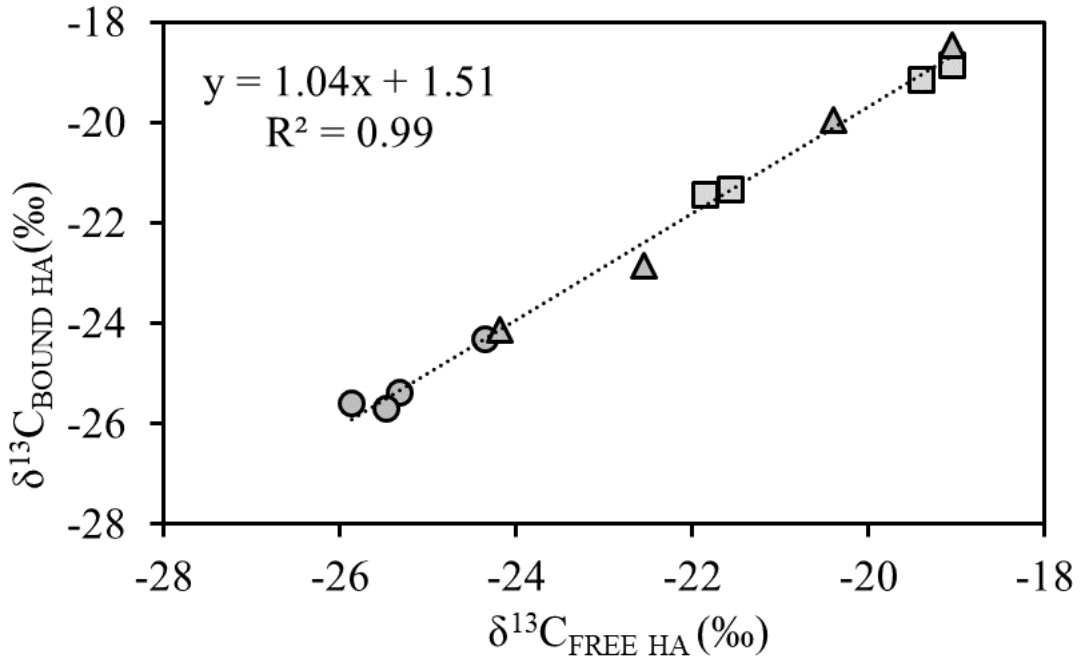

Fig. S3 Linear regression models of ^{13}C depletion of bound HA extracted from AM (●), ASA (■) and BM (▲) saltmarshes versus ^{13}C depletion of the corresponding free HA.

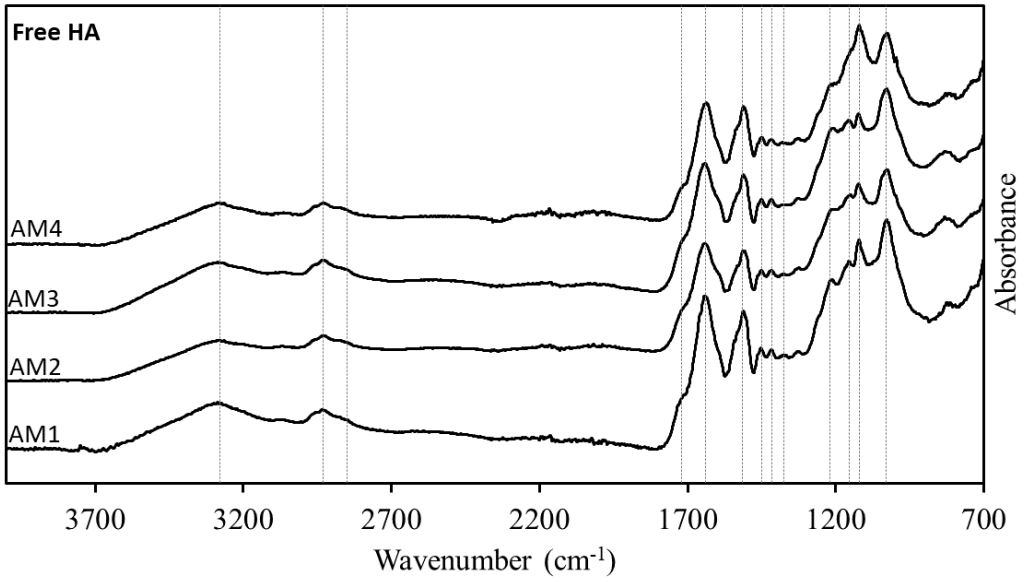

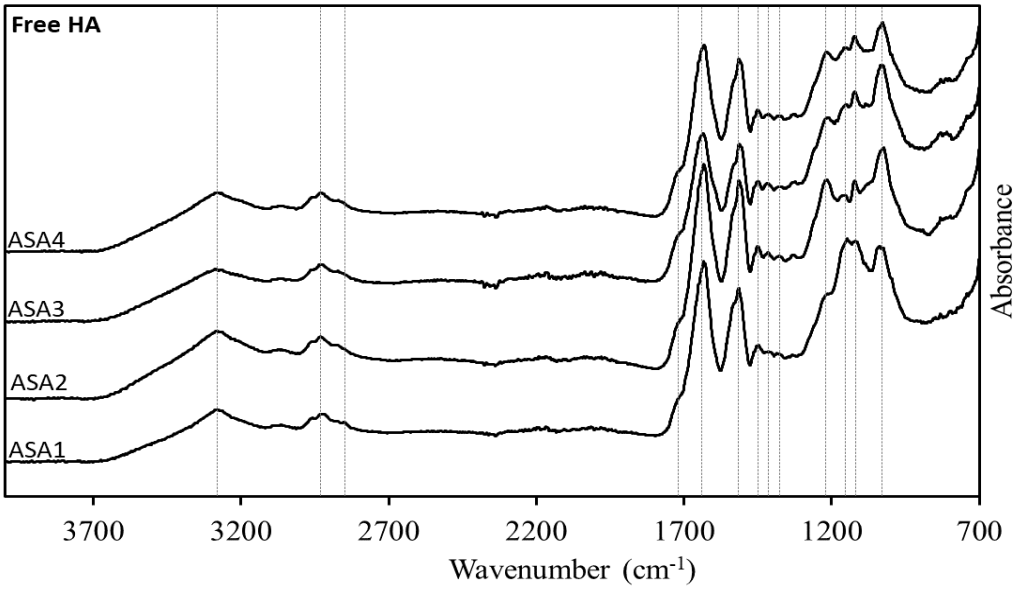

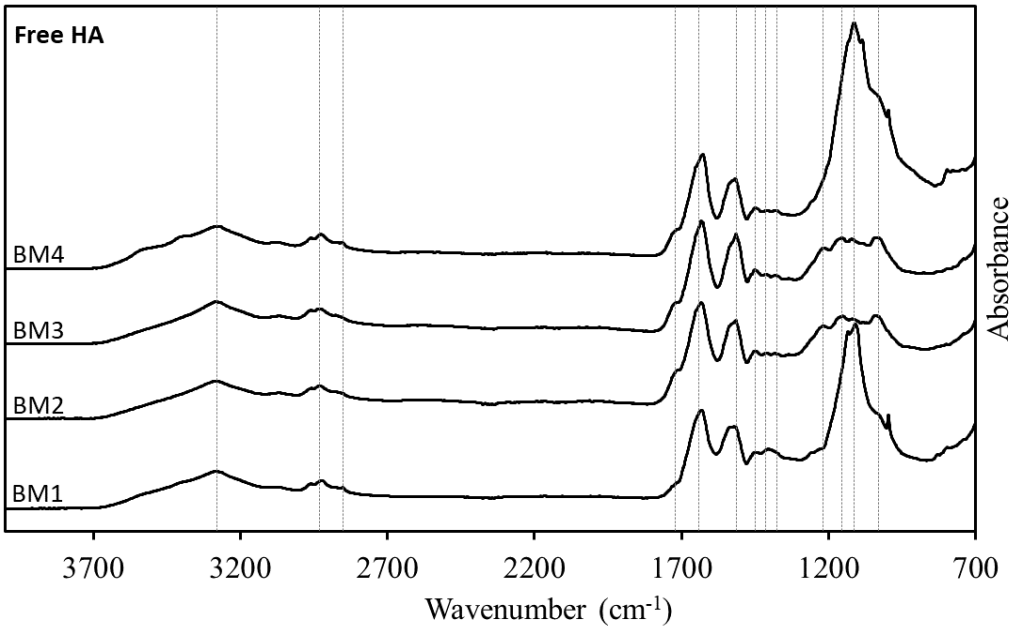

Fig. S4 FT-IR spectra of free HA extracted from AM, ASA and BM saltmarshes.

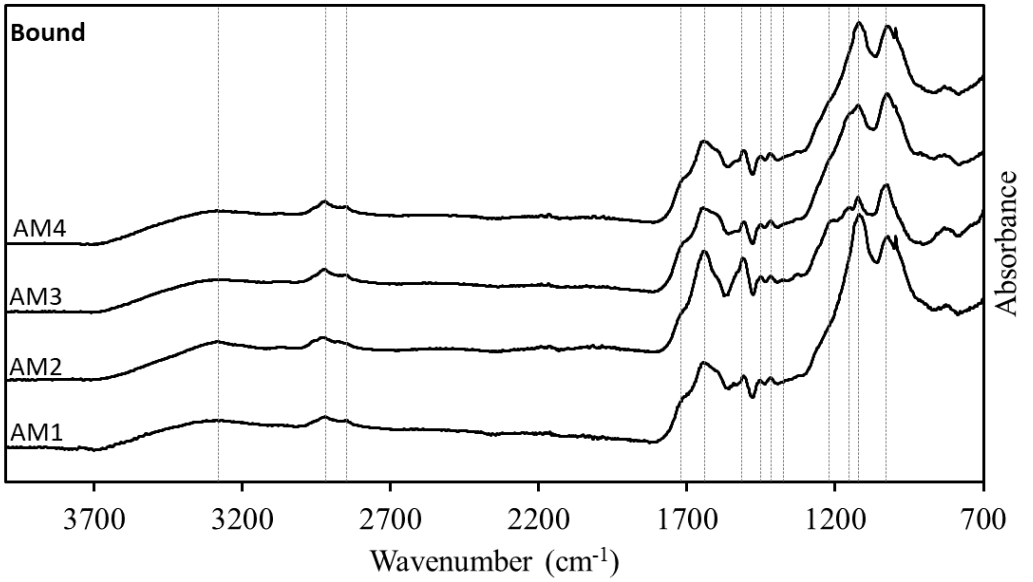

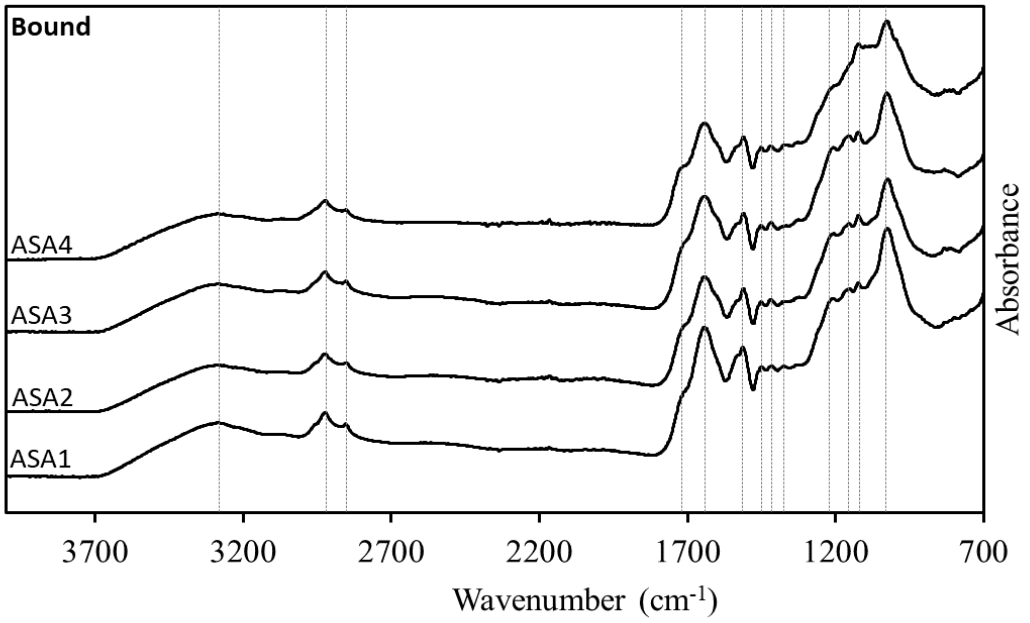

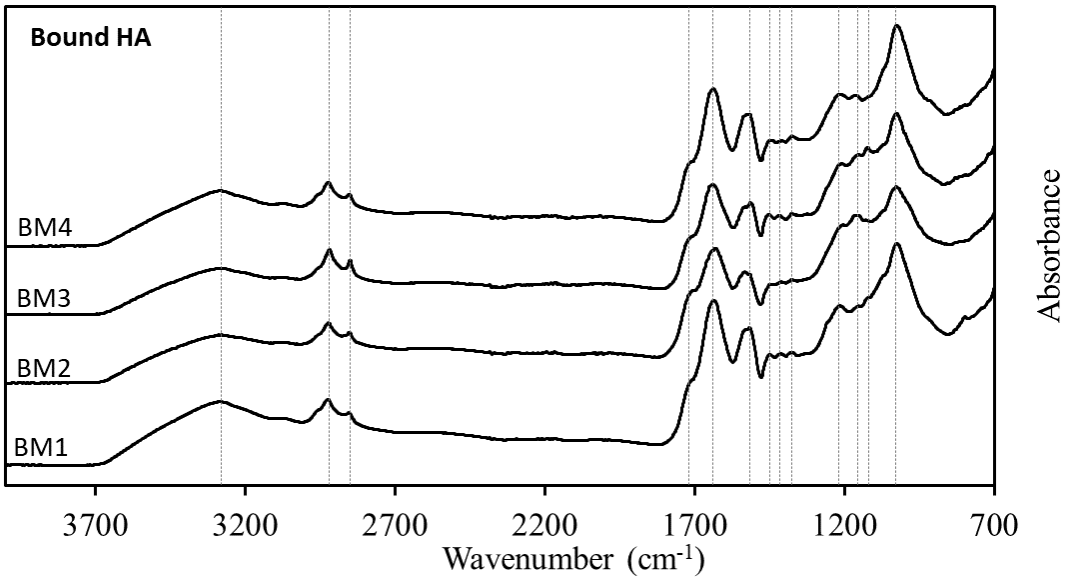

Fig. S5 FT-IR spectra of bound HA extracted from AM, ASA and BM saltmarshes.

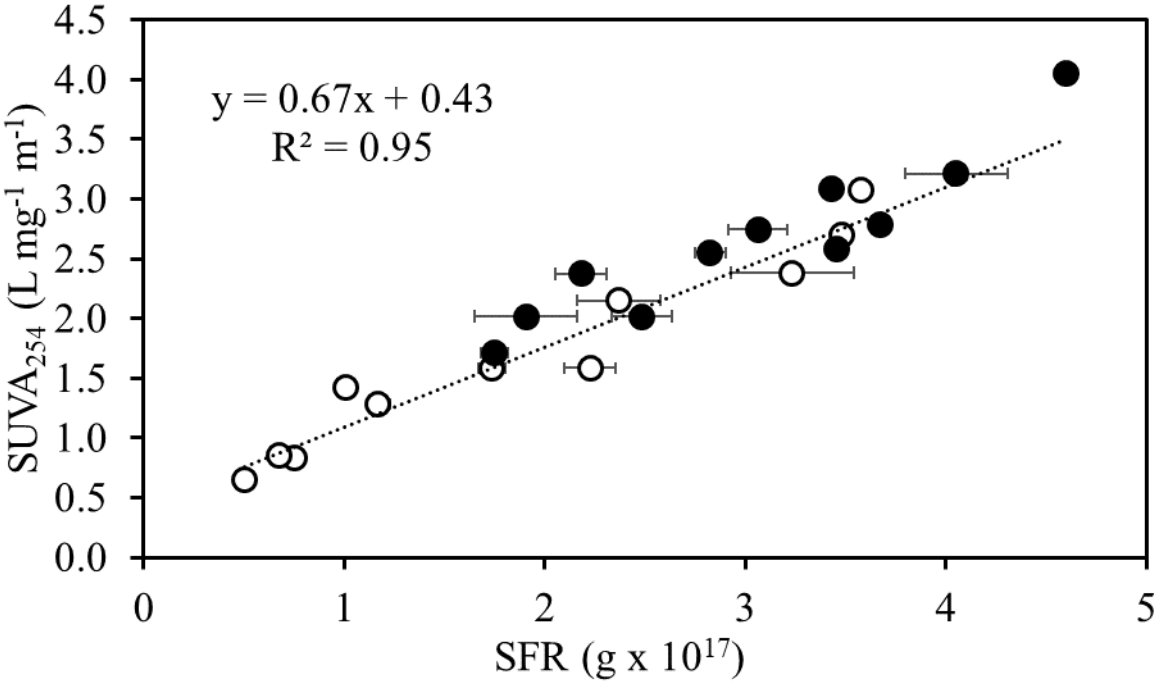

Fig. S6 Linear correlation between specific absorbance at 254 nm and the semiquinone type free radicals concentration of free (empty circles) and bound (black circles) HA.

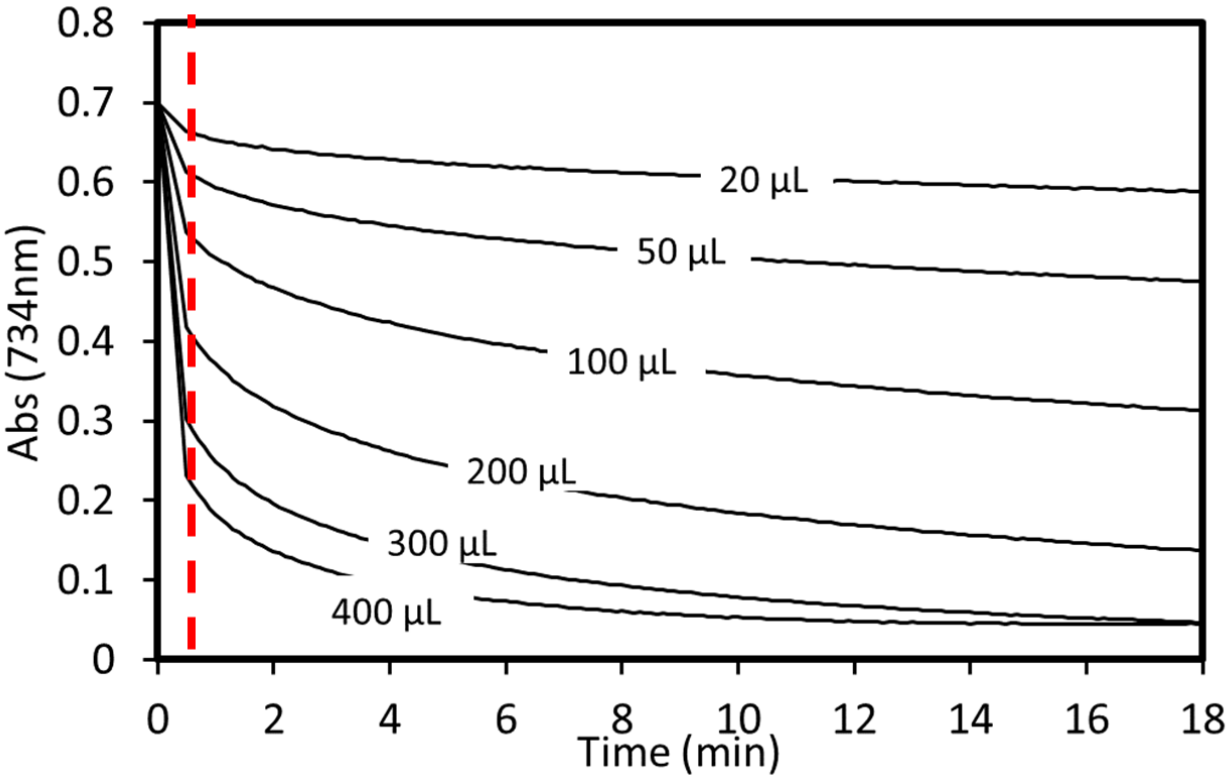

Fig. S7 Time trend of the decrease in absorbance at 734 nm (corresponding to the reduction of $ABTS^{\cdot+}$ to ABTS) after the addition of incresing amounts of HA (AM3 bound HA). Dotted red line indicates the time when the electron donating capacity (EDC) was calculated.

ACKNOWLEDGMENTS

I would like to thank my supervisor, prof. Maria De Nobili, for her guidance through each stage of this three years and for having conveyed her passion on humic substances to me.

I would like to thank also prof. Marco Contin, always present and helpful with everything, and prof. Rosanna Toniolo, for her extreme professionalism and patience during the thousand electrochemical analyses.

I would like to acknowledge the financial support provided by the International Humic Substances Society that allowed me to spend two intensive months at the Embrapa Instrumentation Center (Brazil), under the guidance of Dr. Ladislau Martin Neto and his team. *Muito obrigado por tudo!*

A heartfelt thanks to prof. Christian Millo, who also hosted me again at the Oceanographic Institute of the University of Sao Paulo (Brazil), and to prof. Stefano Covelli, for having given continuity to my master thesis and for the tips for the future.

I would like to thank my lab mates, Ali, Anna, Aldo, Andrea, Elisa and Tania for all the time spent together in the lab, Saturdays and Sundays included. A coffee and one *mandi* to whom is now looking at us from the sky.

An immense thanks to my parents Liteo and Lucia and to my brother Marco, that silently but continuously supported me in these three years.

Finally, a special ευχαριστώ to Thea for her love and her continuous encouragement.